

**Molecular and physiological aspects of alcohol
dehydrogenases in the ethanol metabolism of
*Saccharomyces cerevisiae***

by

Olga de Smidt

Submitted in fulfillment of the requirements
for the degree

Philosophiae Doctor

In the Faculty of Natural and Agricultural Sciences
Department of Microbial, Biochemical and Food Biotechnology
University of the Free State
Bloemfontein
South Africa

May 2007

Promoter: Prof. J. Albertyn
Co-promoter: Prof. J.C. du Preez

Author's note

Whenever we attempt great feats in life it is not so much the hardships or the successes we remember, as the people who helped. I would like to thank my parents for teaching me that I can achieve anything I put my mind to. Your encouragement and support means the world to me, thank you. To the rest of my family who always tried to sound interested in my work, the gesture was much appreciated. A special word of thanks to all my colleagues and friends at the Department. In particular Sanet, I would never have made it this far without you. Thank you also to Eugene who taught me the finer details of working with bioreactors and for all the interesting discussions. All the sample analyses would have been unbearable if not for Piet Botes, who always came to the rescue when a problem arose. Els, thank you for all the time, love and effort, you kept me sane through the last gruelling months. To Jeanine and rest of the Burger family; thank you for always caring about my safety and my sanity. It is with much appreciation that I would also like to thank my High School teachers Joy Roets and Marlene Slabbert. I learned through their diligence and care to love writing and science. I am indebted to my promoters Profs. Albertyn and du Preez for their enthusiastic time and advice. I would also like to express my sincere gratitude towards the Department of Biotechnology and the National Research Foundation for financial support.

Table of contents

1. Introduction	2
2. Literature review	4
2.1 Classification of the alcohol dehydrogenase enzyme	4
2.2 Classical alcohol dehydrogenases ADH I – ADH V	5
2.2.1 Primary and secondary structure	6
2.2.1.1 <i>ADH1</i> encoding ADH I	6
2.2.1.2 <i>ADH2</i> encoding ADH II	7
2.2.1.3 <i>ADH3</i> encoding ADH III	8
2.2.1.4 <i>ADH4</i> encoding ADH IV	9
2.2.1.5 <i>ADH5</i> encoding ADH V	10
2.2.2 Active centres	10
2.2.3 Co-enzymes and metal binding sites	10
2.2.4 Kinetic characteristics	11
2.2.5 Localisation	13
2.2.6 Function and mechanism of action	13
2.2.7 Regulation	16
2.2.7.1 Regulation of <i>ADH2</i> mediated by ADR1	16
2.2.7.2 Other elements participating in <i>ADH2</i> regulation	17
2.2.7.3 The influence of chromatin remodelling on <i>ADH2</i> expression	20
2.2.7.4 Regulation of <i>ADH1</i> , <i>ADH3</i> , <i>ADH4</i> and <i>ADH5</i>	22
2.2.8 Evolutionary development and biochemical adaptation	23
2.3 Other alcohol dehydrogenases	24
2.4 Literature cited	27
3. The effect of medium composition and ethanol toxicity on the growth of <i>Saccharomyces cerevisiae</i> strain W303-1A(a)	35
3.1 Abstract	35

3.2	Introduction	36
3.3	Materials and Methods	37
3.3.1	Strains and media	37
3.3.2	Cultivation conditions	37
3.3.3	Analyses	38
3.4	Results and Discussion	38
3.5	Conclusions	44
3.6	Literature cited	45
4.	Expression of the <i>ADH1</i>, <i>ADH2</i>, <i>ADH3</i>, <i>ADH4</i> and <i>ADH5</i> genes in response to pulse addition of ethanol or glucose to a continuous culture of strain W303-1A(a)	47
4.1	Abstract	47
4.2	Introduction	48
4.3	Materials and Methods	50
4.3.1	Strains and medium	50
4.3.2	Chemostat cultivations	50
4.3.3	Analytical procedures	50
4.3.4	Northern blot analysis	51
4.4	Results and Discussion	52
4.5	Conclusions	58
4.6	Literature cited	60
5.	Growth kinetics and transcription levels of the <i>ADH</i> genes in a recombinant strain over-expressing <i>ADH2</i> in batch cultures	62
5.1	Abstract	62
5.2	Introduction	63
5.3	Materials and Methods	64
5.3.1	Strains and media	64
5.3.2	Construction of an <i>ADH2</i> single deletion mutant (<i>SΔ2a</i>)	64

5.3.3	Construction of recombinant strain S Δ 2aTR_ <i>ADH2</i> over-expressing <i>ADH2</i>	66
5.3.4	Cultivation conditions	66
5.3.5	Analyses	67
5.3.6	Real-time PCR	68
5.4	Results and Discussion	70
5.5	Conclusions	79
5.6	Literature cited	81
6.	Evaluation of multiple <i>ADH</i> knock-out strains of <i>Saccharomyces cerevisiae</i> in bioreactor batch cultivations	83
6.1	Abstract	83
6.2	Introduction	84
6.3	Materials and Methods	86
6.3.1	Strains	86
6.3.2	Media	86
6.3.3	DNA methods	86
6.3.4	Deletion plasmid construction	86
6.3.5	Disruption of <i>ADH2</i> , <i>ADH3</i> , <i>ADH4</i> and <i>ADH5</i> from <i>S. cerevisiae</i> chromosomes	88
6.3.6	Construction of double, triple and quadruple deletion strains D Δ 34a, D Δ 34b, T Δ 345, T Δ 234, T Δ 235, T Δ 245, Q1, Q2, Q3, Q4 and Q5	89
6.3.7	Cultivation conditions	90
6.3.8	Analyses	90
6.3.9	Real-time PCR	90
6.4	Results and Discussion	91
6.4.1	Construction of <i>ADH</i> quadruple deletion mutant strains Q1, Q2, Q3, Q4 and Q5 with molecular and classical techniques	91
6.4.2	Bioreactor cultivation of strains W303-1A(a), Q1, Q2, Q3, Q4 and Q5 with glucose as carbon source	95

6.4.3	Bioreactor cultivation of strains W303-1A(a), Q1, Q2 and Q3 on ethanol as carbon source	106
6.5	Conclusions	111
6.6	Literature cited	115
7.	Concluding remarks and future research	118
8.	Summary	124
9.	Opsomming	125
	Appendices	126

List of Figures

Figure 2.1.	Classification of yeast Zn-containing MDR alcohol dehydrogenases.....	6
Figure 2.2.	Common mechanism for the yeast alcohol dehydrogenase reaction with two ternary enzyme substrate complexes.....	14
Figure 2.3.	Schematic map of the <i>ADH2</i> gene.....	21
Figure 3.1	Growth profile of <i>S. cerevisiae</i> strain W303-1A(a) in complex medium in shake flasks containing different glucose concentrations.....	40
Figure 3.2	Growth profiles of <i>S. cerevisiae</i> W303-1A(a) in complex medium in shake flasks with 5 g ethanol l ⁻¹ as carbon source.....	41
Figure 3.3	Growth profile of strain W303-1A(a) on 10 g glucose l ⁻¹ in a chemically defined medium in shake flasks.....	42
Figure 3.4	Growth profile of strain W303-1A(a) on 5 g ethanol l ⁻¹ in a chemically defined medium in shake flasks.....	42
Figure 3.5	Effect of the exogenous ethanol concentration on the maximum specific growth rate of W303-1A(a) grown at 25°C.....	43
Figure 4.1	Steady-state concentrations of biomass, glucose and ethanol in aerobic glucose-limited chemostat cultures of <i>S. cerevisiae</i> W303-1A(a) in chemically defined medium containing 8 g glucose l ⁻¹	53
Figure 4.2	Metabolite levels during a dynamic response triggered by a 13.2 g.l ⁻¹ glucose pulse.....	55
Figure 4.3	Northern analysis of gene transcription in response to a 13.2 g l ⁻¹ glucose pulse administered to a glucose-limited chemostat culture of strain W303-1A(a).....	55
Figure 4.4	Metabolite levels during a dynamic response triggered by a ethanol pulse. A 7.8 g l ⁻¹ pulse was added (indicated by time 0) to a glucose-limited steady-state culture of strain W303-1A(a) at a dilution rate of 0.17 h ⁻¹	57
Figure 4.5	Northern analysis of gene transcription in response to a 7.8 g l ⁻¹ ethanol pulse administered to a glucose-limited chemostat culture of strain W303-1A(a).....	57

Figure 5.1	(A) PCR amplicon representing the <i>ADH2</i> ORF flank both 5' and 3' by 1000 bp non-coding sequence. (B) The 3017 bp PCR fragment cloned into pGemT-Easy and digested with <i>EcoRI</i> and <i>HindIII</i> for verification. (C) The <i>padh2Δ::URA3</i> plasmid construct verified by digestion with <i>PvuII</i> , <i>NheI</i> and <i>EcoRV</i>	70
Figure 5.2	Nucleotide sequence alignment of the <i>ADH2</i> ORF cloned into pGemT-Easy and the sequence retrieved from the <i>Saccharomyces</i> genome data base.	71
Figure 5.3	Restriction enzyme digestion profile of two independent pCM190L_W:: <i>ADH2</i> plasmid constructs digested with <i>EcoRI</i> and <i>BamHI</i>	72
Figure 5.4	Typical bioreactor cultivation profiles of strains SA2aTR_E and SA2aTR_ADH2 grown aerobically in chemically defined medium without tryptophan with 20 g l ⁻¹ glucose as carbon source.	74
Figure 5.5	Real-time RT-PCR transcription profiles of the <i>ADH1</i> , <i>ADH4</i> and <i>ADH5</i> in strains SA2aTR_E and SA2aTR_ADH2 grown aerobically in chemically defined medium (-TRP) in bioreactors with 20 g l ⁻¹ glucose as carbon source.	76
Figure 5.6	Typical bioreactor cultivation profiles of strains SA2aTR_E and SA2aTR_ADH2 grown aerobically in chemically defined medium without tryptophan with 6.9 and 6.2 g l ⁻¹ ethanol as carbon source.	77
Figure 5.7	Real-time RT-PCR transcription profiles of the <i>ADH1</i> , <i>ADH4</i> and <i>ADH5</i> in strains SA2aTR_E and SA2aTR_ADH2 grown aerobically in chemically defined medium without tryptophan in bioreactors with 6.9 and 6.2 g l ⁻¹ ethanol as carbon source.	78
Figure 6.1	Plasmid constructs pADH1, pADH2, pADH3, pADH4 and pADH5, containing the <i>ADH</i> ORFs and a 1000 bp flanking regions in pGemT-Easy, verified by restriction enzyme digestion.	91
Figure 6.2	Restriction enzyme digestion profiles of the eight deletion plasmid constructs <i>padh1::LEU2</i> , <i>padh1::URA3p</i> , <i>adh1::TRP1</i> , <i>padh1::HIS3</i> , <i>padh2::URA3</i> , <i>padh3::TRP1</i> , <i>padh4::HIS3</i> and <i>padh5::LEU2</i>	92
Figure 6.3	Diagram of double, triple and quadruple deletion strains construction with molecular and classical techniques.	93
Figure 6.4	PCR profiles of the parental and quadruple deletion mutant strains.	94
Figure 6.5	Typical aerobic cultivation profile of <i>S. cerevisiae</i> strain W303-1A(a) grown in chemically defined medium with 16 g glucose l ⁻¹ as initial carbon source.	99

Figure 6.6	Real-time RT-PCR transcription profiles of the <i>ADH1</i> , <i>ADH2</i> , <i>ADH4</i> and <i>ADH5</i> genes of strain W303-1A(a) grown in bioreactors with 16 g glucosel ⁻¹ as carbon source.	100
Figure 6.7	Typical aerobic cultivation and real-time RT-PCR transcription profile of <i>S. cerevisiae</i> strain Q1 grown in chemically defined medium with 10 g glucose l ⁻¹ as initial carbon source.	101
Figure 6.8	Typical aerobic cultivation and real-time RT-PCR transcription profile of <i>S. cerevisiae</i> strain Q2 grown in chemically defined medium with 10 g glucose l ⁻¹ as initial carbon source.	102
Figure 6.9	Typical bioreactor profile of <i>S. cerevisiae</i> strain Q3 grown in chemically defined medium with 10 g glucose l ⁻¹	103
Figure 6.10	Typical aerobic cultivation and real-time RT-PCR transcription profile of <i>S. cerevisiae</i> strain Q4 grown in chemically defined medium with 10 g glucose l ⁻¹	104
Figure 6.11	Typical aerobic cultivation profile and <i>ADH5</i> transcription levels of <i>S. cerevisiae</i> strain Q5 grown in chemically defined medium with 10 g glucose l ⁻¹	105
Figure 6.12	Aerobic cultivation profile and <i>ADH</i> transcription profiles of <i>S. cerevisiae</i> parental strain W303-1A(a) grown in chemically defined medium with 10 g ethanol l ⁻¹	107
Figure 6.13	Aerobic cultivation and <i>ADH1</i> transcription profile of <i>S. cerevisiae</i> strain Q1 grown in chemically defined medium with 7 g ethanol l ⁻¹	108
Figure 6.14	Aerobic cultivation and <i>ADH2</i> transcription profile of <i>S. cerevisiae</i> strain Q2 grown in chemically defined medium with 7 g ethanol l ⁻¹	109
Figure 6.15	Aerobic cultivation profile of <i>S. cerevisiae</i> strain Q3 grown in chemically defined medium with 7 g ethanol l ⁻¹	110

List of Tables

Table 3.1	Growth parameters of <i>S. cerevisiae</i> strain W303-1A(a) in shake flasks on different glucose and ethanol concentrations in a complex and a chemically defined medium.	39
Table 5.1	Growth parameters of <i>S. cerevisiae</i> strains SΔ2aTR_E and SΔ2aTR_ADH2 in bioreactor cultures grown on glucose or ethanol.	75
Table 6.1	Growth parameters of <i>S. cerevisiae</i> strains W303-1A(a), Q1, Q2, Q3, Q4 and Q5 in bioreactor batch cultures grown on glucose.	98
Table 6.2	Growth parameters of <i>S. cerevisiae</i> strains W303-1A(a), Q1, Q2, and Q3 grown on ethanol in aerobic bioreactor cultures.	110

1	Introduction.....	Error! Bookmark not defined.
2	Literature review	4
2.1	<i>Classification of the alcohol dehydrogenase enzymes.....</i>	4
2.2	<i>Classical alcohol dehydrogenases ADH I – ADH V.....</i>	5
2.2.1.	Primary and secondary structure.....	6
2.2.1.1	<i>ADH1</i> encoding ADH I.....	6
2.2.1.2	<i>ADH2</i> encoding ADH II.....	7
2.2.1.3	<i>ADH3</i> encoding ADH III	8
2.2.1.4	<i>ADH4</i> encoding ADH IV	9
2.2.1.5	<i>ADH5</i> encoding ADHV	10
2.2.2	Active centres	10
2.2.3	Co-enzymes and metal binding sites	10
2.2.4	Kinetic characteristics.....	11
2.2.5	Localization	13
2.2.6	Function and mechanism of action	13
2.2.7	<i>Regulation</i>	16
2.2.7.1	Regulation of <i>ADH2</i> mediated by ADR1	16
2.2.7.2	Other elements participating in <i>ADH2</i> regulation.....	17
2.2.7.3	The influence of chromatin remodelling on <i>ADH2</i> expression.....	20
2.2.7.4	Regulation of <i>ADH1</i> , <i>ADH3</i> , <i>ADH4</i> and <i>ADH5</i>	22
2.2.8	Evolutionary development and biochemical adaptation	23
2.3	<i>Other alcohol dehydrogenases</i>	24
Figure 2.1.	Classification of yeast Zn-containing MDR alcohol dehydrogenases.....	6
Figure 2.2.	Common mechanism for the yeast alcohol dehydrogenase reaction with two ternary enzyme substrate complexes.....	14
Figure 2.3.	Schematic map of the <i>ADH2</i> gene.....	21

CHAPTER 1

Molecular and physiological aspects of alcohol dehydrogenases in the ethanol metabolism of *Saccharomyces cerevisiae*

When *Saccharomyces cerevisiae* is grown on a fermentable carbon source such as glucose, the fermentative alcohol dehydrogenase ADH I (Ciriacy, 1979), catalyses the regeneration of NAD⁺ from NADH and produces ethanol from acetaldehyde (Denis *et al.*, 1983a). Apparently, it is a constitutive enzyme, although, according to Bennetzen and Hall (1982) and Denis *et al.* (1983a), its biosynthesis can be completely or partly repressed by growth under conditions of extreme aerobiosis or on non-fermentable substrates. When the fermentable carbon source is depleted, a variety of other enzymes are derepressed in order to utilise the previously excreted ethanol via oxidative respiration and gluconeogenesis (Lutstorf & Megnet, 1968; Wills, 1976). To provide both the carbon source and energy for this system, the yeast cell requires an efficient method for oxidising this previously excreted ethanol. ADH II is a catabolite repressible isoenzyme which primarily functions in the cell to oxidise ethanol to acetaldehyde, which can be metabolised via the tricarboxylic acid cycle or act as intermediate product in gluconeogenesis (Beier *et al.*, 1985; Young & Pilgrim, 1985)

ADH III is a mitochondrial isoenzyme that takes part in the respiratory metabolism by forming part of the ethanol acetaldehyde shuttle that is important for shuttling mitochondrial NADH to the cytosol under anaerobic conditions (Bakker *et al.*, 2000). ADH IV expression is undetectable and may be a “cryptic” gene with no function or simply a gene that is not used under laboratory conditions (Williamson & Paquin, 1987). *ADH5* is expressed at a more or less a constant level during the ethanol production phase following a glucose pulse administered to a glucose-limited chemostat culture of *S. cerevisiae* (van den Berg *et al.*, 1998). The possibility that it might have acquired a peculiar function in the *S. cerevisiae* metabolism, distinct from that of the other cytoplasmic ADHs, cannot be overlooked (Ladriere *et al.*, 2000).

A number of deletion mutants unable to express one or more of the *ADH* genes have been studied by various workers over the past 40 years. Investigations of mutants harbouring a single deletion showed that a deletion of the *ADH1* gene tends to result in slower growth on glucose (Kusano *et al.*, 1998) and production of more acetaldehyde (Wills, 1976) and glycerol (Wills &

Phelps, 1975) than the wild type yeast. Single deletion mutants of *ADH2* or *ADH3* showed no discernible mutant phenotype other than the lack of ADH II or ADH III activity (Wills & Phelps, 1975; Young & Pilgrim, 1985). The *adh2* mutant can also grow satisfactorily on ethanol as the sole carbon source (Wills & Phelps, 1975).

Studies on deletion mutants lacking two or more ADHs demonstrated *adh1adh2* deletion mutants to have a decreased growth rate on glucose (Kusano *et al.*, 1998), but still had the ability to produce ethanol (Wills & Phelps, 1975). Smith *et al.* (2004) found that single deletions of *adh3* or a double deletion of *adh3* and *adh5* did not show a discernible difference in ethanol yield on glucose when compared to wild type cells. An investigation conducted by Ciriacy (1975b) on a triple deletion mutant of *adh1adh2adh3* revealed that it grew poorly in a medium containing a high concentration of glucose and not at all anaerobically. Young and Pilgrim (1985) found this mutant useful to demonstrate that *ADH3* codes for an active ADH enzyme. Expression of the *ADH3* gene restored ADH activity in the “adh null” background. Smith *et al.* (2004) showed that the *adh1adh3adh5* triple deletion mutant had lower ethanol production rates on glucose. Drewke *et al.* (1990) was able to demonstrate ethanol production in a quadruple deletion mutant lacking *adh1* to *adh4*. All these deletion mutants provided information on the participation of the alcohol dehydrogenases in the yeast metabolism and gave rise to many still unanswered questions about the role of each enzyme; Answers which could contribute to a coherent picture and important insights into the ethanol metabolism of *S. cerevisiae*.

In this study the role of each alcohol dehydrogenase iso-enzyme was investigated, by determining its expression in the *S. cerevisiae* chromosome on molecular level. The ADH expression profiles were explored in the wild type yeast in carbon-limited chemostat cultures subjected to the pulse addition of carbon substrate at steady state. The expression of each individual iso-enzyme was investigated by batch cultivation of quadruple deletion mutants harbouring only one functional ADH, with glucose or ethanol as carbon sources. Since ADH II is the main enzyme involved in ethanol utilisation and is subject to extreme regulation, the impact it had on the metabolism when relieved from regulation was investigated. This objective was approached by monitoring the expression of *ADH2* in a multicopy vector under control of a constitutive promoter in a background void of ADH II activity.

CHAPTER 2

Literature review

Saccharomyces cerevisiae is, without a doubt, the most important micro-organism commercially exploited by humans. No other micro-organism has been more intimately associated with the progress and well-being of the human race than *Saccharomyces cerevisiae* and its closely related species. Their contribution to human progress has been based very largely on their capacity of conducting ethanolic fermentation of sugary feedstocks. Two major pathways are involved in the energy metabolism of *S. cerevisiae*: glycolysis and aerobic oxidation. Ethanol is one of the key substrates involved in linking these two separate pathways. The enzymes responsible for this last step are the alcohol dehydrogenases (ADHs) (Fowler *et al.*, 1972).

The ADH systems from various organisms have been the subject of thorough analysis as to the molecular structure, the mode of catalysis and, notably in *S. cerevisiae*, their physiological significance. The *S. cerevisiae* system turned out to be exceptionally attractive to study because of its genetic accessibility to both classical and molecular genetic techniques. The easy availability of yeast cells has also promoted the biochemical analysis of yeast ADH in the early days of enzyme biochemistry. Physiologically, the ADH reaction in *S. cerevisiae* and in related species plays a dual and quite critical role in sugar metabolism. Almost all of the sugar is used fermentatively, regardless of the availability of oxygen, and a specific ADH isozyme serves to regenerate the glycolytic NAD^+ by reduction of acetaldehyde to ethanol. After depletion of the fermentable sugar, oxidation of the accumulated ethanol occurs, again by the action of specific ADH isozymes. Thus, in *S. cerevisiae* the ADH reaction links fermentative and oxidative carbon metabolism, allowing the optimal use of the sugar carbon (Ciriacy, 1997).

2.1 Classification of the alcohol dehydrogenase enzymes

ADHs (E.C. 1.1.1.1) are oxidoreductases that catalyse the reversible oxidation of alcohols to aldehydes or ketones, with the concomitant reduction of NAD^+ or NADP^+ . ADHs constitute a large group of enzymes that can be subdivided into at least three distinct

enzyme superfamilies: medium chain (MDR) and short chain (Kallberg *et al.*, 2002) dehydrogenases/reductases, and iron activated alcohol dehydrogenases (Jornvall *et al.*, 1987; Reid & Fewson, 1994). The MDR superfamily is divided into different enzyme families with regard to structural and functional relationships (Jornvall *et al.*, 2001). The family consists of enzymes with a subunit size of approximately 350 amino acid residues, dimeric or tetrameric, with two domains in each subunit: one catalytic and one responsible for binding with the nucleotide NAD⁺ or NADP⁺. Many enzymes of the MDR family have zinc in their active site and have a sequence motif known as the zinc-containing ADH signature: GHEX₂GX₅(G,A)X₂(I,V,A,C,S) (Persson *et al.*, 1993).

Sequencing of the *S. cerevisiae* genome was completed in April 1996 and revealed the existence of approximately 6000 open reading frames (ORFs), including a number of alcohol dehydrogenases or sequences possibly related to these enzymes. The genes coding for classical alcohol dehydrogenases include *ADH1*, *ADH2*, *ADH3*, *ADH4* and *ADH5* (Ciriacy, 1975a; Feldmann *et al.*, 1994; Lutstorf & Megnet, 1968; Walton *et al.*, 1986). Other genes include *SFA1*, *BDH1* (Gonzalez *et al.*, 2000), *BDH2* (YAL061W), *SOR1* putative *SOR2* (YAL246C), *XDH1*, the cinammyl alcohol dehydrogenase *CDH1* (YCR105W) and the recently proposed *ADH6* (YMR218C) and *ADH7* (YCR105W) (Gonzalez *et al.*, 2000; Larroy *et al.*, 2002b; Larroy *et al.*, 2002a; van Iersel *et al.*, 1997; Wehner *et al.*, 1993). The organisation of most of the above genes is outlined in Figure 2.1. Below follows a detailed discussion of the classical alcohol dehydrogenases ADH I – ADH V, with an overview of a select few of the other enzymes.

2.2 Classical alcohol dehydrogenases ADH I – ADH V

In *S. cerevisiae*, there are five genes that encode the alcohol dehydrogenases of the medium chain zinc-containing superfamily involved in ethanol metabolism, namely *ADH1* to *ADH5*. Lutstorf & Megnet (1968) demonstrated multiple forms of alcohol dehydrogenase named ADH I, ADH II, ADH III, and ADH IV by starch gel electrophoresis in a haploid strain of *Saccharomyces cerevisiae*.

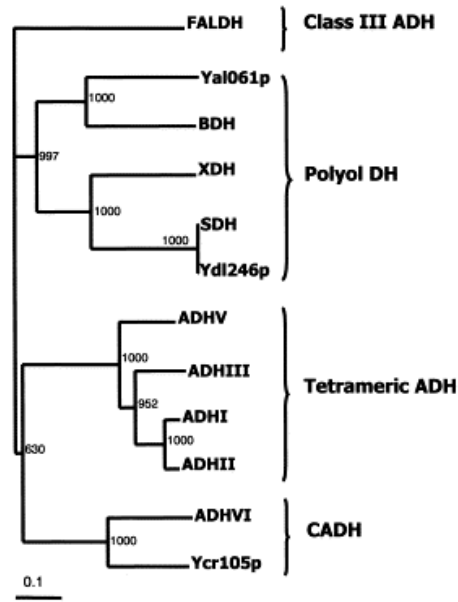


Figure 2.1. Classification of yeast Zn-containing MDR alcohol dehydrogenases. Unrooted phylogenetic tree relating the Zn-containing MDR enzymes from *S. cerevisiae*. Numbers indicate the bootstrap analysis (1000 bootstrap replicates). (Larroy *et al.*, 2003).

2.2.1. Primary and secondary structure

Most of the work on yeast ADH genetics is due to the masterful analysis of Ciriacy. Genetic analysis performed on several haploid *adh* mutants led to the identification of four unlinked genes. The ADH patterns observed are not iso-enzymes coded for by different alleles of one gene, but by different genes altogether: one locus for the fermentative and one for the mitochondrial enzyme with two other loci for the glucose repressible ADHs (Ciriacy, 1975b).

2.2.1.1 *ADHI* encoding ADH I

Yeast alcohol dehydrogenase was the first pyridine nucleotide-dependent dehydrogenase to be crystallised. Physicochemical methods showed that the protein has a molecular weight of 150 kDa and contains 36 free sulphhydryl groups. The active enzyme contains four identical reactive sites and in all probability consists of four similar, if not identical, polypeptide chains (Harris, 1964).

Determination of the primary structure of ADH I in *S. cerevisiae* marked the first case of gene cloning by functional complementation. Many residues are unevenly distributed in the protein and proline and cysteine are over-represented in the N-terminal half, which may be correlated with evolutionary and functional relationships. In the yeast enzyme almost 60% of all valine residues are adjacent to other branched-chain residues (Jornvall, 1977b). Hydrophobic regions are common and long segments without any charged residues are present. The distribution of small residues, proline and hydrophobic residues may be particularly important to the folding of the protein and can be related to probable properties of the tertiary structure, while glycines and repetitive structures may be of special interest in tracing distant evolutionary relationships. A comparison among alcohol dehydrogenases of different species, including *S. cerevisiae* and horse liver, showed extensive variations indicating the type of changes that might be expected between different enzymes and established that alterations of even distantly related dehydrogenase structures may be large (Jornvall, 1977a).

Yeast ADH I seems to be a good model for the study of the stability of complex enzymes. Effects of the environment on structure can easily be tested by measuring the inactivation of reduced and oxidised ADH I. Ca^{2+} stabilises *S. cerevisiae* ADH I by preventing the dissociation of the reduced form of the enzyme and by preventing the unfolding of the oxidised form of the enzyme. It is also reasonable to believe that ADH I binds Mg^{2+} *in vivo* (De Bolle *et al.*, 1997). De Bolle and co workers addressed the question of which residues are actually involved in tetrameric association. They constructed chimeric enzymes of different combinations of ADH I and ADH II sequences. In-depth biochemical analysis led to the conclusion that Cys277 participates in a disulphide bridge that might be important for the thermostability of the native ADH I enzyme (De Bolle *et al.*, 1995).

2.2.1.2 *ADH2* encoding ADH II

By the early 1980s the structural genes coding for both ADH I (*ADH1*) and ADH II (*ADH2*) were identified genetically (Ciriacy, 1975a), cloned (Williamson *et al.*, 1980; Williamson *et al.*, 1981) and their DNA sequences determined (Bennetzen & Hall, 1982; Russell *et al.*, 1983b). High homology was evident at both nucleotide sequence level

(90%) and in amino acid sequence (95%). The amino acid sequences of ADH I and ADH II showed only 22 differences out of 347 residues and no differences in the groups directly involved in catalysis (Ganzhorn *et al.*, 1987).

2.2.1.3 *ADH3* encoding ADH III

It was clear that nuclear DNA codes for the synthesis of the mitochondrial bound alcohol dehydrogenase enzyme, since ADH III is present in respiratory deficient mutants (Wiesenfeld *et al.*, 1975). These researchers also assigned ADH III its tetrameric structure as proposed by Harris (1964) for the cytoplasmic enzyme ADH I. Young & Pilgrim (1985) isolated and sequenced the *ADH3* gene and nucleotide sequence analysis indicated 73% and 74% identity with *ADH1* and *ADH2*, respectively. The amino acid identity between the predicted ADH III polypeptide and ADH I and ADH II was 79% and 80%, respectively, with the only striking difference being the number of lysine residues (24-31). All of the active site, cofactor-binding, and non-catalytic zinc-binding residues identified for *S. cerevisiae* ADH I by Jornvall (1977b) are conserved in both ADH II and ADH III.

The open reading frame encoding ADH III has a highly basic 27 amino acid amino terminal extension relative to ADH I and ADH II. Gene fusion showed that the amino terminus of ADH III contains the information for targeting the protein to, and transporting it into the mitochondrion (van Loon & Young, 1986). All the information required for targeting and import is located in the first 14 amino acids of the leader peptide. It has two functional domains: the amino-proximal half which is required for recognition, uptake by mitochondria and intra mitochondrial sorting and the amino-distal half that is required for proteolytic processing (Pilgrim & Young, 1987). Import of ADH III does not require cleavage of the presequence. Mutational analysis indicated that a broad spectrum of alterations, both point mutations and deletions, affect both mitochondrial import and precursor processing. No entirely redundant elements have been observed, since all mutations have led to an altered phenotype at one or more levels. It is proposed that the amino acid sequence and secondary structure(s) of the leader sequence, as well as the adjacent sequences in the mature amino terminus of ADH III, all

contribute information for normal mitochondrial binding, importing and processing (Mooney *et al.*, 1990).

2.2.1.4 *ADH4* encoding ADH IV

ADH4 is the most distal marker on the left arm of chromosome VII and both restriction- and genetic analysis of the chromosome copy of *ADH4* indicate that it is situated near a telomere (Walton *et al.*, 1986). Paquin & Williamson (1986) described *ADH4* as a new isozyme of, or regulating the expression of an alcohol dehydrogenase. Sequencing analysis of *ADH4* revealed a long open reading frame that is not homologous to other yeast ADHs and is only distantly related to other characterised eukaryotic ADH enzymes (Paquin & Williamson, 1986). While the homology between ADH I and ADH II is very high, the sequence of ADH IV is completely different. Analysis of the sequence of the hypothetical ADH IV protein shows that it does not contain structurally or functionally important amino acid residues that are conserved between yeast ADH I and horse liver ADH. The hypothetical *ADH4* gene product does, however, show a strong homology to the iron-activated ADH from the bacterium *Zymomonas mobilis*. This homology suggests that *ADH4* does encode an alcohol dehydrogenase, but one distinct from any others that have been described in eukaryotes (Williamson & Paquin, 1987).

The presence of a TATAA sequence upstream of the transcription start and the moderate codon bias suggest that it may be a functional yeast gene. Its location near the end of chromosome VII is interesting in view of the fact that many of the genes located at the ends of chromosomes in *S. cerevisiae* encode enzymes involved in fermentation and glycolysis (Mortimer & Schild, 1985). Unlike ADH I, ADH II and ADH III, which are thought to function as tetramers (Leskovac *et al.*, 2002), ADH IV is a dimeric protein that normally occurs in low concentrations in laboratory strains. This protein was purified by over-expressing the *ADH4* gene on a multicopy plasmid (Drewke & Ciriacy, 1988). Contrary to Williamson and Paquin's (1987) suggestion, ADH IV is activated by zinc ions, like the other yeast alcohol dehydrogenase isozymes, and not by ferrous ions as is the case with the structurally similar alcohol dehydrogenase from *Zymomonas mobilis* (Drewke & Ciriacy, 1988).

2.2.1.5 *ADH5* encoding ADHV

ADH5 was first identified through sequencing of chromosome II (Feldmann *et al.*, 1994) and shares 76%, 77%, and 70% sequence identity with *ADH1*, *ADH2* and *ADH3* respectively (Feldmann *et al.*, 1994; Ladriere *et al.*, 2000).

2.2.2 Active centres

Relationships known from tertiary structures of dehydrogenases show that the constituent monomers are separated into two domains, namely a 'coenzyme-binding' domain and a 'catalytic' domain. The three dimensional structure of the active site of the *S. cerevisiae* enzyme reveals the presence of a hydrogen bonded proton relay system: His-51...NAD⁺...Thr-48...H₂O(RCH₂OH)...Zn⁺⁺, stretching from His-51 on the surface of the enzyme to the active site zinc atom in the substrate binding site (Leskovac *et al.*, 1998). On the basis that each individual chain contains one reactive sulphhydryl group and, by binding one atom of zinc and one mole of NAD⁺/NADP⁺, it is capable of forming an independent "active centre" within the quaternary structure of the active tetramer (Harris, 1964). ADH I has a methionine residue at position 294, whereas isozyme ADH II and ADH III have leucine. Apart from these differences the active sites of the *S. cerevisiae* enzymes are the same (Ganzhorn *et al.*, 1987). It has been proposed that the shape or the accessibility of the catalytic pocket appears to be different in the yeast and horse liver enzymes and that it is possible to alter the specificity of the enzyme without sacrificing catalytic power (Green *et al.*, 1993). Such approaches are limited by the lack of data on the tertiary and quaternary structure of *S. cerevisiae* ADH. Crystallisations of ADH I have repeatedly been reported, but the crystals are seemingly not very useful in X-ray diffraction studies (Ramaswamy *et al.*, 1994; Wills *et al.*, 1982).

2.2.3 Co-enzymes and metal binding sites

Early studies showed the active enzyme, isolated as a pure crystalline protein, binds four moles NAD⁺ and four atoms of zinc. Zinc atoms are essential for maintaining the quaternary structure of the enzyme and both zinc and the coenzyme are bound at, or near to, each of the four reactive cysteines (Harris, 1964). Zinc is one of the principal trace elements in biology, with structural or enzymatic roles in hundreds of proteins (Vallee &

Falchuk, 1993). *S. cerevisiae* ADH I, ADH II and ADH III contain one catalytic zinc atom and a second zinc atom which plays a prominent conformational role, probably through stabilisation of the tertiary structure. The second zinc is located at the periphery of the molecule and is bound by four conserved Cys residues clustered around positions 97-111. The external localisation of this structural zinc affects local conformations of the enzyme, but could also easily affect such an exposed zinc atom, for example by its chelation (Magonet *et al.*, 1992). The different coenzyme-binding domains have extensive similarities, are composed of two ‘mononucleotide-binding units’ and resemble the tertiary structures of kinases and some other proteins (Rossman *et al.*, 1975)

The positive charge on the nicotinamide ring is crucial for the enhanced binding of alcohol to the enzyme; insertion of the positive charge in this hydrophobic environment facilitates formation of the negatively charged alcoholate ion. The important role of the zinc atom in alcohol oxidation is to stabilise the alcoholate ion for the hydride transfer step in the reverse direction. Zinc functions as an electron attractor, which gives rise to an increased electrophilic character of the aldehyde, consequently facilitating the transfer of a hydride ion to the aldehyde. Thus the proposed mechanism is essentially electrophilic catalysis mediated by the active site zinc atom (Leskovac *et al.*, 2002).

2.2.4 Kinetic characteristics

The first biochemical data on ADH I and ADH II showed that the kinetic properties of both enzymes favour alcohol production. Under the conditions of high ethanol concentration and the efficient removal of acetaldehyde, both enzymes could function in the oxidation of ethanol (Heick *et al.*, 1969). Wills (1976) later stated that ADH I is normally constitutive under laboratory conditions, has a high K_m value (17 000 – 20 000 $\mu\text{mol l}^{-1}$) for ethanol (Thomson *et al.*, 2005) and therefore seems chiefly responsible for the production of ethanol during anaerobic growth. If levels of ethanol inside the cell are low, ADH II will produce acetaldehyde and NADH at a faster rate than ADH I (Wills *et al.*, 1982). Kinetic investigation of commercially available ADH showed it capable of oxidising all primary alcohols with chain lengths of between two and ten carbon atoms (Schopp & Aurich, 1976) and the activity of ADH I decreases as the chain length of the

primary alcohols increases (Ganzhorn *et al.*, 1987). Substrate specificity of ADH I is restricted to primary unbranched aliphatic alcohols and any branching diminishes the activity of the enzyme and lowers its efficiency (Leskovac *et al.*, 2002). Cyclic alcohols (benzyl alcohol, cyclohexanol) are not oxidised in detectable amounts (Drewke & Ciriacy, 1988) and thiol compounds exert no effect on this isozyme (Cheng & Lek, 1992). It was recently reported that over-expressed ADH I reduced formaldehyde (FA) to methanol *in vivo* (Grey *et al.*, 1996) and was able to provide a considerable degree of protection against cadmium (Yu *et al.*, 1991).

ADH II has a low K_m for ethanol (600 – 800 $\mu\text{mol l}^{-1}$) and is found only in aerobically grown yeast cells (Thomson *et al.*, 2005; Wills, 1976). These findings coincide with its role as major ethanol oxidiser. For all alcohols, normalised reaction rates with ADH II were about three-fold faster than with ADH I (Leskovac *et al.*, 2002). Some contradiction is found in the literature regarding the kinetic characteristics of ADH I and ADH II. Some reports state remarkably similar normalised reaction activities for both ADH I and ADH II under conditions of low substrate concentration, even though the kinetic characteristics of the enzymes are very different (Dickinson & Dack, 2001).

The mitochondrial enzyme (ADH III) showed great affinity for alcohols with double bonds conjugated to the alcohol function (Wiesenfeld *et al.*, 1975). The methionine (ADH I) or leucine (ADH II and ADH III) at position 294 by itself has no interaction with ethanol or propanol (Ganzhorn *et al.*, 1987).

ADH IV has different substrate specificity and pH profiles when compared to other alcohol dehydrogenase isozymes (Drewke & Ciriacy, 1988). It has been shown that alcohol dehydrogenases I, II, and III are not strongly substrate specific and that aliphatic alcohols of up to six carbons can be oxidised (Ganzhorn *et al.*, 1987). ADH IV is seemingly more specific, with isomers of aliphatic alcohols as well as secondary alcohols and glycerol not used at all. Although ADH II and ADH IV differ remarkably in almost all the kinetic parameters (Lutstorf & Megnet, 1968), the latter resembles ADH I in its kinetic constants. The purified enzyme also has a very low specific activity. Its substrate spectrum is even narrower than those of the other isozymes: only ethanol and *n*-propanol are oxidised by ADH IV. No data on the kinetic characteristics of ADH V is presently available.

2.2.5 Localisation

Eukaryotic cells are organised into a complex network of membranes and compartments, which are specialised for various biological functions. A comprehensive knowledge of the location of proteins within these cellular micro-environments is critical for understanding their functions and interactions. In the late 1960s the presence of at least three NAD-dependent alcohol dehydrogenases in baker's yeast was known (Heick *et al.*, 1969). Two of these enzymes were located in the cytosol (ADH I and ADH II) and fractionation experiments placed ADH III in the mitochondrial matrix (van Loon & Young, 1986).

Drewke & Ciriacy (1988) suggested that it is unlikely that ADH IV is proteolytically processed as has been demonstrated for ADH III (Pilgrim & Young, 1987) and that ADH IV is therefore a cytoplasmic enzyme. Although they state functional and biochemical evidence for this, no published data to date report on these facts. Furthermore Overkamp *et al.* (2000) and Bakker *et al.* (2000) obtained evidence, when studying the mechanisms of oxidation of cytosolic NADH by the mitochondrion, that *ADH3* was not the sole mitochondrial ADH. At that time ADH IV and Ydl114W were the only probable candidates with no assigned function or localisation. Huh and co-workers (2003) described the construction and analysis of a collection of yeast strains expressing full-length, chromosomally tagged green fluorescent protein fusion proteins. The use of the GFP tag and co-localisation with RFP-tagged reference proteins allowed them to resolve many related subcellular compartments with confidence, especially in the case of proteins for which little functional data exists. They established that ADH V is located in the cytoplasm and not only ADH III, but also ADH IV are mitochondrial enzymes. If this is the case, an explanation is yet to be provided for the absence of the amino terminal leader peptide sequence in ADH IV.

2.2.6 Function and mechanism of action

Basically ADH I, ADH III, ADH IV, ADH V reduce acetaldehyde to ethanol during glucose fermentation, while ADH II catalyses the reverse reaction of oxidising ethanol to acetaldehyde (Bennetzen & Hall, 1982; Drewke & Ciriacy, 1988; Russell *et al.*, 1983b; Smith *et al.*, 2004; Young & Pilgrim, 1985). The role of ADH I in the cytosol was

described in the 1960s as the major ethanol producer (Heick et al., 1969). During the mid 1970s it was generally agreed that the characterisation of the ADH iso-enzymes should be subject to different responses to glucose repression, heat stability and association with yeast mitochondria. Yet, functions were still only assigned to ADH I and ADH III, with a reference to the other multiple forms, as participants in an oxidative pathway when ethanol is utilised by yeast cells as carbon source (Ciriacy, 1975b).

The main reaction catalysed by ADH is, in principle, very simple: An alcohol group is oxidised by the removal of a proton from the hydroxyl group and by the transfer of a hydride ion from the adjacent carbon atom to NAD^+ (Eklund & Branden, 1987). Schopp & Aurich (1976) performed kinetic studies on alcohol dehydrogenase prepared from dried bakers yeast and found that the enzyme oxidised primary alcohols according to a rapid equilibrium random order mechanism (Figure 2.2).

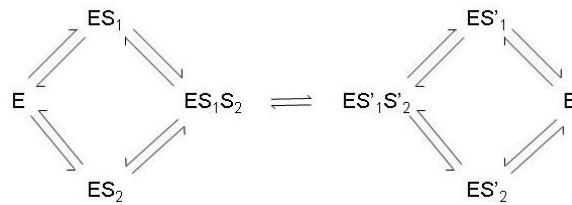


Figure 2.2. Common mechanism for the yeast alcohol dehydrogenase reaction with two ternary enzyme substrate complexes. E = ADH, $S_1 = \text{NAD}^+$, $S_2 = \text{Ethanol}$, $S'_1 = \text{NADH}$, $S'_2 = \text{aldehyde}$ (Schopp & Aurich, 1976)

According to the Michaelis constants, ADH I seems to be chiefly responsible for the production of ethanol from acetaldehyde in cells grown anaerobically, whereas ADH II primarily functions to convert ethanol accumulated during aerobic growth to acetaldehyde, with the concomitant reduction of NAD^+ . ADH I can also accomplish this task, though presumably less efficiently. These two enzymes contribute to the economy of the cell by stabilising the NAD^+ - NADH ratio. The possibility of inter-substitution therefore seems to exist for these isozymes; for instance, cells lacking ADH II activity

can grow on ethanol as carbon source under aerobic conditions (Wills, 1976; Wills *et al.*, 1982).

Wenger and Bernofsky (1971) reported that mitochondrial ADH III was responsible in part for the coupled respiration of yeast mitochondria with ethanol as a substrate. Disruption mutants of *ADH3* showed no discernible mutant phenotype other than the lack of ADH III activity (Young & Pilgrim, 1985). Null mutations in *ADH3* did not confer a phenotype under aerobic conditions (Young & Pilgrim, 1985), but under anaerobic conditions these mutant cells grow noticeably slower than wild type cells (Bakker *et al.*, 2000). Bakker *et al.* (2000) also demonstrated that ADH III is involved in the shuttling of mitochondrial NADH to the cytosol, where it can be reoxidized by the external NADH dehydrogenases. Their results support the hypothesis that ADH III forms part of the ethanol-acetaldehyde shuttle that is necessary for the reoxidation of mitochondrial NADH under anaerobic conditions.

Williamson & Paquin (1987) were unable to detect *ADH4* transcripts on Northern blots of laboratory strains grown on glucose or ethanol. Activity has not been observed except upon insertion of a Ty transposon at *ADH4* or amplification of *ADH4*. It may be a “cryptic” gene with no function or simply a gene that is not used under laboratory conditions. Genetic and physiological analysis showed that disruption of *ADH4* does not influence the viability of the yeast cell, nor is the enzyme responsible for the decrease in ethanol formation in *adh1-adh4* quadruple deletion mutants (Drewke *et al.*, 1990). It has recently been suggested that *ADH4* encodes the major cytosolic alcohol dehydrogenase in the two brewing strains 2DGR19 and NCYC1245. Elevated *ADH4* mRNA levels could be detected and high ethanol production took place in tall tube wort fermenters (Mizuno *et al.*, 2006).

Drewke *et al.* (1990) found that a deletion lacking *adh1* to *adh4* was still able to produce ethanol when grown on glucose as a carbon source. It is reasonable to believe that ADH V might be the enzyme capable of producing ethanol from acetaldehyde.

A search was undertaken to discover the genes and enzymes used by *S. cerevisiae* in the catabolism of leucine to isoamyl alcohol (Dickinson *et al.*, 1997), valine to isobutanol (Dickinson *et al.*, 1998) and isoleucine to active amyl alcohol (Dickinson *et*

al., 2000). As long as the yeast had one functional enzyme out of ADH I-ADH V or SFA1, it was viable and any one of these six enzymes was sufficient for the final stage of amino acid catabolism, namely the conversion of an aldehyde to a long chain or a complex alcohol (Dickinson *et al.*, 2003).

2.2.7 Regulation

2.2.7.1 Regulation of *ADH2* mediated by *ADR1*

The earliest study of regulation of the alcohol dehydrogenase genes was documented by Ciriacy (1975b). Growth studies performed on several different deletion mutants showed that mutation in linked genes of *ADH2* provided the first defining proof of a controlling site involved in carbon catabolite repression in a eukaryote (Ciriacy, 1976). The first gene associated with this function was *ADR1*, a positive regulatory gene specifically activating the expression of the structural gene *ADH2* under derepressed conditions (Ciriacy, 1979). *ADR1* codes for the *trans* acting protein (ADR1) containing two zinc fingers and a region amino terminal to the fingers, which together are essential for DNA binding (Blumberg *et al.*, 1987). Initiation of transcription from most known eukaryotic promoters is positively regulated by the binding of specific transcriptional activator proteins to the enhancer region of upstream activation sequence (UAS) of a promoter (Giniger *et al.*, 1985), (Hope & Struhl, 1985). Two unusual features upstream of the *ADH2* promoter, a 22 bp perfect dyad sequence and a (dA)₂₀ tract were identified (Russell *et al.*, 1983a). The *ADH2* promoter may normally be in an inactive conformation in the yeast chromosome and derepression requires positive activation by ADR1 which is mediated through the 22 bp perfect dyad (UAS1) (Beier *et al.*, 1985). ADR1 binds as a monomer to its binding site and two monomers bind noncooperatively via Cys₂His₂ class zinc finger domains to fill the halves of the 22 bp palindromic UAS1. The ADR1 monomers are able to form one of two complexes: complex I corresponds to the binding of one molecule to the *cis* acting element UAS1 and complex II corresponds to the binding of two molecules to UAS1 (Thukral *et al.*, 1991).

A GC rich, 20 bp sequence (UAS2) upstream of UAS1 was identified and proposed to act synergistically as a binding site for a protein that interacts with ADR1 to activate the expression of *ADH2* (Yu *et al.*, 1989). *In vitro* binding data to this *cis* acting

element suggest that ADR1 binds with low affinity to UAS2, most likely at the AGGAGA sequence. Other interpretations, such as an indirect effect or a direct protein-protein interaction are also possible but seem less likely (Donoviel *et al.*, 1995).

Synthesis of the ADR1 protein is 10 to 16-fold greater during growth on ethanol than during growth on glucose. This derepression in *ADR1* protein translation was found to occur within 40 to 60 min of glucose depletion. Glucose, therefore, represses *ADH2* expression by greatly decreasing the rate of ADR1 protein synthesis. ADR1 turns over with a half-life of about 3 h to 4 h during growth on glucose. This short half-life suggests a mechanism for controlling cellular levels of ADR1 and for removing altered or damaged forms of *ADR1* which may potentially decrease the efficiency of *ADH2* regulation (Vallari *et al.*, 1992). Cook & Denis (1993) established that a 510 bp untranslated leader sequence of the *ADR1* mRNA plays a role in the increased rate of *ADR1* mRNA degradation under glucose growth conditions as compared to growth on ethanol. Other positive factors influencing *ADH2* expression were proposed since excess ADR1 could not overcome a three to four-fold inhibition in *ADH2* transcription caused by multiple promoters on a multicopy vector (Irani *et al.*, 1987). Alteration of cellular physiology in numerous ways can lead to constitutive *ADH2* expression when the requirement for the major activator, ADR1 is satisfied (Voronkova *et al.*, 2006).

2.2.7.2 Other elements participating in *ADH2* regulation

Genetic and biochemical analysis showed that expression of the ADH II structural gene is under the control of at least 24 other unlinked genetic elements or proteins. These include *ADR3*, *CCR1*, *ADR4*, *ADR6*, *CRE1*, *CRE2*, *CCR4*, *NOT1*, *NOT2*, *NOT3*, *NOT4*, *SRB9*, *SRB10*, *SRB11*, *cAPK*, *SCH9*, *ADR7*, *ADR8*, *ADR9*, *SAF1*, *SAF2*, *SAF3*, *REG1* and *BCY1* most of which influence *ADH2* expression mainly indirectly. Several of the genes appear likely to do so through control of ADR1, whether by mRNA translation, phosphorylation or protein interaction.

Cis dominance and tight linkage to the ADH II structural gene demonstrates that *ADR3* is a *cis*-acting regulatory locus required for glucose regulation of the *ADH2* gene (Beier & Young, 1982). *CCR1* codes for a constitutive protein that acts in concert with or through ADR1, probably post translational (Denis & Gallo, 1986). The *CCR1*

gene is allelic to *SNF1* coding for a protein kinase and it is, therefore, possible that a phosphorylation dependent step catalysed by CCR1 is required for full ADR1 function (Denis, 1987). *ADR4* specifies a negative regulatory factor because of its complete recessiveness. It is not yet established whether *ADR4* acts specifically on the *ADR1* or *ADH2* gene or whether its gene product constitutes a regulatory element with a pleiotropic action spectrum (Ciriacy, 1979; Denis *et al.*, 1981). *ADR6* appears to require an *ADH2* sequence located downstream to or including the TATAA box and may act subsequent to ADR1 but prior to translation of *ADH2* mRNA (Taguchi & Young, 1987). The protein is predominantly nuclear in location, consistent with its role as an activator of *ADH2* transcription and the gene contains an open reading frame encoding a protein that has a potential metal binding finger domain near its carboxy terminus (O'Hara *et al.*, 1988).

CRE1, *CRE2*, and *CCR4* affect transcription independently of the upstream regulatory sequences. The allelism of *CRE2* to *SPT6* suggested that the *CRE* genes and *CCR4* are not specific to the regulation of carbon metabolism and function as general effectors of transcriptional processes (Denis, 1984; Denis & Malvar, 1990). *CCR4* contains two distinct glutamine and leucine rich regions that presumably play an important role in protein interactions that mediate the regulatory role of ADH II (Malvar *et al.*, 1992). It has also been implicated in the maintenance of chromatin structure (Denis & Malvar, 1990) The *NOT* genes encode a group of factors involved in repressing the transcription of *HIS3* from a non-canonical TATA (Collart & Struhl, 1994). Mass spectrometry and two hybrid analysis identified NOT1-NOT5 as proteins associated with the CCR4 complex, implying that it should also be positively involved in gene transcription. Mutations in the *NOT* genes (except *NOT5*) caused a reduction of *ADH2* gene expression under derepressed conditions (Liu *et al.*, 1998). The *SRB9*, *SRB10*, and *SRB11* genes code for proteins which co-immunoprecipitate the CCR4 and NOT proteins, and defects in these SRB proteins affect expression at the *ADH2* locus in a manner similar to that observed for defects in CCR4 complex components (Liu *et al.*, 2001).

Although cAPK inactivates *ADH2* expression by inhibiting ADR1 function through phosphorylation, either directly or of another protein required for ADR1 activity, it does not appear responsible for the glucose to ethanol transition in controlling *ADH2*

expression (Cherry *et al.*, 1989; Denis *et al.*, 1992). *SCH9* appears to activate *ADH2* expression by turning off *ADR1* function independently of *cAPK*. *SCH9* derepression does not operate exclusively through *ADR1*. Since *SCH9* does not act through *UAS1*, it may control factors that act through other activation sequences or through factors controlling the general transcriptional machinery. The multiple protein kinases (*cAPK*, *CCR1*, *SCH9*) involved in carbon catabolite repression in *S. cerevisiae* apparently do not possess a single phosphorylation cascade as in the case of protein kinases regulating several mammalian systems (Denis & Audino, 1991). *ADR7*, *ADR8*, and *ADR9* are *trans*-acting elements unlinked to *ADR1* that affect *ADH2* expression under both repressing and derepressing growth conditions. The gene products allow *ADH2* expression to efficiently derepress in the absence of *ADR1* as do *CRE1* and *CRE2* (Karnitz *et al.*, 1992).

The *SAF* gene products (*SAF1*, *SAF2*, *SAF3*) are required for maintaining high levels of *ADR1* RNA under glucose growth conditions, but have little effect under ethanol conditions. Whereas the physiological role of the *SAF* genes is unclear, two models have been suggested: the *SAF* genes may be required for basal transcription of *ADR1* during growth on glucose. This model is consistent with an *ADR1* promoter that lacks upstream activation sequences or with *SAF* products acting in a *UAS*-independent fashion. Alternatively, the *SAF* gene products may act through *UAS* elements to elevate *ADR1* mRNA above a minimal glucose-repressed level. The *SAF* genes appear to be expressed with both ethanol and glucose as carbon sources and no direct evidence exists that they influence genes other than *ADR1* and *ADH2* (Cook & Denis, 1993).

Glucose can repress *ADH2* expression by mechanisms that act independently of phosphorylation. One mechanism that may account for some of this repression involves the inhibition of *ADR1* expression (Dombek *et al.*, 1993). The *REG1* gene encodes a nuclearly localised protein which expression is not regulated by glucose availability. *REG1* is the first negative genetic element identified that affects *ADH2* expression through an *ADR1* dependent pathway via an additional step in transcriptional activation that does not involve the phosphorylation-dephosphorylation of *ADR1* (Niederacher & Entian, 1991). *BCY1* encodes the regulatory subunit of *cAPK*, and influenced *ADH2* expression in an *ADR1*-dependent manner (Donoviel *et al.*, 1995).

CAT8 has an essential role during the adaptation of yeast on ethanol by controlling the induction of many genes in response to glucose depletion (Haurie *et al.*, 2001). A functional carbon source responsive element (CSRE) variant within UAS2 specifically interacts in vitro with the CAT8 activator and contributes to transcriptional derepression of *ADH2* synergistically with the ADR1 dependent UAS1 element (Walther & Schuller, 2001).

In contrast to the situation with most genes subject to catabolite repression, there is no evidence for a *MIG1* binding site in the *ADH2* promoter (Denis & Audino, 1991).

2.2.7.3 The influence of chromatin remodelling on *ADH2* expression

Yeast have to respond very rapidly to environmental changes, therefore their chromatin, even when transcriptionally inactive, is maintained in a state of "transcriptional readiness". The ADH system serves as an ideal model to detect localised differences in chromatin structure which can reflect changes in transcriptional activity. The possibility exist that a decrease in transcriptional activity changes the structure of chromatin in the whole *ADH2* region for instance, by a change of nucleosome spacing (Sledziewski & Young, 1982). Under repressing conditions UAS1 and UAS2 are a nucleosome free region, the TATA box and RNA initiation sequence (RIS) is protected by nucleosomes -1 and +1, and a 20 bp poly (dA-dT) tract is included in the DNA wrapped around nucleosome -1 (Figure 2.3). Nucleosome mapping data show that glucose exerts its inhibitory effect by keeping the relevant promoter sequences (TATA box and RIS) in a nucleosomal configuration, thus precluding their engagement with the transcription machinery. Nucleosome destabilisation represents a prerequisite for transcription at the *ADH2* promoter, since the kinetics of nucleosome disruption do not correlate with the kinetics of mRNA accumulation. *ADH2* transcription is not influenced while chromatin rearrangement is undetectable, suggesting that the two events are independent (Verdone *et al.*, 1997).

Chromatin remodelling that occurs at the *S. cerevisiae ADH2* promoter upon derepression is characterised by two distinct structural alterations. The first, early remodelling step occurs in the absence of transcription and consists of a localised

modification induced by the ADR1 DNA binding domain at the level of the nucleosome-1. The second type of structural alteration, induced when the activation domain is also present, is more stable and involves both nucleosomes -1 and +1. The existence of two steps in the process of chromatin remodelling suggests that at least two

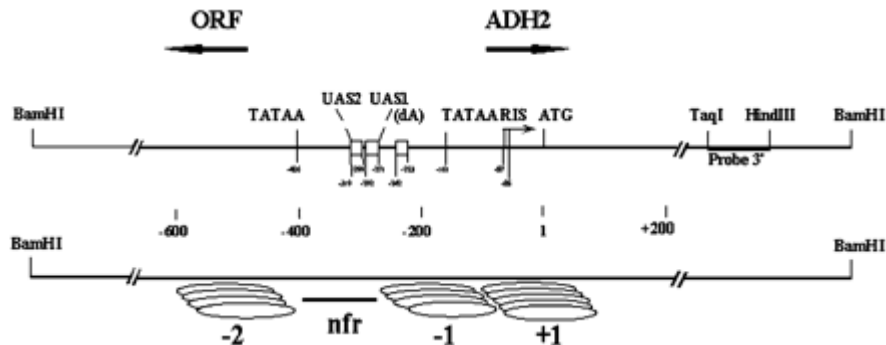


Figure 2.3. Schematic map of the *ADH2* gene. The positions of the relevant elements are given relative to the ATG (A is at position +1). *RIS*, RNA initiation site; *ORF*, open reading frame; *nfr*, nucleosome-free region. Each group of ovals represents a family of multiple overlapping nucleosomes, the borders of which were mapped at high resolution (Verdone *et al.*, 1997).

functions can be attributed to ADR1. First, the protein reconfigures nucleosomes in the immediate vicinity of its binding site, allowing the basal promoter elements to assume the most appropriate structure for the subsequent activation. Secondly, the protein recruits the transcription machinery through its activation domain, allowing mRNA accumulation. This DNA binding factor, therefore, plays a role in overcoming nucleosome exerted repression as a prerequisite for transcriptional activation and not merely as a consequence of RNA polymerase II recruitment (Di Mauro *et al.*, 2000).

Three possible states of the *ADH2* promoter have been proposed. In the absence of ADR1, the *ADH2* promoter remains structurally and functionally inactive when the cells are shifted to derepressing conditions. In the presence of the ADR1 DNA binding domain alone, a localised modification on the -1 nucleosome in the vicinity of the UAS1 sequence, occurs: the promoter is structurally derepressed but functionally inactive. When the ADR1 activation domain is also present, a distinct structural

alteration occurs at the transcribing *ADH2* locus: the promoter is fully derepressed and functionally active. The three possible states of the promoter, due to the absence or the presence of different ADR1 portions, can be considered as an ordered sequence of events occurring at the *ADH2* locus during derepression (Di Mauro *et al.*, 2000).

Verdone and co-workers (2002) analysed the *in vivo* chromatin structure and the kinetics of transcriptional activation of the *S. cerevisiae ADH2* promoter as a function of genetically modified histone acetylation levels. In an exponentially growing wild-type strain in the presence of glucose, equilibrium existed among the various histone acetyltransferases and deacetylases. When this equilibrium was altered by abolishing the function of either or both deacetylases RPD3 and HDA1, an imbalance was created, leading to hyperacetylation of specific modifications of the structure of both nucleosomes -1 and +1. By genetically altering the steady-state pattern of histone acetylation at the repressed *ADH2* promoter, the structure of the TATA box containing nucleosome is destabilised, the promoter becomes accessible to ADR1, and when the cells are shifted to derepressing conditions, the kinetics of mRNA accumulation is faster. Histone deacetylation/acetylation is, therefore, directly involved in altering the chromatin structure at the *ADH2* promoter, influencing the binding of the major transcriptional activator with a concomitant effect on the kinetics of mRNA accumulation.

2.2.7.4 Regulation of *ADH1*, *ADH3*, *ADH4* and *ADH5*

Initially it was stated that regulatory genes affecting ADH II mRNA expression appear to have no effect on *ADH1* expression (Denis *et al.*, 1983b). It was later established that deletion of the genes *CCR4* and *CAF1* not only influenced the repression of *ADH2*, but brought about a phenotype with enhanced expression of *ADH1* (Liu *et al.*, 2001).

A conserved sequence UAS_{RPG} present in various glycolytic genes and ribosomal protein genes also exist in the upstream region of *ADH1* and appears essential for efficient transcription (Santangelo & Tornow, 1990). However, this seems to be true only for cells in the exponential growth phase, since the efficiency of the promoter is virtually indistinguishable with or without the UAS_{RPG} during the ethanol consumption growth phase. In glucose grown cells, the region between -700 bp and -412 bp containing the UAS_{RPG} is needed for the *ADH1* promoter activity to start during the early

exponential growth phase. The promoter region -750 bp upstream of the *ADH1* promoter features the presence of an ADR1 binding site. It is therefore tempting to speculate that the down regulation of the long *ADH1* promoter is indeed due to activation of the upstream promoter by ADR1. Thus, it is possible that the presence of ethanol in the culture medium rather than the absence of glucose decreased the activity of the long *ADH1* promoter in glucose grown cells (Ruohonen *et al.*, 1995).

Whereas the complex regulation of *ADH2* has made it an attractive model system for the genetic dissection of its transcriptional control, the regulation of the remaining three enzymes has not received as much attention. Scant data is available regarding up or down-regulation of these genes, but no evidence exists regarding genetic elements constituting this action.

Similar to the behaviour of enzymes of the tricarboxylic acid cycle (Heick *et al.*, 1969), *ADH3* is repressed by glucose (although repression is not as severe as that of *ADH2*) (Ciriacy, 1975a; Young & Pilgrim, 1985) and appears again after glucose is depleted from the medium. *ADH4* expression is up-regulated by lithium, a compound that is toxic to yeast cells grown on galactose, but is down-regulated by DMSO (Bro *et al.*, 2003; Zhang *et al.*, 2003). Under conditions where ADH I is non-functional, spontaneous chromosomal amplification of *ADH4* was able to rescue the mutant phenotype (Dorsey *et al.*, 1992; Dorsey *et al.*, 1993). *ADH5* expression is unaffected by DMSO (Zhang *et al.*, 2003) and its transcription is significantly increased in a *S. cerevisiae* mutant strain able to grow anaerobically on xylose, a carbon source not normally utilised by yeast in the absence of oxygen (Sonderegger *et al.*, 2004).

2.2.8 Evolutionary development and biochemical adaptation

Many researchers have ventured into research on the origin of the alcohol dehydrogenase isozymes. In the late 1960s, when multiple forms were first reported, Lutstorf & Megnet (1968) entertained the idea that ADH III might be a hybrid originating from the other isozymes. From another perspective, Young and Pilgrim (1985) proposed that the cytosolic isozymes ADH I and ADH II evolved from an ancestral gene for a mitochondrial ADH protein by mutations that resulted in loss of the targeting sequence for the mitochondrion. The similarity between isozymes I and II confirms that the

corresponding structural genes *ADH1* and *ADH2* are derived from an ancestral gene duplication. The functional properties of the isozymes would have been of value shortly after the appearance of free oxygen in the atmosphere. It is, therefore, surprising that the isozymes are so similar and it is highly unlikely that the duplication could have arisen that long ago (Wills & Jornvall, 1979).

The finding that ADH IV has a very low specific activity and might not function for either fermentation nor ethanol utilisation, led Drewke and Ciriacy's (1988) to believe that it might represent a protein that has undergone evolutionary changes as a consequence of not being essential for growth of the yeast cells. Ladriere *et al.* (2000) suggested it not unlikely that *ADH1* and *ADH5* are derived from a direct common ancestor. The rate of sequence divergence has thus been higher for *ADH5* than for any of the other ADHs and, as a general rule, *ADH5* is more distantly related to any other yeast ADH than the other *S. cerevisiae* ADHs. Thomson and co-workers (Thomson *et al.*, 2005) succeeded in resurrecting the last common ancestor of ADH I and ADH II called ADH_A. Kinetic behaviour suggested that the ancestor was optimised to make instead of consume ethanol. This is consistent with the hypothesis that before the *ADH1-ADH2* duplication, yeast did not accumulate ethanol for later consumption but rather used ADH_A to recycle NADH generated in the glycolytic pathway. Silent nucleotide dating suggests that the *ADH1-ADH2* duplication occurred near the time of duplication of several other proteins involved in the accumulation of ethanol, possibly in the Cretaceous age when fleshy fruits arose.

2.3 Other alcohol dehydrogenases

Over expression of the 1152 bp ORF *SFA1* (YDL168W) confers hyper-resistance of yeast to formaldehyde. Interestingly, this protein has a higher homology to several ADHs of human and rodents than to the four known ADHs of *S. cerevisiae* (Fernandez *et al.*, 1995; Wehner *et al.*, 1993). An ADH exhibiting glutathione (GSH) dependent FA oxidation characterised in *E. coli* (Gutheil *et al.*, 1992) suggested the preliminary classification of the *SFA1*-encoded enzyme activity as an ADH of class III. *SFA1* forms homodimers of 41 kDa in accordance with other ADHs of class III and GSH dependent formaldehyde dehydrogenases that form homodimers of this size. Its true substrate is S-

hydroxymethylglutathione and induction is possible by ethanol (Wehner *et al.*, 1993). Yeasts exposed to hazardous environments with a potentially higher content of formaldehyde would benefit from an enzyme catalytically more efficient in such situations. With kinetics to support this function, SFA1 may, therefore, be involved in formaldehyde detoxification (Fernandez *et al.*, 1995).

The gene *ADH6* (Gonzalez *et al.*, 2000) codes for a dimeric enzyme ADH VI which exhibits conservation of the zinc-signature, as well as amino acid sequences in the substrate and coenzyme binding domains, characteristic of the zinc containing MDR enzymes. The purified ADH VI shows a strict specificity for NADPH and accepts a wide range of compounds as substrates, including linear and branched chain primary alcohols and aldehydes, substituted cinnamyl alcohols and aldehydes as well as substituted benzaldehydes and their corresponding alcohols (Larroy *et al.*, 2002a). It is able to produce 2,3-butanediol from acetoin during fermentation, and under oxidative conditions allows the yeast to use 2,3-butanediol as a carbon and energy source (Gonzalez *et al.*, 2000). The specificity of the substrate and cofactor strongly supports the physiological involvement of ADH VI in aldehyde reduction rather than in alcohol oxidation. The potential role of ADH VI in *S. cerevisiae* is not easy to ascertain when simply considering its structural similarity to plant cinnamyl ADHs (CADs). Alternatively, ADH VI might have arisen from its ability to convert veratraldehyde and anisaldehyde into their corresponding alcohols. Therefore, it may give the yeast the opportunity to live in ligninolytic environments where products derived from lignin biodegradation may be available. Another potential function may include the biosynthesis of fusel alcohols (Larroy *et al.*, 2002a) and most certainly NADP(H) homeostasis (Larroy *et al.*, 2003). Recently, genome-wide transcription analysis was employed to identify the *ADH6* gene to encode NADPH-dependent 5-hydroxymethyl furfural (HMF) reduction activity (Petersson *et al.*, 2006).

The purified *ADH7* (YCR105W) gene product, named ADH VII, is a homodimer of which the reductase activity is about five-fold that of the dehydrogenase activity and cinnamaldehydes seem to be the best substrates for this enzyme (Larroy *et al.*, 2002b). The phylogenetic tree constructed from the MDRs identified in the genomes

of *E. coli*, *S. cerevisiae*, *D. melanogaster* and *C. elegans* placed ADH VII in a family of enzymes structurally related to cinnamyl alcohol dehydrogenases (Jornvall *et al.*, 2001).

Despite the enormous amount of information available on the kinetics and regulation of the *S. cerevisiae* alcohol dehydrogenases, the understanding of the physiological role of each enzyme *in vivo* warrants further investigation.

2.4 Literature cited

- Bakker, B. M., C. Bro, P. Kotter, M. A. Luttk, J. P. van Dijken and J. T. Pronk.** 2000. The mitochondrial alcohol dehydrogenase Adh3p is involved in a redox shuttle in *Saccharomyces cerevisiae*. *J. Bacteriol.* **182**: 4730-4737.
- Beier, D. R., A. Sledziewski and E. T. Young.** 1985. Deletion analysis identifies a region, upstream of the *ADH2* gene of *Saccharomyces cerevisiae*, which is required for ADR1-mediated derepression. *Mol. Cell Biol.* **5**: 1743-1749.
- Beier, D. R. and E. T. Young.** 1982. Characterization of a regulatory region upstream of the *ADR2* locus of *S. cerevisiae*. *Nature* **300**: 724-728.
- Bennetzen, J. L. and B. D. Hall.** 1982. The primary structure of the *Saccharomyces cerevisiae* gene for alcohol dehydrogenase. *J. Biol. Chem.* **257**: 3018-3025.
- Blumberg, H., A. Eisen, A. Sledziewski, D. Bader and E. T. Young.** 1987. Two zinc fingers of a yeast regulatory protein shown by genetic evidence to be essential for its function. *Nature.* **328**: 443-445.
- Bro, C., B. Regenberg, G. Lagniel, J. Labarre, M. Montero-Lomeli and J. Nielsen.** 2003. Transcriptional, proteomic, and metabolic responses to lithium in galactose-grown yeast cells. *J Biol. Chem.* **278**: 32141-32149.
- Cheng, L. Y. and L. H. Lek.** 1992. Inhibition of alcohol dehydrogenases by thiol compounds. *FEBS Lett.* **300**: 251-253.
- Cherry, J. R., T. R. Johnson, C. Dollard, J. R. Shuster and C. L. Denis.** 1989. Cyclic AMP-dependent protein kinase phosphorylates and inactivates the yeast transcriptional activator ADR1. *Cell* **56**: 409-419.
- Ciriacy, M.** 1975a. Genetics of alcohol dehydrogenase in *Saccharomyces cerevisiae* : I. Isolation and genetic analysis of *adh* mutants. *Mutation Research* **29**: 315-325.
- Ciriacy, M.** 1975b. Genetics of alcohol dehydrogenase in *Saccharomyces cerevisiae*. II. Two loci controlling synthesis of the glucose-repressible ADH II. *Mol. Gen. Genet.* **138**: 157-164.
- Ciriacy, M.** 1976. Cis-dominant regulatory mutations affecting the formation of glucose-repressible alcohol dehydrogenase (ADHII) in *Saccharomyces cerevisiae*. *Mol. Gen. Genet.* **145**: 327-333.
- Ciriacy, M.** 1979. Isolation and characterization of further cis- and trans-acting regulatory elements involved in the synthesis of glucose-repressible alcohol dehydrogenase (ADHII) in *Saccharomyces cerevisiae*. *Mol. Gen. Genet.* **176**: 427-431.
- Ciriacy, M.** 1997. Alcohol dehydrogenases. In Yeast sugar metabolism. Zimmermann, F. K. and Entian, K. D. *Technomic publishing co.inc.* pp. 213-223.
- Collart, M. A. and K. Struhl.** 1994. *NOT1*(CDC39), *NOT2*(CDC36), *NOT3*, and *NOT4* encode a global-negative regulator of transcription that differentially affects TATA-element utilization. *Genes Dev.* **8**: 525-537.
- Cook, W. J. and C. L. Denis.** 1993. Identification of three genes required for the glucose-dependent transcription of the yeast transcriptional activator ADR1. *Curr. Genet.* **23**: 192-200.

- De Bolle, X., C. Vinals, J. Fastrez and E. Feytmans.** 1997. Bivalent cations stabilize yeast alcohol dehydrogenase I. *Biochem. J.* **323 (Pt 2):** 409-413.
- De Bolle, X., C. Vinals, D. Prozzi, J. Y. Paquet, R. Leplae, E. Depiereux, J. Vandenhoute and E. Feytmans.** 1995. Identification of residues potentially involved in the interactions between subunits in yeast alcohol dehydrogenases. *Eur. J. Biochem.* **231:** 214-219.
- Denis, C. L.** 1984. Identification of new genes involved in the regulation of yeast alcohol dehydrogenase II. *Genetics* **108:** 833-844.
- Denis, C. L.** 1987. The effects of *ADR1* and *CCR1* gene dosage on the regulation of the glucose-repressible alcohol dehydrogenase from *Saccharomyces cerevisiae*. *Mol. Gen. Genet.* **208:** 101-106.
- Denis, C. L. and D. C. Audino.** 1991. The CCR1 (SNF1) and SCH9 protein kinases act independently of cAMP-dependent protein kinase and the transcriptional activator ADR1 in controlling yeast *ADH2* expression. *Mol. Gen. Genet.* **229:** 395-399.
- Denis, C. L., M. Ciriacy and E. T. Young.** 1981. A positive regulatory gene is required for accumulation of the functional messenger RNA for the glucose-repressible alcohol dehydrogenase from *Saccharomyces cerevisiae*. *J. Mol. Biol.* **148:** 355-368.
- Denis, C. L., J. Ferguson and E. T. Young.** 1983a. mRNA levels for the fermentative alcohol dehydrogenase of *Saccharomyces cerevisiae* decrease upon growth on a nonfermentable carbon source. *J. Biol. Chem.* **258:** 1165-1171.
- Denis, C. L., J. Ferguson and E. T. Young.** 1983b. mRNA levels for the fermentative alcohol dehydrogenase of *Saccharomyces cerevisiae* decrease upon growth on a nonfermentable carbon source. *J. Biol. Chem.* **258:** 1165-1171.
- Denis, C. L., S. C. Fontaine, D. Chase, B. E. Kemp and L. T. Bemis.** 1992. ADR1c mutations enhance the ability of ADR1 to activate transcription by a mechanism that is independent of effects on cyclic AMP-dependent protein kinase phosphorylation of Ser-230. *Mol. Cell Biol.* **12:** 1507-1514.
- Denis, C. L. and C. Gallo.** 1986. Constitutive RNA synthesis for the yeast activator ADR1 and identification of the ADR1-5c mutation: implications in posttranslational control of *ADR1*. *Mol. Cell Biol.* **6:** 4026-4030.
- Denis, C. L. and T. Malvar.** 1990. The CCR4 gene from *Saccharomyces cerevisiae* is required for both nonfermentative and spt-mediated gene expression. *Genetics* **124:** 283-291.
- Di Mauro, E., S. G. Kendrew and M. Caserta.** 2000. Two distinct nucleosome alterations characterize chromatin remodeling at the *Saccharomyces cerevisiae ADH2* promoter. *J Biol. Chem.* **275:** 7612-7618.
- Dickinson, F. M. and S. Dack.** 2001. The activity of yeast ADH I and ADH II with long-chain alcohols and diols. *Chem. Biol. Interact.* **130-132:** 417-423.
- Dickinson, J. R., S. J. Harrison, J. A. Dickinson and M. J. Hewlins.** 2000. An investigation of the metabolism of isoleucine to active amyl alcohol in *Saccharomyces cerevisiae*. *J Biol. Chem.* **275:** 10937-10942.
- Dickinson, J. R., S. J. Harrison and M. J. Hewlins.** 1998. An investigation of the metabolism of valine to isobutyl alcohol in *Saccharomyces cerevisiae*. *J Biol. Chem.* **273:** 25751-25756.

- Dickinson, J. R., M. M. Lanterman, D. J. Danner, B. M. Pearson, P. Sanz, S. J. Harrison and M. J. Hewlins.** 1997. A ^{13}C nuclear magnetic resonance investigation of the metabolism of leucine to isoamyl alcohol in *Saccharomyces cerevisiae*. *J Biol. Chem.* **272**: 26871-26878.
- Dickinson, J. R., L. E. Salgado and M. J. Hewlins.** 2003. The catabolism of amino acids to long chain and complex alcohols in *Saccharomyces cerevisiae*. *J. Biol. Chem.* **278**: 8028-8034.
- Dombek, K. M., S. Camier and E. T. Young.** 1993. *ADH2* expression is repressed by REG1 independently of mutations that alter the phosphorylation of the yeast transcription factor ADR1. *Mol. Cell Biol.* **13**: 4391-4399.
- Donoviel, M. S., N. Kacherovsky and E. T. Young.** 1995. Synergistic activation of *ADH2* expression is sensitive to upstream activation sequence 2 (UAS2) orientation, copy number and UAS1-UAS2 helical phasing. *Mol. Cell Biol.* **15**: 3442-3449.
- Dorsey, M., C. Peterson, K. Bray and C. E. Paquin.** 1992. Spontaneous amplification of the *ADH4* gene in *Saccharomyces cerevisiae*. *Genetics* **132**: 943-950.
- Dorsey, M. J., P. Hoeh and C. E. Paquin.** 1993. Phenotypic identification of amplifications of the *ADH4* and *CUP1* genes of *Saccharomyces cerevisiae*. *Curr. Genet.* **23**: 392-396.
- Drewke, C. and M. Ciriacy.** 1988. Overexpression, purification and properties of alcohol dehydrogenase IV from *Saccharomyces cerevisiae*. *Biochim. Biophys. Acta.* **950**: 54-60.
- Drewke, C., J. Thielen and M. Ciriacy.** 1990. Ethanol formation in *adh0* mutants reveals the existence of a novel acetaldehyde-reducing activity in *Saccharomyces cerevisiae*. *J Bacteriol.* **172**: 3909-3917.
- Eklund H. and C.I. Branden.** 1987. Crystal structure, coenzyme conformations, and protein interactions. In: Dolphin DNY, ed. *Pyridine nucleotide coenzymes*. New York: Wiley. pp 51-98.
- Feldmann, H., M. Aigle, G. Aljinovic, B. Andre, M. C. Baclet, C. Barthe, A. Baur, A. M. Becam, N. Biteau and E. Boles .** 1994. Complete DNA sequence of yeast chromosome II. *EMBO J.* **13**: 5795-5809.
- Fernandez, M. R., J. A. Biosca, A. Norin, H. Jornvall and X. Pares.** 1995. Class III alcohol dehydrogenase from *Saccharomyces cerevisiae*: structural and enzymatic features differ toward the human/mammalian forms in a manner consistent with functional needs in formaldehyde detoxication. *FEBS Lett.* **370**: 23-26.
- Fowler, P. W., A. J. Ball and D. E. Griffiths.** 1972. The control of alcohol dehydrogenase isozyme synthesis in *Saccharomyces cerevisiae*. *Can. J. Biochem.* **50**: 35-43.
- Ganzhorn, A. J., D. W. Green, A. D. Hershey, R. M. Gould and B. V. Plapp.** 1987. Kinetic characterization of yeast alcohol dehydrogenases. Amino acid residue 294 and substrate specificity. *J. Biol. Chem.* **262**: 3754-3761.
- Giniger, E., S. M. Varnum and M. Ptashne.** 1985. Specific DNA binding of GAL4, a positive regulatory protein of yeast. *Cell* **40**: 767-774.
- Gonzalez, E., M. R. Fernandez, C. Larroy, L. Sola, M. A. Pericas, X. Pares, and J. A. Biosca.** 2000. Characterization of a (2R,3R)-2,3-butanediol dehydrogenase as the *Saccharomyces cerevisiae* YAL060W gene product. Disruption and induction of the gene. *J. Biol. Chem.* **275**: 35876-35885.

- Green, D. W., H. W. Sun and B. V. Plapp.** 1993. Inversion of the substrate specificity of yeast alcohol dehydrogenase. *J. Biol. Chem.* **268**: 7792-7798.
- Grey, M., M. Schmidt and M. Brendel.** 1996. Overexpression of *ADHI* confers hyper-resistance to formaldehyde in *Saccharomyces cerevisiae*. *Curr. Genet.* **29**: 437-440.
- Gutheil, W. G., B. Holmquist and B. L. Vallee.** 1992. Purification, characterization, and partial sequence of the glutathione-dependent formaldehyde dehydrogenase from *Escherichia coli*: a class III alcohol dehydrogenase. *Biochemistry* **31**: 475-481.
- Harris, J. L.** 1964. Structure and activity of enzymes. In The structure and catalytic activity of thiol dehydrogenases. Hartley, B. S. and Harris, J. L. *Academic press.* pp. 97-109.
- Haurie, V., M. Perrot, T. Mini, P. Jenö, F. Sagliocco and H. Boucherie.** 2001. The transcriptional activator Cat8p provides a major contribution to the reprogramming of carbon metabolism during the diauxic shift in *Saccharomyces cerevisiae*. *J. Biol. Chem.* **276**: 76-85.
- Heick, H. M. C., J. Willemot and N. Begin-heick.** 1969. The subcellular localization of alcohol dehydrogenase activity in baker's yeast. *Biochim. Biophys. Acta.* **191**: 493-501.
- Hope, I. A. and K. Struhl.** 1985. GCN4 protein, synthesized in vitro, binds *HIS3* regulatory sequences: implications for general control of amino acid biosynthetic genes in yeast. *Cell* **43**: 177-188.
- Huh, W. K., J. V. Falvo, L. C. Gerke, A. S. Carroll, R. W. Howson, J. S. Weissman and E. K. O'Shea.** 2003. Global analysis of protein localization in budding yeast. *Nature* **425**: 686-691.
- Irani, M., W. E. Taylor and E. T. Young.** 1987. Transcription of the *ADH2* gene in *Saccharomyces cerevisiae* is limited by positive factors that bind competitively to its intact promoter region on multicopy plasmids. *Mol. Cell Biol.* **7**: 1233-1241.
- Jornvall, H.** 1977a. Alcohol dehydrogenase: structural studies, functional aspects and evolutionary conclusions in relation to steroid binding. *Biochem Soc. Trans.* **5**: 636-639.
- Jornvall, H.** 1977b. The primary structure of yeast alcohol dehydrogenase. *Eur. J. Biochem.* **72**: 425-442.
- Jornvall, H., B. Persson and J. Jeffery.** 1987. Characteristics of alcohol/polyol dehydrogenases. The zinc-containing long-chain alcohol dehydrogenases. *Eur J Biochem.* **167**: 195-201.
- Jornvall, H., J. Shafqat and B. Persson.** 2001. Variations and constant patterns in eukaryotic MDR enzymes. Conclusions from novel structures and characterized genomes. *Chem. Biol. Interact.* **130-132**: 491-498.
- Kallberg, Y., U. Oppermann, H. Jornvall and B. Persson.** 2002. Short-chain dehydrogenases/reductases (SDRs). *Eur. J. Biochem.* **269**: 4409-4417.
- Karnitz, L., M. Morrison and E. T. Young.** 1992. Identification and characterization of three genes that affect expression of *ADH2* in *Saccharomyces cerevisiae*. *Genetics* **132**: 351-359.
- Kusano, M., Y. Sakai, N. Kato, H. Yoshimoto, H. Sone and Y. Tamai.** 1998. Hemiacetal dehydrogenation activity of alcohol dehydrogenases in *Saccharomyces cerevisiae*. *Biosci. Biotechnol. Biochem.* **62**: 1956-1961.

- Ladriere, J. M., I. Georis, M. Guerineau and J. Vandenhaute.** 2000. *Kluyveromyces marxianus* exhibits an ancestral *Saccharomyces cerevisiae* genome organization downstream of *ADH2*. *Gene* **255**: 83-91.
- Larroy, C., M. R. Fernandez, E. Gonzalez, X. Pares and J. A. Biosca.** 2002a. Characterization of the *Saccharomyces cerevisiae* YMR318C (*ADH6*) gene product as a broad specificity NADPH-dependent alcohol dehydrogenase: relevance in aldehyde reduction. *Biochem. J.* **361**: 163-172.
- Larroy, C., X. Pares and J. A. Biosca.** 2002b. Characterization of a *Saccharomyces cerevisiae* NADP(H)-dependent alcohol dehydrogenase (ADHVII), a member of the cinnamyl alcohol dehydrogenase family. *Eur. J. Biochem.* **269**: 5738-5745.
- Larroy, C., F. M. Rosario, E. Gonzalez, X. Pares and J. A. Biosca.** 2003. Properties and functional significance of *Saccharomyces cerevisiae* ADHVI. *Chem. Biol. Interact.* **143-144**: 229-238.
- Leskovac, V., S. Trivic and B. M. Anderson.** 1998. Use of competitive dead-end inhibitors to determine the chemical mechanism of action of yeast alcohol dehydrogenase. *Mol. Cell Biochem.* **178**: 219-227.
- Leskovac, V., S. Trivic and D. Pericin.** 2002. The three zinc-containing alcohol dehydrogenases from baker's yeast, *Saccharomyces cerevisiae*. *FEMS Yeast Res.* **2**: 481-494.
- Liu, H. Y., V. Badarinarayana, D. C. Audino, J. Rappsilber, M. Mann and C. L. Denis.** 1998. The NOT proteins are part of the CCR4 transcriptional complex and affect gene expression both positively and negatively. *EMBO J.* **17**: 1096-1106.
- Liu, H. Y., Y. C. Chiang, J. Pan, J. Chen, C. Salvatore, D. C. Audino, V. Badarinarayana, V. Palaniswamy, B. Anderson and C. L. Denis.** 2001. Characterization of CAF4 and CAF16 reveals a functional connection between the CCR4-NOT complex and a subset of SRB proteins of the RNA polymerase II holoenzyme. *J Biol. Chem.* **276**: 7541-7548.
- Lutstorf, U. and R. Megnet.** 1968. Multiple forms of alcohol dehydrogenase in *Saccharomyces cerevisiae*. I. Physiological control of ADH-2 and properties of ADH-2 and ADH-4. *Arch. Biochem. Biophys.* **126**: 933-944.
- Magonet, E., P. Hayen, D. Delforge, E. Delaive and J. Remacle.** 1992. Importance of the structural zinc atom for the stability of yeast alcohol dehydrogenase. *Biochem. J.* **287 (Pt 2)**: 361-365.
- Malvar, T., R. W. Biron, D. B. Kaback and C. L. Denis.** 1992. The CCR4 protein from *Saccharomyces cerevisiae* contains a leucine-rich repeat region which is required for its control of *ADH2* gene expression. *Genetics* **132**: 951-962.
- Mizuno, A., H. Tabei and M. Iwahuti.** 2006. Characterization of low-acetic-acid-producing yeast isolated from 2-deoxyglucose-resistant mutants and its application to high-gravity brewing. *J Biosci. Bioeng.* **101**: 31-37.
- Mooney, D. T., D. B. Pilgrim and E. T. Young.** 1990. Mutant alcohol dehydrogenase (ADH III) presequences that affect both in vitro mitochondrial import and in vitro processing by the matrix protease. *Mol. Cell Biol.* **10**: 2801-2808.
- Mortimer, R. K. and D. Schild.** 1985. Genetic map of *Saccharomyces cerevisiae*, edition 9. *Microbiol. Rev.* **49**: 181-213.
- Niederacher, D. and K. D. Entian.** 1991. Characterization of Hex2 protein, a negative regulatory element necessary for glucose repression in yeast. *Eur J Biochem.* **200**: 311-319.

- O'Hara, P. J., H. Horowitz, G. Eichinger and E. T. Young.** 1988. The yeast *ADR6* gene encodes homopolymeric amino acid sequences and a potential metal-binding domain. *Nucleic Acids Res.* **16:** 10153-10169.
- Overkamp, K. M., B. M. Bakker, P. Kotter, A. van Tuijl, S. de Vries, J. P. van Dijken and J. T. Pronk.** 2000. In vivo analysis of the mechanisms for oxidation of cytosolic NADH by *Saccharomyces cerevisiae* mitochondria. *J. Bacteriol.* **182:** 2823-2830.
- Paquin, C. E. and V. M. Williamson.** 1986. Ty insertions at two loci account for most of the spontaneous antimycin A resistance mutations during growth at 15 degrees C of *Saccharomyces cerevisiae* strains lacking *ADH1*. *Mol. Cell Biol.* **6:** 70-79.
- Persson, B., J. Hallborn, M. Walfridsson, B. Hahn-Hägerdal, S. Keranen, M. Penttila and H. Jornvall.** 1993. Dual relationships of xylitol and alcohol dehydrogenases in families of two protein types. *FEBS Lett.* **324:** 9-14.
- Petersson, A., J. R. M. Almeida, T. Modig, K. Karhumaa, B. Hahn-Hägerdal, M. F. Gorwa-Grauslund and G. Lidén.** 2006. A 5-hydroxymethyl furfural reducing enzyme encoded by the *Saccharomyces cerevisiae ADH6* gene conveys HMF tolerance. *Yeast* **23:** 455-464.
- Pilgrim, D. and E. T. Young.** 1987. Primary structure requirements for correct sorting of the yeast mitochondrial protein ADH III to the yeast mitochondrial matrix space. *Mol. Cell Biol.* **7:** 294-304.
- Ramaswamy, S., D. A. Kratzer, A. D. Hershey, P. H. Rogers, A. Arnone, H. Eklund and B. V. Plapp.** 1994. Crystallization and preliminary crystallographic studies of *Saccharomyces cerevisiae* alcohol dehydrogenase I. *J. Mol. Biol.* **235:** 777-779.
- Reid, M. F. and C. A. Fewson.** 1994. Molecular characterization of microbial alcohol dehydrogenases. *Crit Rev. Microbiol.* **20:** 13-56.
- Rossmann, M. G., A. Liljas, C. I. Branden and L. J. Banaszak.** 1975. The enzymes. Boyer, P. *Academic press.* pp. 61-102.
- Ruohonen, L., M. K. Aalto and S. Keranen.** 1995. Modifications to the *ADH1* promoter of *Saccharomyces cerevisiae* for efficient production of heterologous proteins. *J. Biotechnol.* **39:** 193-203.
- Russell, D. W., M. Smith, D. Cox, V. M. Williamson and E. T. Young.** 1983a. DNA sequences of two yeast promoter-up mutants. *Nature* **304:** 652-654.
- Russell, D. W., M. Smith, V. M. Williamson and E. T. Young.** 1983b. Nucleotide sequence of the yeast alcohol dehydrogenase II gene. *J. Biol. Chem.* **258:** 2674-2682.
- Santangelo, G. M. and J. Tornow.** 1990. Efficient transcription of the glycolytic gene *ADH1* and three translational component genes requires the GCR1 product, which can act through TUF/GRF/RAP binding sites. *Mol. Cell Biol.* **10:** 859-862.
- Schopp, W. and H. Aurich.** 1976. Kinetics and reaction mechanism of yeast alcohol dehydrogenase with long-chain primary alcohols. *Biochem. J.* **157:** 15-22.
- Sledziewski, A. and E. T. Young.** 1982. Chromatin conformational changes accompany transcriptional activation of a glucose-repressed gene in *Saccharomyces cerevisiae*. *Proc. Natl. Acad. Sci. U. S. A.* **79:** 253-256.

- Smith, M. G., S. G. Des Etages and M. Snyder.** 2004. Microbial synergy via an ethanol-triggered pathway. *Mol. Cell Biol.* **24**: 3874-3884.
- Sonderegger, M., M. Jeppsson, B. Hahn-Hagerdal and U. Sauer.** 2004. Molecular basis for anaerobic growth of *Saccharomyces cerevisiae* on xylose, investigated by global gene expression and metabolic flux analysis. *Appl. Environ. Microbiol.* **70**: 2307-2317.
- Taguchi, A. K. and E. T. Young.** 1987. The identification and characterization of *ADR6*, a gene required for sporulation and for expression of the alcohol dehydrogenase II isozyme from *Saccharomyces cerevisiae*. *Genetics* **116**: 523-530.
- Thomson, J. M., E. A. Gaucher, M. F. Burgan, D. W. De Kee, T. Li, J. P. Aris and S. A. Benner.** 2005. Resurrecting ancestral alcohol dehydrogenases from yeast. *Nat. Genet.* **37**: 630-635.
- Thukral, S. K., A. Eisen and E. T. Young.** 1991. Two monomers of yeast transcription factor ADR1 bind a palindromic sequence symmetrically to activate *ADH2* expression. *Mol. Cell Biol.* **11**: 1566-1577.
- Vallari, R. C., W. J. Cook, D. C. Audino, M. J. Morgan, D. E. Jensen, A. P. Laudano and C. L. Denis.** 1992. Glucose repression of the yeast *ADH2* gene occurs through multiple mechanisms, including control of the protein synthesis of its transcriptional activator, ADR1. *Mol. Cell Biol.* **12**: 1663-1673.
- Vallee, B. L. and K. H. Falchuk.** 1993. The biochemical basis of zinc physiology. *Physiol Rev.* **73**: 79-118.
- van den Berg, M. A., P. Jong-Gubbels and H. Y. Steensma.** 1998. Transient mRNA responses in chemostat cultures as a method of defining putative regulatory elements: application to genes involved in *Saccharomyces cerevisiae* acetyl-coenzyme A metabolism. *Yeast* **14**: 1089-1104.
- van Iersel, M. F., M. H. Eppink, W. J. van Berkel, F. M. Rombouts and T. Abee.** 1997. Purification and characterization of a novel NADP-dependent branched-chain alcohol dehydrogenase from *Saccharomyces cerevisiae*. *Appl. Environ. Microbiol.* **63**: 4079-4082.
- van Loon, A. P. and E. T. Young.** 1986. Intracellular sorting of alcohol dehydrogenase isoenzymes in yeast: a cytosolic location reflects absence of an amino-terminal targeting sequence for the mitochondrion. *EMBO J.* **5**: 161-165.
- Verdone, L., F. Cesari, C. L. Denis, E. Di Mauro and M. Caserta.** 1997. Factors affecting *Saccharomyces cerevisiae ADH2* chromatin remodeling and transcription. *J Biol. Chem.* **272**: 30828-30834.
- Verdone, L., J. Wu, K. Van Riper, N. Kacherovsky, M. Vogelauer, E. T. Young, M. Grunstein, E. Di Mauro and M. Caserta.** 2002. Hyperacetylation of chromatin at the *ADH2* promoter allows Adr1 to bind in repressed conditions. *EMBO J.* **21**: 1101-1111.
- Voronkova, V., N. Kacherovsky, C. Tachibana, D. Yu and E. T. Young.** 2006. Snf1-dependent and Snf1-independent constitutive pathways of *ADH2* expression in *Saccharomyces cerevisiae*. *Genetics* **12**: 2123-2138.
- Walther, K. and H. J. Schuller.** 2001. Adr1 and Cat8 synergistically activate the glucose-regulated alcohol dehydrogenase gene *ADH2* of the yeast *Saccharomyces cerevisiae*. *Microbiol.* **147**: 2037-2044.

- Walton, J. D., C. E. Paquin, K. Kaneko and V. M. Williamson.** 1986. Resistance to antimycin A in yeast by amplification of *ADH4* on a linear, 42 kb palindromic plasmid. *Cell* **46**: 857-863.
- Wehner, E. P., E. Rao and M. Brendel.** 1993. Molecular structure and genetic regulation of *SFA*, a gene responsible for resistance to formaldehyde in *Saccharomyces cerevisiae*, and characterization of its protein product. *Mol. Gen. Genet.* **237**: 351-358.
- Wenger, J. I. and C. Bernofsky.** 1971. Mitochondrial alcohol dehydrogenase from *Saccharomyces cerevisiae*. *Biochim. Biophys. Acta.* **227**: 479-490.
- Wiesenfeld, M., L. Schimpfessel and R. Crokaert.** 1975. Multiple forms of mitochondrial alcohol dehydrogenase in *Saccharomyces cerevisiae*. *Biochim. Biophys. Acta.* **405**: 500-512.
- Williamson, V. M., J. Bennetzen, E. T. Young, K. Nasmyth and B. D. Hall.** 1980. Isolation of the structural gene for alcohol dehydrogenase by genetic complementation in yeast. *Nature* **283**: 214-216.
- Williamson, V. M. and C. E. Paquin.** 1987. Homology of *Saccharomyces cerevisiae ADH4* to an iron-activated alcohol dehydrogenase from *Zymomonas mobilis*. *Mol. Gen. Genet.* **209**: 374-381.
- Williamson, V. M., E. T. Young and M. Ciriacy.** 1981. Transposable elements associated with constitutive expression of yeast alcohol dehydrogenase II. *Cell* **23**: 605-614.
- Wills, C.** 1976. Production of yeast alcohol dehydrogenase isoenzymes by selection. *Nature* **261**: 26-29.
- Wills, C. and H. Jornvall.** 1979. The two major isozymes of yeast alcohol dehydrogenase. *Eur. J. Biochem.* **99**: 323-331.
- Wills, C., P. Kratofil and T. Martin.** 1982. Functional mutants of yeast alcohol dehydrogenase. *Basic Life Sci.* **19**: 305-329.
- Wills, C. and J. Phelps.** 1975. A technique for the isolation of yeast alcohol dehydrogenase mutants with altered substrate specificity. *Arch. Biochem Biophys.* **167**: 627-637.
- Young, E. T. and D. Pilgrim.** 1985. Isolation and DNA sequence of *ADH3*, a nuclear gene encoding the mitochondrial isozyme of alcohol dehydrogenase in *Saccharomyces cerevisiae*. *Mol. Cell Biol.* **5**: 3024-3034.
- Yu, J., M. S. Donoviel and E. T. Young.** 1989. Adjacent upstream activation sequence elements synergistically regulate transcription of *ADH2* in *Saccharomyces cerevisiae*. *Mol. Cell Biol.* **9**: 34-42.
- Yu, W., I. G. Macreadie and D. R. Winge.** 1991. Protection against cadmium toxicity in yeast by alcohol dehydrogenase. *J Inorg. Biochem.* **44**: 155-161.
- Zhang, W., D. L. Needham, M. Coffin, A. Rooker, P. Hurban, M. M. Tanzer and J. R. Shuster.** 2003. Microarray analyses of the metabolic responses of *Saccharomyces cerevisiae* to organic solvent dimethyl sulfoxide. *J Ind. Microbiol. Biotechnol.* **30**: 57-69.

The effect of medium composition and ethanol toxicity on the growth of	
<i>Saccharomyces cerevisiae</i> strain W303-1A.....	35
Abstract.....	35
3.2 Introduction.....	35
3.2 Introduction.....	36
3.3 Materials and Methods.....	37
3.3.1 Strains and media.....	37
3.3.2 Cultivation conditions.....	37
3.3.3 Analyses.....	38
3.4 Results and Discussion.....	38
3.5 Conclusions.....	44
3.6 Literature cited.....	45
Figure 3.1	Growth profile of <i>S. cerevisiae</i> strain W303-1A(a) in complex medium in shake flasks containing different glucose concentrations, 37.6 g l ⁻¹ (●), 22.9 g l ⁻¹ (■), 11.3 g l ⁻¹ (▼).....
	40
Figure 3.2	Growth profiles of <i>S. cerevisiae</i> W303-1A(a) in complex medium in shake flasks with 5 g ethanol l ⁻¹ as carbon source (A). Growth profiles where peptone (B) and yeast extract (C) were excluded from the medium are also shown. Biomass (●) and ethanol (▲) concentrations were measured over a period of 70 h.
	41
Figure 3.3	Growth profile of strain W303-1A(a) on 10 g glucose l ⁻¹ in a chemically defined medium in shake flasks. Biomass (●), glucose (■) and ethanol (▲) concentrations are indicated in the graph.....
	42
Figure 3.4	Growth profile of strain W303-1A(a) on 5 g ethanol l ⁻¹ in a chemically defined medium in shake flasks. Biomass (●) and ethanol (▲) concentrations are indicated in the graph.....
	42
Figure 3.5	Effect of the exogenous ethanol concentration on the maximum specific growth rate (μ_{\max}) of W303-1A(a) grown at 25°C
	43
Table 3.1	Growth parameters of <i>S. cerevisiae</i> strain W303-1A(a) in shake flasks on different glucose and ethanol concentrations in a complex and a chemically defined medium.
	39

CHAPTER 3

The effect of medium composition and ethanol toxicity on the growth of *Saccharomyces cerevisiae* strain W303-1A(a).

Abstract

The growth of *Saccharomyces cerevisiae* strain W303-1A(a) was evaluated in complex and chemically defined media using glucose or ethanol as carbon source. In complex medium, the strain had a low maximum specific growth rate (μ_{\max}) of 0.28 h^{-1} on glucose and produced ethanol at a volumetric rate of $0.204 \text{ g l}^{-1} \text{ h}^{-1}$, but was unable to utilise the ethanol produced from glucose over a period of 45 h. In complex medium ethanol was utilised at a slow rate of $0.086 \text{ g l}^{-1} \text{ h}^{-1}$ with incomplete utilisation of $5 \text{ g ethanol l}^{-1}$ even after 70 h. When the ethanol concentration exceeded a threshold value of 10 g l^{-1} the μ_{\max} value was significantly decreased. In the chemically defined medium with glucose as carbon source, however, all of the glucose was consumed during the first 20 h as well as all of the produced ethanol within 45 h. Furthermore, the μ_{\max} value was increased to 0.42 h^{-1} and the rate of ethanol production was $0.597 \text{ g l}^{-1} \text{ h}^{-1}$. When grown in the chemically defined medium on ethanol as the initial carbon source, the ethanol was utilised at a volumetric rate of uptake of $0.176 \text{ g l}^{-1} \text{ h}^{-1}$ with complete utilisation within 45 h. These observations suggest that subsequent growth experiments should be carried out in chemically defined medium with ethanol concentrations below 10 g l^{-1} .

3.2 Introduction

In especially physiological studies of microorganisms, it is important to ensure that a well formulated culture medium is used so as not to impose an unknown nutrient limitation. Unaccounted for nutrient limitations can result in misinterpretation of experimental data (Lagunas, 1986). Most yeast species produce satisfactory biomass on YPD medium containing yeast extract, peptone and glucose as carbon source. Yeast extract originates from lysed yeast cells and consists primarily of oxidised amino acids, but also includes nutrients such as vitamins (especially B vitamins) and minerals. Peptone is a protein derivative and is a broadly used component of yeast culture media because it is a rich source of amino acids and nitrogen (Martinez *et al.*, 2006). Magnesium is an essential cofactor for many of the glycolytic enzymes and has been identified as a limiting nutrient in fermentation broth containing peptone and yeast extract (Dombek & Ingram, 1986; Dombek & Ingram, 1987).

Several groups have reported improvements in alcoholic fermentation and final ethanol concentration by broth supplementation with additives such as lipids, proteins and vitamins (Casey *et al.*, 1983; Casey *et al.*, 1984; 1987; Janssens *et al.*, 1983). The addition of inositol to the culture medium improved the ethanol yield during fermentation and phospholipid synthesis, with the yeast cells producing more saturated fatty acids (Chi *et al.*, 1999).

Ethanol exerts different and separable effects on the specific growth rate of the yeast population, its viability and its specific rate of fermentation (D'Amore & Stewart, 1987). The amount of ethanol able to cause a decrease in growth rate is highly dependent on the yeast strain and medium composition and values ranging from 10 to 35 g ethanol l⁻¹ are cited in the literature (Casey *et al.*, 1984) When growing *S. cerevisiae* on sugars as carbon substrate, the inhibitory effect of the produced ethanol should also be considered.

The main aim of the investigation reported here was to evaluate the effect of the culture medium on the growth parameters of *Saccharomyces cerevisiae* strain W303-1A(a) in batch cultures. The ethanol tolerance of this strain was also determined to avoid severe inhibitory effects of ethanol, since it was essential for the subsequent experiments that the culture medium allowed complete utilisation of ethanol produced from glucose, or when added as sole carbon source.

3.3 Materials and Methods

3.3.1 Strains and media

The experiments in this chapter were conducted on *S. cerevisiae* strain W303-1A(a) (Appendix C). Cultivations were performed in complex as well as chemically defined media (Appendix A).

3.3.2 Cultivation conditions

Evaluating the effects of medium components. Aerobic cultivations were carried out in 500 ml Erlenmeyer flasks with stoppers of non-absorbent cotton wool, each containing 200 ml of the appropriate medium and either glucose or ethanol as carbon source. The glucose concentrations ranged from 11.3 g l⁻¹ to 37.6 g l⁻¹ and the ethanol concentrations were either 5 g l⁻¹ or 20 g l⁻¹. All shake flask cultivations were carried out at an initial pH of 5.5 at 30°C on a rotary shaker at 200 r min⁻¹. For experiments using glucose as carbon substrate, an inoculum was prepared in a 250 ml shake flask containing 50 ml of the relevant medium with 10 g glucose l⁻¹ and grown for 9 to 12 h. Similar inocula were prepared for experiments using ethanol as carbon substrate, but were grown for three more hours after the glucose had been depleted (derepressed conditions) before being transferred to the 500 ml flasks. These were inoculated with the pre-inocula to give an initial OD₆₀₀ of ca. 0.2.

Determining ethanol toxicity levels. The cells were grown in a temperature gradient incubator (Scientific Industries Inc., Bohemia, New York) at 25°C. Each of the L-shaped 30 ml test tubes contained 11 ml chemically defined medium and were located in 30 equidistant wells in the aluminium bar, which rocked gently to provide agitation. Oscillation was gradually increased from 25 to 50 per min over a period of 10 h. The appropriate volume of ethanol was added to each set of tubes and the concentrations determined by gas chromatography. Each tube was inoculated from an actively growing shake flask culture to an initial OD₆₀₀ value of ca. 0.04. Growth was considered to have occurred where the maximum specific growth rate exceeded 0.03 h⁻¹.

3.3.3 Analyses

Culture turbidity was monitored at 600 nm with a BioPhotometer (Eppendorf, Hamburg, Germany) and converted to dry biomass using a standard curve. Cells were harvested during late exponential phase, cooled on ice, centrifuged at 3 000 r min⁻¹ for 5 min, washed twice with distilled water and dried at 105°C overnight prior to gravimetric determination of the dry biomass concentration. The ethanol concentrations in the supernatant was determined with a 2010 gas chromatograph (Shimadzu) equipped with an SGE PBX-70 column (30 m x 0.25 ID) at an over temperature of 180°C, with 30 ml nitrogen carrier gas min⁻¹. Glucose concentrations were determined with a Sugar Analyser I high-performance liquid chromatograph equipped with a refractive index detector and a Waters Sugarpack I column (Waters Associates, Milford, MA, USA) operating at 85°C with an eluent (degassed water) flow rate of 0.5 ml min⁻¹.

3.4 Results and Discussion

Initially strain W303-1A(a) was grown in the complex medium as described by du Preez *et al.* (2001). Different glucose concentrations were added as carbon source and growth in shake flasks was monitored over a period of 45 h. The μ_{\max} value was not significantly influenced by the initial glucose concentration (Table 3.1, Figure 3.1A). The glucose was completely consumed in the culture medium with an initial glucose concentration of 22.9 g l⁻¹ or less, where as some residual glucose was still detected in the medium with and initial glucose concentration of 37.6 g l⁻¹ after 45 h (Figure 3.1B). Ethanol was produced at similar volumetric rates (Table 3.1), but no significant ethanol assimilation was apparent even after 45 h (Figure 3.1C).

Strain W303-1A(a) was able to grow on ethanol as added carbon source in complex medium in shake flasks (Figure 3.2A). At an initial ethanol concentration of 5 g l⁻¹ the ethanol was consumed at a volumetric rate of 0.086 g l⁻¹ h⁻¹, but residual ethanol was still detected after 70 h (Table 3.1, Figure 3.2A). The effect of the culture medium composition on the poor ethanol utilisation was investigated by the omission of certain constituents. In complex medium without peptone the maximum specific growth rate was 0.08 h⁻¹ compared to 0.17 h⁻¹ in the complete complex medium. Similarly, the rate of ethanol

Table 3.1 Growth parameters of *S. cerevisiae* strain W303-1A(a) in shake flasks on different glucose and ethanol concentrations in a complex and a chemically defined medium.

Medium	Substrate	g l ⁻¹	Growth parameters		
			μ _{max} , h ⁻¹	Q _s ^{max} , g l ⁻¹ h ⁻¹	Q _p ^{max} , g l ⁻¹ h ⁻¹
Complex	Glucose	11.3	0.28	0.6	0.204
		22.9	0.3	0.712	0.296
		37.6	0.27	0.918	0.259
	Ethanol	5	0.17	0.086	
Chemically defined	Glucose	10	0.42	0.974	0.597
	Ethanol	5	0.19	0.176	

Growth rates were calculated by linear regression analysis of the exponential growth data. Q_s and Q_p were calculated from the maximum slopes of the glucose and ethanol concentration curves respectively.

utilisation was only 0.029 g l⁻¹ h⁻¹ compared to 0.086 g l⁻¹ h⁻¹ in the complete complex medium, which resulted in a considerable amount of residual ethanol after 70 h (Figure 3.2B). The exclusion of yeast extract had no discernable influence on the growth parameters (Figure 3.2C). This apparent requirement for peptone was probably due to the auxotrophic nature of the yeast strain.

Since ethanol metabolism was the main focus point of this study, a well formulated medium was essential to avoid unknown nutrient limitations so as to facilitate maximal utilisation of ethanol. Subsequently, a chemically defined medium was formulated based on the media used by various other researchers for a number of different yeast strains. Amino acid concentrations were derived from the media of de Kock *et al.* (2000) and Flikweert *et al.* (1996), vitamin components from Schulze *et al.* (1995) and trace element concentrations as described by du Preez & van der Walt (1983), whereas the macro elements were derived from media described by Verduyn *et al.* (1990) and du Preez *et al.* (2001). Uracil, adenine, tryptophan, histidine and leucine were added to satisfy the auxotrophic requirements of strain W303-1A(a) (Cakar *et al.*, 1999; Pronk, 2002). The composition of the chemically defined medium is given in appendix A.

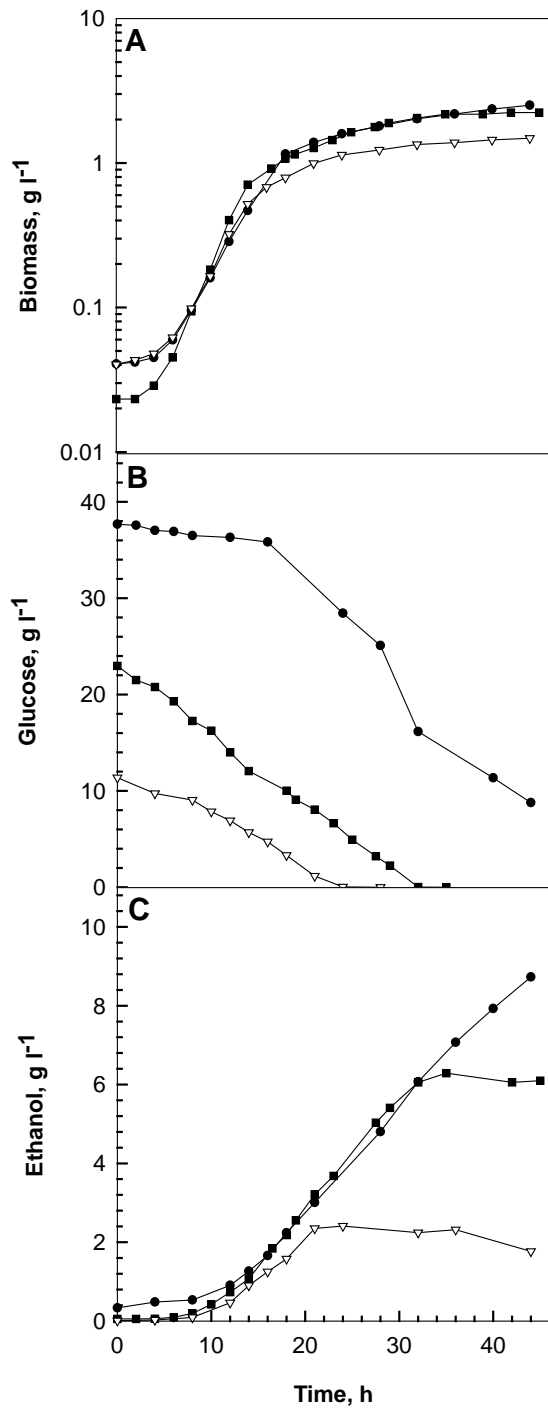


Figure 3.1 Growth profile of *S. cerevisiae* strain W303-1A(a) in complex medium in shake flasks containing different glucose concentrations, 37.6 g l⁻¹ (●), 22.9 g l⁻¹ (■), 11.3 g l⁻¹ (▽)

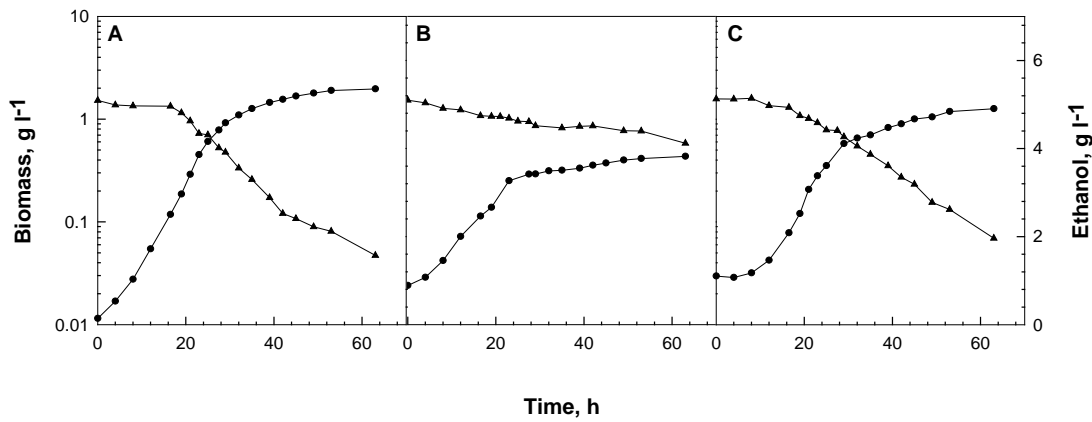


Figure 3.2 Growth profiles of *S. cerevisiae* W303-1A(a) in complex medium in shake flasks with 5 g ethanol l⁻¹ as carbon source (A). Growth profiles where peptone (B) and yeast extract (C) were excluded from the medium are also shown. Biomass (●) and ethanol (▲) concentrations were measured over a period of 70 h.

In the chemically defined medium with glucose as carbon source, strain W303-1A(a) consumed all of the glucose during the first 20 h, as well as all of the produced ethanol within 45 h (Figure 3.3). The other growth parameters were also considerably greater, compared to growth in the complex medium (Table 3.1) and resembled values available in literature (Boubekeur *et al.*, 2001). The strain was also able to utilise all the available ethanol within 45 hours when grown in the chemically defined medium containing 5 g ethanol l⁻¹ as carbon source (Figure 3.4).

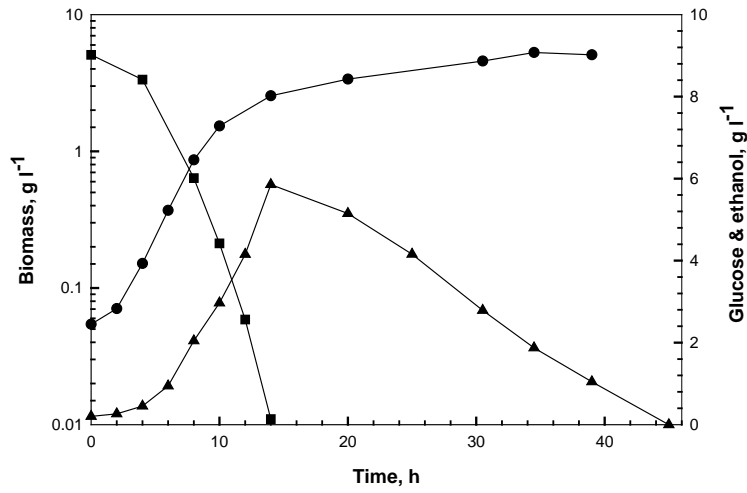


Figure 3.3 Growth profile of strain W303-1A(a) on 10 g glucose l⁻¹ in a chemically defined medium in shake flasks. Biomass (●), glucose (■) and ethanol (▲) concentrations are indicated in the graph.

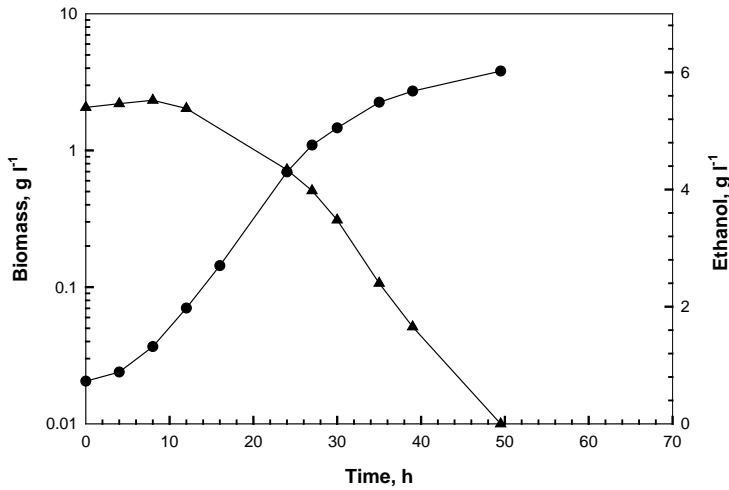


Figure 3.4 Growth profile of strain W303-1A(a) on 5 g ethanol l⁻¹ in a chemically defined medium in shake flasks. Biomass (●) and ethanol (▲) concentrations are indicated in the graph.

Investigation of the effect of externally added ethanol showed that at concentrations of between 0 to 10 g l⁻¹ less than 10% inhibition of the μ_{\max} value occurred (Figure 3.5). However, at ethanol concentrations greater than 10 g l⁻¹ an inverse linear correlation between the ethanol concentration and the μ_{\max} value was found ($R^2 = 0.9931$), with a concentration of 72 g l⁻¹ completely inhibiting growth. Therefore, for subsequent experiments the externally added ethanol concentrations were kept below 10 g l⁻¹.

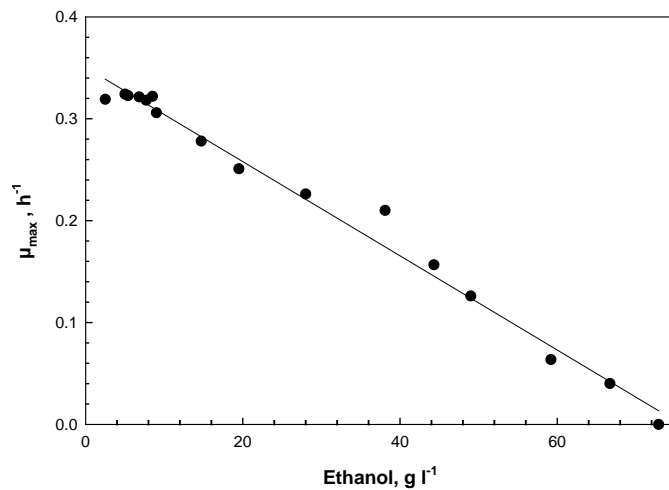


Figure 3.5 Effect of the exogenous ethanol concentration on the maximum specific growth rate (μ_{\max}) of W303-1A(a) grown at 25°C

3.5 Conclusions

S. cerevisiae strain W303-1A(a) utilised produced or externally added ethanol at a low rate when grown in complex medium. Apparently the complex medium failed to satisfy the demanding nutritional requirements of this auxotrophic yeast strain, judging from the growth parameters shown in Table 3.1. The use of a chemically defined medium resulted in a higher μ_{\max} value of 0.19 h^{-1} compared to 0.17 h^{-1} in the complex medium. The rate of ethanol utilisation also increased from 0.087 in the complex medium to $0.176 \text{ g l}^{-1} \text{ h}^{-1}$ in the chemically defined medium and all of the ethanol was consumed within 50 h. Ethanol inhibited growth and fermentation of strain W303-1A(a) and when the ethanol concentration exceeded a value of 10 g l^{-1} the growth rate was significantly inhibited.

3.6 Literature cited

- Boubekeur, S., N. Camougrand, O. Bunoust, M. Rigoulet and B. Guerin.** 2001. Participation of acetaldehyde dehydrogenases in ethanol and pyruvate metabolism of the yeast *Saccharomyces cerevisiae*. *Eur J Biochem.* **268**: 5057-5065.
- Cakar, Z. P., U. Sauer and J. E. Bailey.** 1999. Metabolic engineering of yeast: the perils of auxotrophic hosts. *Biotechnol. Lett.* **21**: 611-616.
- Casey, G. P., C. A. Magnus and W. M. Inglelew.** 1983. High gravity brewing: Nutrient enhanced production of high concentrations of ethanol by brewing yeast. *Biotechnol. Lett.* **5**: 429-434.
- Casey, G. P., C. A. Magnus and W. M. Inglelew.** 1984. High-gravity brewing: Effects of nutrition on yeast composition, fermentative ability, and alcohol production. *Appl. Environ. Microbiol.* **48**: 639-646.
- Chi, Z., S. D. Kohlwein and F. Paltauf.** 1999. Role of phosphatidylinositol (PI) in ethanol production and ethanol tolerance by a high ethanol producing yeast. *J. Ind Microbiol Biotechnol.* **22**: 58-63.
- D'Amore, T. and G. G. Stewart.** 1987. Ethanol tolerance of yeast, review. *Enzyme Microb. Technol.* **9**: 322-330.
- de Kock, S. H., J. C. du Preez and S. G. Kilian.** 2000. The effect of vitamins and amino acids on glucose uptake in aerobic chemostat cultures of three *Saccharomyces cerevisiae* strains. *Syst. Appl. Microbiol.* **23**: 41-46.
- Dombek, K. M. and L. O. Ingram.** 1986. Magnesium limitation and its role in apparent toxicity of ethanol during yeast fermentation. *Appl. Environ. Microbiol.* **52**: 975-981.
- Dombek, K. M. and L. O. Ingram.** 1987. Ethanol production during batch fermentation with *Saccharomyces cerevisiae*: changes in glycolytic enzymes and internal pH. *Appl. Environ. Microbiol.* **53**: 1286-1291.
- du Preez, J. C., J. E. Mare, J. Albertyn and S. G. Kilian.** 2001. Transcriptional repression of *ADH2*-regulated β -xylanase production by ethanol in recombinant strains of *Saccharomyces cerevisiae*. *FEMS Yeast Res.* **1**: 233-240.
- du Preez, J. C. and J. P. van der Walt.** 1983. Fermentation of D-xylose to ethanol by a strain of *Candida shehatae*. *Biotechnol. Lett.* **5**: 357-362.
- Flikweert, M. T., L. van der Zanden, W. M. T. M. Janssen, H. Y. Steensma, J. P. van Dijken and J. T. Pronk.** 1996. Pyruvate decarboxylase: An indispensable enzyme for growth of *Saccharomyces cerevisiae* on glucose. *Yeast* **12**: 247-257.
- Janssens, J. H., N. Burris, A. Woodward and R. B. Bailey.** 1983. Lipid-enhanced ethanol production by *Kluyveromyces fragilis*. *Appl. Environ. Microbiol.* **45**: 598-602.
- Lagunas, R.** 1986. Misconceptions about the energy metabolism of *Saccharomyces cerevisiae*. *Yeast* **2**: 221-228.
- Martinez, C., C. Gertosio, A. Labbe, R. Perez and M. A. Ganga.** 2006. Production of *Rhodotorula glutinis*: a yeast that secretes α -L-arabinofuranosidase. *Elec. J. Biotechnol.* **9**: 407-413.
- Pronk, J. T.** 2002. Auxotrophic yeast strains in fundamental and applied research. *Appl. Environ. Microbiol.* **68**: 2095-2100.

Schulze, U., M. E. Larsen and J. Villadsen. 1995. Determination of intracellular trehalose and glycogen in *Saccharomyces cerevisiae*. *Anal. Biochem.* **228**: 143-149.

Verduyn, C., E. Postma, W. A. Scheffers and J. P. van Dijken. 1990. Physiology of *Saccharomyces cerevisiae* in anaerobic glucose-limited chemostat cultures. *J. Gen. Microbiol.* **136**: 395-403.

Expression of the <i>ADH1</i> , <i>ADH2</i> , <i>ADH3</i> , <i>ADH4</i> and <i>ADH5</i> in response to pulse addition of ethanol or glucose to a continuous culture of strain W303-1A(a)	
Abstract.....	47
4.2 Introduction.....	47
4.2 Introduction.....	48
4.3 Materials and Methods.....	50
4.3.1 Strains and medium.....	50
4.3.2 Chemostat cultivation	50
4.3.3 Analytical procedures	50
4.3.4 Northern blot analysis.....	51
4.4 Results and Discussion	52
4.5 Conclusions.....	58
4.6 Literature cited.....	60
Figure 4.1	Steady-state concentrations of biomass (●), glucose (■) and ethanol (▲) in aerobic glucose-limited chemostat cultures of <i>S. cerevisiae</i> W303-1A(a) in chemically defined medium containing 8 g glucose l ⁻¹ 53
Figure 4.2	Metabolite levels during a dynamic response triggered by a glucose pulse. A 13.2 g l ⁻¹ pulse was added at time 0 to a glucose-limited steady-state culture of strain W303-1A(a) at a dilution rate of 0.17 h ⁻¹ . (Δ)..... 55
Figure 4.3	Northern analysis of gene transcription in response to a 13.2 g l ⁻¹ glucose pulse administered to a glucose-limited chemostat culture of strain W303-1A(a). Northern blot x-rays (A), RNA normalised against actin are indicated by the bars and expressed in % (B). The scales indicated on left in B represent 0-250%. Sampling times correspond with the metabolic profile depicted in Figure 2. The transcription of <i>ADH4</i> was not shown, since it could not be detected under these experimental conditions and <i>ADH5</i> levels were too low for quantification. 55
Figure 4.4	Metabolite levels during a dynamic response triggered by an ethanol pulse. A 7.8 g l ⁻¹ pulse was added (indicated by time 0) to a glucose-limited steady-state culture of strain W303-1A(a) at a dilution rate of 0.17 h ⁻¹ . Symbols: ethanol (▲), acetic acid (◻) and theoretical ethanol washout curve (Δ). 57
Figure 4.5	Northern analysis of gene transcription in response to a 7.8 g l ⁻¹ ethanol pulse administered to a glucose-limited chemostat culture of strain W303-1A(a). Northern blot x-rays (A), RNA normalised against actin are indicated by the bars and expressed in % (B). The scales indicated on left in B represent 0-250%. Sampling times correspond with the metabolic profile depicted in Figure 4. The transcription of <i>ADH4</i> was not shown, since it could not be detected under the experimental conditions and <i>ADH5</i> levels were too low for quantification. 57

CHAPTER 4

Expression of the *ADH1*, *ADH2*, *ADH3*, *ADH4* and *ADH5* genes in response to pulse addition of ethanol or glucose to a continuous culture of strain W303-1A(a)

Abstract

A chemostat culture of *Saccharomyces cerevisiae* strain W303-1A(a) at a dilution rate of 0.17 h^{-1} with a glucose feed concentration of 8 g l^{-1} was pulsed with 13.2 or 7.8 g l^{-1} glucose or ethanol, respectively. mRNA levels of *ADH1* to *ADH5* were monitored by Northern blot analyses during the transient response, until no residual carbon substrate could be detected. *ADH1* transcription was induced by glucose, but with some degree of repression by produced or added ethanol also evident. The expression of *ADH2* was repressed by glucose and, contrary to literature, was also repressed by ethanol. Full transcription could only be detected after the ethanol had completely disappeared from the culture. *ADH3* expression levels remained elevated while ethanol could be detected in the culture medium, suggesting that the ADH III mitochondrial enzyme could be another candidate for the first step in ethanol utilisation. *ADH4* expression was not detected and *ADH5* transcription was too low for quantification with the method used.

4.2 Introduction

Enzyme activities in the metabolic network of *Saccharomyces cerevisiae* are regulated at various levels. Among the most important is carbon source-dependent transcriptional regulation of genes, of which glucose repression is the most extensively studied example. In the presence of excess glucose, genes involved in the respiratory glucose metabolism or in the utilisation of less-favoured carbon sources are repressed (Gancedo, 1998; Ronne, 1995)

During the last few decades the function and regulation of the alcohol dehydrogenase enzymes of *S. cerevisiae* have been investigated by numerous authors (Denis *et al.*, 1983; Dombek *et al.*, 1993; Lutstorf & Megnet, 1968; Ruohonen *et al.*, 1995; Williamson & Paquin, 1987; Young & Pilgrim, 1985). Despite the wealth of knowledge that exists regarding the regulation of especially *ADH2* (Ciriacy, 1997), most experimental studies on transcriptional regulation in *S. cerevisiae* were done under ill defined physiological conditions, using shake flask cultures under either repressed or derepressed conditions (Sierkstra *et al.*, 1992). Chemostat cultivation offers an interesting alternative, since it allows reproducible experiments under aerobic, pH-controlled conditions. Fresh medium with a growth rate limiting concentration of glucose is pumped through the growth chamber at a constant rate, and a constant efflux of cells and medium from the growth chamber occurs at the same rate, ensuring cells in a well-defined physiological state (du Preez *et al.*, 2001; van den Berg *et al.*, 1996; van den Berg *et al.*, 1998).

Du Preez *et al.* (2001) investigated the expression of the *Trichoderma reesei* xylanase (*XYN2*) gene in *S. cerevisiae* that had been transformed using episomal multicopy plasmids with a promoter-terminator expression cassette derived from *S. cerevisiae ADH2*. By using chemostat cultures it was shown that *XYN2* transcription, under control of the *ADH2* promoter, was repressed by both glucose and ethanol. According to literature, the *ADH2* gene is derepressed in the presence of ethanol (Ciriacy, 1975; Denis *et al.*, 1981; Denis & Malvar, 1990) and the finding that ethanol repressed the *ADH2* promoter was contrary to expectation. This unrecognised facet of *ADH2* regulation also gave rise to questions regarding the regulation of the other iso-enzymes. The determination of physiological parameters influencing the regulation of *ADH1* and

ADH2 is of interest, since their promoters, especially that of *ADH2*, have been used in production of heterologous proteins (Cousens *et al.*, 1987; Lee & DaSilva, 2005; Ruohonen *et al.*, 1995). In addition, investigation of the effects of glucose and ethanol on the regulation of *ADH3*, *ADH4* and *ADH5* could assist in the elucidation of their currently undefined roles in ethanol metabolism.

The aim of the work reported in this chapter was to ascertain the expression levels of *ADH1* to *ADH5* in response to the pulse addition of glucose or ethanol to a glucose-limited chemostat culture of wild type strain W303-1A(a), especially to determine whether ethanol would result in transcriptional repression of genomic *ADH2*.

4.3 Materials and Methods

4.3.1 Strains and medium

S. cerevisiae strain W303-1A(a) was used, cultivated in carbon-limited chemically defined medium. The medium composition is given in Appendix A and the strain genotype in Appendix C, Table A.

4.3.2 Chemostat cultivation

Aerobic continuous culture experiments were conducted in a 2 litre Multigen F-2000 bioreactor (New Brunswick Scientific, Edison, NJ, USA) equipped with an exhaust gas condenser (reflux cooler), a pH electrode (Mettler Toledo, Halstead, Great Britain) and a polarographic oxygen electrode (Ingold AG, Urdorf, Switzerland), with a working volume of 650 to 700 ml. Silicone rubber tubing with peristaltic pumps (Watson Marlow Ltd, Cornwall, England) were used for the medium feed and level control by withdrawal of excess culture from the culture surface. These cultivations were conducted at 30°C with the pH controlled at pH 5.5 (± 0.1) by automatic titration with 3 M KOH. The dissolved oxygen tension was maintained above 20% of saturation using an aeration rate of 1000 ml min⁻¹ and manual adjustment of the stirrer speed within a range of 350 to 600 r min⁻¹. The chemostat was operated at a dilution rate of 0.17 h⁻¹ with a glucose concentration of 8 g l⁻¹ in the feed. Pulse experiments were conducted by administering pulses of glucose or ethanol directly into the culture at steady state, to give final concentrations of 13.2 and 7.8 g l⁻¹ respectively. Samples were taken directly from the culture at steady state, usually after three to five residence times, except when shifts from the respiratory to the respiro-fermentative region were carried out, in which case at least eight residence times were allowed before sampling. A steady state was defined as occurring when the culture turbidity varied less than $\pm 7\%$ for at least three consecutive residence times with no upward or downward trend.

4.3.3 Analytical procedures

Culture turbidity was monitored with a Photolab S6 photometer (WTW, Weilheim, Germany) at 690 nm and biomass was gravimetrically determined in duplicate by drying

centrifuged and washed samples at 105°C to constant weight. The ethanol, glucose and acetic concentrations were monitored over time following each pulse. The ethanol concentration of each sample was determined as described in Chapter 3. For determination of acetic acid, the samples were acidified with formic acid (7.5% v/v, final concentration) and assayed using the same analytical procedure as for determining the ethanol concentrations. The glucose concentration of the feed medium and the continuous culture supernatants were also determined as described in Chapter 3. Samples containing less than 1 g glucose l⁻¹ were analysed with a D-glucose bioanalysis kit (Boehringer Mannheim, Mannheim, Germany) with a detection limit of 4 mg glucose l⁻¹. For these assays, 10 ml samples were rapidly inactivated by aspirating into 30 ml bottles containing 500 µl ice-cold 5 M HCl and immediately put on ice. The pH of the supernatants was adjusted to neutrality with 5 M NaOH, centrifuged and stored at -20°C until the enzymatic determination of D-glucose was performed. The dilution factor of each sample was incorporated in the subsequent calculations.

Assuming that no ethanol uptake or evaporation occurred, the theoretical decrease in the ethanol concentration over time due to wash-out was calculated using the equation $P_t = P_o e^{-Dt}$, where P_t was the ethanol concentration at time t , P_o the initial ethanol concentration and D the dilution rate.

4.3.4 Northern blot analysis

During the pulse experiments samples were collected, centrifuged and the cell pellets were stored at -80°C. Total RNA was isolated according to the method described by Kohrer & Domdey (1991), 10 µg electrophoresed in formaldehyde agarose gels and blotted onto HybondTM N⁺ nylon membranes (Amersham) (Pelle & Murphy, 1993). Protocols for RNA isolation and Northern blotting are given in Appendix M and N. The blots were hybridised to PCR derived probes performed on plasmid DNA with High Fidelity Taq polymerase (Roche Applied Science) at reaction conditions described in Appendix F (Prog. 2). The plasmid template for each probe is listed in Appendix E and primers in Appendix D (Table B). The primer sequences for amplification of the ADH probes were obtained from van den Berg *et al.* (1998). The probes for *ADH1*, *ADH3*, *ADH4* and *ADH5* were amplified from the plasmid constructs in Figures O, AB, AF and AJ, respectively, using primer pairs ADH1-3F/ADH1-3R, ADH3-4F/ADH3-4R, ADH4-

4F/ADH4-4R and ADH5-4F/ADH5-4R. These four probes were labelled directly with PCR using radio-active (α - ^{32}P) dCTP (Amersham Biosciences, Biotech, UK). A special protocol was followed for the *ADH2* probe because of its high homology with *ADH1*. Therefore, a fragment downstream from the ORF was amplified, resulting in hybridisation of the probe to the untranslated regions of the mRNA (van den Berg *et al.*, 1998). A large fragment was amplified from plasmid DNA (Appendix E, Figure B) using primer pair ADH2-6F and ADH2-6R. The amplified fragment was digested with *Sau3A*, which cuts directly after the stop codon and yields a 325 bp fragment downstream of the ORF. This fragment was excised from agarose gel, cleaned using the GFX™ PCR DNA and gel band purification kit (GE Healthcare, Buckinghamshire, UK) and ^{32}P labelled using the High Prime labelling kit (Roche Applied Science) according to the instructions of the manufacturer. The *ACT1* probe used as an internal standard was obtained by cutting a 1140 bp fragment using *Bam*HI and *Hind*III from a plasmid containing the *ACT1* gene. This fragment was labelled ^{32}P in the same way as described for *ADH2*. Quantification was done using Quantity One version 4.5 values obtained were normalised against actin.

4.4 Results and Discussion

In aerobic glucose-limited chemostat cultures using chemically defined medium, *S. cerevisiae* W303-1A(a) exhibited respiratory growth at low dilution rates in a range of 0.074 to 0.2 h⁻¹ with high biomass yield coefficients, no ethanol production and as little as 0.015 g l⁻¹ residual glucose at steady state (Figure 4.1). On increasing the dilution rate from 0.21 to 0.34 h⁻¹, a point was reached where the limited respiratory capacity of the cells apparently was saturated; above that critical value, the metabolism of the yeast

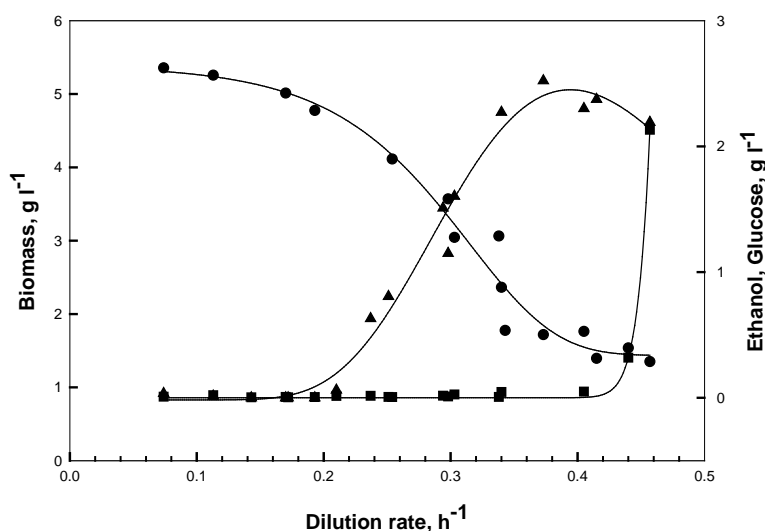


Figure 4.1 Steady-state concentrations of biomass (●), glucose (■) and ethanol (▲) in aerobic glucose-limited chemostat cultures of *S. cerevisiae* W303-1A(a) in chemically defined medium containing 8 g glucose l⁻¹.

shifted towards a respiro-fermentative (oxido-reductive) state with aerobic ethanol production taking place. The subsequent pulse experiments were performed at a dilution rate of 0.17 h⁻¹, where respiratory growth occurred and no ethanol production could be detected.

Transcription of the *ADH* genes was analysed during the transient response to a glucose and an ethanol pulse administered to a steady-state culture. This allowed a direct comparison of the regulation effect of glucose, ethanol and acetic acid. During the transient response, four phases could be distinguished according to the detectable carbon compounds: glucose, ethanol, acetic acid and none (Figure 4.2). The yeast consumed the excess glucose during the first 180 min while producing ethanol and acetic acid. This was followed directly by the consumption of ethanol from 180 to 780 min, which led to additional acetic acid production. The strain utilised the produced ethanol seeing that the experimental values did not follow the theoretical washout curve (Figure 4.2). Finally, acetic acid was consumed during the time interval of 780 to 960 min and no excess carbon was present from 960 to 1080 min.

ADH1 was slightly induced following the glucose pulse, but the level of mRNA dropped during the phase of ethanol assimilation from 210 to 540 min until ethanol had reached a concentration of 0.89 g l⁻¹. This decrease was expected since the activity of the *ADH1* promoter decreases towards the end of the glucose consumption phase (Ruohonen *et al.*, 1995). Below an ethanol concentration of 0.89 g l⁻¹ (t = 540 min, Figure 4.3) the amount of *ADH1* mRNA increased and stayed elevated throughout the acetic acid phase. On depletion of acetic acid the levels returned to the basal level detectable before the pulse was administered (Figure 4.3).

In contradiction to earlier findings of Yu *et al.* (1989), Dombek *et al.* (1993) and Denis *et al.* (1983) with shake flask cultivations, *ADH2* mRNA was detected during glucose-limited and glucose-excess growth. Furthermore, no derepression by ethanol was observed during the ethanol phase (t = 180 to 780 min, Figure 4.3). Ethanol even appeared to repress *ADH2* transcription, since full transcription could only be detected after the ethanol had disappeared completely from the culture.

Contrary to the findings of Young and Pilgrim (1985), glucose-induced repression of *ADH3* mRNA levels was not detected. *ADH3* levels showed an increase towards the ethanol phase and high levels of expression were detected throughout the ethanol phase of the pulse (Figure 4.3). As previously reported by Williamson & Paquin (1987) and van den Berg *et al.* (1998), *ADH4* mRNA was not detected. Van den Berg *et al.* (1998) suggested that a T-element in close proximity to the two Abf1 sites might mediate this silencing. They also reported rather strong and relatively constant levels of expression for *ADH5* in strain T2-3D during a similar pulse experiment. With strain W303-1A(a), however, a faint transcript of *ADH5* mRNA, too low for quantification, was detected (Figure 4.3).

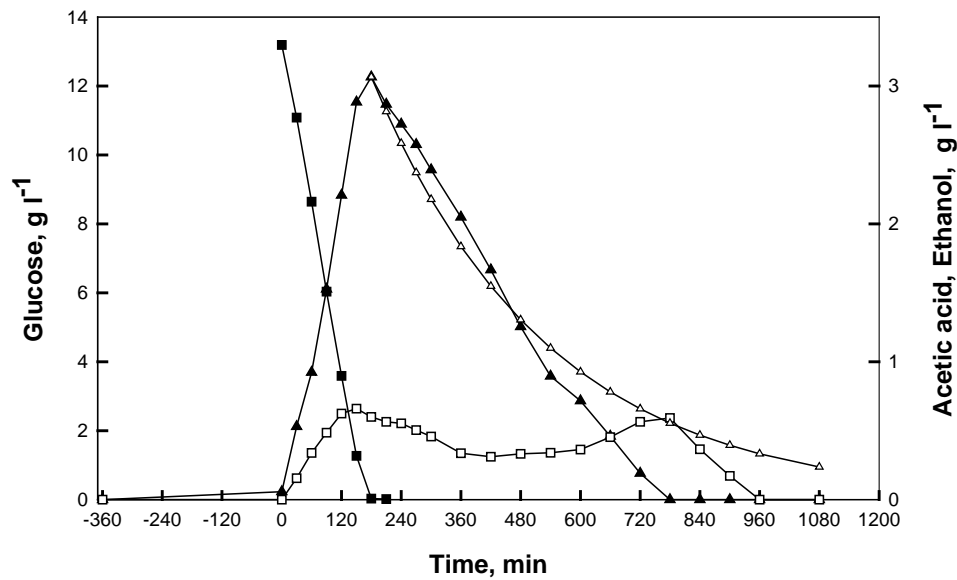


Figure 4.2 Metabolite levels during a dynamic response triggered by a glucose pulse. A 13.2 g l⁻¹ pulse was added at time 0 to a glucose-limited steady-state culture of strain W303-1A(a) at a dilution rate of 0.17 h⁻¹. Symbols: glucose (■), ethanol (▲), acetic acid (□) and theoretical ethanol washout curve (Δ).

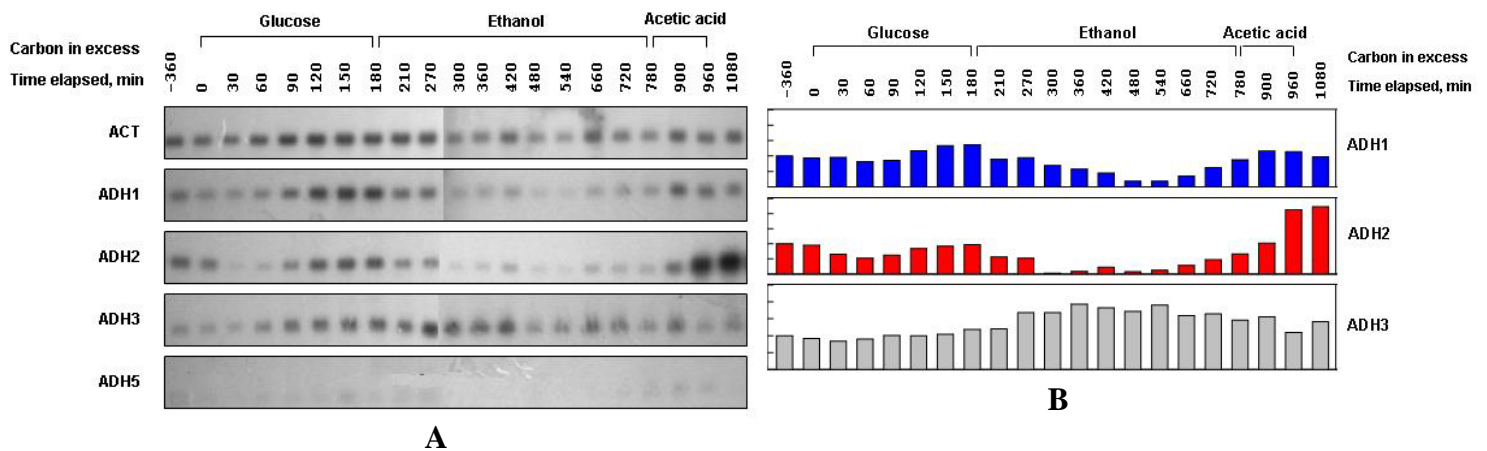


Figure 4.3 Northern analysis of gene transcription in response to a 13.2 g l⁻¹ glucose pulse administered to a glucose-limited chemostat culture of strain W303-1A(a). Northern blot x-rays (A), RNA normalised against actin are indicated by the bars and expressed in % (B). The scales indicated on left in B represent 0-250%. The transcription of *ADH4* was not shown, since it could not be detected under these experimental conditions and *ADH5* levels were too low for quantification.

A pulse experiment with 7.8 g ethanol l⁻¹ was also performed on strain W303-1A(a) grown under the same conditions (Figure 4.4). During the subsequent response an ethanol and acetic acid phase could be distinguished. The ethanol concentrations were always below the theoretical washout curve, indicating that ethanol consumption took place. Ethanol was consumed by the culture over a period of 12 h (t = 0 to 720 min, Figure 4.4) with the concomitant formation of acetic acid. During the second response phase the culture continued to utilise the acetic acid during the time interval of 720 to 960 min and no excess carbon substrate was present from 960 to 1080 min (Figure 4.4). *ADH1* levels decreased only slightly in response to the ethanol pulse, while *ADH2* transcription levels decreased dramatically and remained low during the ethanol phase. An increase in *ADH2* mRNA levels was only visible after no more ethanol could be detected in the culture (Figure 4.5). *ADH3* transcription was induced by ethanol and remained high until all the ethanol was utilised (t = 60 to 720 min, Figure 4.5). *ADH4* could once again not be detected under these conditions and *ADH5* transcription was faint towards the end of the ethanol phase, but too low for quantification.

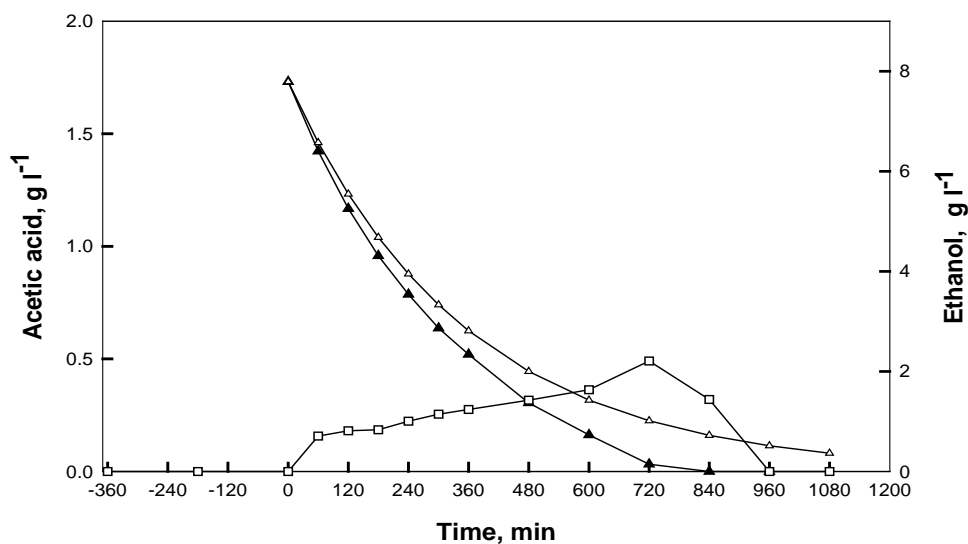


Figure 4.4 Metabolite levels during a dynamic response triggered by a ethanol pulse. A 7.8 g l^{-1} pulse was added (indicated by time 0) to a glucose-limited steady-state culture of strain W303-1A(a) at a dilution rate of 0.17 h^{-1} . Symbols: ethanol (\blacktriangle), acetic acid (\square), and theoretical ethanol washout curve (\triangle).

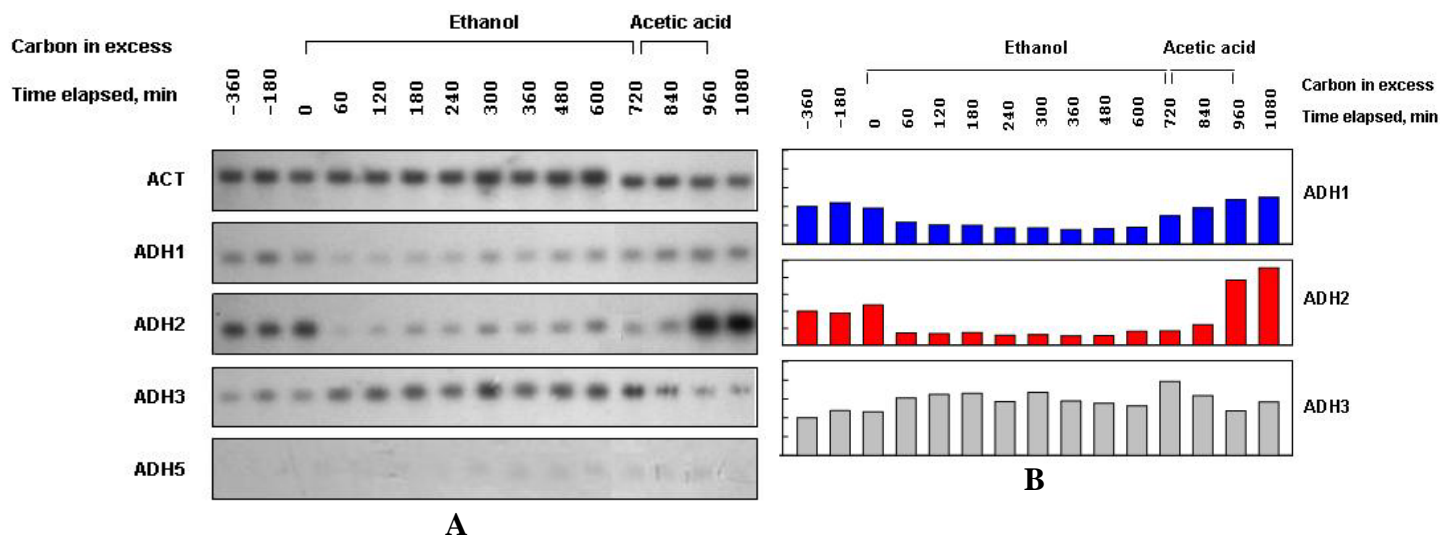


Figure 4.5 Northern analysis of gene transcription in response to a 7.8 g l^{-1} ethanol pulse administered to a glucose-limited chemostat culture of strain W303-1A(a). Northern blot x-rays (A), RNA normalised against actin are indicated by the bars and expressed in % (B). The scales indicated on left in B represent 0-250%. Sampling times correspond with the metabolic profile depicted in Figure 4. The transcription of *ADH4* was not shown, since it could not be detected under the experimental conditions and *ADH5* levels were too low for quantification.

4.5 Conclusions

Transcription of the *ADH* genes was analysed during the transient response to a glucose and an ethanol pulse in a glucose-limited chemostat culture. Most transcription studies so far have dealt with one gene in static systems using shake flask cultures (Pronk *et al.*, 1996). Bioreactor cultures are better experimental systems since the parameter of interest can be varied while maintaining all other parameters constant.

The increase in *ADHI* transcription during the glucose phase of a glucose pulse correlated with the fact that the ADH I enzyme is the main fermentative enzyme responsible for ethanol formation in the cell (Ciriacy, 1979; Heick *et al.*, 1969). Although it has been stated that the *ADHI* promoter is turned off when cells enter the ethanol consumption phase (Denis *et al.*, 1983; Ruohonen *et al.*, 1995), it is evident from the data reported here that *ADHI* mRNA was still detectable whether the culture medium contained produced or added ethanol. *ADH2* transcription was repressed by glucose as reported by various authors (Ciriacy, 1978; Cook & Denis, 1993; Denis *et al.*, 1983; Dombek *et al.*, 1993; Lutstorf & Megnet, 1968), but contrary to the findings of Young and Pilgrim (1985) and in accordance with reports of van den Berg *et al.* (1998) and du Preez *et al.* (2001), was also repressed by ethanol. Seeing that ADH II is generally believed to be the major enzyme responsible for the first step of ethanol utilisation (Lutstorf & Megnet, 1968), it is remarkable that an enzyme that uses ethanol as a substrate (Leskovac *et al.*, 2002; Thomson *et al.*, 2005; Wills, 1976; Wills *et al.*, 1982) was repressed at transcriptional level when growing on ethanol and derepressed on acetic acid. These findings as well as the high and constant expression levels of *ADH3* during the ethanol phases of both pulse experiments, allows some speculation on the accepted roles of ADH I and ADH II as the main fermentative and oxidative enzymes, respectively. The induction of the *ADH3* gene during the ethanol phase of the pulses suggested that the mitochondrial ADH III enzyme could also be involved in the first step in ethanol utilisation. This also raised the question of whether the enzymes were able to functionally substitute for each other when all five genes were present in the genome.

In accordance with previous data, *ADH4* expression could not be detected (van den Berg *et al.*, 1998; Williamson & Paquin, 1987). Although *ADH5* transcription levels detected here were too low for quantification, it is an interesting prospect to investigate *ADH5* expression in an *adh* null background. Since a previous study by Drewke *et al.* (1990) reported ethanol production in such a strain, investigating *ADH5* expression with a more sensitive detection method could provide valuable information on its role in the ethanol metabolism.

4.6 Literature cited

- Ciriacy, M.** 1975. Genetics of alcohol dehydrogenase in *Saccharomyces cerevisiae*. II. Two loci controlling synthesis of the glucose-repressible ADH II. *Mol. Gen. Genet.* **138**: 157-164.
- Ciriacy, M.** 1978. A yeast mutant with glucose-resistant formation of mitochondrial enzymes. *Mol. Gen. Genet.* **159**: 329-335.
- Ciriacy, M.** 1979. Isolation and characterization of further cis- and trans-acting regulatory elements involved in the synthesis of glucose-repressible alcohol dehydrogenase (ADHII) in *Saccharomyces cerevisiae*. *Mol. Gen. Genet.* **176**: 427-431.
- Ciriacy, M.** 1997. Alcohol dehydrogenases. In Yeast sugar metabolism. Zimmermann, F. K. and Entian, K. D. *Technomic publishing co.inc.* pp. 213-223.
- Cook, W. J. and C. L. Denis.** 1993. Identification of three genes required for the glucose-dependent transcription of the yeast transcriptional activator ADR1. *Curr. Genet.* **23**: 192-200.
- Cousens, L. S., J. R. Shuster, C. Gallegos, L. L. Ku, M. M. Stempien, M. S. Urdea, R. Sanchez-Pescador, A. Taylor and P. Tekamp-Olson.** 1987. High level expression of proinsulin in the yeast, *Saccharomyces cerevisiae*. *Gene* **61**: 265-275.
- Denis, C. L., M. Ciriacy and E. T. Young.** 1981. A positive regulatory gene is required for accumulation of the functional messenger RNA for the glucose-repressible alcohol dehydrogenase from *Saccharomyces cerevisiae*. *J. Mol. Biol.* **148**: 355-368.
- Denis, C. L., J. Ferguson and E. T. Young.** 1983. mRNA levels for the fermentative alcohol dehydrogenase of *Saccharomyces cerevisiae* decrease upon growth on a nonfermentable carbon source. *J. Biol. Chem.* **258**: 1165-1171.
- Denis, C. L. and T. Malvar.** 1990. The *CCR4* gene from *Saccharomyces cerevisiae* is required for both nonfermentative and spt-mediated gene expression. *Genetics* **124**: 283-291.
- Dombek, K. M., S. Camier and E. T. Young.** 1993. *ADH2* expression is repressed by REG1 independently of mutations that alter the phosphorylation of the yeast transcription factor ADR1. *Mol. Cell Biol.* **13**: 4391-4399.
- Drewke, C., J. Thielen and M. Ciriacy.** 1990. Ethanol formation in *adh0* mutants reveals the existence of a novel acetaldehyde-reducing activity in *Saccharomyces cerevisiae*. *J. Bacteriol.* **172**: 3909-3917.
- du Preez, J. C., J. E. Mare, J. Albertyn and S. G. Kilian.** 2001. Transcriptional repression of *ADH2*-regulated beta-xylanase production by ethanol in recombinant strains of *Saccharomyces cerevisiae*. *FEMS Yeast Res.* **1**: 233-240.
- Gancedo, J. M.** 1998. Yeast carbon catabolite repression. *Microbiol. Mol. Biol. Rev.* **62**: 334-361.
- Heick, H. M. C., J. Willemot and N. Begin-heick.** 1969. The subcellular localization of alcohol dehydrogenase activity in baker's yeast. *Biochim. Biophys. Acta.* **191**: 493-501.
- Kohrer, K. and H. Domdey.** 1991. Preparation of high molecular weight RNA. *Methods Enzymol.* **194**: 398-405.

- Lee, K. M. and N. A. DaSilva.** 2005. Evaluation of the *Saccharomyces cerevisiae* ADH2 promoter for protein synthesis. *Yeast* **22**: 431-440.
- Leskovac, V., S. Trivic and D. Pericin.** 2002. The three zinc-containing alcohol dehydrogenases from baker's yeast, *Saccharomyces cerevisiae*. *FEMS Yeast Res.* **2**: 481-494.
- Lutstorf, U. and R. Megnet.** 1968. Multiple forms of alcohol dehydrogenase in *Saccharomyces cerevisiae*. I. Physiological control of ADH-2 and properties of ADH-2 and ADH-4. *Arch. Biochem. Biophys.* **126**: 933-944.
- Pelle, R. and N. B. Murphy.** 1993. Northern hybridization: rapid and simple electrophoretic conditions. *Nucleic Acids Res.* **21**: 2783-2784.
- Pronk, J. T., S. H. Yde and J. P. van Dijken.** 1996. Pyruvate metabolism in *Saccharomyces cerevisiae*. *Yeast* **12**: 1607-1633.
- Ronne, H.** 1995. Glucose repression in fungi. *Trends Genet.* **11**: 12-17.
- Ruohonen, L., M. K. Aalto and S. Keranen.** 1995. Modifications to the ADH1 promoter of *Saccharomyces cerevisiae* for efficient production of heterologous proteins. *J. Biotechnol.* **39**: 193-203.
- Sierkstra, L. N., J. M. Verbakel and C. T. Verrips.** 1992. Analysis of transcription and translation of glycolytic enzymes in glucose-limited continuous cultures of *Saccharomyces cerevisiae*. *J. Gen. Microbiol.* **138**: 2559-2566.
- Thomson, J. M., E. A. Gaucher, M. F. Burgan, D. W. De Kee, T. Li, J. P. Aris and S. A. Benner.** 2005. Resurrecting ancestral alcohol dehydrogenases from yeast. *Nat. Genet.* **37**: 630-635.
- van den Berg, M. A., P. Jong-Gubbels, C. J. Kortland, J. P. van Dijken, J. T. Pronk and H. Y. Steensma.** 1996. The two acetyl-coenzyme A synthetases of *Saccharomyces cerevisiae* differ with respect to kinetic properties and transcriptional regulation. *J. Biol. Chem.* **271**: 28953-28959.
- van den Berg, M. A., P. Jong-Gubbels and H. Y. Steensma.** 1998. Transient mRNA responses in chemostat cultures as a method of defining putative regulatory elements: application to genes involved in *Saccharomyces cerevisiae* acetyl-coenzyme A metabolism. *Yeast* **14**: 1089-1104.
- Williamson, V. M. and C. E. Paquin.** 1987. Homology of *Saccharomyces cerevisiae* ADH4 to an iron-activated alcohol dehydrogenase from *Zymomonas mobilis*. *Mol. Gen. Genet.* **209**: 374-381.
- Wills, C.** 1976. Controlling protein evolution. *Fed. Proc.* **35**: 2098-2101.
- Wills, C., P. Kratofil and T. Martin.** 1982. Functional mutants of yeast alcohol dehydrogenase. *Basic Life Sci.* **19**: 305-329.
- Young, E. T. and D. Pilgrim.** 1985. Isolation and DNA sequence of ADH3, a nuclear gene encoding the mitochondrial isozyme of alcohol dehydrogenase in *Saccharomyces cerevisiae*. *Mol. Cell Biol.* **5**: 3024-3034.
- Yu, J., M. S. Donoviel and E. T. Young.** 1989. Adjacent upstream activation sequence elements synergistically regulate transcription of ADH2 in *Saccharomyces cerevisiae*. *Mol. Cell Biol.* **9**: 34-42.

Growth kinetics and transcription levels of the ADH genes in a recombinant strain over-expressing <i>ADH2</i> in batch cultures	62
Abstract.....	62
5.2 Introduction.....	63
5.3 Materials and Methods.....	64
5.3.1 Strains and media.....	64
5.3.2 Construction of an <i>ADH2</i> single deletion mutant (SΔ2a).....	64
5.3.3 Construction of recombinant strain SΔ2aTR_ <i>ADH2</i> over-expressing <i>ADH2</i>	66
5.3.4 Cultivation conditions.....	66
5.3.5 Analyses.....	67
5.3.6 Real time PCR.....	68
5.4 Results and Discussion	70
5.5 Conclusions.....	79
5.6 Literature cited.....	81

Figure 5.1 (A) PCR amplicon representing the *ADH2* ORF flank both 5' and 3' by 1000 bp non-coding sequence, lane 1. (B) The 3017 bp PCR fragment cloned into pGemT-Easy and digested with *EcoRI* and *HindIII* for verification, lane 2. (C) The *padh2Δ::URA3* plasmid construct verified by digestion with *PvuII*, *NheI* and *EcoRV*, lane 3. The lanes designated M represent λ III marker DNA of which the band lengths can be viewed in Appendix P. Band lengths are indicated in base pairs. 70

Figure 5.2 Nucleotide sequence alignment of the *ADH2* ORF cloned into pGemT-Easy and the sequence retrieved from the *Saccharomyces* genome data base (*adh2* *sgd*). The alignment was performed with DNassist software. 71

Figure 5.3 Restriction enzyme digestion profile of two independent pCM190L_W::*ADH2* plasmid constructs digested with *EcoRI* and *BamHI* (lanes 1 & 2). Lane M represents λ III marker DNA (Appendix P). 72

Figure 5.4 Typical bioreactor cultivation profiles of strains SΔ2aTR_E (A,B) and SΔ2aTR_*ADH2* (C, D) grown aerobically in chemically defined medium

	without tryptophan with 20 g l ⁻¹ glucose as carbon source. Symbols: Biomass (●), glucose (■), ethanol (▲), Acetic acid (□) and glycerol (○). The metabolite concentrations are representative of independent duplicate experiments.	74
Figure 5.5	Real-time RT-PCR transcription profiles of the <i>ADH1</i> , <i>ADH4</i> and <i>ADH5</i> in strains SΔ2aTR_E (A, C, E) and SΔ2aTR_ADH2 (B, D, F) grown aerobically in chemically defined medium (-TRP) in bioreactors with 20 g l ⁻¹ glucose as carbon source. The glucose (■) and ethanol (▲) concentrations were derived from Figure 5.4.	76
Figure 5.6	Typical bioreactor cultivation profiles of strains SΔ2aTR_E (A) and SΔ2aTR_ADH2 (B) grown aerobically in chemically defined medium without tryptophan with 6.9 and 6.2 g l ⁻¹ ethanol as carbon source. Symbols: Biomass (●) and ethanol (▲). The metabolite concentrations are representative of independent duplicate experiments.	77
Figure 5.7	Real-time RT-PCR transcription profiles of the <i>ADH1</i> , <i>ADH4</i> and <i>ADH5</i> in strains SΔ2aTR_E (A, C, E) and SΔ2aTR_ADH2 (B, D, F) grown aerobically in chemically defined medium without tryptophan in bioreactors with 6.9 and 6.2 g l ⁻¹ ethanol as carbon source. The ethanol (▲) concentrations were derived from Figure 5.6.	78
Table 5.1	Growth parameters of <i>S. cerevisiae</i> strains SΔ2aTR_E and SΔ2aTR_ADH2 in bioreactor cultures grown on glucose or ethanol.	75

CHAPTER 5

Growth kinetics and transcription levels of the *ADH* genes in a recombinant strain over-expressing *ADH2* in batch cultures

Abstract

Strain S Δ 2a lacking the *ADH2* structural gene was constructed by partially replacing the ORF with the *URA3* marker gene. Isogenic strains S Δ 2aTR_E and S Δ 2aTR_*ADH2* were constructed from S Δ 2a using standard transformation techniques. Strain S Δ 2aTR_*ADH2* over-expressed the *ADH2* gene on a multicopy episomal vector pCM190L_W and control strain S Δ 2aTR_E contained only the empty pCM190L_W vector. Bioreactor cultivations of these strains in chemically defined medium with glucose or ethanol as carbon source, showed no discernable difference in the growth parameters. Real-time RT-PCR was employed to monitor the expression levels of the other *ADH* genes. *ADH1* transcription levels of both strains were detected with both carbon sources and showed elevated levels during the ethanol assimilation phase of diauxic growth. *ADH4* transcription was detected during the ethanol assimilation phase of diauxic growth. However, when the same strains were grown on ethanol as a carbon source, the transcription of *ADH4* was only detected when ethanol reached a concentration of 0.103 g l⁻¹. This study also revealed that the *ADH5* gene was the only *ADH* gene monitored which showed a different transcription profile for the strain over-expressing *ADH2* when grown on glucose. Transcription of *ADH5* in the S Δ 2aTR_*ADH2* strain indicated a possible contribution towards ethanol production. Unfortunately, *ADH3* transcription was not monitored due to the lack of an acceptable TaqMan probe.

5.2 Introduction

The earliest studies of regulation of the *ADH* genes of *S. cerevisiae* was documented by Ciriacy (1975). *ADH2* showed typical catabolite repression (Gancedo, 1998) where the presence of glucose repressed the transcription several fold (Price *et al.*, 1990). The *ADH2* structural gene is subject to rigorous regulation by at least 24 unlinked genetic elements or proteins (discussed in detail in Chapter 2). Possible repression by ethanol has recently been proposed by van den Berg *et al.* (1998), du Preez *et al.* (2001) and in chapter 4 of this study, where *ADH2* transcription levels decreased upon the pulse addition of ethanol to continuous cultures of various strains. It would be interesting to observe the function of the *ADH2* ORF where it is relieved from any repression.

The expression of foreign genes in *S. cerevisiae* is commonly regulated by native yeast promoters. Inducible promoters like *CUP1* and *GAL1* are employed to control the time and level of gene expression (Romanos *et al.*, 1992). The tetracycline (tet) inducible gene expression system developed by Gossen & Bujard (1992) is useful for controlling the expression of targeted genes and for determining the roles of the gene products in cellular functions. In the tet expression system the expression of a target gene under transcriptional control of a tet operator Cytochrome C hybrid promoter (tetO₇-CYC1) is fully activated in growth medium without doxycycline (tetracycline analogue)(Gossen & Bujard, 1992). This innovative system allows the expression of indigenous or foreign genes in yeast without any induction.

This aim of this chapter was to investigate whether over-expression of the native *ADH2* gene under control of a foreign unregulated promoter had any impact on the metabolism and the transcription profiles of the other *ADH* genes. Batch cultivations were performed in bioreactors with both glucose and ethanol as carbon sources.

5.3 Materials and Methods

5.3.1 Strains and media

The W303-1A(a), S Δ 2a, S Δ 2aTR_E and S Δ 2aTR_ADH2 strains were used in this study. W303-1A(a) was used for the construction of strain S Δ 2a, which contains a single deletion of the ADH2 gene. S Δ 2aTR_E and S Δ 2aTR_ADH2 are recombinant strains representing S Δ 2a transformed with the empty pCM190L_W plasmid and recombinant pCM190L_W::ADH2 construct respectively. Batch cultivations were performed in chemically defined medium containing glucose or ethanol as carbon source. Selective pressure was exercised by excluding tryptophan from the medium. *Escherichia coli* strain Top 10F used for propagation of plasmid constructs were plated on LB medium and yeast transformation and screenings on YNB dropout medium. The different media are presented in Appendix A and the strain genotypes are available in Appendix C, Table A.

5.3.2 Construction of an ADH2 single deletion mutant (S Δ 2a)

The ADH2 ORF flanked by 1000 bp non-coding regions was amplified from 118 ng W303-1A(a) genomic DNA with Expand Long Template Taq polymerase (Roche Applied Science) using the reaction mixtures and conditions described in Appendix F (Prog. 1). Primer pair ADH2-1F/ADH2-1R was employed (Appendix D, Table B) at an annealing temperature of 55°C. The pADH2 plasmid (Appendix E, Figure B) was constructed by ligating this 3017 bp PCR amplicon (Appendix E, Figure Z) into the pGemT-Easy vector (Appendix E, Figure A) and propagating it in *E. coli* cells as described by Sambrook & Russel (2001) (Appendix H & I). pADH2 was isolated from *E. coli* cells using the standard method described by Becker *et al.* (1990) (Appendix K) and subjected to restriction enzyme digestion (Appendix G) for verification. The 3017 bp fragment was also sub-cloned by excision with *EcoRI* and ligated into a single *EcoRI* site of the pUC18 vector (Appendix E, Figure C). This was necessary to facilitate the cloning of the 3' non-coding region during construction of the deletion plasmid. During two subsequent cloning events the 5'- and 3' non-coding regions of ADH2 were inserted into

the pJJ244 vector (Appendix E, Figure K) flanking the *URA3* yeast marker gene. A 1048 bp fragment extending from the *EcoRI* site in the 5' non-coding region to the *EcoRV* site 66 bp within the *ADH2* coding sequence of p*ADH2* was excised and ligated into *EcoRI* and *SmaI* digested pJJ244. A 1347 bp fragment extending from the *HindIII* site 286 bp in the *ADH2* coding region to the *HindIII* site in the pUC18 multiple cloning site was excised and cloned into pJJ244 digested at a single *HindIII* site. The *padh2Δ::URA3* deletion plasmid (Appendix E, Figure Y) therefore, has the flanking regions of the *ADH2* gene and 649 bp of the *ADH2* ORF replaced by the *URA3* marker gene verified by restriction enzyme digestion with *PvuII*, *NheI* and *EcoRV*.

The 3425 bp *adh2Δ::URA3* PCR construct (Appendix E, Figure AA) was amplified with Expand Long Template Taq polymerase using 50 ng of the plasmid *padh2Δ::URA3* as template and primer pair ADH2-1F/ADH2-1R (Appendix D, Table B) at an annealing temperature of 55°C. PCR reaction mixtures and conditions are described in Appendix F (Prog. 1). The linear PCR product was transformed to W303-1A(a) yeast cells using the method described by Chen *et al.* (1992) (Appendix J) and plated on YNB dropout plates without uracil. Colonies that appeared after 2 days of incubation at 30°C were verified by analytical PCR.

A number of colonies were chosen at random and genomic DNA was isolated using the method described by Labuschagne & Albertyn (2007) (Appendix K). This DNA served as template in the verification PCR of which the reaction mixtures and conditions are shown in Appendix F (Prog. 3). Taq polymerase supplied by New England Biolabs and primer pair ADH2-3F/URA3-1F (Appendix D, Table B) were used at an annealing temperature of 52°C. The ADH2-3F primer hybridised to the genomic DNA 100 bp further upstream from the ADH2-1F primer and the URA3-1F primer hybridised to the *URA3* marker gene. Amplification of the desired 1282 bp fragment was only possible if the gene replacement occurred at the preferred chromosomal location (Appendix E, Figure AA). Transformants with the correct genetic profile were designated SΔ2a and preserved in 15% glycerol and stored at – 80°C as described in Appendix B.

5.3.3 Construction of recombinant strain SΔ2aTR_ADH2 over-expressing ADH2

The *ADH2* ORF was amplified from 118 ng W303-1A(a) genomic DNA with High Fidelity Taq polymerase (Roche Applied Science) under reaction conditions described in Appendix F (Prog. 3). Primer pair ADH2-5F/ADH2-4R (Appendix D, Table B) were used at an annealing temperature of 53°C. Since the primers used for producing this amplicon did not distinguish between *ADH1* and *ADH2* and produced two bands of exactly the same length, the PCR products were cloned into the pGemT-Easy vector (Appendix H & I) and submitted to *EcoRI* digestion to confirm insertion. Four colonies were chosen at random and submitted to bidirectional sequencing with primers Sp6 and T7 (Appendix D, Table B). Sequencing was performed on a ABI Prism 377 DNA sequencer with the ABI Prism™ Big Dye terminator™ V3.0 cycle sequencing ready reaction kit (Applied Biosystems).

The *ADH2* ORF from the chosen plasmid (Appendix E, Figure D) was excised with restriction sites *Bam*HI, introduced by primer ADH2-5F at the start codon of the *ADH2* gene, and *Not*I in the multiple cloning site of the pGemT-Easy vector. The linear fragment was site directionally ligated into the multiple cloning site of the pCM190L_W shuttle vector (Appendix E, Figure E) and propagated in Top 10F *E. coli* cells. The pCM190L_W::*ADH2* plasmid construct (Appendix E, Figure F) was submitted to enzyme digestion analyses for verification. This construct was transformed into the SΔ2a strain as described in Appendix J and plated on YNB dropout medium without uracil and tryptophan. A control strain SΔ2aTR_E, which is simply strain SΔ2a transformed with the empty pCM190L_W vector, was included in the batch cultivation studies as negative control. The absence and over-expression of *ADH2* were verified with real-time RT-PCR.

5.3.4 Cultivation conditions

Aerobic batch cultivations experiments were conducted in 2 litre Multigen F-2000 bioreactors (New Brunswick Scientific, Edison, NJ, USA) equipped with exhaust gas condensers (reflux cooler), pH electrodes (Mettler Toledo, Halstead, Great Britain) and polarographic oxygen electrodes (Ingold AG, Urdorf, Switzerland), with a working

volume of 1 000 ml. These cultivations were conducted at 30°C with the pH controlled at pH 5.5 (\pm 0.1) by automatic titration with 3 M KOH. The dissolved oxygen tension was maintained above 20% of saturation by manual adjustment of the aeration rate and the stirrer speed within a range of 350 to 600 r min⁻¹.

For the cultivations on 20 g glucose l⁻¹ as carbon source pre-inocula were prepared by reviving cells from cryo-storage on YPD plates for 2 to 3 days at 30°C as described in Appendix B. These cells were used to inoculate a 250 ml Erlenmeyer flask containing 50 ml chemically defined medium with 20 g glucose l⁻¹. After incubation for 11 h at 30°C on a rotary shaker, 2.5 ml of the latter culture was transferred to a new Erlenmeyer flask containing fresh medium and incubated under the same conditions. This step was repeated before 30 ml of the exponentially growing cells served as inoculum for aerobic bioreactor cultivations. For the ethanol growth studies, pre-inocula were also prepared by revival and subsequent cultivation in 250 ml Erlenmeyer flask containing 50 ml chemically defined medium with 20 g glucose l⁻¹. After 21 h of incubation (6 h after glucose depletion) 15 ml of the shake flask culture was used to inoculate the bioreactors containing chemically defined medium with 7 g ethanol l⁻¹.

5.3.5 Analyses

Culture turbidity was monitored at 600 nm with a BioPhotometer (Eppendorf, Hamburg, Germany) and converted to dry biomass using a standard curve. Cells were harvested during late exponential phase, cooled on ice, centrifuged at 3 000 r min⁻¹ for 5 min, washed twice with distilled water and dried at 105°C overnight prior to gravimetric determination of the dry biomass concentration. The glucose and ethanol concentrations were determined as described in Chapter 3 and the acetic acid concentrations as mentioned in Chapter 4. Glycerol concentrations were determined with a Hewlett Packard 1100 high-performance liquid chromatograph equipped with a refractive index detector and a Phenomenex Luna 5u NH2 100A column operating at 35°C with an eluent (degassed 75% acetonitrile) flow rate of 2 ml.min⁻¹.

5.3.6 Real time PCR

Total RNA was extracted from periodically taken samples using the method described by Kohrer & Domdey (1991) (Appendix M) and quantified on the Nanodrop ND 1000 Spectrophotometer (NanoDrop Technologies, Wilmington, USA) Real-time RT-PCR was performed on total RNA pre-treated with DNaseI enzyme as described in Appendix O. The absence of genomic DNA was confirmed by PCR amplification without the reverse transcription step.

Amplification and detection were carried out in a 72 ring Rotor Gene 3000 (Corbett Research, Sydney, Australia). The fluorescently labelled oligonucleotide TaqMan probes and PCR primers for the *ADH* genes were designed with the FastPCR probe and primer design tool available on the Internet (Institute of Biotechnology, University of Helsinki, Finland: <http://www.biocenter.helsinki.fi/bi>). The ADH probes and primers were manufactured and supplied by Inqaba Biotech (Johannesburg, South Africa). The probes were labelled at the 5' end with the reporter dye 6-carboxyfluorescein (FAM) and with Black whole quencher (BHQ1) at the 3' end. Unfortunately no suitable probe could be designed for *ADH3* despite numerous attempts, therefore the transcription levels of this gene was not monitored. The fluorescently labelled probe and ACT-fw/ACT-as primers for the housekeeping gene *ACT1* was designed, manufactured and supplied by (Ambion, Austin, Texas). The ACT probe was labelled at the 5' end with JOE and quenched at the 3' end with TAMRA. The sequences of the primers are given in Appendix D, Table B and that of the TaqMan probes in Table C. Specificity was tested by using total RNA isolated from batch cultures of single deletion mutant of each gene. The primers and probes were deemed specific when no signal was obtained from a PCR performed on total RNA originating from a strain where the target gene was absent from the genome. Each multiplex PCR was performed in a 10 µl reaction mixture with the 2x SensiMix One-Step Kit (Quantace, London, UK). The final concentrations of all the reaction constituents and reaction conditions are given in Appendix O.

For semi-quantification of the transcripts a standard curve was constructed using DNA of each gene as standard. For this, plasmid constructs containing the ORF of *ACT1* and each of the *ADH* genes (Appendix E, Figure B, O, AF, AJ) were used as templates and a portion of each ORF was PCR amplified. Primer pairs ACT1-1F/ACT1-1R was

used for amplifying a portion of *ACT1*, ADH2-6F/uni2-R for *ADH1* and *ADH2*, ADH4-4F/ADH4-4R for *ADH4* and ADH5-4F/ADH5-1R for *ADH5* (Appendix D, Table B). The Taq DNA polymerase (New England Biolabs), other reaction component concentrations and reaction conditions are shown in Appendix F, Programme 5. PCR products were separated in a 1% agarose gel, DNA was eluted from the gel and spectrophotometrically quantified in quadruplicate. Copy numbers were calculated using the amount of DNA (ng) and the length of template (bp) (<http://www.uri.edu/research/gsc/resources/cndna.html>). The real-time RT-PCR reaction for each gene was set up using serial 10-fold dilutions of the amplified fragment as the DNA template. Three independent replicates were used for normalisation. Standard curves were used by the Rotor Gene 3000 Analyses software for calculation of C_T values and copy numbers. Copy numbers were normalised against Actin and plotted on a log scale for interpretation.

5.4 Results and Discussion

Strain S Δ 2a, which contained a single deletion in the *ADH2* gene was constructed by replacement of the ORF with the *URA3* yeast marker gene. The 3017 bp *ADH2* ORF flanked on both sides with 1000 bp non-coding sequence was amplified from the genome of strain W303-1A(a) and cloned into the pGemT-Easy vector (Figure 5.1A). Cloning and orientation was verified by the presence of 2834 bp, 1740 bp and 1296 bp fragments upon digestion with restriction enzymes *EcoRI* and *HindIII* (Figure 5.1B). The 3017 bp fragment was also sub-cloned into the pUC18 vector by means of *EcoRI*. The 5' and 3' non-coding regions were cloned into the pJJ244 vector as described in the Materials and Methods, resulting in 649 bp of the *ADH2* ORF replaced by the *URA3* marker gene. This plasmid construct, *padh2* Δ ::*URA3* (Appendix E, Figure Y), was digested with *PvuII*,

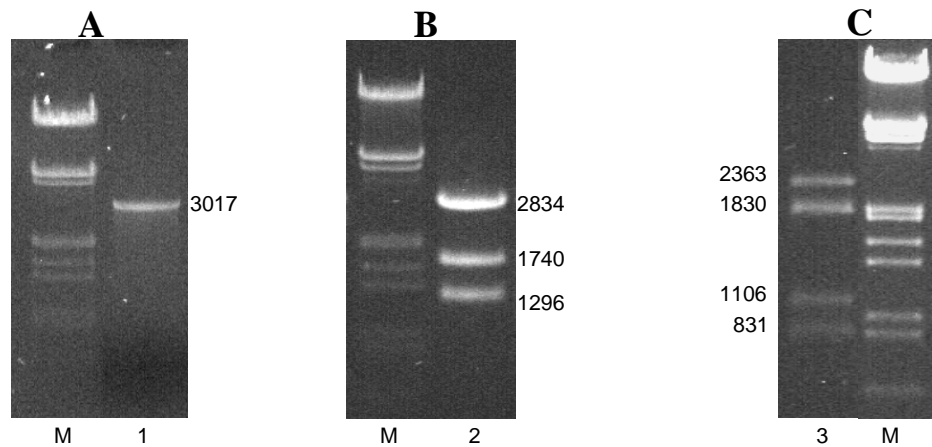


Figure 5.1 (A) PCR amplicon representing the *ADH2* ORF flank both 5' and 3' by 1000 bp non-coding sequence, lane 1. (B) The 3017 bp PCR fragment cloned into pGemT-Easy and digested with *EcoRI* and *HindIII* for verification, lane 2. (C) The *padh2* Δ ::*URA3* plasmid construct verified by digestion with *PvuII*, *NheI* and *EcoRV*, lane 3. The lanes designated M represent λ III marker DNA of which the band lengths can be viewed in Appendix P. Band lengths are indicated in base pairs.

NheI and *EcoRV* which yielded four bands of 2363 bp, 1830 bp, 1106 bp and 831 bp in length (Figure 5.1C). PCR amplicon derived from using this construct as template DNA was transformed to W303-1A(a) yeast cells. Positive colonies were selected on YNB dropout medium without uracil and screened for the deletion with PCR.

The SΔ2aTR_ADH2 strain contained the *ADH2* gene in a multi-copy episomal vector with a Tetracycline operator Cytochrome C hybrid promoter that insures constitutive expression of the target gene without any induction. The *ADH2* ORF was amplified from genomic DNA, cloned into the pGemT-Easy vector and confirmed by sequencing analysis (Figure 5.2). The gene was excised from pGemT-Easy and inserted

adh2 sgd	1	ATGCTATTCCAGAACTCAAAAAGCCATTATCTTCTACGAATCCAACGGCAAGTTGGAGCATAAAGGATATCC	73
adh2 cloned	1	ATGCTATTCCAGAACTCAAAAAGCCATTATCTTCTACGAATCCAACGGCAAGTTGGAGCATAAAGGATATCC	73
adh2 sgd	74	CAGTTCCAAAGCCAAAGCCCAACGAATTGTTAATCAACGTCAAGTACTCTGGTGTCTGCCACACCGATTGCA	146
adh2 cloned	74	CAGTTCCAAAGCCAAAGCCCAACGAATTGTTAATCAACGTCAAGTACTCTGGTGTCTGCCACACCGATTGCA	146
adh2 sgd	147	CGCTTGGCATGGTACTGGCCATTGCCAACTAAGTTACCATTAGTTGGTGGTCACGAAGGTGCCGGTGTCTGTT	219
adh2 cloned	147	CGCTTGGCATGGTACTGGCCATTGCCAACTAAGTTACCATTAGTTGGTGGTCACGAAGGTGCCGGTGTCTGTT	219
adh2 sgd	220	GTCCGCATGGGTGAAAACGTTAAGGGCTGGAAGATCGGTGACTACGCCGGTATCAAATGGTTGAACGGTTCTT	292
adh2 cloned	220	GTCCGCATGGGTGAAAACGTTAAGGGCTGGAAGATCGGTGACTACGCCGGTATCAAATGGTTGAACGGTTCTT	292
adh2 sgd	293	GTATGGCCTGTGAATACTGTGAATTGGGTAACGAATCCAACGTCTCAGCTGACTTGTCTGGTTACACCCA	365
adh2 cloned	293	GTATGGCCTGTGAATACTGTGAATTGGGTAACGAATCCAACGTCTCAGCTGACTTGTCTGGTTACACCCA	365
adh2 sgd	366	CGACGGTCTTTCCAAGAATACGCTACCGCTGACGCTGTTCAAGCCGCTCACATTCTCAAGGTACTGACTTG	438
adh2 cloned	366	CGACGGTCTTTCCAAGAATACGCTACCGCTGACGCTGTTCAAGCCGCTCACATTCTCAAGGTACTGACTTG	438
adh2 sgd	439	GCTGAAGTCGCGCCAATCTTGTGTGCTGGTATCACCCTATACAAGGCTTTGAAGTCTGCCAACTTGAGAGCAG	511
adh2 cloned	439	GCTGAAGTCGCGCCAATCTTGTGTGCTGGTATCACCCTATACAAGGCTTTGAAGTCTGCCAACTTGAGAGCAG	511
adh2 sgd	512	GCCACTGGGCGGCCATTCTGGTGTCTGCTGGTGGTCTAGGTTCTTTGGCTGTTCAATATGCTAAGGCGATGGG	584
adh2 cloned	512	GCCACTGGGCGGCCATTCTGGTGTCTGCTGGTGGTCTAGGTTCTTTGGCTGTTCAATATGCTAAGGCGATGGG	584
adh2 sgd	585	TTACAGAGTCTTAGGTATTGATGGTGGTCCAGGAAAGGAAGAAATTGTTACCTCGCTCGGTGGTGAAGTATTC	657
adh2 cloned	585	TTACAGAGTCTTAGGTATTGATGGTGGTCCAGGAAAGGAAGAAATTGTTACCTCGCTCGGTGGTGAAGTATTC	657
adh2 sgd	658	ATCGACTTCACCAAAGAGAAGGACATTGTTAGCGCAGTCGTTAAGGCTACCAACGGCGGTGCCACGGTATCA	730
adh2 cloned	658	ATCGACTTCACCAAAGAGAAGGACATTGTTAGCGCAGTCGTTAAGGCTACCAACGGCGGTGCCACGGTATCA	730
adh2 sgd	731	TCAATGTTCCGTTTCCGAAGCCGCTATCGAAGCTTCTACCAGATACTGTAGGGCGAACGGTACTGTTGTCTT	803
adh2 cloned	731	TCAATGTTCCGTTTCCGAAGCCGCTATCGAAGCTTCTACCAGATACTGTAGGGCGAACGGTACTGTTGTCTT	803
adh2 sgd	804	GGTTGGTTTGCAGCCGGTGCAAAGTGTCTCTCTGATGTCTTCAACCACGTTGTCAAGTCTATCTCCATTGTC	876
adh2 cloned	804	GGTTGGTTTGCAGCCGGTGCAAAGTGTCTCTCTGATGTCTTCAACCACGTTGTCAAGTCTATCTCCATTGTC	876
adh2 sgd	877	GGCTCTTACGTGGGGAACAGAGCTGATACCAGAGAAGCCTTAGATTTCTTTGCCAGAGGTCTAGTCAAGTCTC	949
adh2 cloned	877	GGCTCTTACGTGGGGAACAGAGCTGATACCAGAGAAGCCTTAGATTTCTTTGCCAGAGGTCTAGTCAAGTCTC	949
adh2 sgd	950	CAATAAAGGTAGTTGGCTTATCCAGTTTACCAGAAAATTACGAAAAGATGGAGAAGGGCCAAATGTGGTAG	1022
adh2 cloned	950	CAATAAAGGTAGTTGGCTTATCCAGTTTACCAGAAAATTACGAAAAGATGGAGAAGGGCCAAATGTGGTAG	1022
adh2 sgd	1023	ATACGTTGTTGACACTTCTAAATAA	1047
adh2 cloned	1023	ATACGTTGTTGACACTTCTAAATAA	1047

Figure 5.2 Nucleotide sequence alignment of the *ADH2* ORF cloned into pGemT-Easy and the sequence retrieved from the *Saccharomyces* genome data base (adh2 sgd). The alignment was performed with DNassist software.

into multiple cloning site of the pCM190L_W vector by means of *Bam*HI-*Not*I site directional ligation. This pCM190L_W::*ADH2* plasmid construct (Appendix E, Figure F) was verified by a 5227 bp, 2507 bp, 1071 bp band pattern when digested with *Eco*RI and *Bam*HI (Figure 5.3) and transformed into strain SΔ2a. Recombinants were selected on YNB dropout medium without uracil and tryptophan. A control strain for the batch cultivations were generated by transformation of the SΔ2a strain with the empty pCM190L_W vector. According to the real-time RT-PCR data, the control strain SΔ2aTR_E showed no transcription of *ADH2*, while the recombinant SΔ2aTR_*ADH2* strain expressed the gene in the order of 4 million copies μl^{-1} . The recombinant strain showed a 10-fold increase in *ADH2* copy number when grown under derepressed conditions compared to the wild type W303-1A(a) strain.

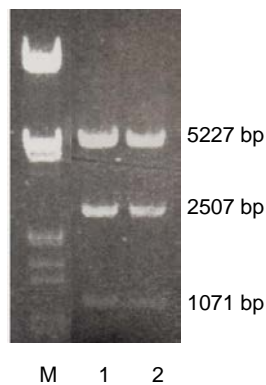


Figure 5.3 Restriction enzyme digestion profile of two independent pCM190L_W::*ADH2* plasmid constructs digested with *Eco*RI and *Bam*HI (lanes 1 & 2). Lane M represents λ III marker DNA (Appendix P).

The control SΔ2aTR_E and recombinant SΔ2aTR_ADH2 strains were grown in bioreactors containing chemically defined medium and 20g l⁻¹ glucose as carbon source (Figure 5.4). There was no difference in the growth rates between the two strains: both strains grew exponentially with a specific growth rate of 0.43 h⁻¹ (Table 5.1). Growth on glucose was accompanied by the formation of ethanol and small amounts of acetic acid and glycerol (Figure 5.4 B, D). Both strains were able to grow on the produced ethanol at specific growth rates of 0.03 and 0.02 h⁻¹. The specific growth rate on ethanol is dependent on the medium composition (Beck & von Meyenburg, 1968) and although chemically defined medium was used here, the low specific growth rates on ethanol was probably due to the auxotrophic requirement for tryptophan. The two strains also produced and utilised ethanol at similar volumetric rates (Table 5.1). Only marginal differences were visible for the amounts of glycerol and acetic acid produced by strains SΔ2aTR_E and SΔ2aTR_ADH2 reflected by the yield coefficients in Table 5.1.

When considering the transcription levels of *ADH1*, *ADH4* and *ADH5* it is evident from Figure 5.5 that the *ADH1* transcription profiles are similar whether *ADH2* is absent or present in abundance. *ADH1* levels stayed elevated during the growth on glucose, as it is responsible for the ethanol formation during this phase (Ciriacy & Breitenbach, 1979; Heick *et al.*, 1969). Contrary to the suggestions of Denis & Young (1983) and Ruohonen *et al.* (1995), the *ADH1* expression levels increased further while ethanol was consumed, an event notable in both strains (Figure 5.5 A, B). Contrary to the findings of Williamson & Paquin (1987) and van den Berg *et al.* (1998), *ADH4* transcription was detected during the ethanol consumption phase of growth (Figure 5.5 C, D). In an *adh2* nul background (Figure 5.5 C) *ADH4* transcription was detected at ethanol concentrations of below 6 g l⁻¹ and were elevated while ethanol could be detected in the medium. When *ADH2* was over-expressed (Figure 5.5 D) similar *ADH4* transcription levels were detected, but declined as ethanol consumption progressed. The *ADH5* transcription profiles were the only case in which significant differences was evident between the two strains (Figure 5.5 E, F). Expression of the *ADH5* gene in the

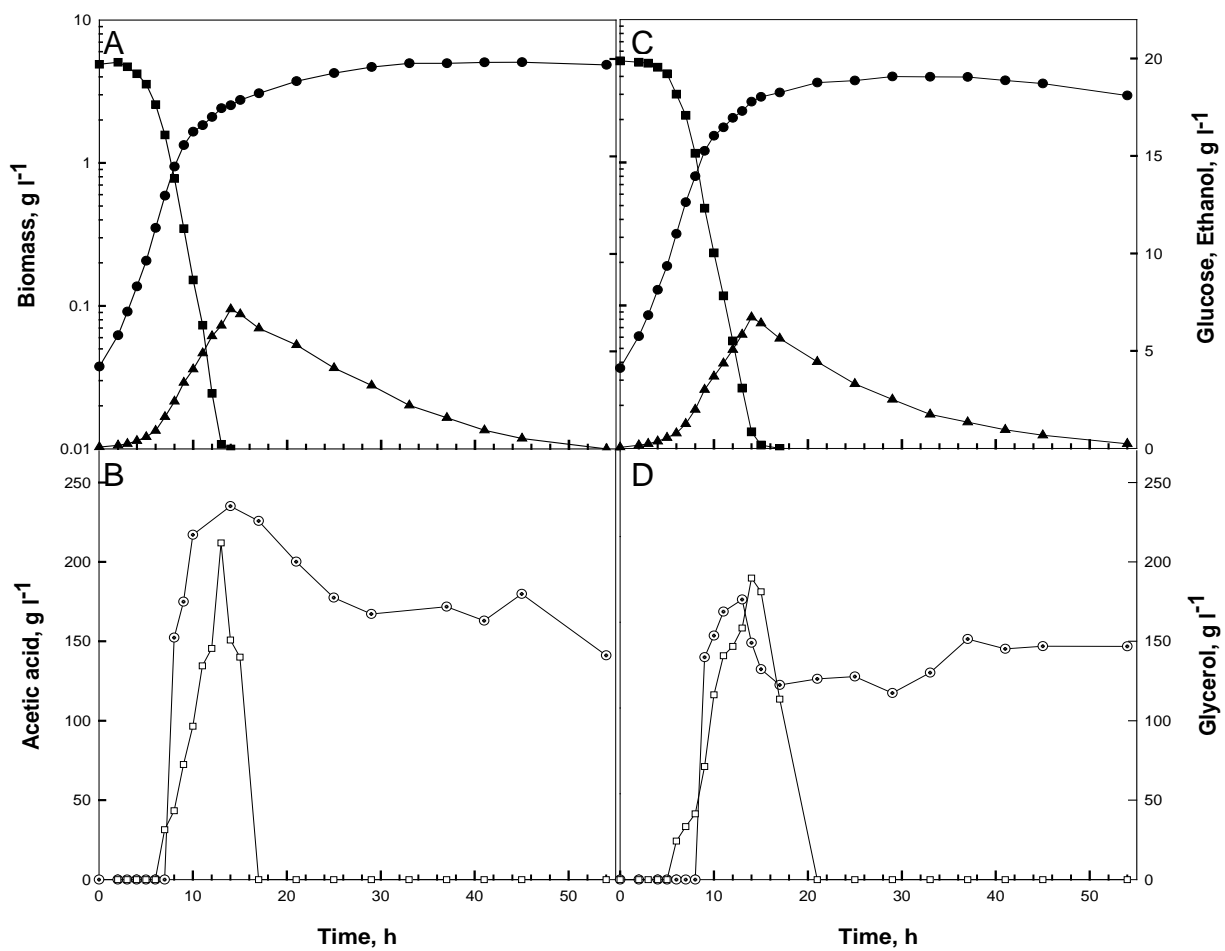


Figure 5.4 Typical bioreactor cultivation profiles of strains *SΔ2aTR_E* (A,B) and *SΔ2aTR_ADH2* (C, D) grown aerobically in chemically defined medium without tryptophan with 20 g l⁻¹ glucose as carbon source. Symbols: Biomass (●), glucose (■), ethanol (▲), Acetic acid (□) and glycerol (○). The metabolite concentrations are representative of independent duplicate experiments.

Table 5.1 Growth parameters of *S. cerevisiae* strains SΔ2aTR_E and SΔ2aTR_ADH2 in bioreactor cultures grown on glucose or ethanol. The mean values of duplicate experiments are given.

Parameter	Strain	
	SΔ2aTR_E	SΔ2aTR_ADH2
Carbon source: Glucose		
μ_{\max} glucose, h ⁻¹	0.43 ± 0.025	0.43 ± 0.02
μ_{\max} ethanol, h ⁻¹	0.03 ± 0.005	0.02 ± 0.001
$Y_{x/s}$	0.12 ± 0.001	0.14 ± 0.007
$Y_{p/s}$ ethanol	0.35 ± 0.01	0.34 ± 0.01
$Y_{p/s}$ glycerol	0.015 ± 0.002	0.011 ± 0.001
$Y_{p/s}$ acetic acid	0.011 ± 0.009	0.009 ± 0
Q_p^{\max} , g l ⁻¹ h ⁻¹	0.76 ± 0.03	0.77 ± 0.004
Q_s^{\max} , g l ⁻¹ h ⁻¹	0.25 ± 0.003	0.23 ± 0.02
Carbon source: Ethanol		
μ_{\max} , h ⁻¹	0.15 ± 0.002	0.15 ± 0.005
$Y_{x/s}$	0.61 ± 0.02	0.51 ± 0.002
Q_s^{\max} , g l ⁻¹ h ⁻¹	0.39 ± 0.01	0.37 ± 0.03
Q_s^{\max} (0-18 h), g l ⁻¹ h ⁻¹	0.031 ± 0.002	0.089 ± 0.03

μ_{\max}	Maximum specific growth rate on carbon stated, calculated by linear regression analysis of exponential growth data
$Y_{x/s}$	Biomass yield coefficient (g dry biomass/g carbon)
$Y_{p/s}$ ethanol	Ethanol yield coefficient (g ethanol/g glucose)
$Y_{p/s}$ glycerol	Glycerol yield coefficient (g glycerol produced/g glucose assimilated)
$Y_{p/s}$ acetic acid	Acetic acid yield coefficient (g acetic acid produced/g glucose assimilated)
Q_p^{\max}	Maximum volumetric rate of ethanol production, calculated from the maximum slope of the ethanol concentration curve
Q_s^{\max}	Maximum volumetric rate of ethanol assimilation, calculated from the maximum slope of the ethanol concentration curve

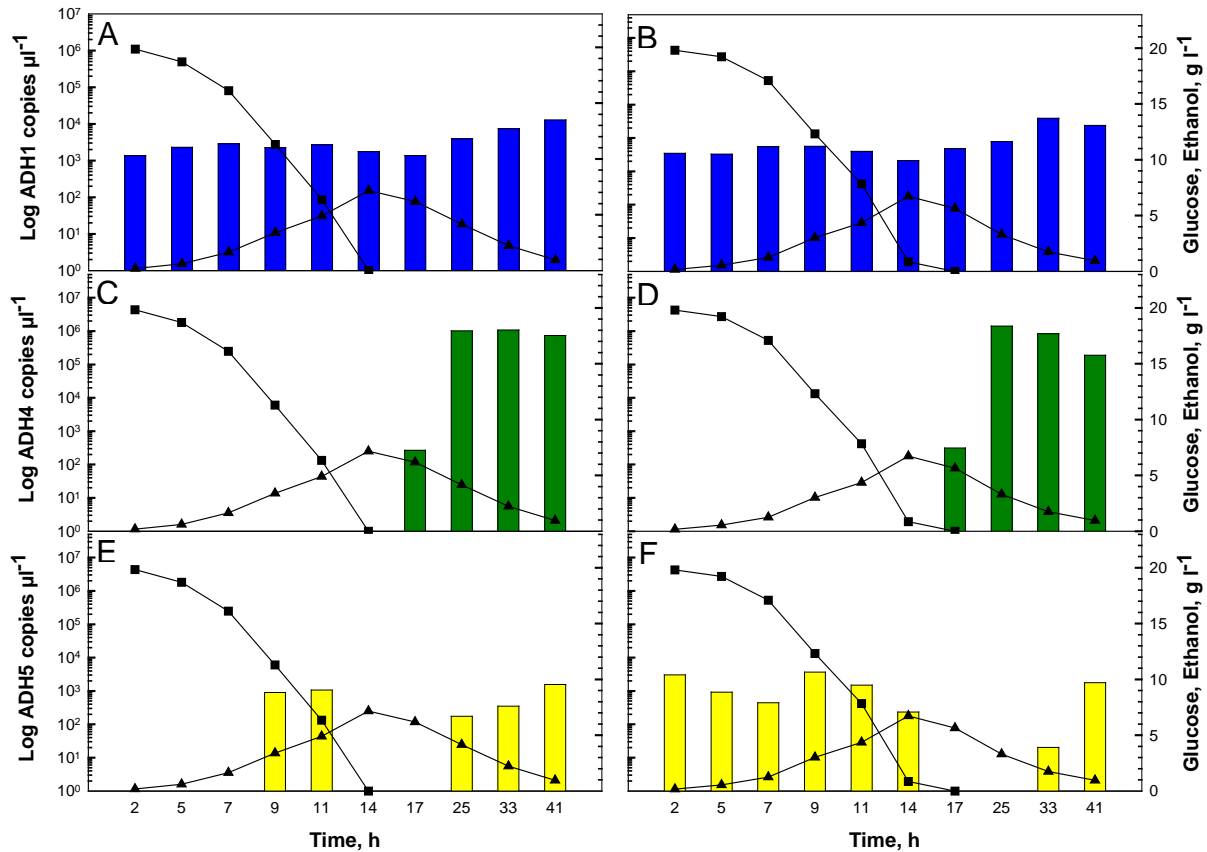


Figure 5.5 Real-time RT-PCR transcription profiles of the *ADH1*, *ADH4* and *ADH5* in strains *SΔ2aTR_E* (A, C, E) and *SΔ2aTR_ADH2* (B, D, F) grown aerobically in chemically defined medium (-TRP) in bioreactors with 20 g l⁻¹ glucose as carbon source. The glucose (■) and ethanol (▲) concentrations were derived from Figure 5.4.

SΔ2aTR_E strain was detected during the final stage of glucose consumption, after which it disappeared from the culture. Transcription was again evident when the ethanol concentration was below 4.4 g l⁻¹ and increased gradually towards ethanol depletion. In the case where *ADH2* was over-expressed (Figure 5.5 F), *ADH5* transcription was detected in fluctuating levels while glucose consumption took place. Expression ceased upon glucose depletion and only appeared again when the ethanol concentration reached 1.7 g l⁻¹.

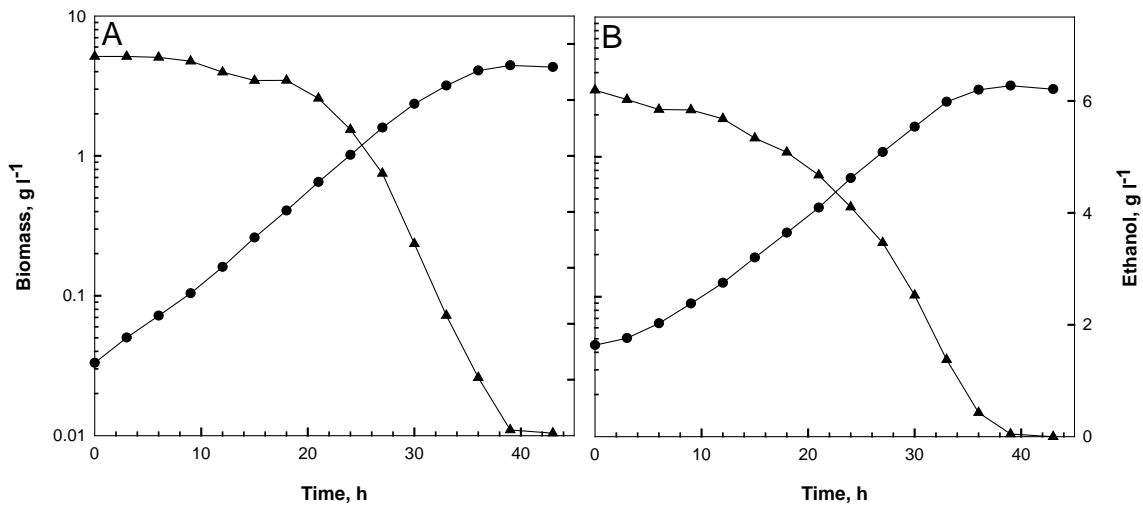


Figure 5.6 Typical bioreactor cultivation profiles of strains *SΔ2aTR_E* (A) and *SΔ2aTR_ADH2* (B) grown aerobically in chemically defined medium without tryptophan with 6.9 and 6.2 g l⁻¹ ethanol as carbon source. Symbols: Biomass (●) and ethanol (▲). The metabolite concentrations are representative of independent duplicate experiments.

Strains *SΔ2aTR_E* and *SΔ2aTR_ADH2* were also grown on 6.9 and 6.2 g l⁻¹ ethanol, respectively (Figure 5.6). Both strains grew on ethanol with similar specific growth rates of 0.15 h⁻¹ (Table 5.1). The initial volumetric rate of ethanol uptake (0-18 h) was slower for strain *SΔ2aTR_E* (0.031 g l⁻¹ h⁻¹) than for *SΔ2aTR_ADH2* (0.089 g l⁻¹ h⁻¹) and the biomass yield coefficients showed notable differences as well (Table 5.1). It should be taken into consideration that the cultivations were performed in two separate bioreactors and ethanol evaporation was not taken into account. It is then reasonable to assume that although setup differences were kept to a minimum, ethanol lost through stripping from the medium by aeration could have contributed to the variation in growth parameters. Contrary to the findings of Denis *et al.* (1983), high levels of *ADH1* transcription was detected during the growth on ethanol for both strains. The levels appeared to increase as the ethanol was consumed by the cells (Figure 5.7 A, B). *ADH4* levels were only detectable when the ethanol concentrations was as low as 0.103 g l⁻¹ for strain *SΔ2aTR_E* (Figure 5.7 C) and 0.048 g l⁻¹ for strain *SΔ2aTR_ADH2* (Figure 5.7 D). It was evident

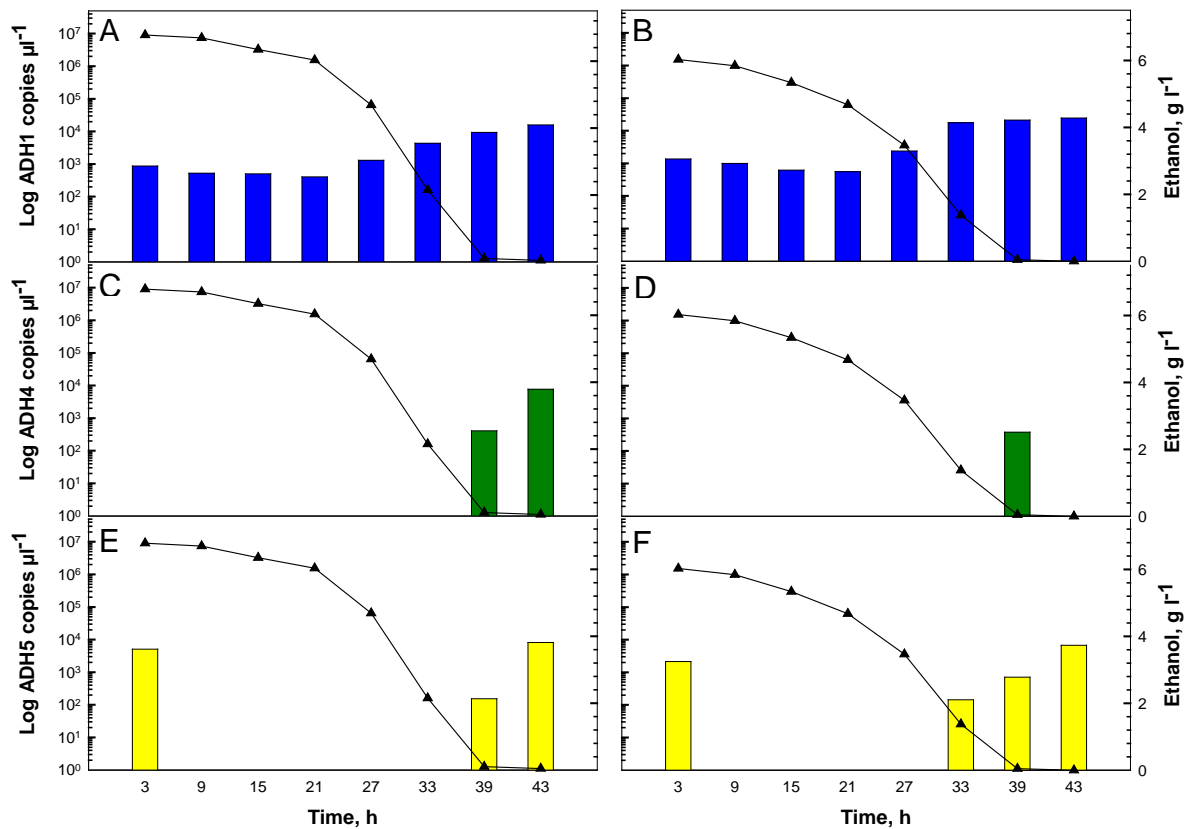


Figure 5.7 Real-time RT-PCR transcription profiles of the *ADH1*, *ADH4* and *ADH5* in strains *SΔ2aTR_E* (A, C, E) and *SΔ2aTR_ADH2* (B, D, F) grown aerobically in chemically defined medium without tryptophan in bioreactors with 6.9 and 6.2 g l⁻¹ ethanol as carbon source. The ethanol (▲) concentrations were derived from Figure 5.6.

that the presence of *ADH4* mRNA prevailed after ethanol depletion when *ADH2* was absent from the genome, while it was not detected when *ADH2* was over-expressed. *ADH5* transcription ceased after 3 h and only reappeared when the ethanol concentrations dropped below 0.103 g l⁻¹ and 1.3 g l⁻¹ (Figure 5.7 E, F).

5.5 Conclusions

When *S. cerevisiae* strain SΔ2aTR_E (harbouring the empty pCM190L_W vector in a genetic background with the *ADH2* gene disrupted by *URA3*) and strain SΔ2aTR_ADH2 (an isogenic strain over-expressing *ADH2*) were grown in bioreactors with glucose or ethanol as carbon source, no significant differences in the growth parameters were observed. The fact that an *ADH2* negative strain was able to grow on ethanol was in accordance with previously reported data by Wills & Phelps (1975). The lack of differences in growth parameters observed in this study was not unique. Previous studies also showed no significant metabolite accumulation or decreases when certain enzyme levels were increased (Ciriacy & Breitenbach, 1979; Navas *et al.*, 1993).

This investigation contradicted previous observations by Denis *et al.* (1983) that *ADH1* transcription decreased upon glucose depletion. *ADH1* transcription was not only detected during the glucose assimilation phase, but the transcription levels became elevated during the ethanol assimilation phase of diauxic growth (Figure 5.5 A & B). Transcription levels of the *ADH1* gene was also elevated in both strains during growth on externally added ethanol. The possibility that *ADH1* transcription was affected by the *ADH2* structural gene expression had been ruled out, since no significant differences in the transcription profiles were detected whether *ADH2* expression was absent or in abundance. It is well established that the ADH I protein is transcriptionally regulated, since the amount of mRNA was proportional to the amount of active ADH I enzyme (Denis *et al.*, 1983). Consequently, in this case ADH I played a major role in not only ethanol production, but also in ethanol assimilation.

Previous reports stated that *ADH4* was probably not expressed in laboratory strains and that ADH IV activity could be detected only upon over-expression of the structural gene. It was, therefore, very probable that ADH IV is not involved in the fermentation of glucose (Drewke & Ciriacy, 1988; Williamson *et al.*, 1983). In this study, *ADH4* was detected with the sensitive real-time RT-PCR method and transcription of this gene was evident during the ethanol assimilation phase of diauxic growth. However, when the same strains were grown on ethanol as a carbon source, the transcription of *ADH4* was only detected when ethanol had decreased to a concentration of 0.103 g l⁻¹. It is reasonable to conclude that the source of ethanol had an impact on

transcription, since the levels of expression were higher during the ethanol assimilation phase of diauxic growth than during growth on added ethanol. Similar findings have also been reported for *ADH2* expression (Denis, 1984; du Preez *et al.*, 2001). Judging by the transcription levels of *ADH4* it is safe to say that in this case ADH IV did not contribute to the production of ethanol during growth on glucose. It seems possible that ADH IV could play a role in ethanol assimilation during diauxic growth, but a correlation between the amount of mRNA and the enzyme activity or protein concentration needs to be established for confirmation.

This study also revealed that the *ADH5* gene was the only *ADH* gene monitored which showed a different transcription profile in the strain over-expressing *ADH2* when grown on glucose. Transcription of *ADH5* in the *SΔ2aTR_ADH2* strain indicated a possible contribution towards ethanol production.

The possibility also exists that the ADH enzymes behave differently when only one is expressed in a background void of all the others. Data reporting ethanol production in a strain lacking *ADH1* to *ADH4* (Drewke *et al.*, 1990) support this suggestion and this warrants further investigation.

5.6 Literature cited

- Beck, C. and H. K von Meyenburg.** 1968. Enzyme pattern and aerobic growth of *Saccharomyces cerevisiae* under various degrees of glucose limitation. *J Bacteriol.* **96:** 479-486.
- Becker, J. M., G. A. Caldwell and E. A. Zachgo.** 1990. Biotechnology, a laboratory course. Becker, J. M, Caldwell, G. A, and Zachgo, E. A. *Academic Press.* pp.
- Chen, D. C., B. C. Yang and T. T. Kuo.** 1992. One-step transformation of yeast in stationary phase. *Curr. Genet.* **21:** 83-84.
- Ciriacy, M.** 1975. Genetics of alcohol dehydrogenase in *Saccharomyces cerevisiae* : I. Isolation and genetic analysis of *adh* mutants. *Mutation Research.* **29:** 315-325.
- Ciriacy, M. and I. Breitenbach.** 1979. Physiological effects of seven different blocks in glycolysis in *Saccharomyces cerevisiae*. *J Bacteriol.* **139:** 152-160.
- Denis, C. L.** 1984. Identification of new genes involved in the regulation of yeast alcohol dehydrogenase II. *Genetics* **108:** 833-844.
- Denis, C. L., J. Ferguson and E. T. Young.** 1983. mRNA levels for the fermentative alcohol dehydrogenase of *Saccharomyces cerevisiae* decrease upon growth on a non-fermentable carbon source. *J. Biol. Chem.* **258:** 1165-1171.
- Denis, C. L. and E. T. Young.** 1983. Isolation and characterization of the positive regulatory gene *ADR1* from *Saccharomyces cerevisiae*. *Mol. Cell Biol.* **3:** 360-370.
- Drewke, C. and M. Ciriacy.** 1988. Over-expression, purification and properties of alcohol dehydrogenase IV from *Saccharomyces cerevisiae*. *Biochim. Biophys. Acta.* **950:** 54-60.
- Drewke, C., J. Thielen and M. Ciriacy.** 1990. Ethanol formation in *adh0* mutants reveals the existence of a novel acetaldehyde-reducing activity in *Saccharomyces cerevisiae*. *J Bacteriol.* **172:** 3909-3917.
- du Preez, J. C., J. E. Mare, J. Albertyn and S. G. Kilian.** 2001. Transcriptional repression of *ADH2*-regulated β -xylanase production by ethanol in recombinant strains of *Saccharomyces cerevisiae*. *FEMS Yeast Res.* **1:** 233-240.
- Gancedo, J. M.** 1998. Yeast carbon catabolite repression. *Microbiol. Mol. Biol. Rev.* **62:** 334-361.
- Gossen, M. and H. Bujard.** 1992. Tight control of gene expression in mammalian cells by tetracycline-responsive promoters. *Proc. Natl. Acad. Sci. U. S. A.* **89:** 5547-5551.
- Heick, H. M. C., J. Willemot and N. Begin-heick.** 1969. The subcellular localization of alcohol dehydrogenase activity in baker's yeast. *Biochim. Biophys. Acta.* **191:** 493-501.
- Kohrer, K. and H. Domdey.** 1991. Preparation of high molecular weight RNA. *Methods Enzymol.* **194:** 398-405.
- Labuschagne, M. and J. Albertyn.** 2007. Cloning of an epoxide hydrolase-encoding gene from *Rhodotorula mucilaginosa* and functional expression in *Yarrowia lipolytica*. *Yeast* **24:** 69-78.

- Navas, M. A., S. Cerdan and J. M. Gancedo.** 1993. Futile cycles in *Saccharomyces cerevisiae* strains expressing the gluconeogenic enzymes during growth on glucose. *Proc. Natl. Acad. Sci. U. S. A.* **90**: 1290-1294.
- Price, V. L., W. E. Taylor, W. Clevenger, M. Worthington and E. T. Young.** 1990. Expression of heterologous proteins in *Saccharomyces cerevisiae* using the *ADH2* promoter. *Methods Enzymol.* **185**: 308-318.
- Romanos, M. A., C. A. Scorer and J. J. Clare.** 1992. Foreign gene expression in yeast: a review. *Yeast* **8**: 423-488.
- Ruohonen, L., M. K. Aalto and S. Keranen.** 1995. Modifications to the *ADHI* promoter of *Saccharomyces cerevisiae* for efficient production of heterologous proteins. *J. Biotechnol.* **39**: 193-203.
- Sambrook, J. and D. W. Russel.** 2001. Molecular cloning: A laboratory manual. *Cold Spring Harbour.*
- van den Berg, M. A., P. Jong-Gubbels and H. Y. Steensma.** 1998. Transient mRNA responses in chemostat cultures as a method of defining putative regulatory elements: application to genes involved in *Saccharomyces cerevisiae* acetyl-coenzyme A metabolism. *Yeast* **14**: 1089-1104.
- Williamson, V. M., D. Cox, E. T. Young, D. W. Russell and M. Smith.** 1983. Characterization of transposable element-associated mutations that alter yeast alcohol dehydrogenase II expression. *Mol. Cell Biol.* **3**: 20-31.
- Williamson, V. M. and C. E. Paquin.** 1987. Homology of *Saccharomyces cerevisiae ADH4* to an iron-activated alcohol dehydrogenase from *Zymomonas mobilis*. *Mol. Gen. Genet.* **209**: 374-381.
- Wills, C. and J. Phelps.** 1975. A technique for the isolation of yeast alcohol dehydrogenase mutants with altered substrate specificity. *Arch. Biochem Biophys.* **167**: 627-637.

6	Evaluation of multiple <i>ADH</i> knock-out strains of <i>S. cerevisiae</i> in bioreactor batch cultivations.....	83
6.1	Abstract.....	83
6.2	Introduction.....	84
6.3	Materials and Methods.....	86
6.3.1	Strains	86
6.3.2	Media	86
6.3.3	DNA methods	86
6.3.4	Deletion plasmid construction	86
6.3.5	Disruption of <i>ADH2</i> , <i>ADH3</i> , <i>ADH4</i> and <i>ADH5</i> from <i>S. cerevisiae</i> chromosomes	88
6.3.6	Construction of double, triple and quadruple deletion strains D Δ 34a, D Δ 34b, T Δ 345, T Δ 234, T Δ 235, T Δ 245, Q1, Q2, Q3, Q4 and Q5	89
6.3.7	Cultivation conditions.....	90
6.3.8	Analyses.....	90
6.3.9	Real-time RT-PCR.....	90
6.4	Results and Discussion	91
6.4.1	Construction of <i>ADH</i> quadruple deletion mutant strains Q1, Q2, Q3, Q4 and Q5 by molecular and classical techniques	91
6.4.2	Bioreactor cultivation of strains W303-1A(a), Q1, Q2, Q3 Q4 and Q5 on glucose as carbon source.....	95
6.4.3	Bioreactor cultivation of strains W303-1A(a), Q1, Q2 and Q3 on ethanol as carbon source.....	106
6.5	Conclusions.....	111
6.6	References cited.....	115
Figure 6.1	Plasmid constructs p <i>ADH1</i> , p <i>ADH2</i> , p <i>ADH3</i> , p <i>ADH4</i> and p <i>ADH5</i> , containing the <i>ADH</i> ORFs and a 1000 bp flanking regions in pGemT-Easy, verified by restriction enzyme digestion.	91
Figure 6.2	Restriction enzyme digestion profiles of the eight deletion plasmid constructs p <i>adh1::LEU2</i> , p <i>adh1::URA3p</i> , p <i>adh1::TRP1</i> , p <i>adh1::HIS3</i> , p <i>adh2::URA3</i> , p <i>adh3::TRP1</i> , p <i>adh4::HIS3</i> and p <i>adh5::LEU2</i>	92
Figure 6.3	Diagram of double, triple and quadruple deletion strains construction with molecular and classical techniques.	93
Figure 6.4	PCR profiles of the parental and quadruple deletion mutant strains.	94
Figure 6.5	Typical aerobic cultivation profile of <i>S. cerevisiae</i> strain W303-1A(a) grown in chemically defined medium with 16 g glucose l ⁻¹ as initial carbon source.	99
Figure 6.6	Real-time RT-PCR transcription profiles of the <i>ADH1</i> , <i>ADH2</i> , <i>ADH4</i> and <i>ADH5</i> genes of strain W303-1A(a) grown in bioreactors with 16 g glucose l ⁻¹ as carbon source.....	100

Figure 6.7	Typical aerobic cultivation and real-time RT-PCR transcription profile of <i>S. cerevisiae</i> strain Q1 grown in chemically defined medium with 10 g glucose l ⁻¹ as initial carbon source.	101
Figure 6.8	Typical aerobic cultivation and real-time RT-PCR transcription profile of <i>S. cerevisiae</i> strain Q2 grown in chemically defined medium with 10 g glucose l ⁻¹ as initial carbon source.	102
Figure 6.9	Typical bioreactor profile of <i>S. cerevisiae</i> strain Q3 grown in chemically defined medium with 10 g glucose l ⁻¹	103
Figure 6.10	Typical aerobic cultivation and real-time RT-PCR transcription profile of <i>S. cerevisiae</i> strain Q4 grown in chemically defined medium with 10 g glucose l ⁻¹	104
Figure 6.11	Typical aerobic cultivation profile and <i>ADH5</i> transcription levels of <i>S. cerevisiae</i> strain Q5 grown in chemically defined medium with 10 g glucose l ⁻¹	105
Figure 6.12	Aerobic cultivation profile and <i>ADH</i> transcription profiles of <i>S. cerevisiae</i> parental strain W303-1A(a) grown in chemically defined medium with 7 g ethanol l ⁻¹	107
Figure 6.13	Aerobic cultivation and <i>ADH1</i> transcription profile of <i>S. cerevisiae</i> strain Q1 grown in chemically defined medium with 7 g ethanol l ⁻¹	108
Figure 6.14	Aerobic cultivation and <i>ADH2</i> transcription profile of <i>S. cerevisiae</i> strain Q2 grown in chemically defined medium with 7 g ethanol l ⁻¹	109
Figure 6.15	Aerobic cultivation profile of <i>S. cerevisiae</i> strain Q3 grown in chemically defined medium with 7 g ethanol l ⁻¹	110
Table 6.1	Growth parameters of <i>S. cerevisiae</i> strains W303-1A(a), Q1, Q2, Q3, Q4 and Q5 in bioreactor batch cultures grown on glucose.	98
Table 6.2	Growth parameters of <i>S. cerevisiae</i> strains W303-1A(a), Q1, Q2, and Q3 grown on ethanol in aerobic bioreactor cultures.	110

CHAPTER 6

Evaluation of multiple *ADH* knock-out strains of *Saccharomyces cerevisiae* in bioreactor batch cultivations

Abstract

The physiological importance of each alcohol dehydrogenase (ADH) was investigated in strains Q1, Q2, Q3, Q4 and Q5 irreversibly in which in the five *ADH* genes had been deleted in different combinations. Batch cultivations were performed in a chemically defined medium supplemented with glucose or ethanol. The ADH I in strain Q1 was the only ADH able to efficiently catalyse the reduction of acetaldehyde to ethanol with the regeneration of NAD⁺. The oxidation of produced or added ethanol could also be attributed to ADH I. Growth of strains lacking the *ADH1* gene resulted in the formation of glycerol as a major fermentation product concomitant with a significant production of acetaldehyde. Strains Q2 and Q3, expressing only ADH II or ADH III, respectively, were able to produce ethanol from glucose. Transcription levels of the *ADH4* gene in the quadruple deletion mutant strain Q4 showed that the gene product ADH IV was not responsible for the production of ethanol during growth on glucose and the strain was neither able to utilise the produced ethanol nor grow on added ethanol. When ethanol was produced from glucose, the *ADH5* gene was not transcribed at sufficient levels to suggest that ADH V was responsible for ethanol production in strain Q5. The *ADH5* gene product also did not participate in the oxidation of ethanol, since strain Q5 was unable to grow on ethanol.

6.2 Introduction

The yeast *Saccharomyces cerevisiae* is capable of fermentation with production of ethanol and can utilise this substrate as sole carbon source. Alcohol dehydrogenases play a central role in this metabolism, catalysing the interconversion of ethanol and acetaldehyde. Moreover, as nicotinamide adenine dinucleotide takes part in the reaction, alcohol dehydrogenase is involved in the general “coenzyme equilibration” mechanisms of the cell (Wiesenfeld *et al.*, 1975).

ADH I is the fermentative enzyme catalysing the reduction of acetaldehyde to ethanol during alcoholic fermentation (Ciriacy, 1975a; Heick *et al.*, 1969; Lutstorf & Megnet, 1968). ADH II is an isoenzyme biosynthetically regulated by catabolite repression and its function in the cell is related to the oxidation of ethanol to acetaldehyde, which can be metabolised via the tricarboxylic acid cycle or act as an intermediate product in gluconeogenesis (Beier *et al.*, 1985; Young & Pilgrim, 1985). Mitochondrial ADH III is in part coupled to respiration during growth on ethanol by shuttling mitochondrial NADH to the cytosol (Bakker *et al.*, 2000; Wenger & Bernofsky, 1971; Young & Pilgrim, 1985). No distinct function has thus far been assigned to the ADH IV and ADH V isozymes. ADH IV is seemingly not expressed in laboratory strains (Williamson & Paquin, 1987), but *ADH4* transcription can be detected at high levels in certain brewing strains during ethanol production (Mizuno *et al.*, 2006). ADH V might play a role in ethanol production in a genetic background in which none of the other four ADHs are functional (Drewke *et al.*, 1990).

The available literature allows speculation on the ability of the ADH enzymes to substitute functions. For instance, Wills & Phelps (1975) demonstrated that strains lacking the *ADH2* gene were still able to grow on ethanol as a substrate. Under extreme conditions, like the prolonged alcoholic fermentation of grape must, ADH II not only takes part in the production of higher alcohols, but also in the reduction of acetaldehyde to ethanol (Millan *et al.*, 1990). Over-expression of the *ADH4* gene through Ty-insertions also allowed fermentable growth on glucose in a strain lacking a functional *ADH1* gene (Paquin & Williamson, 1986).

The introduction of defined mutations in the structural *ADH* genes were employed in this study to obtain information on the physiological role of each ADH enzyme. This investigation was focused on the role of each enzyme in ethanol metabolism in terms of the expression of its structural gene in quadruple deletion mutant, each with only one intact *ADH* gene.

6.3 Materials and Methods

6.3.1 Strains

The work reported here entailed the engineering of strains S Δ 2a, S Δ 2b, S Δ 3, S Δ 4, S Δ 5, D Δ 34a, D Δ 34b, T Δ 345, T Δ 234, T Δ 235, T Δ 245, Q1, Q2, Q3, Q4 and Q5 from parental strains W303-1A(a) and W303-1A(α). Strains Test-a and Test- α were crossed with dissected spores to determine the mating type of the deletion mutants. *Escherichia coli* strain Top 10F' was used for most amplifications and DNA manipulations, whereas strain DH5 α was used where it was necessary to digest the DNA with *Bcl*I. The genotypes of each of the strain is presented in Appendix C, Table A.

6.3.2 Media

Escherichia coli cells, used for propagation of plasmid constructs, were plated on LB medium containing ampicillin (60 μ g ml⁻¹), IPTG (9.6 μ g ml⁻¹) and X-gal (40 μ g ml⁻¹). Yeast transformants were plated on YNB dropout medium and deletion strains were revived on YPD agar plates. Bioreactor cultivations of parental strain W303-1A(a) and mutant strains Q1, Q2, Q3, Q4, and Q5 were performed in chemically defined medium supplemented with glucose or ethanol. The different media compositions are available in Appendix A.

6.3.3 DNA methods

DNA manipulations (Appendix G, H), transformation of *E. coli* (Appendix I) and plasmid DNA extractions (Appendix K) were performed by standard methods (Becker *et al.*, 1990; Sambrook & Russel, 2001). Yeast transformations were performed as described by Chen *et al.* (1992) (Appendix J) and total yeast genomic DNA isolated according to the method of Labuschagne & Albertyn (2007) (Appendix K).

6.3.4 Deletion plasmid construction

The ADH genes flanked both 5' and 3' by non-coding DNA were amplified from W303-1A(a) genomic DNA using Expand Long Template Taq Polymerase (Roche Applied Science). Primer pairs ADH1-1F/ADH1-1R, ADH3-1F/ADH3-1R, ADH4-1F/ADH4-1R

and ADH5-1F/ADH5-1R were used to amplify the *ADH1* (3024 bp), *ADH3* (3100 bp), *ADH4* (3330 bp) and *ADH5* (2982 bp) fragments, respectively. PCR was performed in accordance with Appendix F at an annealing temperature of 50°C, using conditions described in Appendix F, Prog. 1. PCR products were cloned into the pGemT-Easy vector and the resulting plasmids p*ADH1* (Appendix E, Figure O), p*ADH3* (Appendix E, Figure AB), p*ADH4* (Appendix E, Figure AF) and p*ADH5* (Appendix E, Figure AJ) verified by restriction enzyme analysis. Construction of the p*ADH2* plasmid (Appendix E, Figure C) was described in Chapter 5.

Plasmids were constructed by replacing each of the *ADH* genes with a yeast marker gene. Four different deletion plasmids were constructed in which the *ADH1* ORF was replaced by selectable marker genes *LEU2*, *URA3*, *TRP1* and *HIS3*, respectively. This was necessary to facilitate the engineering of the quadruple deletion strains Q2, Q3, Q4 and Q5. A 657 bp segment of the *ADH1* gene was replaced with the *LEU2* marker gene from pJJ250 (Appendix E, Figure M) in the *padh1::LEU2* plasmid (Appendix E, Figure Q) by site directional cloning, harnessing the *BclI-HindIII* sites from p*ADH1* and the *BamHI-HindIII* sites in pJJ250. For the construction of deletion plasmids *padh1::URA3*, *padh1::TRP1* and *padh1::HIS3* (Appendix E, Figures S, U, W), a 1270 bp segment was excised with *BclI* and *BamHI* from p*ADH1* (spanning 942 bp of the *ADH1* ORF and 328 bp into the 3' flanking region) and *BamHI* fragments of the *URA3*, *TRP1* and *HIS3* marker genes from vectors YDp-U, YDp-W, YDp-H (Appendix E, Figures G, H, I) were cloned into the backbone. The *padh2::URA3* plasmid was constructed as described in Chapter 5. The *ADH3* (1143 bp) and *ADH4* (1369) ORFs were replaced by PCR and standard cloning techniques. Chimeric primer pairs ADH3-2F/ADH3-2R and ADH4-2F/ADH4-2R (Appendix D, Table B) were used for deleting the ORFs and concurrently introducing *BamHI* and *XhoI* restriction sites, respectively, for circularisation. The *TRP1* marker gene from pJJ248 (Appendix E, Figure L) was *BamHI-BglII* ligated to the introduced *BamHI* site of the circularised PCR product where *ADH3* was deleted, resulting in the *padh3::TRP1* deletion plasmid (Appendix E, Figure AD). The *ADH4* ORF, deleted by PCR, was replaced by the *HIS3* marker gene from pJJ217 (Appendix E, Figure J) by site directional cloning with restriction sites *BamHI* and *XhoI*. The resulting plasmid designated *padh4::HIS3* is depicted in Appendix E, Figure AH.

The *padh5::LEU2* plasmid (Appendix E, Figure AL) was obtained by deletion of a 1099 bp *XbaI-BclI* fragment of the *ADH5* coding region in *pADH5* and replaced by the *XbaI-BclI* excised *LEU2* marker gene originating from pJJ252 (Appendix E, Figure N). The eight deletion plasmids were verified by restriction enzyme analysis.

6.3.5 Disruption of *ADH2*, *ADH3*, *ADH4* and *ADH5* from *S. cerevisiae* chromosomes

PCR fragments were amplified with Expand Long Template Taq Polymerase (Roche Applied Science) using the deletion plasmids *padh2::URA3*, *padh3::TRP1*, *padh4::HIS3* and *padh5::LEU2* as templates. Amplification commenced at reaction conditions described in Appendix F, Prog. 1 at an annealing temperature of 50°C. Primer pairs ADH2-1F/ADH2-1R, ADH3-1F/ADH3-1R, ADH4-1F/ADH4-1R and ADH5-1F/ADH5-1R were used for each of the templates, respectively. The resulting PCR fragments *adh2Δ::URA3*, *adh3Δ::TRP1*, *adh4Δ::HIS3* and *adh5Δ::LEU2* are shown in Appendix E, Figures AA, AE, AI, and AM. The PCR mixes were used to transform recipient *S. cerevisiae* strain W303-1A(a) by using standard procedures. The *adh2Δ::URA3* fragment was also transformed into isogenic strain W303-1A(α), resulting in strain SΔ2b. Structural genes *ADH2*, *ADH3*, *ADH4* and *ADH5* were thus disrupted in resulting strains SΔ2a, SΔ3, SΔ4 and SΔ5, which were selected for uracil, tryptophan, histidine and leucine prototrophy, respectively. Deletions were confirmed by diagnostic PCR using specific primers that yielded products unique to each disruption. PCRs were performed with Taq polymerase (New England Biolabs) at conditions described in Appendix F, Prog. 3. Primer pairs ADH2-3F/URA3-1F, ADH3-3F/TRP1-1R, ADH4-3F/HIS3-1R and ADH5-3F/LEU2-1R (Appendix D, Table B) were employed to produce fragments confirming *adh2Δ::URA3* (1282 bp), *adh3Δ::TRP1* (1483 bp), *adh4Δ::HIS3* (1610 bp) and *adh5Δ::LEU2* (1628 bp) deletions.

6.3.6 Construction of double, triple and quadruple deletion strains D Δ 34a, D Δ 34b, T Δ 345, T Δ 234, T Δ 235, T Δ 245, Q1, Q2, Q3, Q4 and Q5

Double, triple and quadruple deletion mutants were constructed using transformation (Appendix J) and classical micromanipulation techniques (Appendix L). The construction of each strain is outlined in Figure 6.3. Strain S Δ 3 was crossed with strain S Δ 4, the diploids sporulated and subsequently analysed by tetrad analyses to obtain strains D Δ 34a and D Δ 34b. The triple deletion strain T Δ 234 were fashioned by crossing D Δ 34a with single deletion strain S Δ 2b and T Δ 345 by crossing D Δ 34b with S Δ 5. Strain T Δ 234 was crossed with S Δ 2b and the haploid progeny, resulting from tetrad analyses, carrying triple deletions in *adh2adh3adh5* (T Δ 235) and *adh2adh4adh5* (T Δ 245), were identified by their ability to grow in the absence of uracil, leucine and tryptophan or histidine. For the construction of quadruple deletion strain Q1 the T Δ 345 strain was crossed with S Δ 2b and the dissected haploid progeny displaying uracil, tryptophan, histidine and leucine prototrophy were selected. Transformation was employed to generate the other quadruple deletion strains Q2, Q3, Q4 and Q5. The PCR fragments used for the transformations were amplified with Expand Long Template Taq Polymerase using deletion plasmids *padh1::URA3*, *padh1::TRP1*, *padh1::HIS3* and *padh1::LEU2* as templates. Primer pair ADH1-1F/ADH1-1R were used at an annealing temperature of 55°C and reaction conditions described in Appendix F, Prog. 1. T Δ 345, T Δ 235, T Δ 245 and T Δ 234 were recipient strains transformed with the resulting PCR fragments *adh1 Δ ::URA3* (Appendix E, Figure T), *adh1 Δ ::TRP1* (Appendix E, Figure V), *adh1 Δ ::HIS3* (Appendix E, Figure X) and *adh1 Δ ::LEU2* (Appendix E, Figure R), respectively. All the strains were not only selected for their ability to grow without certain supplements, but deletions were also confirmed by diagnostic PCR.

Q1, Q2, Q3, Q4 and Q5 genotypes were confirmed by PCR using specific primers to confirm the incorporated deletions, as well as the intact *ADH* gene in each strain. Genomic DNA extracted from each strain was used as template and the PCRs were performed according to the conditions described in Appendix F (Prog. 4). Primer pairs ADH1-2F/1RT-R, ADH2-3F/2RT-R, ADH3-3F/ADH3-4R, ADH4-4F/ADH4-4R and ADH5-3F/ADH5-4R were used to amplify fragments verifying the intact genes *ADH1*

(1912 bp), *ADH2* (1650 bp), *ADH3* (1398 bp), *ADH4* (1091 bp) and *ADH5* (1409) ORFs respectively. Primer binding sites are shown in Appendix E, Figures P, Z, AC, AG and AK. Replacement of the *ADH1* gene with marker genes *URA3*, *TRP1*, *HIS3* or *LEU2* was verified under the same PCR conditions by using primer ADH1-2F in combination with primers URA3-1R, TRP1-1R, HIS3-1R and LEU2-1R, respectively. The *ADH2*, *ADH3*, *ADH4* and *ADH5* replacements were verified with primer pairs described in section 6.3.5.

6.3.7 Cultivation conditions

Aerobic batch cultivations in bioreactors were performed and pre-inocula for strains W303-1A(a) and Q1 prepared as described in Chapter 5. Pre-inocula for strains Q2, Q3, Q4 and Q5 were prepared by cultivation for 3 days at 30°C on YPD medium. Cells were then taken from the plate cultures and resuspended in chemically defined medium without a carbon source to a final OD₆₀₀ of *ca.* 10. The appropriate volumes were then inoculated into the bioreactor vessels to give initial OD₆₀₀ values of *ca.* 0.2. Pre-inocula had to be prepared in this way, since growth was severely inhibited in shake flask cultures, probably by the accumulation of acetaldehyde.

6.3.8 Analyses

Culture turbidity, biomass, glucose, ethanol, acetic acid and glycerol concentrations were determined as described in previous chapters. Acetaldehyde concentrations were determined with the same method used for ethanol and acetic acid described in Chapter 4.

6.3.9 Real-time RT-PCR

RNA samples were collected, RNA extracted and pre-treated with DNaseI as described in Chapter 5. The same real-time RT-PCR probes, standards and reaction conditions were also employed for monitoring the mRNA transcription levels in strains W303-1A(a), Q1, Q2, Q4 and Q5. As mentioned in Chapter 5, all attempts to design a TaqMan probe suitable for *ADH3* were unsuccessful.

6.4 Results and Discussion

6.4.1 Construction of *ADH* quadruple deletion mutant strains Q1, Q2, Q3, Q4 and Q5 with molecular and classical techniques

The *ADH* ORFs with a 1000 bp flanking regions were amplified by PCR, cloned into pGemT-Easy and verified by restriction analysis. The p*ADH1* plasmid was identified by the presence of 2834 bp, 2377 bp and 666 bp fragments when digested with *EcoRI* and *BamHI* (Figure 6.1, lane1). p*ADH2* and p*ADH3* were digested with *EcoRI-HindIII* and *SalI-XbaI*, respectively. p*ADH2* was characterised by three bands of 2834 bp, 1740 bp and 1296 bp in length and p*ADH3* by fragments of 4024 bp, 1238 bp and 854 bp (Figure 6.1, lanes 2 & 3). Restriction enzymes combinations *BamHI-XbaI* and *NheI-XbaI* were used to verify the p*ADH4* and p*ADH5* plasmids. Digestion of p*ADH4* resulted in bands of 5316 bp and 1030 bp in length, whereas p*ADH5* was digested into 4228 bp and 1770 bp fragments (Figure 6.1, lanes 4 & 5). Segments of each *ADH* ORF were subsequently replaced by selectable yeast marker genes. The *ADH1* coding region was replaced by the four different marker genes *LEU2*, *URA3*, *TRP1* and *HIS3* to yield the four deletion

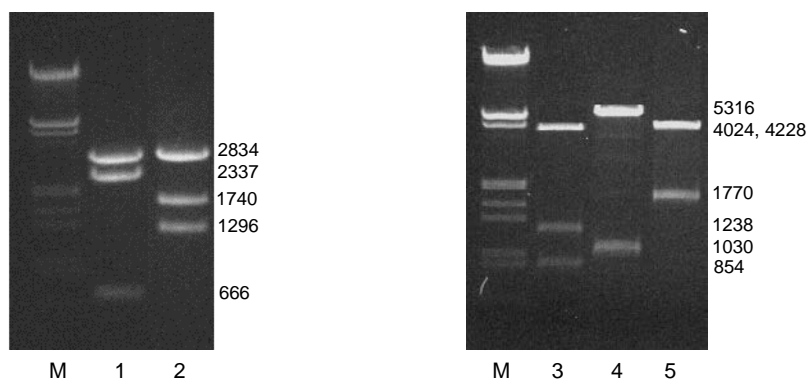


Figure 6.1 Plasmid constructs p*ADH1*, p*ADH2*, p*ADH3*, p*ADH4* and p*ADH5*, containing the *ADH* ORFs and a 1000 bp flanking regions in pGemT-Easy, verified by restriction enzyme digestion. Lane 1: p*ADH1* digested with *EcoRI* and *BamHI*. Lane 2: p*ADH2* digested with *EcoRI* and *HindIII*. Lane 3: p*ADH3* digested with *SalI* and *XbaI*. Lane 4: p*ADH4* digested with *BamHI* and *XbaI*. Lane 5: p*ADH5* digested with *NheI* and *XbaI*. The lanes designated M represent λ III marker DNA of which the band lengths can be viewed in Appendix P

plasmids *padh1::LEU2*, *padh1::URA3*, *padh1::TRP1* and *padh1::HIS3*, respectively. Digestion of *padh1::LEU2* with *EcoRV* and *BamHI* were characterised by the presence of 3 bands of 3948 bp, 1993 bp and 1314 bp in size (Figure 6.2, lane 1). *EcoRV* digestion of *padh1::URA3* resulted in bands of 4663 bp and 1256 bp in length (Figure 6.2, lane 6). Double digestions of *padh1::TRP1* and *padh1::HIS3* with *XbaI-PstI* and *EcoRV-NheI* resulted in fragment combinations 4297 bp/1340 bp and 4326 bp/1643 bp, respectively (Figure 6.2, lanes 7 & 8). *padh2::URA3* were subjected to multiple digestion with *PvuI-EcoRV-NheI* which resulted in four fragments 2363 bp, 1830 bp, 1106 bp and 831 bp in sizes (Figure 6.2, lane 2). Four bands 2997 bp, 1287 bp, 681 bp and 612 bp in length were obtained when *padh3::TRP1* was digested with *EcoRI* and *HindIII* (Figure 6.2, lane 3). The deletion plasmids *padh4::HIS3* and *padh5::LEU2* were digested with enzyme combinations *NheI-BamHI-SalI* and *NheI-EcoRV-XbaI*, where the different digestion

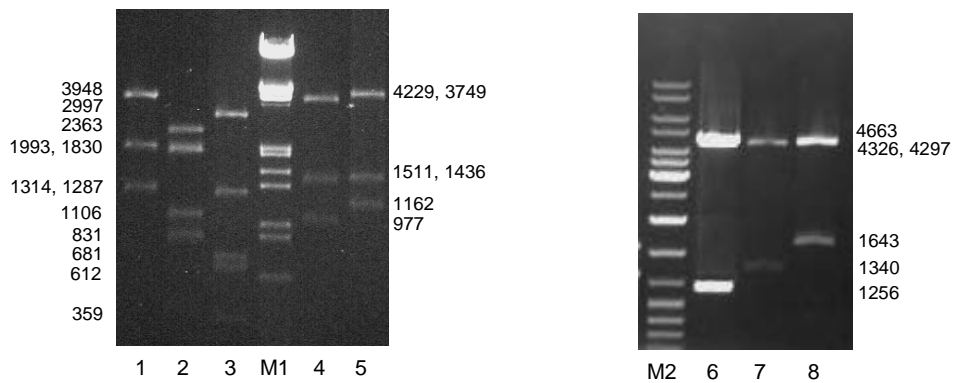


Figure 6.2 Restriction enzyme digestion profiles of the eight deletion plasmid constructs where the *ADH* ORFs were replaced with selective marker genes. The *padh1::LEU2* digested with *EcoRV* and *BamHI* is shown in lane 1. Lanes 6, 7 and 8 represent the *padh1::URA3*, *padh1::TRP1* and *padh1::HIS3* plasmid constructs digested with *EcoRV*, *XbaI-PstI* and *EcoRV-NheI*, respectively. *padh2::URA3* digested with *PvuI*, *EcoRV* and *NheI* (lane 2). *padh3::TRP1* digested with *EcoRI* and *HindIII* (lane 3). *NheI-BamHI-SalI* digestion of *padh4::HIS3* is depicted in lane 4 and *NheI-EcoRV-XbaI* digested *padh5::LEU2* in lane 5. The lane designated M1 represents λ III marker DNA and lane M2 O'GeneRuler. The band lengths of the marker DNA are available in Appendix P. Band lengths are given in base pairs.

profiles resulting in fragments of 3749 bp, 1436 bp, 977 bp and 4229 bp, 151 bp, 1162 bp identified each construct (Figure 6.2, lanes 4 & 5). PCR fragments were amplified from the deletion plasmids *padh2::URA3*, *padh3::TRP1*, *padh4::HIS3* and *padh5::LEU2* and transformed into isogenic strains W303-1A(a) and W303-1A(α). The resulting single deletion mutant strains S Δ 2a, S Δ 2b, S Δ 3, S Δ 4 and S Δ 5 were employed in the construction of several double, triple and quadruple deletion strain by means of classical micromanipulation techniques. Transformation was also used for the engineering of selected quadruple strains. The elaborate system used to produce the quadruple deletion strains Q1, Q2, Q3, Q4 and Q5 are depicted in Figure 6.3.

The genotypes of the quadruple deletion mutant strains were verified by diagnostic PCR. PCR fragments were obtained only for the specific intact *ADH* gene in each of the strains and the fragment lengths resembled that of the parental strain W303-1A(a) (Figure 6.4A). Strain Q1 was characterised by the presence of a 1912 bp fragment representing the intact *ADHI* gene and 1282 bp, 1482 bp, 1610 bp and 1628 bp representing the *adh2 Δ ::URA3*, *adh3 Δ ::TRP1*, *adh4 Δ ::HIS3* and *adh5 Δ ::LEU2* deletions, respectively (Figure 6.4B). Strains Q2, Q3, Q4 and Q5 were similarly screened and each presented a unique PCR profile (Figure 6.4).

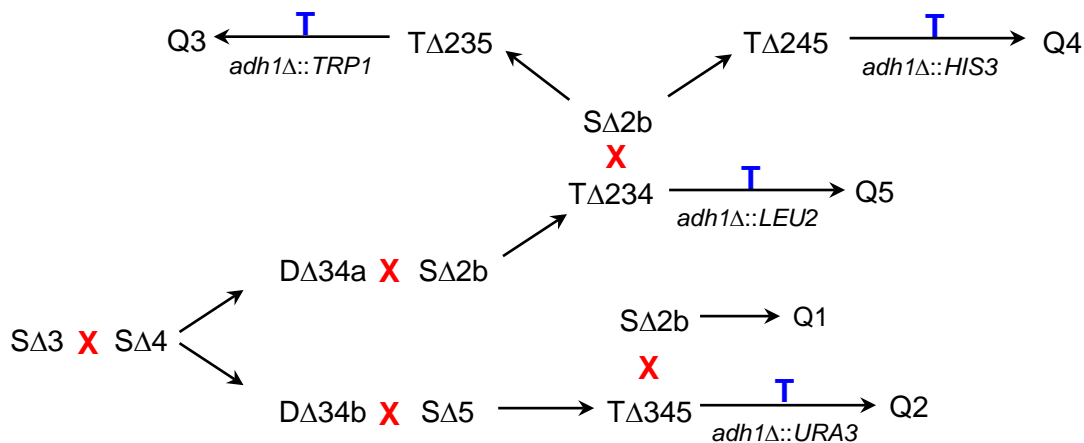


Figure 6.3 Diagram of double, triple and quadruple deletion strains. The strain genotypes can be viewed in Appendix C, Table A. Crossing of strains with different mating types are indicated by **X**. In the cases of Q2, Q3, Q4 and Q5 where the strains were constructed with transformation (**T**) as well, the transformation constructs used are indicated beneath the arrows.

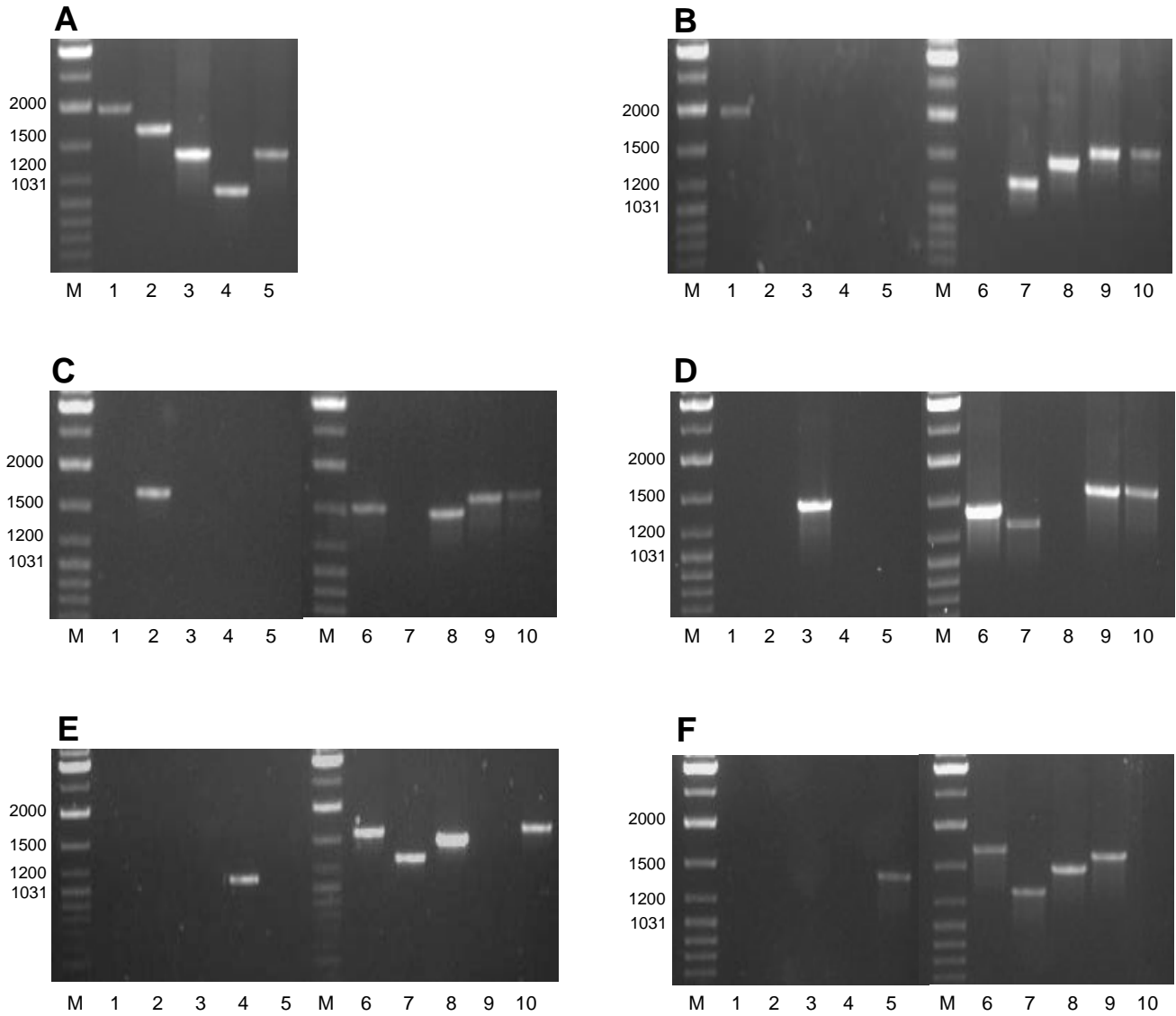


Figure 6.4 PCR profiles of the parental and quadruple deletion mutant strains. (A) Parental strain W303-1A(a) depicting amplified fragments of the intact *ADH1* (1912 bp), *ADH2* (1650 bp), *ADH3* (1398 bp), *ADH4* (1091 bp) and *ADH5* (1409 bp) genes as reference. B to F represent the genetic profiles of strains Q1, Q2, Q3, Q4 and Q5, respectively. Lanes 1 to 5 show amplification of the native intact *ADH1*, *ADH2*, *ADH3*, *ADH4* and *ADH5* genes, respectively. No amplification indicates deletion of the relative *ADH* gene. Lanes 6 indicates replacement of the *ADH1* gene with either *URA3* (1524 bp, lane C6), *TRP1* (1381 bp, lane D6), *HIS3* (1590 bp, lane E6) or *LEU2* (1704 bp, lane F6). Lane 7 shows the replacement of *ADH2* with *URA3* (1282 bp), lane 8 *ADH3* replaced by *TRP1* (1483), lane 9 *ADH4* replaced by *HIS3* (1610 bp) and lane 10 depicts *ADH5* deleted and replaced by the *LEU2* marker gene (1628 bp). Lanes M represent marker DNA O'GeneRuler (Appendix P).

6.4.2 Bioreactor cultivation of strains W303-1A(a), Q1, Q2, Q3 Q4 and Q5 on glucose as carbon source

The importance of each ADH enzyme in the ethanol metabolism was elucidated by culturing the five engineered strains Q1, Q2, Q3, Q4 and Q5, defective in all *ADH* genes except the one mentioned in the above designation, in bioreactors on glucose and ethanol. The strains were evaluated in terms of their growth kinetics and the transcription levels of the *ADH* gene/s present. The data presented are representative of independent duplicate experiments. The W303-1A(a) parental strain grew rapidly on glucose with a specific growth rate of 0.44 h^{-1} . All the glucose was utilised at a maximum volumetric rate of $2.315 \text{ g l}^{-1} \text{ h}^{-1}$ with the concomitant formation of ethanol, glycerol and acetic acid. After depletion of glucose from the culture medium, ethanol and acetic acid were utilised, while glycerol was still detected after 39 h (Figure 6.5, Table 6.1). During glucose utilisation, high levels of *ADH1* expression were detected, which agreed with the concept that ADH I were responsible for ethanol production (Figure 6.6A) (Ciriacy, 1979; Heick *et al.*, 1969). *ADH2* transcription was visibly but not completely repressed by glucose (Figure 6.6B). *ADH4* transcription was not detected in the presence of glucose and low levels of *ADH5* mRNA appeared when the glucose concentrations had decreased to 6.66 and 1.69 g l^{-1} (Figure 6.6C, D). During the ethanol assimilation phase of diauxic growth, *ADH1* transcription decreased as indicated by the 4.6 to 5.6-fold in mRNA levels, after which the levels gradually increased while ethanol was utilised (Figure 6.6A). *ADH2* mRNA levels increased 470 to 500-fold upon depletion of glucose and, although high levels were detected during ethanol utilisation, a visible decrease correlated with the decrease in ethanol concentrations (Figure 6.6B). *ADH4* and *ADH5* transcription levels were detected when ethanol concentrations were 4.6 g l^{-1} . The transcription of both these genes were detected while ethanol was present in the medium and *ADH5* levels gradually increased until the ethanol reached a concentration of 2 g l^{-1} (Figure 6.6C, D).

The Q1 strain grew on glucose at a rate of 0.45 h^{-1} , but glucose was assimilated at a slower volumetric rate of $1.771 \text{ g l}^{-1} \text{ h}^{-1}$. Ethanol was also produced and assimilated at slower specific rates of 1.366 and $0.117 \text{ g g}^{-1} \text{ h}^{-1}$, respectively, compared to 1.757 and $1.172 \text{ g l}^{-1} \text{ h}^{-1}$ seen in W303-1A(a). The Q1 strain produced less glycerol, as shown by the glycerol yield coefficients in Table 6.1, and the formation of glycerol was only visible

after 7 h, whereas glycerol was detected in strain W303-1A(a) within 2 h of inoculation (Figure 6.7). Other than the differences mentioned, the growth parameters of strain Q1 largely resembled those of the parental strain W303-1A(a) (Table 6.1). *ADHI* transcription was detected during the glucose consumption phase and was initially repressed only 1.4 to 1.7-fold by the produced ethanol, where after the levels gradually increased during the ethanol assimilation phase of diauxic growth (Figure 6.7C).

The Q2 and Q3 strains demonstrated similar growth kinetics to each other, but vastly different from those of strains Q1 and W303-1A(a). Strains Q2 (Figure 6.8) and Q3 (Figure 6.9) grew on glucose at maximum specific growth rates of 0.21 and 0.19 h⁻¹, respectively, and glucose was assimilated at very slow rates (Table 6.1). These strains were also characterised by the production of high concentrations of glycerol (3.19 and 3.01 g l⁻¹) and acetaldehyde (1.07 and 0.85 g l⁻¹). More glycerol and acetaldehyde were produced from glucose than ethanol (Table 6.1). Depletion of glucose was followed by an acetaldehyde assimilation phase where no significant change in biomass was observed. As can be seen from the broken line in Figure 6.8 and Figure 6.9, assimilation of acetaldehyde did take place because, despite its high volatility, the concentrations during growth decreased more rapidly than the rate of evaporation. The cells grew on the produced ethanol at specific rates of 0.09 and 0.1 h⁻¹ and assimilated this carbon substrate at specific rates of 0.106 and 0.104 g g⁻¹ h⁻¹. *ADH2* transcription in the Q2 strain demonstrated repression by glucose, but the depletion of glucose did not result in immediate alleviation of repression. A 450-fold increase in mRNA levels was detected when the acetaldehyde concentration was 0.28 g l⁻¹ and remained elevated during ethanol assimilation (Figure 6.8C). Unfortunately, *ADH3* transcription could not be monitored due to the lack of an appropriate TaqMan probe.

The Q4 and Q5 strains were able to grow on glucose (Figure 6.10, Figure 6.11), but did so at very slow rates when compared to the W303-1A(a) and Q1 strains. Strains Q4 and Q5 produced even less ethanol from glucose and at lower specific rates compared to strains Q2 and Q3 (Table 6.1). A high production of glycerol and acetaldehyde were also characteristic of strains Q4 and Q5 and both were unable to utilise the produced ethanol as carbon source. *ADH4* mRNA was only detected in strain Q4 during the first 5 h of cultivation which could very well be remnants of expression in the inoculum (Figure

6.10C). The presence of *ADH5* mRNA in strain Q5 during the first 5 h of growth and its abrupt disappearance might be explained the same way. Transcription was apparent again after 33 h, but did not coincide with any ethanol assimilation (Figure 6.11C).

Nomenclature for table 6.1

μ_{\max}	Maximum specific growth rate on carbon stated, calculated by linear regression analysis of exponential growth data
$Y_{x/s}$	Biomass yield coefficient (g dry biomass/g carbon)
$Y_{\text{ethanol}/s}$	Ethanol yield coefficient (g ethanol/g glucose)
$Y_{\text{glycerol}/s}$	Glycerol yield coefficient (g glycerol produced/g glucose assimilated)
$Y_{\text{acetaldehyde}/s}$	Acetaldehyde yield coefficient (g acetaldehyde produced/g glucose assimilated)
Q_s^{\max}	Maximum volumetric rate of glucose assimilation, calculated from the maximum slope of the glucose concentration curve
Q_p^{\max}	Maximum volumetric rate of ethanol production, calculated from the maximum slope of the ethanol concentration curve
$q_p^{\max}, \text{ g g}^{-1} \text{ h}^{-1}$	Maximum specific rate of ethanol production (g ethanol/g biomass h)
$q_s^{\max}, \text{ g g}^{-1} \text{ h}^{-1}$	Maximum specific rate of ethanol assimilation (g ethanol/g biomass h)
ND	Not determined

Table 6.1 Growth parameters of *S. cerevisiae* strains W303-1A(a), Q1, Q2, Q3, Q4 and Q5 in bioreactor batch cultures grown on glucose. The mean values of duplicate experiments are given

Parameter	Strain					
	W303-1A(a)	Q1	Q2	Q3	Q4	Q5
$\mu_{\max \text{ glucose}}, \text{h}^{-1}$	0.44 ± 0	0.45 ± 0.007	0.21 ± 0.009	0.19 ± 0.007	0.18 ± 0.008	0.17 ± 0.004
$\mu_{\max \text{ ethanol}}, \text{h}^{-1}$	0.05 ± 0.004	0.04 ± 0	0.09 ± 0	0.1 ± 0.01	ND	ND
$Y_{x/s \text{ glucose}}$	0.15 ± 0.004	0.14 ± 0.01	0.06 ± 0.005	0.07 ± 0.006	0.05 ± 0	0.05 ± 0.008
$Y_{x/s \text{ ethanol}}$	0.38 ± 0.02	0.38 ± 0.03	1.08 ± 0.02	1.4 ± 0.002	ND	ND
$Y_{\text{ethanol}/s}$	0.38 ± 0.004	0.37 ± 0.03	0.13 ± 0.02	0.11 ± 0.001	0.06 ± 0.005	0.06 ± 0.01
$Y_{\text{glycerol}/s}$	0.11 ± 0.02	0.03 ± 0.001	0.32 ± 0.007	0.35 ± 0.01	0.36 ± 0.02	0.34 ± 0.03
$Y_{\text{acetaldehyde}/s}$	ND	ND	0.14 ± 0.02	0.15 ± 0.04	0.14 ± 0.01	0.17 ± 0.01
$Q_s^{\max}, \text{g l}^{-1} \text{h}^{-1}$	2.315 ± 0.05	1.771 ± 0.2	0.843 ± 0.03	0.658 ± 0.07	0.660 ± 0.002	0.609 ± 0.02
$Q_p^{\max}, \text{g l}^{-1} \text{h}^{-1}$	0.859 ± 0.02	0.84 ± 0.01	0.46 ± 0.006	0.063 ± 0.005	0.043 ± 0.004	0.032 ± 0.006
$q_p^{\max}, \text{g g}^{-1} \text{h}^{-1}$	1.757 ± 0.01	1.366 ± 0.04	0.143 ± 0.03	0.141 ± 0.001	0.114 ± 0.01	0.072 ± .004
$q_s^{\max}, \text{g g}^{-1} \text{h}^{-1}$	0.172 ± 0.001	0.117 ± 0.001	0.106 ± 0.01	0.104 ± 0.03	ND	ND

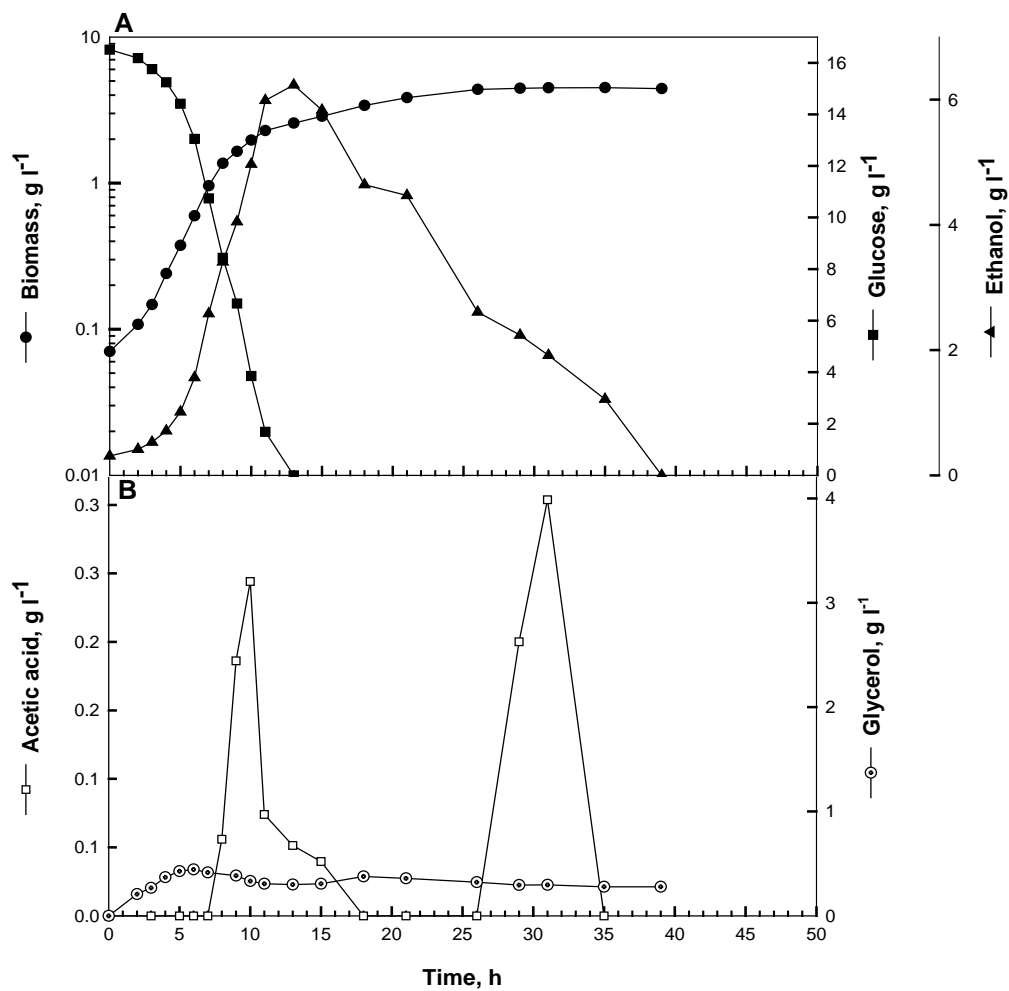


Figure 6.5 Typical aerobic cultivation profile of *S. cerevisiae* strain W303-1A(a) grown in chemically defined medium with 16 g glucose l^{-1} as initial carbon source. The metabolite concentrations are representative of independent duplicate experiments.

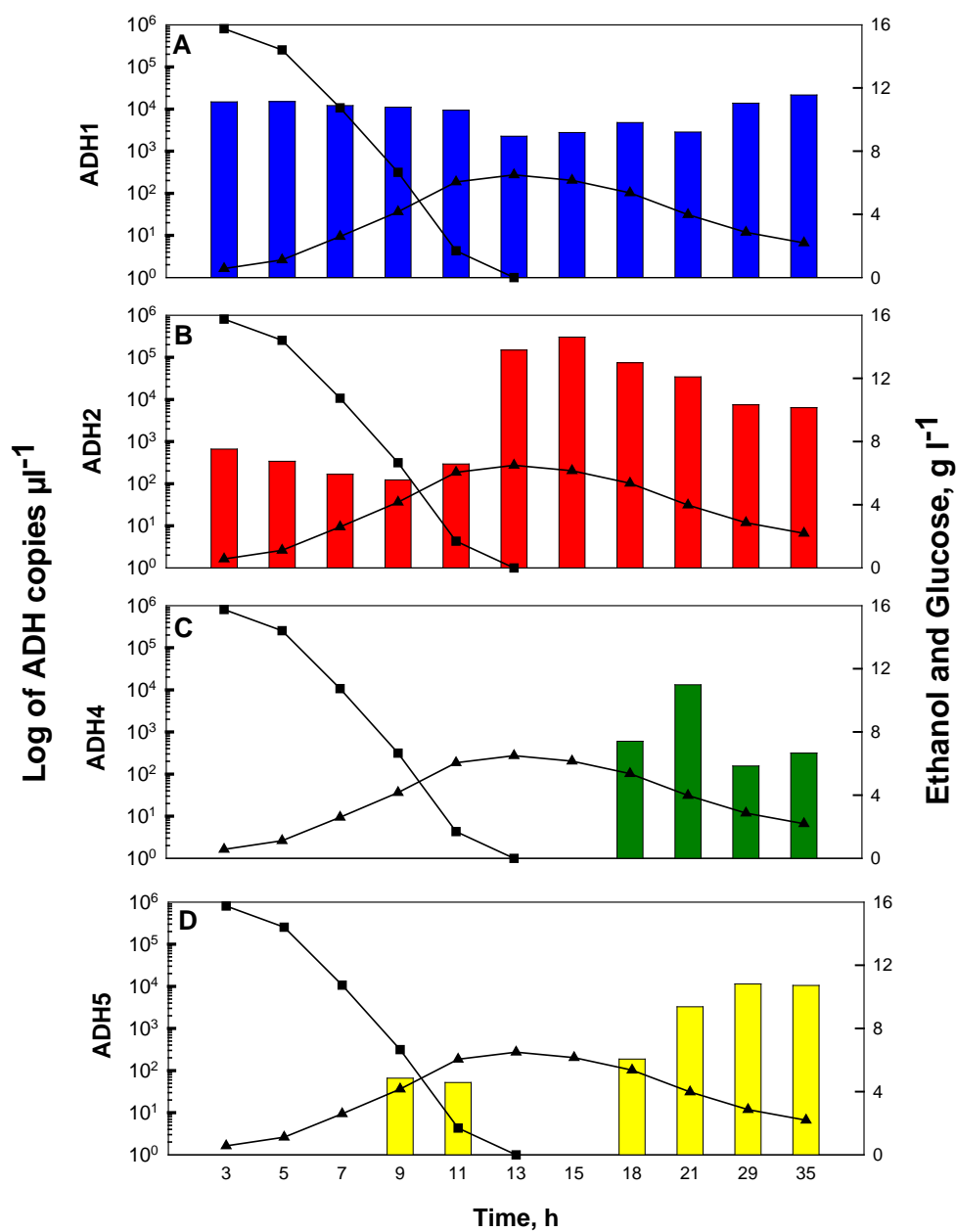


Figure 6.6 Real-time RT-PCR transcription profiles of the *ADH1*, *ADH2*, *ADH4* and *ADH5* genes of strain W303-1A(a) grown in bioreactors with 16 g glucose l⁻¹ as carbon source. Glucose (■) and ethanol (▲) concentrations were derived from Figure 6.1.

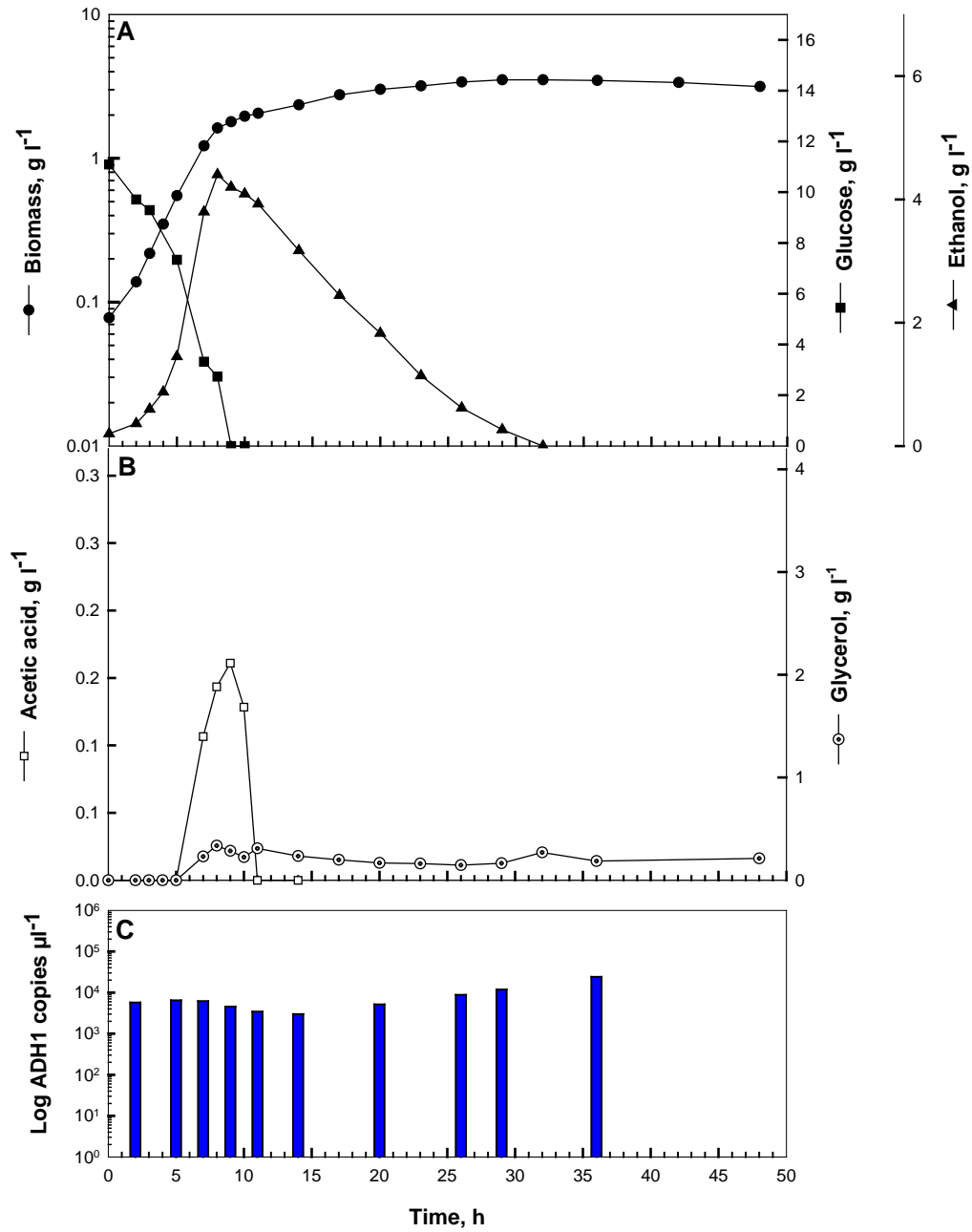


Figure 6.7 (A, B) Typical aerobic cultivation profile of *S. cerevisiae* strain Q1 (expressing only the *ADH1* gene) grown in chemically defined medium with 10 g glucose l⁻¹ as initial carbon source. (C) Real-time RT-PCR transcription profile of the *ADH1* gene.

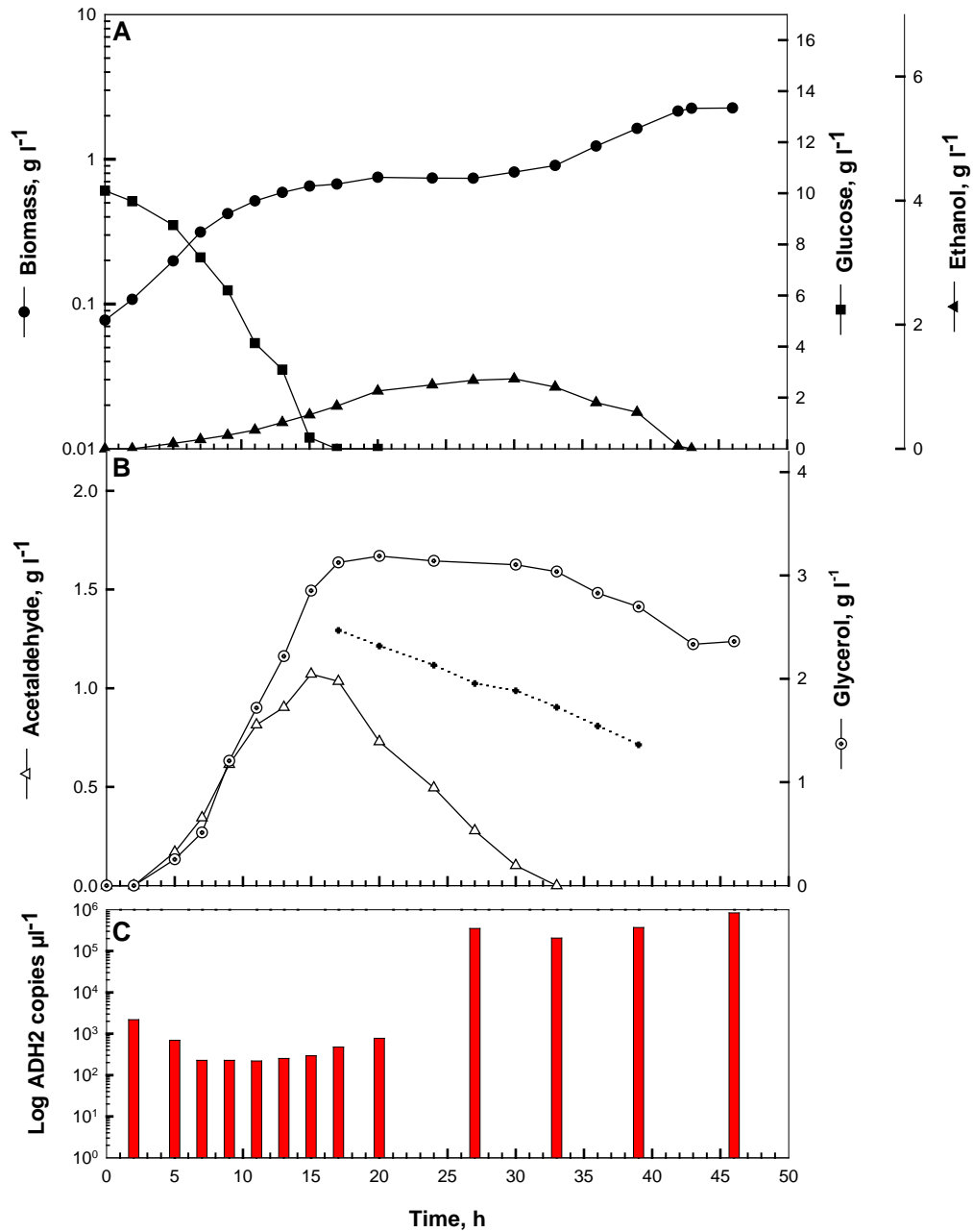


Figure 6.8 (A, B) Typical aerobic cultivation profile of *S. cerevisiae* strain Q2 (expressing only the *ADH2* gene) grown in chemically defined medium with 10 g glucose l⁻¹ as initial carbon source. (C) Real-time RT-PCR transcription profile of the *ADH2* gene. The dotted line is an indication of the measured acetaldehyde evaporation.

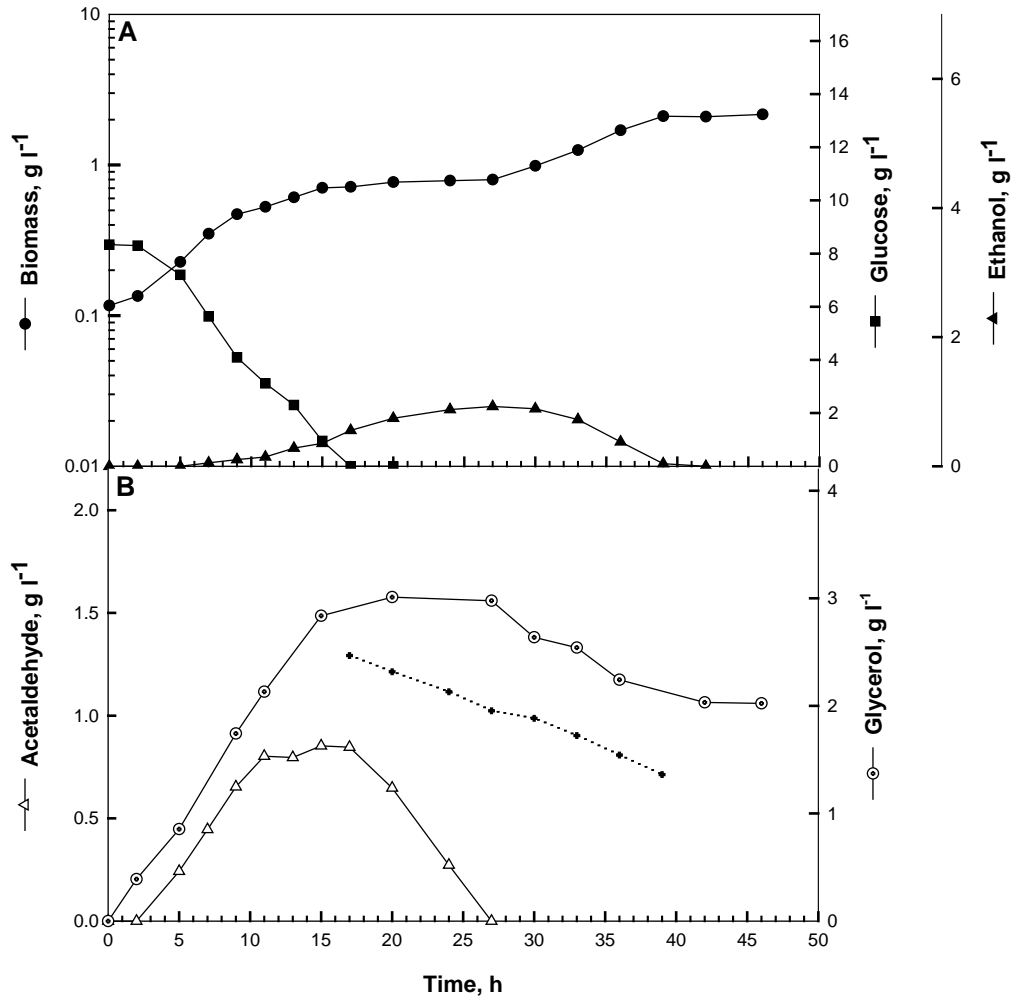


Figure 6.9 Typical bioreactor profile of *S. cerevisiae* strain Q3 (expressing only the *ADH3* gene) grown in chemically defined medium with 10 g glucose l⁻¹ as initial carbon source. The broken line indicates the decrease in acetaldehyde concentration due to evaporation.

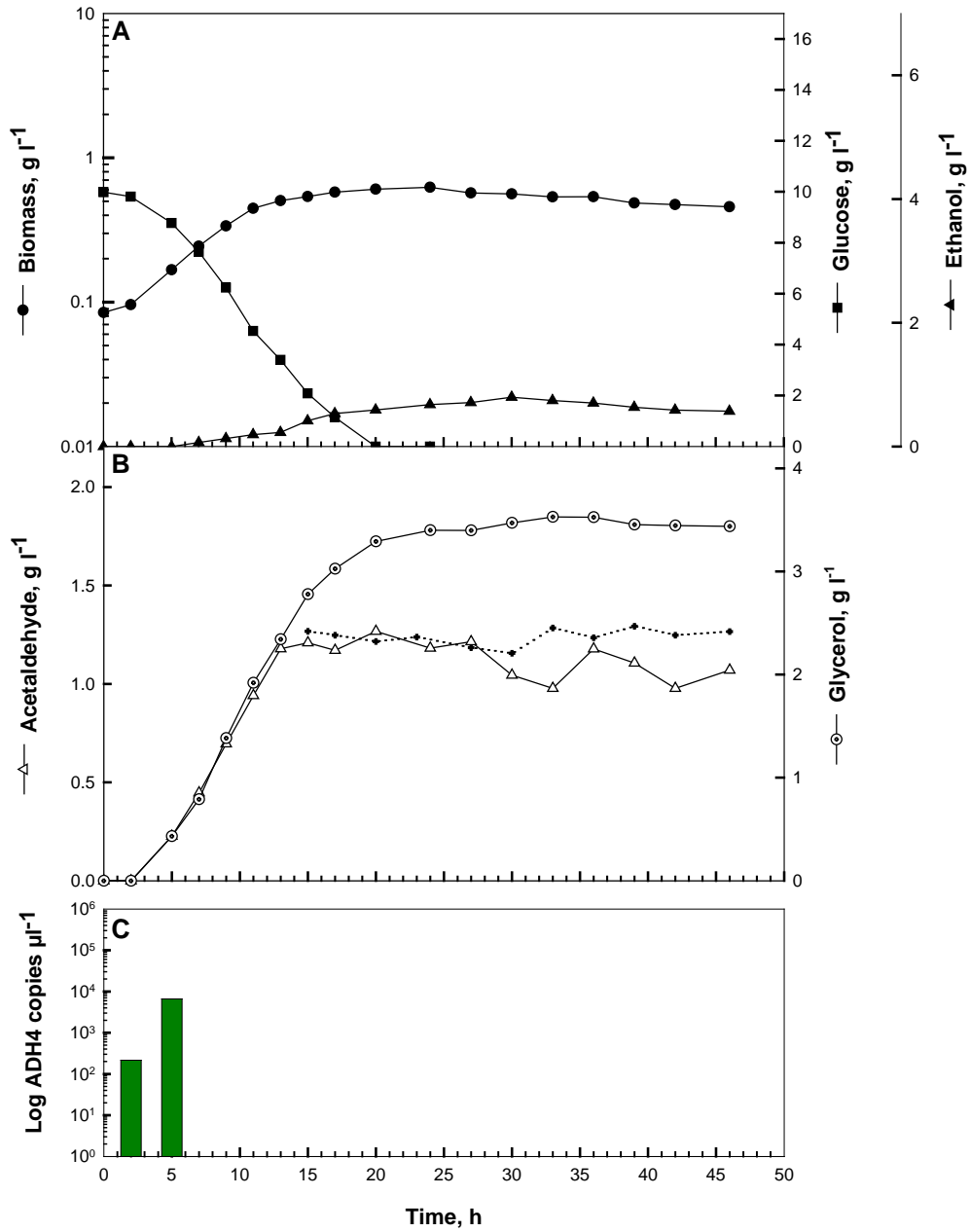


Figure 6.10 (A, B) Typical aerobic cultivation profile of *S. cerevisiae* strain Q4 (expressing only the *ADH4* gene) grown in chemically defined medium with 10 g glucose l⁻¹ as initial carbon source. (C) Real-time RT-PCR transcription profile of the *ADH4* gene. The broken line indicates the decrease in acetaldehyde concentration due to evaporation.

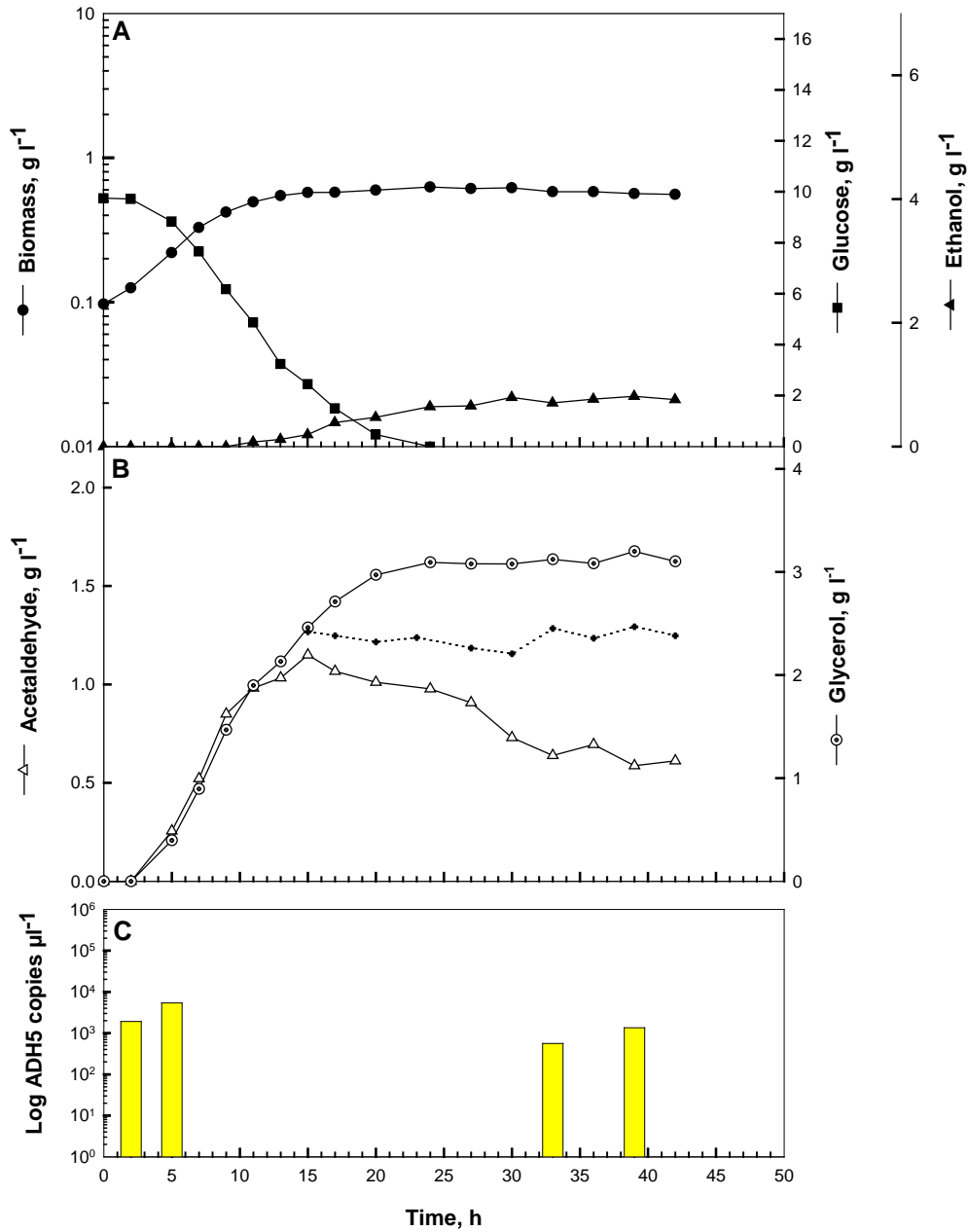


Figure 6.11 (A, B) Typical aerobic cultivation profile of *S. cerevisiae* strain Q5 (expressing only the *ADH5* gene) grown in chemically defined medium with 10 g glucose l⁻¹ as initial carbon source. (C) Real-time RT-PCR transcription profile of the *ADH5* gene. The broken line indicates the decrease in acetaldehyde concentration due to evaporation.

6.4.3 Bioreactor cultivation of strains W303-1A(a), Q1, Q2 and Q3 on ethanol as carbon source

Growth kinetics and transcription profiles of the *ADH* gene/s were compared when the quadruple deletion mutant strains Q1, Q2, Q3 and W303-1A(a) (parental strain) were grown aerobically in bioreactors on ethanol as carbon source. Strains W303-1A(a) grew on ethanol at a specific rate of 0.2 h^{-1} and ethanol was assimilated at a specific rate of $0.44 \text{ g g}^{-1} \text{ h}^{-1}$. The biomass yield coefficient was 0.51 and no other metabolites were detected (Figure 6.12A, Table 6.2). *ADH1* transcription was detected throughout the cultivation and no repression by ethanol was evident (Figure 6.12B). *ADH2* transcription was detected (Figure 6.12C), as would be expected of the gene encoding the primary enzyme responsible for the oxidation of ethanol (Beier *et al.*, 1985; Young & Pilgrim, 1985). The *ADH4* gene was not expressed during growth on ethanol. *ADH5* transcription was detected 3 h after inoculation and no transcription was evident until ethanol concentrations had decreased below 3.2 g l^{-1} . The transcription level gradually increased until ethanol depletion (Figure 6.12D).

Strain Q1, with only the *ADH1* gene intact, was able to grow on ethanol and no marked differences in growth kinetics compared to the W303-1A(a) strain (Figure 6.13A, Table 6.2) were apparent. The *ADH1* transcription profile of Q1 also resembled that of the parental strain with an increase in levels evident when the ethanol concentration had decreased below 1.7 g l^{-1} (Figure 6.13B). The Q2 strain, which contained only the *ADH2* gene, grew on ethanol at a specific rate of 0.2 h^{-1} (Figure 6.14A). The rate of ethanol assimilation was less than that of strain W303-1A(a) (Table 6.2). An *ADH2* expression profile similar to that of the parental W303-1A(a) strain was observed (Figure 6.14B). The Q3 strain, with only the *ADH3* gene in the genome, grew on ethanol at a specific rate of 0.17 h^{-1} , which was slower compared to the other three strains. Strain Q3 also differed from these strains in the sense that very little ethanol (0.5 g l^{-1}) was consumed during the first 15 h of cultivation. When ethanol assimilation did take place, it was at a slower rate (Figure 6.15, Table 6.2). The Q4 and Q5 strains were unable to grow on ethanol as a carbon substrate.

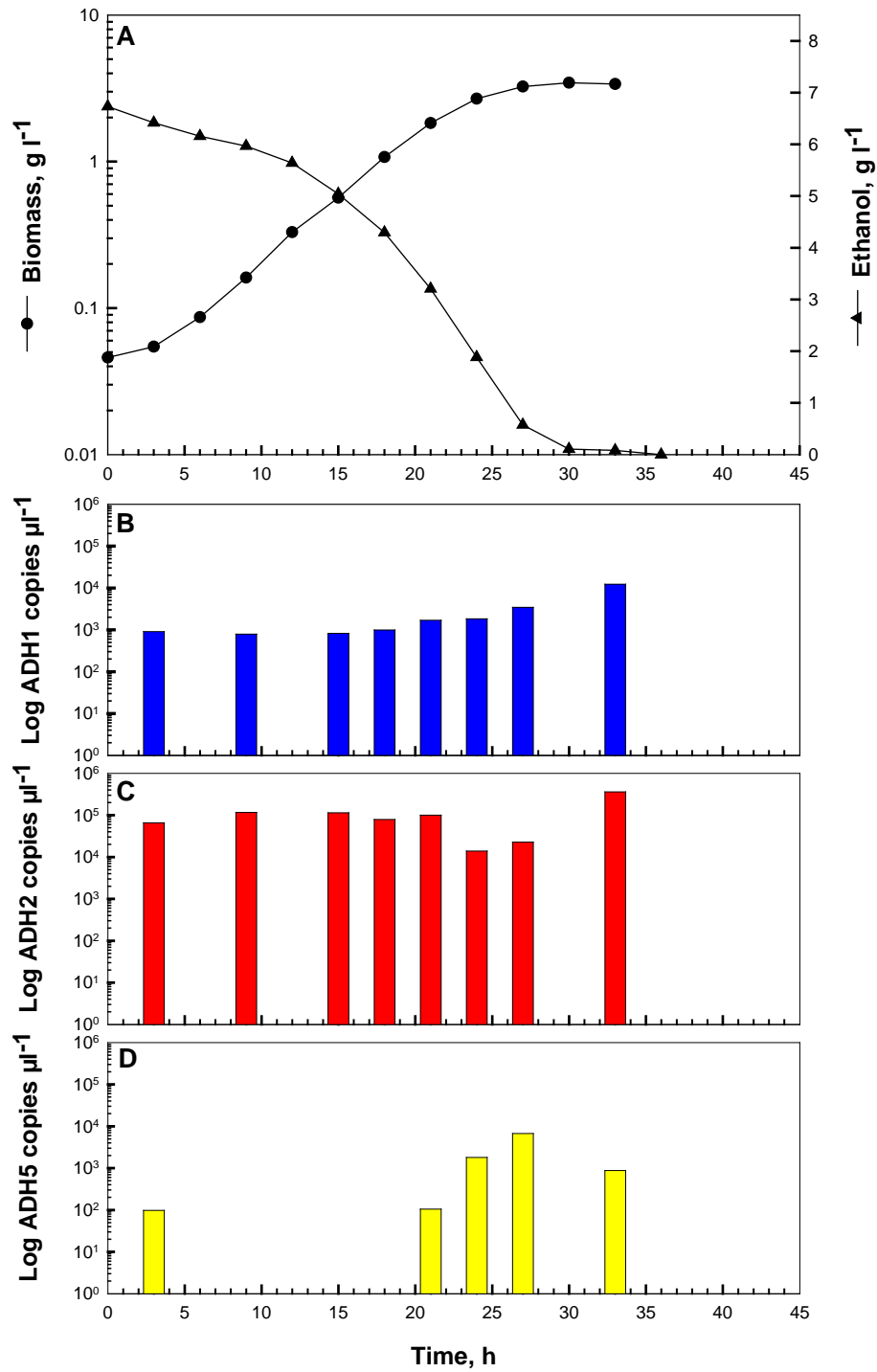


Figure 6.12 (A) Aerobic cultivation profile of *S. cerevisiae* strain W303-1A(a) (parental strain) grown in chemically defined medium with 7 g ethanol l⁻¹ as initial carbon source. (B, C, D) Real-time RT-PCR transcription profile of the *ADH1*, *ADH2* and *ADH5* genes, respectively. The *ADH4* gene was not expressed under these experimental conditions. The values are representative of independent duplicate experiments.

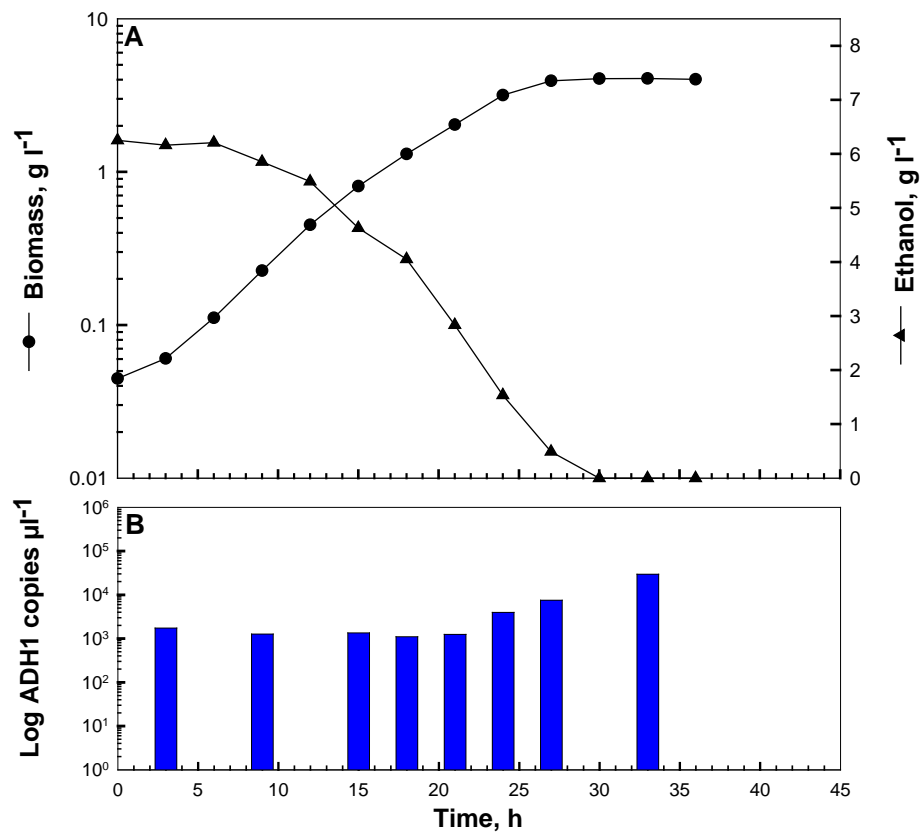


Figure 6.13 (A) Aerobic cultivation profile of *S. cerevisiae* strain Q1 (with only the *ADH1* gene in the genome) grown in chemically defined medium with 7 g ethanol l^{-1} as initial carbon source. (B) Real-time RT-PCR transcription profile of the *ADH1* gene.

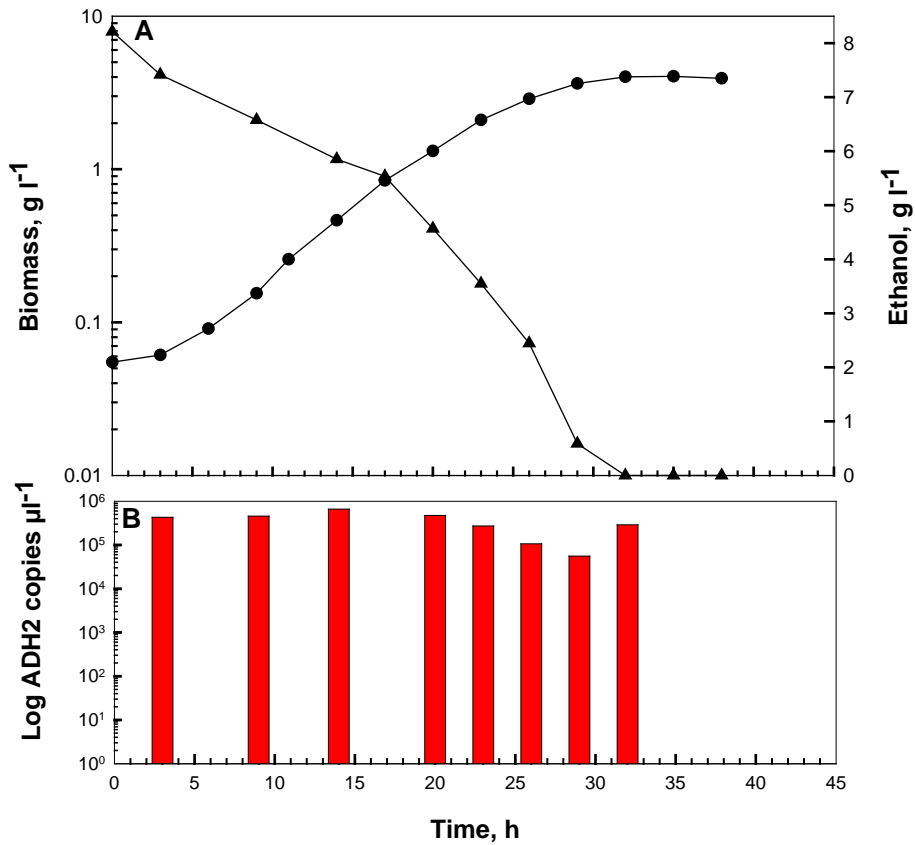


Figure 6.14 (A) Aerobic cultivation profile of *S. cerevisiae* strain Q2 (with only the *ADH2* gene in the genome) grown in chemically defined medium with 7 g ethanol l^{-1} as initial carbon source. (B) Real-time RT-PCR transcription profile of the *ADH2* gene.

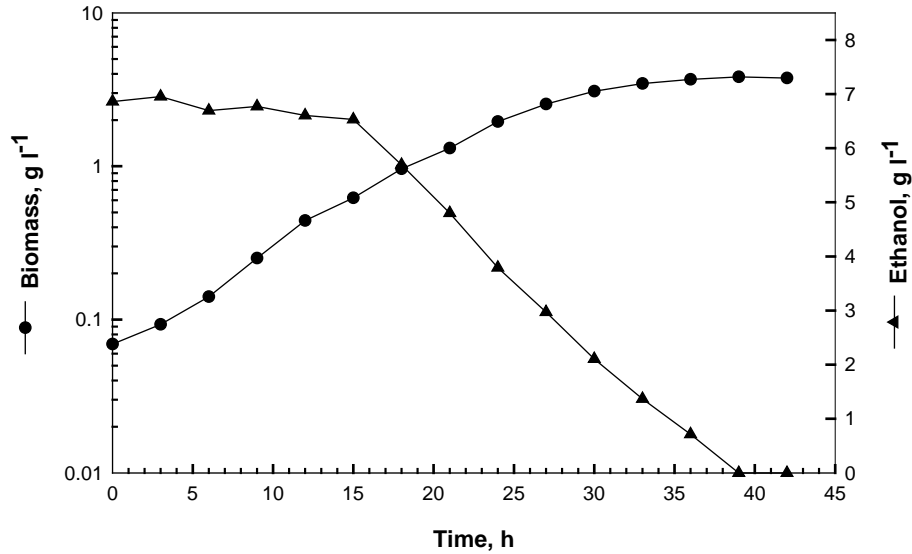


Figure 6.15 Aerobic cultivation profile of *S. cerevisiae* strain Q3 (with only the *ADH3* gene in the genome) grown in chemically defined medium with 7 g ethanol l⁻¹ as initial carbon source.

Table 6.2 Growth parameters of *S. cerevisiae* strains W303-1A(a), Q1, Q2, and Q3 grown on ethanol in aerobic bioreactor cultures. The mean values of duplicate experiments are given

Parameter	Strain			
	W303-1A(a)*	Q1	Q2	Q3
μ_{\max} , h ⁻¹	0.20	0.21 ± 0.001	0.2 ± 0.001	0.17 ± 0.005
Q_s^{\max} , g l ⁻¹ h ⁻¹	0.417	0.385 ± 0.03	0.397 ± 0.003	0.28 ± 0.01
$Y_{x/s}$	0.51	0.57 ± 0.07	0.49 ± 0.004	0.62 ± 0.005
q_s^{\max} , g g ⁻¹ h ⁻¹	0.44	0.23 ± 0.03	0.33 ± 0.03	0.25 ± 0.01

* Data presented for this strain was from one experiment

μ_{\max} Maximum specific growth rate on ethanol, calculated by linear regression analysis of exponential growth data

Q_s^{\max} Maximum volumetric rate of ethanol assimilation, calculated from the maximum slope of the ethanol concentration curve

$Y_{x/s}$ Biomass yield coefficient (g dry biomass/g ethanol)

q_s^{\max} Specific rate of ethanol assimilation (g ethanol g biomass⁻¹ h⁻¹)

6.5 Conclusions

In contrast to previous studies (Johansson; Sjostrom, 1984; Wills & Phelps, 1975), strains were engineered with irreversible defects in the five *ADH* genes in different combinations, thereby avoiding the problem of *in vivo* leakiness of undefined point mutations. The physiological importance of each ADH enzyme was investigated in aerobic bioreactor cultures with glucose and ethanol as carbon sources.

ADH I catalyses the reduction of acetaldehyde to ethanol and plays a key role in sugar metabolism of *S. cerevisiae* through the regeneration of NAD^+ from glycolytic $\text{NADH} + \text{H}^+$ (Ciriacy, 1979; Heick *et al.*, 1969; Lutstorf & Megnet, 1968; Wills & Phelps, 1975) and among the ADHs investigated in this study, ADH I is the only enzyme able to perform this task efficiently. The results also showed that ADH I could oxidise the ethanol produced during growth on glucose or when added as the initial carbon source. The growth kinetics of the Q1 strain on glucose largely resembled that of the W303-1A(a) parental strain, with marginal differences in glycerol production and ethanol assimilation rates. Considering the correlation between mRNA transcription levels and the amount of active ADH I (Denis *et al.*, 1983), it is reasonable to conclude that ADH I in the Q1 strain was capable of oxidising the ethanol produced during growth on glucose, since it was expressed not only during glucose consumption, but also during the ethanol consumption phase of diauxic growth (Figure 6.7). Since ADH I should kinetically be able to oxidise ethanol, but would do so presumable less efficiently (Wills, 1976; Wills *et al.*, 1982), the lower rate of ethanol assimilation could be attributed to the absence of ADH II in strain Q1 when compared to the W303-1A(a) strain where both enzymes were functional. The lower specific rate of ethanol assimilation was also evident when strain Q1 was grown on ethanol as carbon source (Table 6.2). ADH1 transcription in the Q1 strain exhibited less repression following glucose depletion due to the presence of a nonfermentative carbon source, than recorded in literature (Denis *et al.*, 1983; Williamson *et al.*, 1983) or reported here for the parental strain W303-1A(a) (Figure 6.6, Figure 6.7).

The *in vivo* significance of the reaction catalysed by ADH I has been verified by the investigation of mutants deficient in *ADH1*. Such mutants grew slowly on glucose

and this carbon source was converted to glycerol, ethanol and acetaldehyde under aerobic conditions (Table 6.1, Figure 6.8, Figure 6.9, Figure 6.10 & Figure 6.11) (Ciriacy, 1975a; Ciriacy, 1975b; Johansson; Sjostrom, 1984; Wills *et al.*, 1982; Wills & Phelps, 1975). With *ADH1* absent from the genome the operation of Neuberg's second form of fermentation (Neuberg & Kobel, 1934) would be expected to result in high concentrations of glycerol before glucose depletion. This form of fermentation results when dihydroxyacetone phosphate is reduced to glycerol-3-phosphate, which in turn is converted to glycerol. The glycerol formation enables the reoxidation of NADH that is generated during the conversion of sugar into biomass (Pronk *et al.*, 1996). According to Neuberg's third form of fermentation the glycerol produced results in a deficiency in the amount of reduced NAD available for the reduction of acetaldehyde to ethanol. Acetaldehyde, instead of accumulating, should undergo a dismutation to either acetate or ethanol (Neuberg & Kobel, 1934). The effects of acetaldehyde on ethanol-producing micro-organisms are complex due in part to its high volatility. The contribution of acetaldehyde to product inhibition in yeast fermentations is due to the fact that its diffusion from yeast cells is not instantaneous and that acetaldehyde accumulates intracellularly during the fermentation of glucose (Stanley *et al.*, 1997; Stanley & Pamment, 1993). Several cytoplasmic and mitochondrial aldehyde dehydrogenases (ALDH) have been identified and characterised (Thielen & Ciriacy, 1991; Wang *et al.*, 1998) and the dismutation of acetaldehyde in *S. cerevisiae* was proposed to be mediated by mitochondrial ALDH II (Thielen & Ciriacy, 1991). Acetaldehyde causes inhibition effects on yeast growth at a concentration of 0.07 g l⁻¹, which could be connected to inhibition effects on ALDH (Modig *et al.*, 2002). Ciriacy (1978) reported that several mitochondrial enzymes were repressed in *adh1adh2adh3* mutants when grown aerobically on glucose and the slow growth in the quadruple deletion strains could, therefore, at least partially also be ascribed to impaired mitochondrial function.

Previous reports stated that *ADH2* mRNA was not present during growth in a glucose-containing medium (Denis *et al.*, 1981; Williamson *et al.*, 1983) and synthesis was first detected approximately 1 h after release from glucose repression followed by a several hundred-fold increase (Denis *et al.*, 1983; Dombek *et al.*, 1993). With the sensitive real time RT-PCR method used in this study, *ADH2* transcription was detected

while glucose was present in the medium and was subject to partial glucose repression, even when it was the only functional *ADH* (Figure 6.8). The transcription levels in the parental as well as the Q2 strain increased 450 to 500-fold on glucose depletion. It is tempting to speculate whether the apparent acetaldehyde assimilation visible in strain Q2 could be attributed to ADH II activity. It seemed that the increases in *ADH2* transcription levels and ethanol concentrations coincided with the assimilation of the produced acetaldehyde, but mRNA levels for the time interval 21 to 26 h are necessary to fully elucidate this assumption.

ADH III is expressed at lower levels in *S. cerevisiae* cells than ADH I and ADH III (Ciriacy, 1975a; Williamson & Paquin, 1987; Young & Pilgrim, 1985) and is involved in shuttling of mitochondrial reducing equivalents to the cytosol, where the redox balance can be restored by NADH dehydrogenases on the external side of the mitochondrial inner membrane (Bakker *et al.*, 2000). Although *ADH3* levels were not monitored, it was evident from the growth kinetics of strain Q3 that ADH III seemed no more capable of producing ethanol from glucose than the *ADH2* gene product. Under derepressed conditions the Q3 strain did, however, exhibit a capacity to grow on and assimilate ethanol at the same rate as the Q2 strain. These preliminary results indicated that the *ADH3* gene product could fulfil the same function as ADH II in a deletion background.

ADH4 transcription was detected for the first time in a laboratory strain using the sensitive real-time RT-PCR method. *ADH4* mRNA was detected in strain W303-1A(a) during the ethanol assimilation phase of diauxic growth (Figure 6.6C), but the expression might not be related to ethanol consumption. No *ADH4* transcription was detected when strain W303-1A(a) was grown on ethanol (Figure 6.12) and a quadruple deletion mutant Q4, containing only the *ADH4* gene, was unable to grow on ethanol as a carbon source. Although ADH IV does not share sequence or structural similarity with the other four ADHs (Paquin & Williamson, 1986), it is activated by zinc ions and resembled ADH I in terms of kinetic constants (Drewke & Ciriacy, 1988). Although Paquin & Williamson (1986) demonstrated that over-expression of the *ADH4* gene allowed fermentative growth on glucose in a strain lacking a functional *ADH1* gene, the data presented here (Figure

6.10) showed that the *ADH4* gene product, ADH IV could not be responsible for the production of ethanol during growth on glucose.

Drewke and co-workers (1990) showed that residual ethanol production in an *adh1* to *adh4* deletion mutant cannot be attributed to any of the known ADH enzymes. At that time, however, the existence of *ADH5* was not known. The lack of significant *ADH5* transcription during ethanol production resulting from the growth on glucose as reported here, suggested that the *ADH5* gene was not transcribed at sufficiently high levels to suggest that ADH V was responsible for ethanol production in strain Q5. Although *ADH5* transcription was detected during the ethanol consumption phase of diauxic growth in parental strain W303-1A(a) (Figure 6.6), the transcription profile during growth on added ethanol (Figure 6.12) and the inability of strain Q5 to grow on ethanol, suggested that the *ADH5* gene product did not participate in the oxidation of ethanol to acetaldehyde.

6.6 Literature cited

- Bakker, B. M., C. Bro, P. Kotter, M. A. Luttk, J. P. van Dijken and J. T. Pronk.** 2000. The mitochondrial alcohol dehydrogenase Adh3p is involved in a redox shuttle in *Saccharomyces cerevisiae*. *J. Bacteriol.* **182**: 4730-4737.
- Becker, J. M., G. A. Caldwell and E. A. Zachgo.** 1990. Biotechnology, a laboratory course. Becker, J. M, Caldwell, G. A, and Zachgo, E. A. *Academic Press.* pp.
- Beier, D. R., A. Sledziewski and E. T. Young.** 1985. Deletion analysis identifies a region, upstream of the *ADH2* gene of *Saccharomyces cerevisiae*, which is required for ADR1-mediated derepression. *Mol. Cell Biol.* **5**: 1743-1749.
- Chen, D. C., B. C. Yang and T. T. Kuo.** 1992. One-step transformation of yeast in stationary phase. *Curr. Genet.* **21**: 83-84.
- Ciriacy, M.** 1975a. Genetics of alcohol dehydrogenase in *Saccharomyces cerevisiae* : I. Isolation and genetic analysis of *adh* mutants. *Mutation Research.* **29**: 315-325.
- Ciriacy, M.** 1975b. Genetics of alcohol dehydrogenase in *Saccharomyces cerevisiae*. II. Two loci controlling synthesis of the glucose-repressible ADH II. *Mol. Gen. Genet.* **138**: 157-164.
- Ciriacy, M.** 1978. A yeast mutant with glucose-resistant formation of mitochondrial enzymes. *Mol. Gen. Genet.* **159**: 329-335.
- Ciriacy, M.** 1979. Isolation and characterization of further cis- and trans-acting regulatory elements involved in the synthesis of glucose-repressible alcohol dehydrogenase (ADHII) in *Saccharomyces cerevisiae*. *Mol. Gen. Genet.* **176**: 427-431.
- Denis, C. L., M. Ciriacy and E. T. Young.** 1981. A positive regulatory gene is required for accumulation of the functional messenger RNA for the glucose-repressible alcohol dehydrogenase from *Saccharomyces cerevisiae*. *J. Mol. Biol.* **148**: 355-368.
- Denis, C. L., J. Ferguson and E. T. Young.** 1983. mRNA levels for the fermentative alcohol dehydrogenase of *Saccharomyces cerevisiae* decrease upon growth on a nonfermentable carbon source. *J. Biol. Chem.* **258**: 1165-1171.
- Dombek, K. M., S. Camier and E. T. Young.** 1993. *ADH2* expression is repressed by REG1 independently of mutations that alter the phosphorylation of the yeast transcription factor ADR1. *Mol. Cell Biol.* **13**: 4391-4399.
- Drewke, C. and M. Ciriacy.** 1988. Overexpression, purification and properties of alcohol dehydrogenase IV from *Saccharomyces cerevisiae*. *Biochim. Biophys. Acta.* **950**: 54-60.
- Drewke, C., J. Thielen and M. Ciriacy.** 1990. Ethanol formation in *adh0* mutants reveals the existence of a novel acetaldehyde-reducing activity in *Saccharomyces cerevisiae*. *J Bacteriol.* **172**: 3909-3917.
- Heick, H. M. C., J. Willemot and N. Begin-heick.** 1969. The subcellular localization of alcohol dehydrogenase activity in baker's yeast. *Biochim. Biophys. Acta.* **191**: 493-501.
- Johansson, M. and J. E. Sjoström.** 1984. Enhanced production of glycerol in an alcohol dehydrogenase (*ADH1*) deficient mutant of *Saccharomyces cerevisiae*. *Biotechnol. Lett.* **6**: 49-54.

- Labuschagne, M. and J. Albertyn.** 2007. Cloning of an epoxide hydrolase-encoding gene from *Rhodotorula mucilaginosa* and functional expression in *Yarrowia lipolytica*. *Yeast* **24**: 69-78.
- Lutstorf, U. and R. Megnet.** 1968. Multiple forms of alcohol dehydrogenase in *Saccharomyces cerevisiae*. I. Physiological control of ADH-2 and properties of ADH-2 and ADH-4. *Arch. Biochem. Biophys.* **126**: 933-944.
- Millan, C., J. C. Mauricio and J. M. Ortega.** 1990. Alcohol and aldehyde dehydrogenase from *Saccharomyces cerevisiae*: specific activity and influence on the production of acetic acid, ethanol and higher alcohols in the first 48 h of fermentation of grape must. *Microbios.* **64**: 93-101.
- Mizuno, A., H. Tabei and M. Iwahuti.** 2006. Characterization of low-acetic-acid-producing yeast isolated from 2-deoxyglucose-resistant mutants and its application to high-gravity brewing. *J Biosci. Bioeng.* **101**: 31-37.
- Modig, T., G. Liden and M. J. Taherzadeh.** 2002. Inhibition effects of furfural on alcohol dehydrogenase, aldehyde dehydrogenase and pyruvate dehydrogenase. *Biochem J.* **363**: 769-776.
- Neuberg, C. and M. Kobel.** 1934. Present Status of the Problem of Sugar Fermentation. *J Bacteriol.* **28**: 461-471.
- Paquin, C. E. and V. M. Williamson.** 1986. Ty insertions at two loci account for most of the spontaneous antimycin A resistance mutations during growth at 15 degrees C of *Saccharomyces cerevisiae* strains lacking *ADH1*. *Mol. Cell Biol.* **6**: 70-79.
- Pronk, J. T., S. H. Yde and J. P. van Dijken.** 1996. Pyruvate metabolism in *Saccharomyces cerevisiae*. *Yeast* **12**: 1607-1633.
- Sambrook, J. and D. W. Russel.** 2001. Molecular cloning: A laboratory manual. *Cold Spring Harbour.*
- Stanley, G. A., T. J. Hobley and N. B. Pamment.** 1997. Effect of acetaldehyde on *Saccharomyces cerevisiae* and *Zymomonas mobilis* subjected to environmental shocks. *Biotechnol. Bioeng.* **53**: 71-78.
- Stanley, G. A. and N. B. Pamment.** 1993. Transport and intracellular accumulation of acetaldehyde in *Saccharomyces cerevisiae*. *Biotechnol. Bioeng.* **42**: 24-29.
- Thielen, J. and M. Ciriacy.** 1991. Biochemical basis of mitochondrial acetaldehyde dismutation in *Saccharomyces cerevisiae*. *J. Bacteriol.* **173**: 7012-7017.
- Wang, X., C. J. Mann, Y. Bai, L. Ni and H. Weiner.** 1998. Molecular cloning, characterization, and potential roles of cytosolic and mitochondrial aldehyde dehydrogenases in ethanol metabolism in *Saccharomyces cerevisiae*. *J Bacteriol.* **180**: 822-830.
- Wenger, J. I. and C. Bernofsky.** 1971. Mitochondrial alcohol dehydrogenase from *Saccharomyces cerevisiae*. *Biochim. Biophys. Acta.* **227**: 479-490.
- Wiesenfeld, M., L. Schimpfessel, and R. Crokaert.** 1975. Multiple forms of mitochondrial alcohol dehydrogenase in *Saccharomyces cerevisiae*. *Biochim. Biophys. Acta.* **405**: 500-512.
- Williamson, V. M., D. Cox, E. T. Young, D. W. Russell and M. Smith.** 1983. Characterization of transposable element-associated mutations that alter yeast alcohol dehydrogenase II expression. *Mol. Cell Biol.* **3**: 20-31.

- Williamson, V. M. and C. E. Paquin.** 1987. Homology of *Saccharomyces cerevisiae* ADH4 to an iron-activated alcohol dehydrogenase from *Zymomonas mobilis*. *Mol. Gen. Genet.* **209**: 374-381.
- Wills, C.** 1976. Production of yeast alcohol dehydrogenase isoenzymes by selection. *Nature* **261**: 26-29.
- Wills, C., P. Kratofil and T. Martin.** 1982. Functional mutants of yeast alcohol dehydrogenase. *Basic Life Sci.* **19**: 305-329.
- Wills, C. and J. Phelps.** 1975. A technique for the isolation of yeast alcohol dehydrogenase mutants with altered substrate specificity. *Arch. Biochem Biophys.* **167**: 627-637.
- Young, E. T. and D. Pilgrim.** 1985. Isolation and DNA sequence of *ADH3*, a nuclear gene encoding the mitochondrial isozyme of alcohol dehydrogenase in *Saccharomyces cerevisiae*. *Mol. Cell Biol.* **5**: 3024-3034.

CHAPTER 7

Concluding remarks and future research

For the investigation of the role and regulation of the ADH enzymes in *Saccharomyces cerevisiae*, it was essential to use a culture medium that met the nutritional requirements of the yeast strain. However, a complex medium failed to satisfy the demanding nutritional requirements of *S. cerevisiae* auxotrophic strain W303-1A(a). The use of a chemically defined medium resulted in higher specific growth and ethanol utilisation rates compared to the complex medium. When the ethanol concentration exceeded a value of 10 g l⁻¹ the growth rate was significantly inhibited. Therefore, the medium was formulated so that ethanol production did not exceed the latter volume.

The physiological roles and regulation of *ADH1*, *ADH2*, *ADH3*, *ADH4* and *ADH5* were investigated from three different angles. Firstly, by monitoring transcription of the *ADH* genes during the transient response to a glucose and an ethanol pulse in a glucose-limited chemostat culture using Northern blotting. Secondly, by investigating the growth kinetics and transcription levels of the *ADH* genes in a recombinant strain over-expressing *ADH2* in batch cultures. Lastly, by evaluating multiple knock-out strains, each expressing only one ADH gene, in bioreactor batch cultivations. Batch cultivations were performed with glucose or ethanol as carbon sources and mRNA levels were monitored by real-time RT-PCR analyses.

It is well known from literature that ADH I catalyses the reduction of acetaldehyde to ethanol and plays a key role in sugar metabolism of *S. cerevisiae* by allowing regeneration of NAD⁺ from glycolytic NADH + H⁺ (Ciriacy, 1979; Heick *et al.*, 1969; Lutstorf & Megnet, 1968; Wills & Phelps, 1975). Accordingly, *ADH1* transcription levels showed in this study increased in response to a glucose pulse administered to a chemostat culture of strain W303-1A(a), as well as during growth on glucose in batch cultures of strain Q1 (lacking all other *ADH* genes save *ADH1*). *ADH1* transcription in the Q1 strain showed less repression by the presence of a nonfermentative carbon source following glucose depletion than recorded in literature (Denis *et al.*, 1983; Williamson *et al.*, 1983) or reported here for the parental strain. Bioreactor cultivation of

strain Q1 also showed that ADH I, when functioning as the only ADH, could sufficiently oxidise the ethanol produced during growth on glucose or when added as the initial carbon source.

The *in vivo* significance of the reaction catalysed by ADH I was verified by mutants deficient in *ADH1*. Such mutants demonstrated impaired growth on glucose and this carbon was largely converted to glycerol, ethanol and acetaldehyde under aerobic conditions. Glycerol production was attributed to the functioning of Neuberger's second form of fermentation and the slow growth and acetaldehyde accumulation to impaired mitochondrial function.

ADH II is generally believed to be the major enzyme responsible for the first step of ethanol utilisation (Lutstorf & Megnet, 1968). According to the literature, *ADH2* mRNA was not present during growth on a medium containing glucose and synthesis could be detected after glucose depletion (Denis *et al.*, 1981; Williamson *et al.*, 1983); (Denis *et al.*, 1983; Dombek *et al.*, 1993). With the sensitive real-time RT-PCR method used in this study, *ADH2* transcription was, in fact, detected during growth on glucose. When considering the *ADH2* transcription levels following the pulse addition of glucose or ethanol to a chemostat culture, it is remarkable that an enzyme that uses ethanol as a substrate was repressed at transcriptional level when growing on ethanol and derepressed on acetic acid. In an attempt to further investigate this facet of ADH II regulation, repression of the structural gene was alleviated by over-expression on a multicopy vector system unaffected by catabolite repression. In batch cultivations with glucose or ethanol as carbon substrate, the presence of ADH II in excess did not result in significant differences in the growth parameters compared to a strain lacking ADH II activity. In batch cultures of strain Q2 (expressing only ADH II) with glucose as carbon substrate, *ADH2* transcription was subject to glucose repression, even when it was the only functional ADH, but was detected while glucose was present in the medium. The transcription levels suggested that ADH II could be responsible for the conversion of acetaldehyde to ethanol.

Mitochondrial ADH III is in part coupled to respiration during growth on ethanol by shuttling mitochondrial reducing equivalents to the cytosol (Bakker *et al.*, 2000; Wenger & Bernofsky, 1971; Young & Pilgrim, 1985). Northern blot analysis

showed that the *ADH3* gene was induced during the ethanol phase of the pulses suggested that the mitochondrial ADH III enzyme could also be involved in the first step of ethanol utilisation. Although *ADH3* levels were not monitored by real-time RT-PCR, it was evident from the growth kinetics of strain Q3 that ADH III seemed no more capable of sufficiently producing ethanol from glucose than the *ADH2* gene product. Thus it appears that the mitochondrial ADH III activity is not so effective in acetaldehyde reduction as previously proposed (Wills & Phelps, 1975). The growth kinetics of the Q3 strains demonstrated that the *ADH3* gene product could fulfil the same function as ADH II.

In accordance with previous data, *ADH4* expression could not be detected in batch or chemostat cultures using Northern blotting (van den Berg *et al.*, 1998; Williamson & Paquin, 1987). With the sensitive real-time RT-PCR method *ADH4* transcription was detected in batch cultivation during the ethanol consumption phase of diauxic growth of strain W303-1A(a), single deletion strain SΔ2aTR_E and recombinant strain SΔ2aTR_ADH2. None of these strains showed significant *ADH4* transcription levels when grown on ethanol as carbon source. No *ADH4* transcription was detected in the quadruple deletion strain Q4 and this strain was also unable to grow on ethanol as carbon source. It is evident that ADH IV is not involved in the production or assimilation of ethanol and that in the case where transcription was detected, it was probably unrelated to utilisation of this carbon substrate.

Little information is currently available regarding the biochemistry or function of ADH V. In this study *ADH5* expression in chemostat cultures of strain W303-1A(a) could not be detected in quantifiable amounts using Northern blotting. In batch cultivations with glucose as carbon source, a low level of *ADH5* transcription was detected by real-time RT-PCR during the glucose assimilation phase in strain SΔ2aTR_ADH2 and during the ethanol assimilation phase of diauxic growth in strain W303-1A(a). This transcription was in all probability not associated with ethanol utilisation, since the Q5 strain did not show significant transcription of *ADH5* and was unable to grow on ethanol as carbon source.

Since ethanol production in mutants containing an intact ADH5 (such as strain Q5 and as reported by Drewke *et al.*, 1990) could not be attributed to the

functioning of ADH V, it is essential to investigate other possible candidates such as *SFA1* and *ADH6*. *SFA1* showed ethanol inducibility (Wehner *et al.*, 1993) and *SFA1* activity was sufficient for the final stage of amino acid catabolism, namely the conversion of an aldehyde to a long chain or a complex alcohol in an *adhΔ1-5* background (Dickinson *et al.*, 2003). Although Petersson *et al.* (2006) demonstrated NADPH-dependent 5-hydroxymethyl furfural (HMF) reduction activity associated with ADH VI, its substrate and cofactor specificity strongly supports the physiological involvement of ADH VI in aldehyde reduction rather than in alcohol oxidation (Gonzalez *et al.*, 2000). The physiological importance of each ADH enzyme will also be better assessed in carbon-limited chemostat cultures.

7.2 References cited

- Bakker, B. M., C. Bro, P. Kotter, M. A. Lutтик, J. P. van Dijken and J. T. Pronk.** 2000. The mitochondrial alcohol dehydrogenase Adh3p is involved in a redox shuttle in *Saccharomyces cerevisiae*. *J. Bacteriol.* **182**: 4730-4737.
- Ciriacy, M.** 1979. Isolation and characterization of further cis- and trans-acting regulatory elements involved in the synthesis of glucose-repressible alcohol dehydrogenase (ADHII) in *Saccharomyces cerevisiae*. *Mol. Gen. Genet.* **176**: 427-431.
- Denis, C. L., M. Ciriacy and E. T. Young.** 1981. A positive regulatory gene is required for accumulation of the functional messenger RNA for the glucose-repressible alcohol dehydrogenase from *Saccharomyces cerevisiae*. *J. Mol. Biol.* **148**: 355-368.
- Denis, C. L., J. Ferguson and E. T. Young.** 1983. mRNA levels for the fermentative alcohol dehydrogenase of *Saccharomyces cerevisiae* decrease upon growth on a nonfermentable carbon source. *J. Biol. Chem.* **258**: 1165-1171.
- Dickinson, J. R., L. E. Salgado and M. J. Hewlins.** 2003. The catabolism of amino acids to long chain and complex alcohols in *Saccharomyces cerevisiae*. *J. Biol. Chem.* **278**: 8028-8034.
- Dombek, K. M., S. Camier and E. T. Young.** 1993. *ADH2* expression is repressed by REG1 independently of mutations that alter the phosphorylation of the yeast transcription factor ADR1. *Mol. Cell Biol.* **13**: 4391-4399.
- Drewke, C., J. Thielen, and M. Ciriacy.** 1990. Ethanol formation in *adh0* mutants reveals the existence of a novel acetaldehyde-reducing activity in *Saccharomyces cerevisiae*. *J. Bacteriol.* **172**: 3909-3917.
- Gonzalez, E., M. R. Fernandez, C. Larroy, L. Sola, M. A. Pericas, X. Pares and J. A. Biosca.** 2000. Characterization of a (2R,3R)-2,3-butanediol dehydrogenase as the *Saccharomyces cerevisiae* YAL060W gene product. Disruption and induction of the gene. *J. Biol. Chem.* **275**: 35876-35885.
- Heick, H. M. C., J. Willemot and N. Begin-heick.** 1969. The subcellular localization of alcohol dehydrogenase activity in baker's yeast. *Biochim. Biophys. Acta.* **191**: 493-501.
- Lutstorf, U. and R. Megnet.** 1968. Multiple forms of alcohol dehydrogenase in *Saccharomyces cerevisiae*. I. Physiological control of ADH-2 and properties of ADH-2 and ADH-4. *Arch. Biochem. Biophys.* **126**: 933-944.
- Petersson, A., J. R. M. Almeida, T. Modig, K. Karhumaa, B. Hahn-Hägerdal, M. F. Gorwa-Grauslund and G. Lidén.** 2006. A 5-hydroxymethyl furfural reducing enzyme encoded by the *Saccharomyces cerevisiae* *ADH6* gene conveys HMF tolerance. *Yeast* **23**: 455-464.
- van den Berg, M. A., P. Jong-Gubbels and H. Y. Steensma.** 1998. Transient mRNA responses in chemostat cultures as a method of defining putative regulatory elements: application to genes involved in *Saccharomyces cerevisiae* acetyl-coenzyme A metabolism. *Yeast* **14**: 1089-1104.
- Wehner, E. P., E. Rao and M. Brendel.** 1993. Molecular structure and genetic regulation of *SFA*, a gene responsible for resistance to formaldehyde in *Saccharomyces cerevisiae*, and characterization of its protein product. *Mol. Gen. Genet.* **237**: 351-358.

- Wenger, J. I. and C. Bernofsky.** 1971. Mitochondrial alcohol dehydrogenase from *Saccharomyces cerevisiae*. *Biochim. Biophys. Acta.* **227**: 479-490.
- Williamson, V. M., D. Cox, E. T. Young, D. W. Russell and M. Smith.** 1983. Characterization of transposable element-associated mutations that alter yeast alcohol dehydrogenase II expression. *Mol. Cell Biol.* **3**: 20-31.
- Williamson, V. M. and C. E. Paquin.** 1987. Homology of *Saccharomyces cerevisiae ADH4* to an iron-activated alcohol dehydrogenase from *Zymomonas mobilis*. *Mol. Gen. Genet.* **209**: 374-381.
- Wills, C. and J. Phelps.** 1975. A technique for the isolation of yeast alcohol dehydrogenase mutants with altered substrate specificity. *Arch. Biochem Biophys.* **167**: 627-637.
- Young, E. T. and D. Pilgrim.** 1985. Isolation and DNA sequence of *ADH3*, a nuclear gene encoding the mitochondrial isozyme of alcohol dehydrogenase in *Saccharomyces cerevisiae*. *Mol. Cell Biol.* **5**: 3024-3034.

9. Opsomming

Wanneer *Saccharomyces cerevisiae* op 'n fermenteerbare koolstofbron soos glukose geweek word, kataliseer die fermentatiewe alkohol dehidrogenase, ADH I, die regenerering van NAD^+ vanaf NADH en produseer etanol vanaf asetaldehyd. Sodra die fermenteerbare koolstofbron uitgeput is, word 'n aantal ander ensieme se onderdrukking opgehef om die voorheen-uitgeskeide etanol via oksidatiewe respirasie en glukoneogenese te verbruik. Om beide die koolstofbron en energie vir hierdie sisteem te verskaf, het die gissel 'n effektiewe metode nodig om die voorheen-uitgeskeide etanol te oksideer. ADH II is 'n kataboliet-onderdukbare iso-ensiem wat in die sel primêr funksioneer om etanol na asetaldehyd te oksideer, wat dan weer via die trikarboksielsuur-siklus gemetaboliseer kan word, of ook kan optree as 'n intermediêre produk in glukoneogenese. ADH III is 'n mitochondriale iso-ensiem wat deel is van respiratoriese metabolisme deur deelname aan die etanol-asetaldehyd pendelmeganisme wat belangrik is om mitochondriale reduserende ekwivalente na die sitosol te vervoer onder anaërobe toestande. Die fisiologiese rolle en regulering van *ADH1*, *ADH2*, *ADH3*, *ADH4* en *ADH5* is ondersoek deur transkripsievlakke in chemostaat en lotkulture te monitor met die Northern kladtegniek en reële-tyd RT-PCR. Dit is aangetoon dat ADH I die sleutelensiem in die reduksie van asetaldehyd na etanol is, asook dat dit etanol kan oksideer. *ADH2* transkripsievlakke is onderdruk deur glukose en etanol in chemostaatkulture wat met beide hierdie koolstofbronne gepuls is, maar slegs glukose-onderdrukking was duidelik in lotkulture. Northern klad-analise het gewys dat die *ADH3* geen gedurende die etanol-fase van die puls geïnduseer word, wat 'n aanduiding kan wees dat die mitochondriale ADH III ensiem ook betrokke kan wees in die eerste stap van etanolverbruik. Die groeikinetika van 'n stam waar slegs ADH III uitgedruk word, het aangedui dat die *ADH3* geenproduk dieselfde funksie as ADH II kan vervul. *ADH4* transkripsie is waargeneem vir die eerste keer in lotkulture en dit is bewys dat dit nie betrokke was by die produksie of opname van etanol nie. *ADH5* transkripsie is ook vir die eerste keer aangetoon en data dui aan dat ADH V nie by etanol produksie in 'n *adh1-adh4* delesiemutant betrokke is nie.

8. Summary

When *Saccharomyces cerevisiae* is grown on a fermentable carbon source such as glucose, the fermentative alcohol dehydrogenase, ADH I, catalyses the regeneration of NAD⁺ from NADH and produces ethanol from acetaldehyde. When the fermentable carbon source is depleted, a variety of other enzymes are derepressed in order to utilise the previously excreted ethanol via oxidative respiration and gluconeogenesis. To provide both the carbon source and energy for this system, the yeast cell requires an efficient method for oxidising this previously excreted ethanol. ADH II is a catabolite repressible isoenzyme which primarily functions in the cell to oxidise ethanol to acetaldehyde, which can be metabolised via the tricarboxylic acid cycle or act as intermediate product in gluconeogenesis. ADH III is a mitochondrial isoenzyme participating in the respiratory metabolism by forming part of the ethanol-acetaldehyde shuttle that is important for shuttling mitochondrial reducing equivalents to the cytosol under anaerobic conditions. The physiological roles and regulation of *ADH1*, *ADH2*, *ADH3*, *ADH4* and *ADH5* were investigated by monitoring transcription levels in chemostat and batch cultivations with Northern blotting and real-time RT-PCR. ADH I was shown to be the key enzyme in the reduction of acetaldehyde to ethanol and also demonstrated ample ability to oxidise ethanol. *ADH2* transcription was inhibited by glucose and ethanol in chemostat cultures pulsed with both these carbon sources, but only glucose repression was evident in batch cultures. Northern blot analysis showed that the *ADH3* gene was induced during the ethanol phase of the pulses suggested that the mitochondrial ADH III enzyme could also be involved in the first step in ethanol utilisation. The growth kinetics of a strain expressing only ADH III demonstrated that the *ADH3* gene product could fulfil the same function as ADH II. *ADH4* transcription was detected for the first time in batch cultures and was shown not to be involved in the production or assimilation of ethanol. *ADH5* transcription was also demonstrated for the first time and data suggest that ADH V is not involved in ethanol production in a *adh1-adh4* deletion mutant.

Appendices

Table of content

Appendix A. Culture media.....	129
Chemically defined medium.....	129
Complex medium	130
YNB dropout medium	131
LB medium.....	131
YPD medium.....	131
Appendix B. Cell storage.....	131
Appendix C. Strains used in this study	132
Appendix D. Primers and fluorescent probes used in this study	133
Appendix E. Plasmid constructs, PCR products and commercial vectors	135
Appendix F. PCR component concentrations and reaction conditions	148
Expand Long Template reaction components (Roche Applied Science)	148
High Fidelity Taq polymerase reaction components (Roche Applied Science)	148
Taq DNA polymerase reaction components (New England Biolabs)	148
Programme 1: Expand Long template reaction conditions.....	148
Programme 2: Amplification of Northern Blot probes.....	148
Programme 3: Screening with standard PCR	149
Programme 4: Screening with touchdown PCR.....	149
Programme 5: Amplification of Real-time PCR standards	149
Appendix G. Restriction enzyme digestions	149
Appendix H. Ligation reactions.....	149
Appendix I. Transformation of Rubidium chloride competent <i>E. coli</i>	150
Appendix J. Transformation of yeast cells	150
Appendix K. DNA extraction methods	150
Bacterial plasmid DNA extraction using alkaline lysis	150
Yeast genomic DNA extraction.....	151
Appendix L. Construction of deletion mutants with micromanipulation.....	151
Mating and sporulation.....	151
Dissection	151
Replica plate screening.....	152
Appendix M. RNA isolation from <i>S. cerevisiae</i>	152

Appendix N. Northern Blotting	153
Electrophoresis with formaldehyde	153
Capillary transfer to nylon membranes.....	153
Hybridization with radio active probes.....	153
Appendix O. Real-time PCR	154
DNase I treatment.....	154
Component concentrations in each reaction	154
Reaction conditions	154
Appendix P: Marker DNA.....	154
Literature cited.....	155

Appendices

Appendix A. Culture media

Chemically defined medium

Citric acid	: 0.5 g l ⁻¹
NaCl	: 0.1 g l ⁻¹
(NH ₄) ₂ SO ₄	: 5 g l ⁻¹
MgSO ₄ · 7H ₂ O	: 0.4 g l ⁻¹
CaCl ₂ · 2H ₂ O	: 0.02 g l ⁻¹
KH ₂ PO ₄	: 5 g l ⁻¹

Trace elements

- The trace element solution was designed for 10g l⁻¹ biomass, use 1 ml l⁻¹ medium
- Dissolve the following compounds in water, adjust pH with acid

H ₂ O dist	: 950 ml
HCl conc	: 50 ml
FeSO ₄ · 7 H ₂ O	: 35 g
MnSO ₄ · H ₂ O	: 7 g
ZnSO ₄ · 7 H ₂ O	: 11 g
CuSO ₄ · 5 H ₂ O	: 1 g
CoCl ₂	: 2 g
Na ₂ MoO ₄ · 2 H ₂ O	: 1.3 g
H ₃ BO ₃	: 2 g
KI	: 0.35 g
Al ₂ (SO ₄) ₃	: 0.5 g

Vitamin solution

- 1000 fold concentrated stock solution.
- Dissolve 25 mg *d*-Biotin in 10 ml of 0.1 M NaOH
- Add the dissolved biotin to approximately 400 ml of water and adjust pH to 6.5

- Add the following vitamins:

Calcium panthotenate	: 500 mg
Nicotinic acid	: 500 mg
<i>p</i> -Aminobenzoic acid	: 100 mg
Pyrodoxine. HCl	: 500 mg
Thiamine. HCl	: 500 mg

- Adjust the pH to 6.5 then add

<i>m</i> -Inositol	: 12.5 g
--------------------	----------

- Adjust the pH to 6.5, filter sterilise and store at 4°C.

Amino acids and other supplements

Alanine	: 50 mg
Arginine	: 50 mg
Asparagine	: 50 mg
Aspartic acid	: 50 mg
Glutamic acid	: 50 mg
Glutamine	: 50 mg
Glycine	: 50 mg
Histidine	: 50 mg
Isoleucine	: 50 mg
Leucine	: 400 mg
Lysine	: 50 mg
Methionine	: 50 mg
Phenylalanin	: 50 mg
Proline	: 50 mg
Serine	: 50 mg
Threonine	: 50 mg
Tryptophan	: 50 mg
Tyrosine	: 50 mg
Valine	: 50 mg
Cysteine	: 50 mg
Adenine	: 50 mg
Uracil	: 50 mg

- Prepare 100 fold concentrated stock solution of all the compounds except leucine and cysteine.
- Adjust to pH 11 with NaOH, aliquot in 40 ml volumes and store at -20°C.
- Leucine and cysteine were added before use.
- Autoclave citric acid, NaCl, trace elements and 0.2 ml l⁻¹ antifoam (1:1 mixture of Voranol P2000 Polyol and Durapol 3000 antifoaming agents).
- Autoclave each basal salt separate.
- Filter sterilise vitamins and amino acids.
- Dissolve 400 mg leucine in 15 ml 0.2 M NaOH and 50 mg cysteine in 3 ml 1N HCl, filter sterilize.
- Add basal salts, vitamins and amino acids to the citric acid mixture and make up with water. The pH should be 5.5.

References: (Cakar *et al.*, 1999; du Preez & van der Walt, 1983; Flikweert *et al.*, 1996; Pronk, 2002; Schulze *et al.*, 1995; Verduyn *et al.*, 1990)

Complex medium

Yeast extract	: 2 g.l ⁻¹
Peptone	: 4 g.l ⁻¹
MgSO ₄ . 7H ₂ O	: 0.4 g.l ⁻¹
CaCl ₂ .2H ₂ O	: 0.02 g.l ⁻¹
KH ₂ PO ₄	: 2 g.l ⁻¹
Trace elements	: 0.5 g.l ⁻¹
Silicone antifoam	: 0.5 g.l ⁻¹
pH 5.5	

Reference: (du Preez *et al.*, 2001)

YNB dropout medium

Yeast nitrogen base (DIFCO) : 6.7 g l⁻¹
Glucose : 10 g l⁻¹
amino acid supplement (BIO 101®) : 0.6 g l⁻¹
pH 6.2

Add 50 mg histidin, uracil, leucine or tryptophan when required.

LB medium

Tryptone : 10 g l⁻¹
Yeast Extract : 5 g l⁻¹
NaCl : 10 g l⁻¹

YPD medium

Yeast extract : 10 g l⁻¹
Peptone : 20 g l⁻¹
Glucose : 20 g l⁻¹

Reference: (Sambrook & Russel, 2001)

Appendix B. Cell storage

1. Grow the cells on YPD plates (or selection media for transformants) for 2-3 days.
2. Aliquot 1 ml volumes of 15% glycerol in sterile cryotubes.
3. Scrape an ample amount of the cells from the plate using a loop.
4. Resuspend thoroughly in the glycerol and store at -80°C.
5. To revive, scrape some crystals from the surface with an inoculation loop.
6. Place on YPD plate, allow to thaw and streak out.

Reference: (Becker *et al.*, 1990)

Appendix C. Strains used in this study

Table A: Yeast and bacterial strains used in this study

Yeast strains	Genotype	Ref #	Origin
W303-1A(a)	W303-1A, <i>MATa, his3, leu2, trp1, ura3</i>	OdS1	Thomas & Rothstein, 1989
W303-1A(α)	W303-1A, <i>MATα, his3, leu2, trp1, ura3</i>	OdS2	Thomas & Rothstein, 1989
Test-a	W303-1A, <i>MATa, ade3, ura1, gal1</i>	OdS3	Thomas & Rothstein, 1989
Test- α	W303-1A, <i>MATα, ade3, ura1, gal1</i>	OdS4	Thomas & Rothstein, 1989
S Δ 2a	W303-1A, <i>MATa, adh3Δ::URA3</i>	OdS11	This study
S Δ 2b	W303-1A, <i>MATα, adh2Δ::URA3</i>	OdS16	This study
S Δ 3	W303-1A, <i>MATα, adh3Δ::TRP1</i>	OdS25	This study
S Δ 4	W303-1A, <i>MATa, adh4Δ::HIS3</i>	OdS29	This study
S Δ 5	W303-1A, <i>MATa, adh5Δ::LEU2</i>	OdS32	This study
D Δ 34a	W303-1A, <i>MATa, adh3Δ::TRP1, adh4Δ::HIS3</i>	OdS46	This study
D Δ 34b	W303-1A, <i>MATα, adh3Δ::TRP1, adh4Δ::HIS3</i>	OdS47	This study
T Δ 345	W303-1A, <i>MATa, adh3Δ::TRP1, adh4Δ::HIS3, adh5Δ::LEU2</i>	OdS53	This study
T Δ 234	W303-1A, <i>MATa, adh2Δ::URA3, adh3Δ::TRP1, adh4Δ::HIS3</i>	OdS59	This study
T Δ 235	W303-1A, <i>MATα, adh2Δ::URA3, adh3Δ::TRP1, adh5Δ::LEU2</i>	OdS81	This study
T Δ 245	W303-1A, <i>MATa, adh2Δ::URA3, adh4Δ::HIS3, adh5Δ::LEU2</i>	OdS83	This study
Q1	W303-1A, <i>MATa, adh2Δ::URA3, adh3Δ::TRP1, adh4Δ::HIS3, adh5Δ::LEU2</i>	OdS94	This study
Q2	W303-1A, <i>MATa, adh1Δ::URA32, adh3Δ::TRP1, adh4Δ::HIS3, adh5Δ::LEU2</i>	OdS121	This study
Q3	W303-1A, <i>MATa, adh1Δ::TRP1, adh2Δ::URA3, adh4Δ::HIS3, adh5Δ::LEU2</i>	OdS124	This study
Q4	W303-1A, <i>MATα, adh1Δ::HIS3, adh2Δ::URA3, adh3Δ::TRP1, adh5Δ::LEU2</i>	OdS123	This study
Q5	W303-1A, <i>MATa, adh1Δ::LEU2, adh2Δ::URA3, adh3Δ::TRP1, adh4Δ::HIS3</i>	OdS114	This study
S Δ 2aTR_E	W303-1A, <i>MATa, adh2Δ::URA3</i> (S Δ 2a) transformed with pCM190L-W	OdS100	This study
S Δ 2aTR_ADH2	W303-1A, <i>MATa, adh2Δ::URA3</i> (S Δ 2a) transformed with pCM190L-W::ADH2	OdS103	This study
<i>E. coli</i> strains			
Top 10F	<i>mcrA</i> , D (mrr-hsdRMS-mcrBC), F80D <i>lacZ</i> M15, <i>DlacX74, deoR, recA1, araD129, D(ara, leu), 7697, galU, galK, lrp, rpsL, endA1, nupG, F'</i>		New England Biolabs
DH5 α	<i>endA1, hsdR17</i> ($r_K^- m_K^+$) supE44, thi-1, <i>recA1, gyrA</i> (Nal ^r) <i>relA1, D(lacIZYA-argF)U169, deoR</i> (f80d <i>lacD(lacZ)M15</i>)		New England Biolabs

S Δ : Single deletion followed by the *ADH* gene deleted

DA: Double deletion followed by the *ADH* genes deleted

T Δ : Triple deletion followed by the *ADH* genes deleted

Q : Quadruple deletion followed by the *ADH* gene still intact

TR-S Δ 2a : Transformed with either the empty pCM190L_W or construct expression *ADH2*

Appendix D. Primers and fluorescent probes used in this study

Table B. Primers used in this study

Name	Sequence (5' - 3')	bp	T _m (°C)
ACT1-1F	GAG GTT GCT GCT TTG GTT ATT G	22	60.8
ACT1-1R	TTG TGG TGA ACG ATA GAT GGA C	22	60.8
ACT-fw	TTT GTC CTT GTA CTC TTC CGG TAG	24	61
ACT-as	GTG AGG TAG AGA GAA ACC AGC GT	23	62.4
ADH1-1F	AGA CGC GCA TAA CCG CTA GA	20	59.7
ADH1-1R	TAA GAT GTG CGC ATC TTG GGA	21	57.9
ADH1-2F	TGC CGA AAG AAC CTG AGT GC	20	59
ADH1-3F	TAA GCG AAT TTC TTA TGA TTT ATG	24	47.5
ADH1-3R	GGT ATT GTC CTC TGA GG	17	48.5
ADH2-1F	CGG ATC AAC TGG CAC CAT CT	20	58.3
ADH2-1R	TTT TCT CCC TCA CTG CAT CCC	21	58.3
ADH2-3F	GAG CGT TGA ATC GGT GAT GC	20	57.6
ADH2-4R	ATA AGC TTT TAT TTA GAA GTG TCA ACA ACG	30	55.4
ADH2-5F	ATG GAT CCA TGT CTA TTC CAG AAA CTC	27	63
ADH2-6F	GCA CGC TTG GCA TGG TGA CT	20	61.2
ADH2-6R	CGT TCG TAC TAG CAA CAT GG	20	53.4
ADH3-1F	AAG ATC AAG GAA ACA TGT CGG	21	54.2
ADH3-1R	ATG TGT TGC CCG CCT AGT AT	20	54.2
ADH3-2F	TCG GAT CCG GAA AAG GGC AAG ATT TTG G	28	64.9
ADH3-2R	TCG GAT CCC TGG TGA ACA ATG TTG ACG	27	64
ADH3-3F	ATC GCT TAA CCT GGC TAG TTG	21	56
ADH3-4F	TGC GAA TGA GCA GCA GCC	18	59
ADH3-4R	GAG TCT TAG GGA TTG CAG C	19	52.9
ADH4-1F	TTT TGC AGG ATT CGG GGT TA	20	55.8
ADH4-1R	TTT ATC AGG CAT GCT GCT GA	20	55.9
ADH4-2F	TGC TCG AGT GAT GCC TGC CAT TTG	23	63.7
ADH4-2R	TGC TCG AGG GCA TAC GTG ATC C	22	62.3
ADH4-3F	ATG CCT TTC GAA CCA CTT TGA G	22	57.2
ADH4-4F	ATG TCT TCC GTT ACT GGG	18	51.4
ADH4-4R	GGT TAG TCA AAT GGC AGG C	19	54
ADH5-1F	GAA TTT GCT TTT TGG TTT CGA	21	51.8
ADH5-1R	AAC GAA TAC TTT CGC AGT GG	20	54.3
ADH5-3F	TGC GGT AGC GAC AGA TTG TAG	21	58
ADH5-4F	TTG TGA CAT CTG CTG ACG CG	20	58.1
ADH5-4R	TTC GTT AGG CTT AGG TTC C	19	51.6
HIS3-1R	CGC AAT CTG AAT CTT GGT TTC	21	52.7
LEU2-1R	TTC GGC TGT GAT TTC TTG ACC	21	56.8

Table B. Primers used in this study (continued)

Name	Sequence (5' - 3')	bp	T _m (°C)
pCM190L-3F	TAC CCT ATG GCA TGC ATG TGC TCT G	25	66.2
Sp 6	TAT TTA GGT GAC ACT ATA G	19	30.7
T7	TAA TAC GAC TCA CTA TAG GG	20	38.8
TRP1-1R	AAT GGA CCA GAA CTA CCT GTG AA	23	57.4
URA3-1F	GGG TGA ACG TTA CAG AAA AGC A	22	57.1
URA3-1R	TAG TTG GCA GCA ACA GGA CTA	22	59.8
1RT-F	GGA AGA ATT ATT CAG ATC CAT CGG TGG TG	29	66
1RT-R	AAC GGT GGT ACC GTT AGC TCT AAC	24	64.5
2RT-F	ACA AGG CTT TGA AGT CTG CCA AC	23	62.7
2RT-R	TCG CCT TAG CAT ATT GAA CAG CCA	24	62.8
4RT-F	TGC CAC CTG CTT TGA CTG CTG C	22	66.4
4RT-R	ACC GTC TTT GTA TGC AGC GAC	21	62.5
5RT-F	AGG CCA CTA ATG GCG GTT CTC	21	64.5
5RT-R	ACC AAC CAG GAC GAC AGT ACC	21	64.5
Uni2-R	GCC AAC TAC CTT TAT TGG AGA CTT	24	56.3

Table C: Fluorescent labelled probes used in this study

Name	Fluorophore	Sequence (5' - 3')	Quencher	bp	T _m (°C)
ACT probe	JOE	ACG ACG TGA GTA ACA CCA TCA CCG GAA	TAMRA	27	66.5
ADH1 probe	FAM	CGT CAG TGG CCT TTA GAA CAG CAC CGA	BHQ-1	27	69.16
ADH2 probe	FAM	ACC AGC AGC ACC AGA AAT GGC CG	BHQ-1	23	68.12
ADH4 probe	FAM	TCA ATA CCC TTC AAA GCA CAG GCA TCG G	BHQ-1	28	67.54
ADH5 probe	FAM	TAC CTC GTA GAA GCC TCG ATA GCT GCT	BHQ-1	27	67.64

Appendix E. Plasmid constructs, PCR products and commercial vectors

Charts were modelled with pDraw32 software. This program does not include the primer length when calculating the base pair allocation, manual addition of the primer length is thus necessary for calculation of band lengths.

- Purple primers
- Blue Enzymes with one restriction site
- Red enzymes with two restriction sites
- Other enzymes with three or more restriction sites

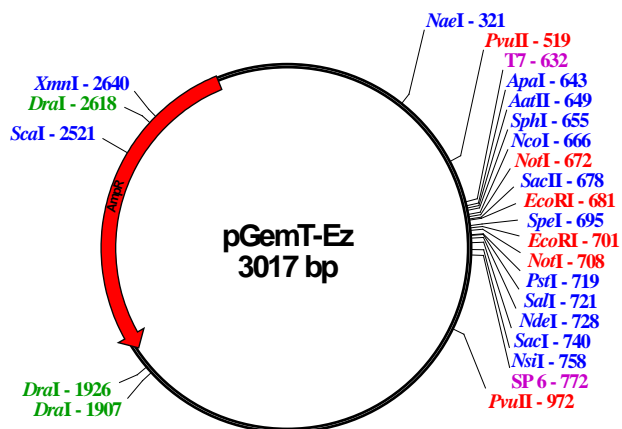


Figure A. pGemT-Easy with engineered T-overhangs to facilitate PCR products cloning (Promega)

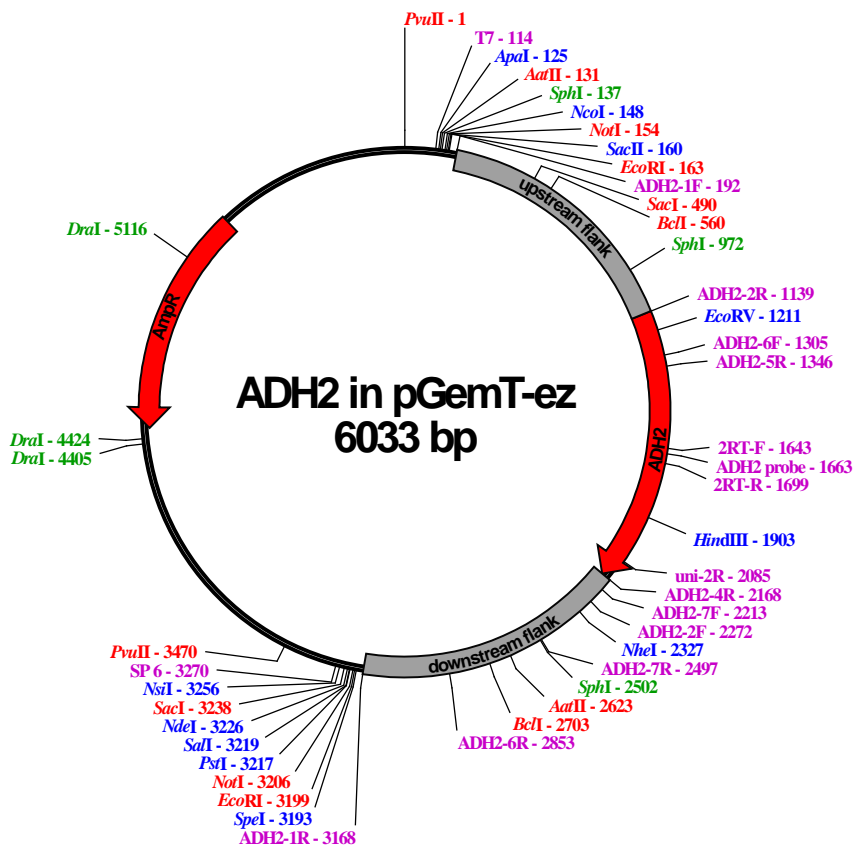


Figure B: pADH2. ADH2 ORF and 1000bp flanking regions up- and downstream cloned into pGemT-Easy

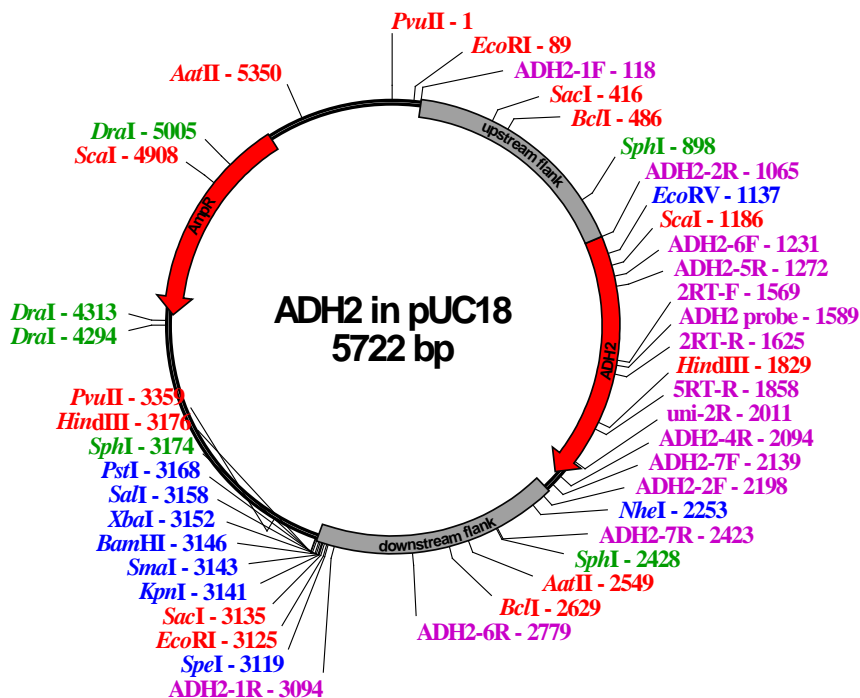


Figure C: pUC18::ADH2. ADH2 ORF and 1000bp flanking regions up- and downstream cloned into pUC18

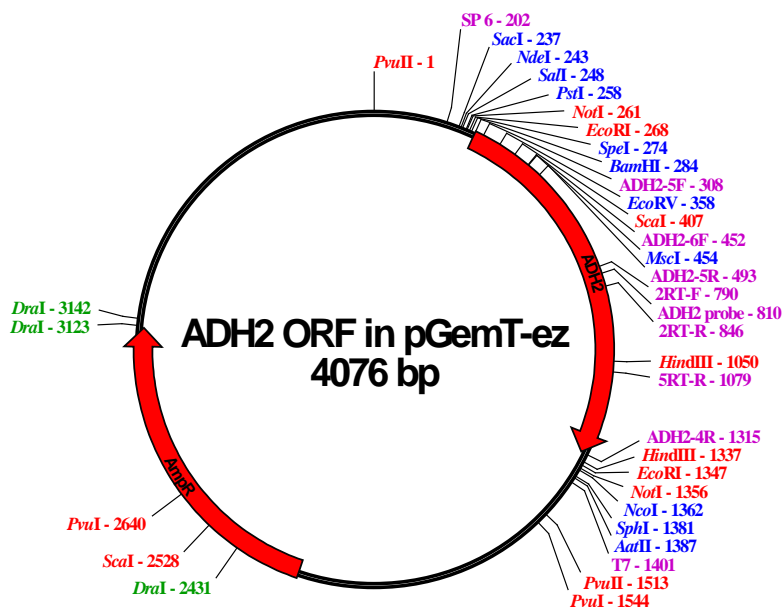


Figure D: ADH2 ORF cloned into pGemT-Easy

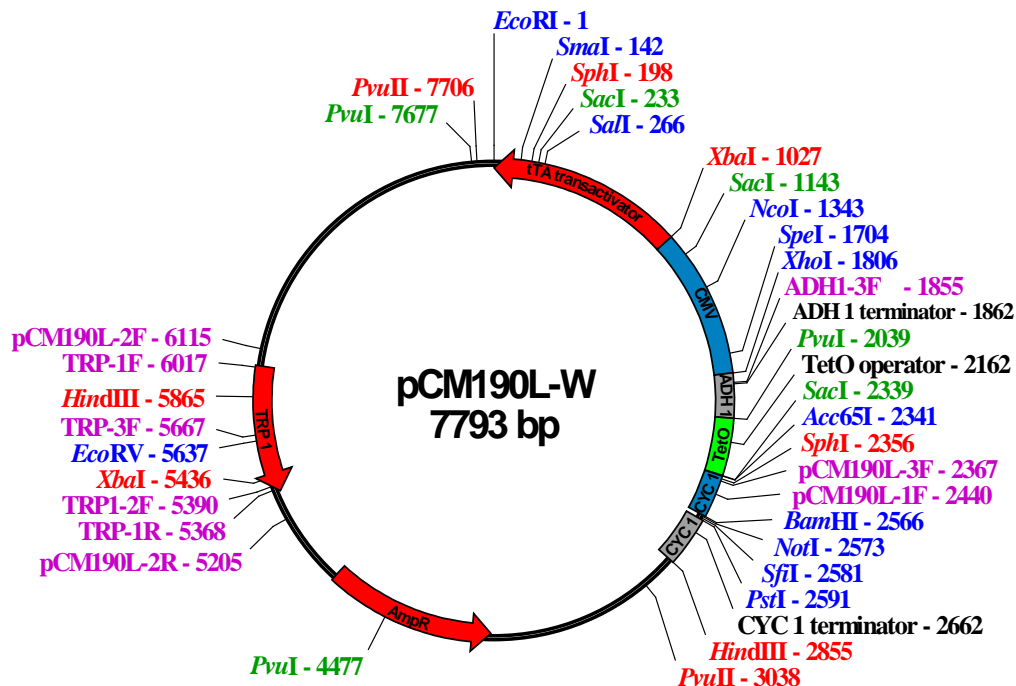


Figure E. pCM190L_W. Shuttle vector with Amp^R and TRP marker genes.

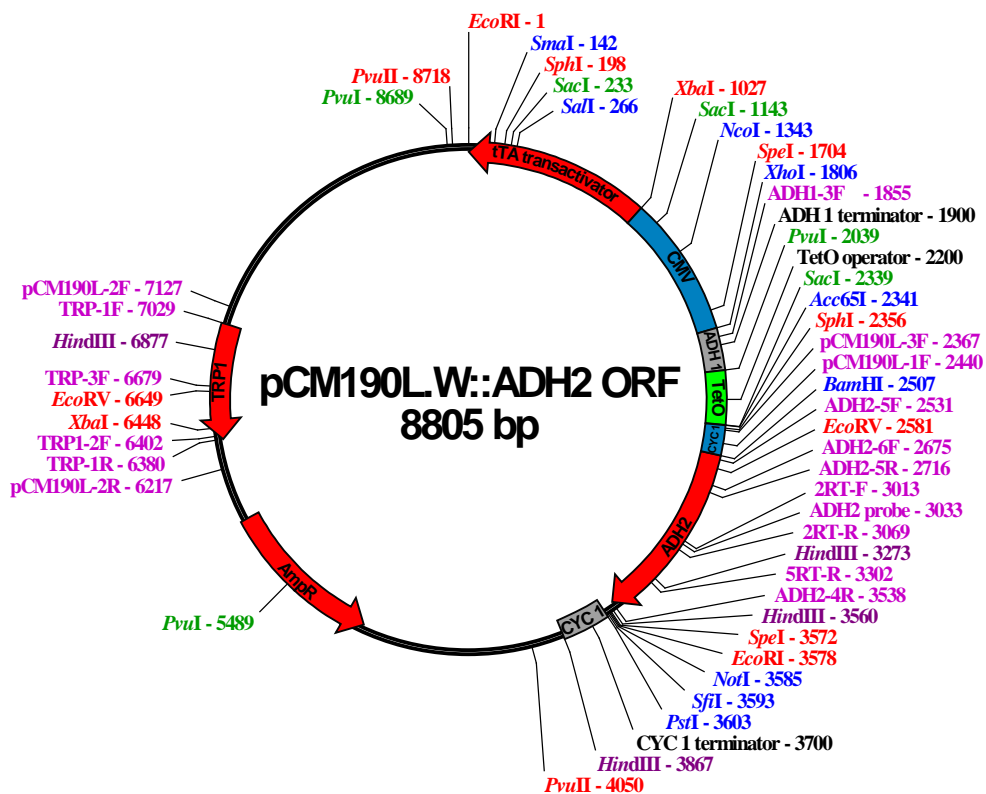


Figure F: pCM190L_W::ADH2. ADH2 ORF from figure D sub-cloned into pCM190L_W

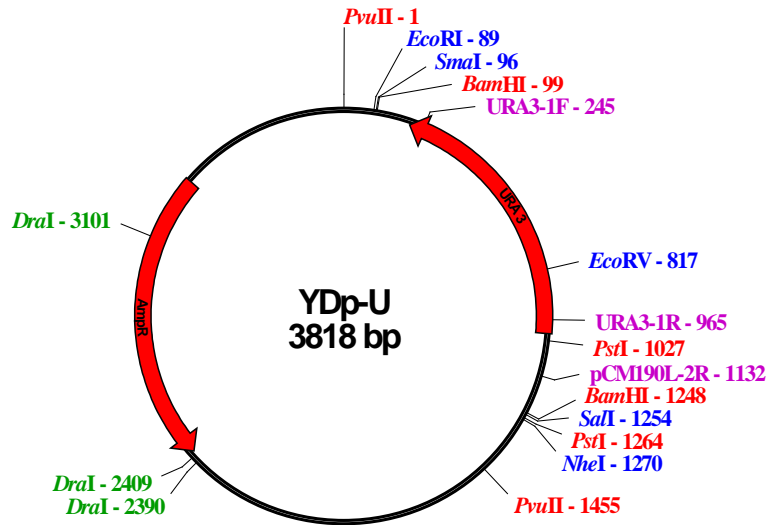


Figure G: YDp-U plasmid carrying the *URA3* yeast marker gene

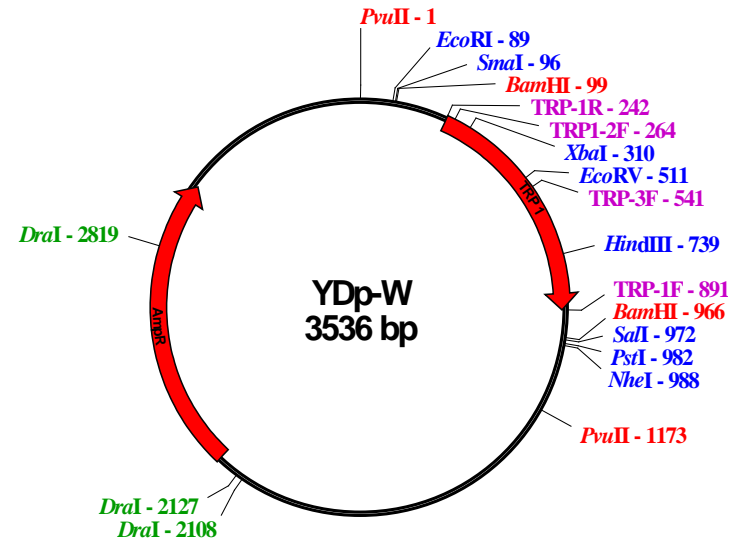


Figure H: YDp-W plasmid carrying the *TRP1* yeast marker gene

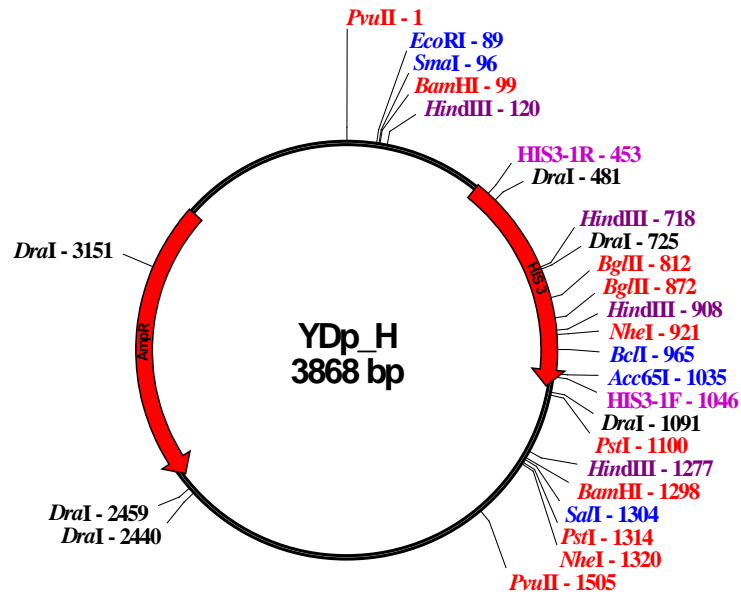


Figure I: YDp-H plasmid carrying the *HIS3* yeast marker gene

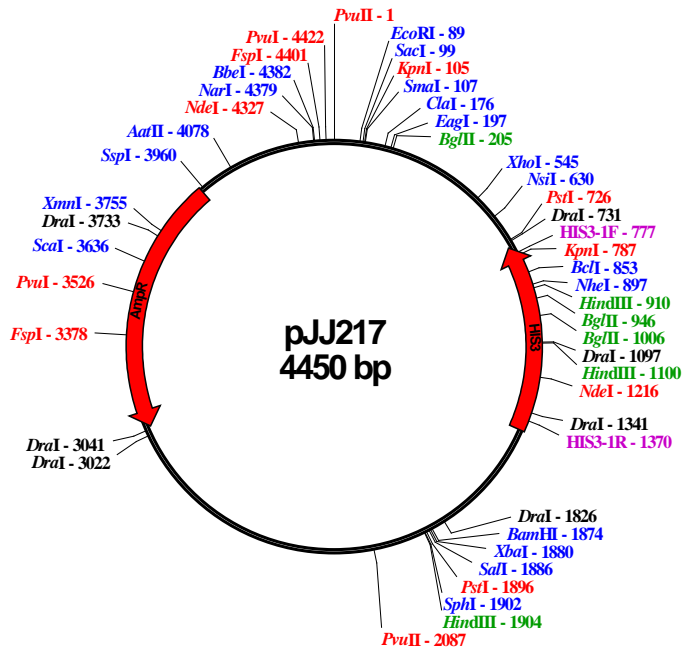


Figure J: pJJ217 plasmid carrying the *HIS3* yeast marker gene

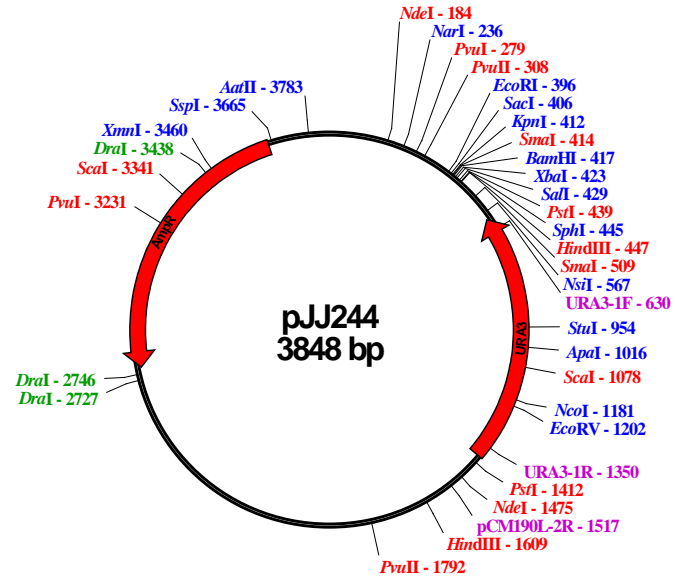


Figure K: pJJ244 plasmid carrying the *URA3* yeast marker gene

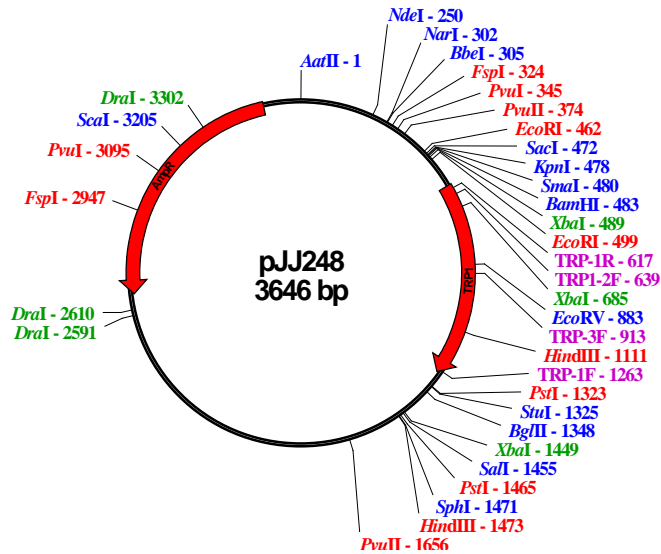


Figure L: pJJ248 plasmid carrying the *TRP1* yeast marker gene

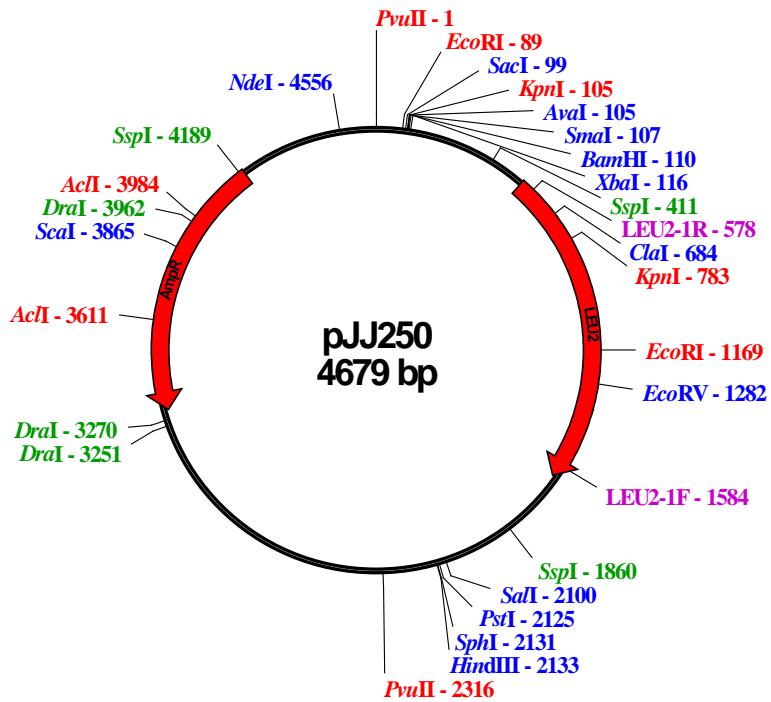


Figure M: pJJ250 plasmid carrying the *LEU2* yeast marker gene

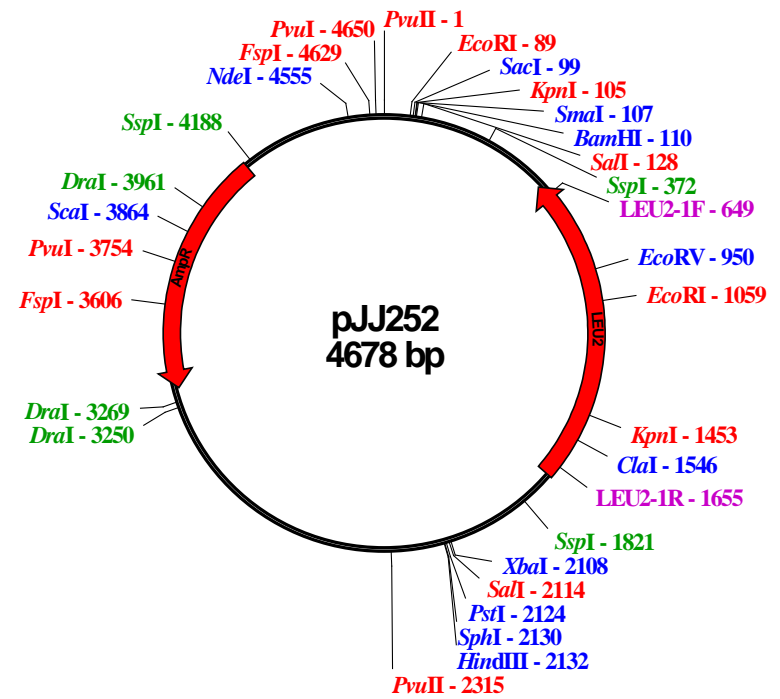


Figure N: pJJ252 plasmid carrying the *LEU2* yeast marker gene (other orientation)

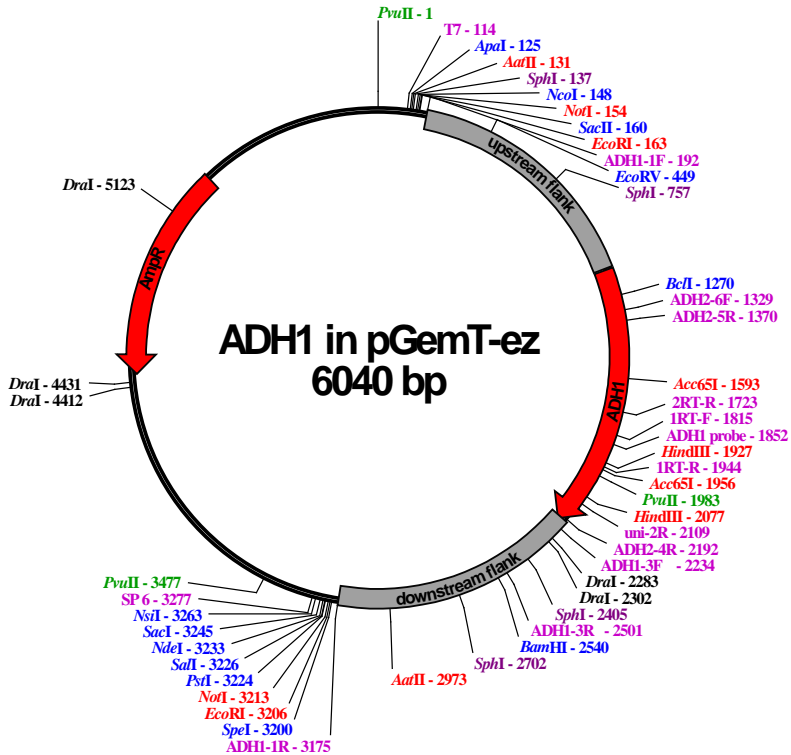


Figure O: pADH1. ADH1 ORF and 1000bp flanking regions up- and downstream cloned into pGemT-Easy

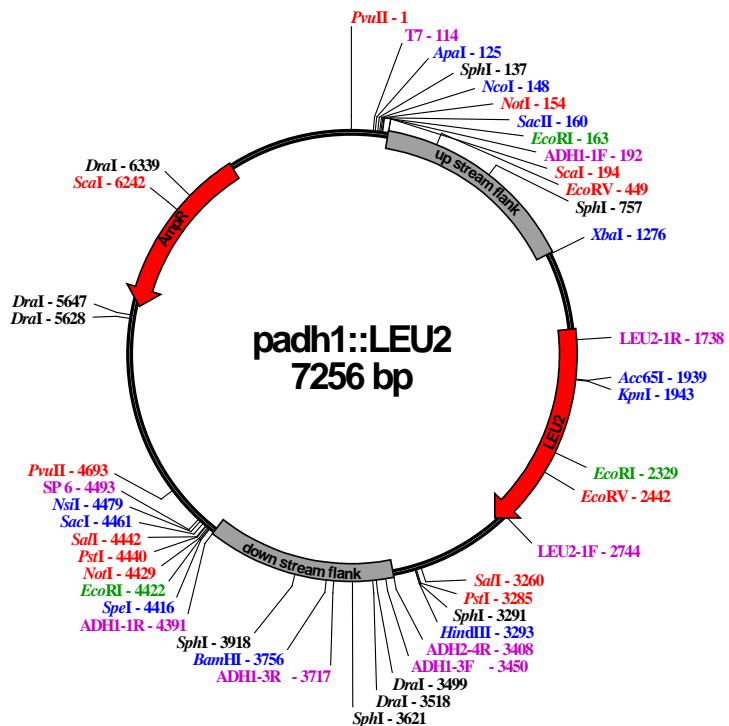


Figure Q: padh1Δ::LEU2. ADH1 ORF from pADH1 removed with BclI and HindIII and replaced with the LEU2 marker gene from pJJ250

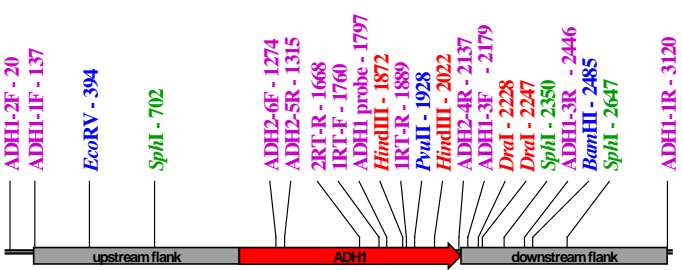


Figure P: ADH1 ORF and flanking regions also including 117 bp further upstream of the cloned fragment for screening

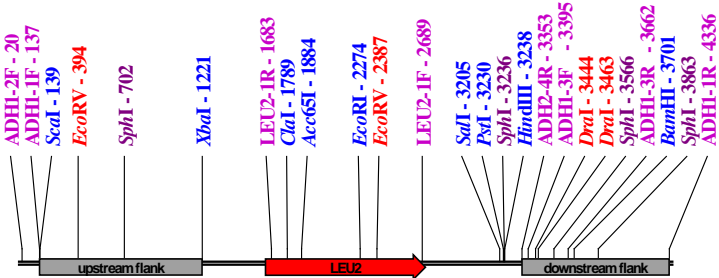


Figure R: LEU2 and ADH1 flanking regions also including 117 bp further upstream of the cloned fragment for screening

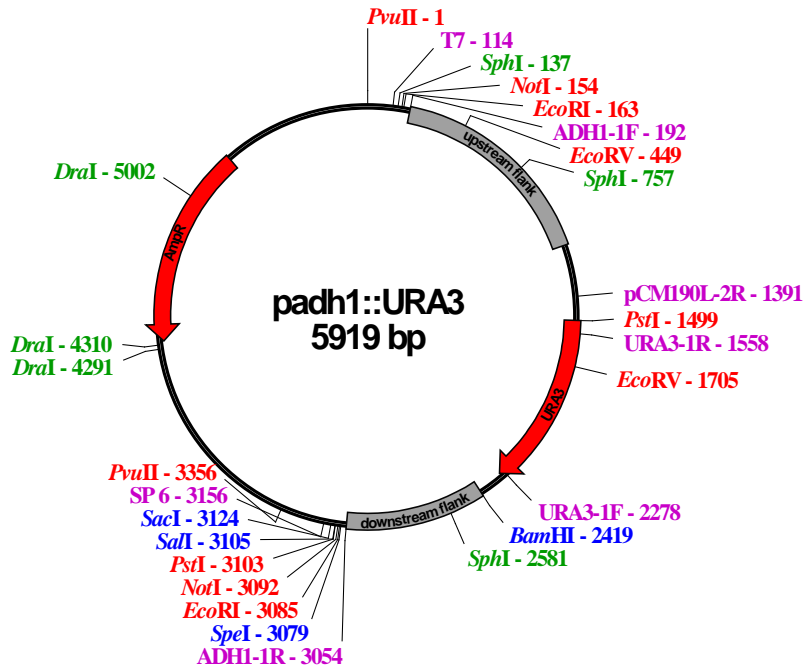


Figure S: *padh1Δ::URA3*. *ADHI* ORF from *pADHI* removed with *BclI* and *BamHI* and replaced with the *URA3* marker gene from YDp-U

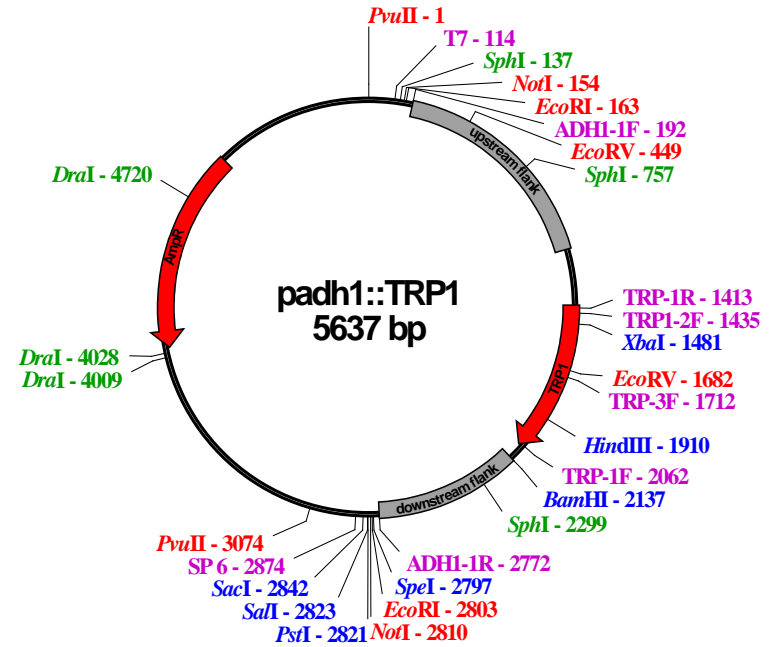


Figure U *padh1Δ::TRP1*. *ADHI* ORF from *pADHI* removed with *BclI* and *BamHI* and replaced with the *TRP1* marker gene from YDp-W

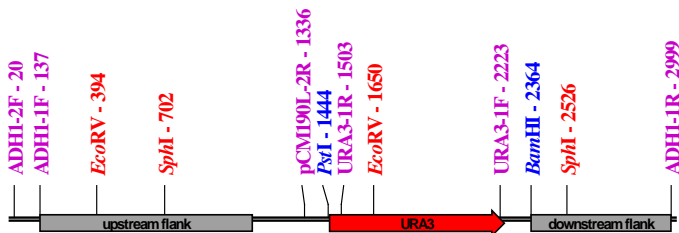


Figure T: *URA3* and *ADHI* flanking regions also including 117 bp further upstream of the cloned fragment for screening

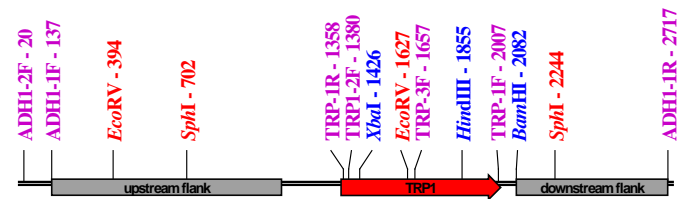


Figure V: *TRP1* and *ADHI* flanking regions also including 117 bp further upstream of the cloned fragment for screening

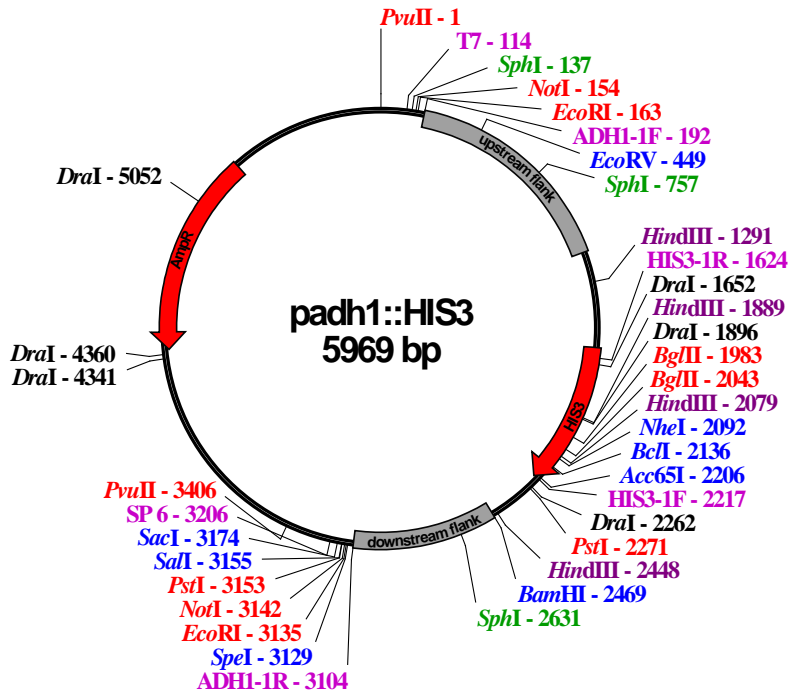


Figure W: *padh1Δ::HIS3*. *ADHI* ORF from p*ADHI* removed with *BclII* and *BamHI* and replaced with the *HIS3* marker gene from YDp-H

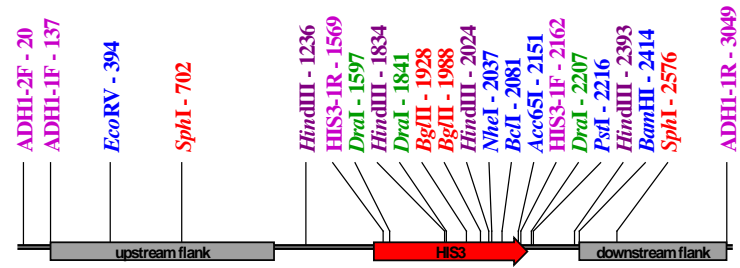


Figure X: *HIS3* and *ADHI* flanking regions also including 117 bp further upstream of the cloned fragment for screening

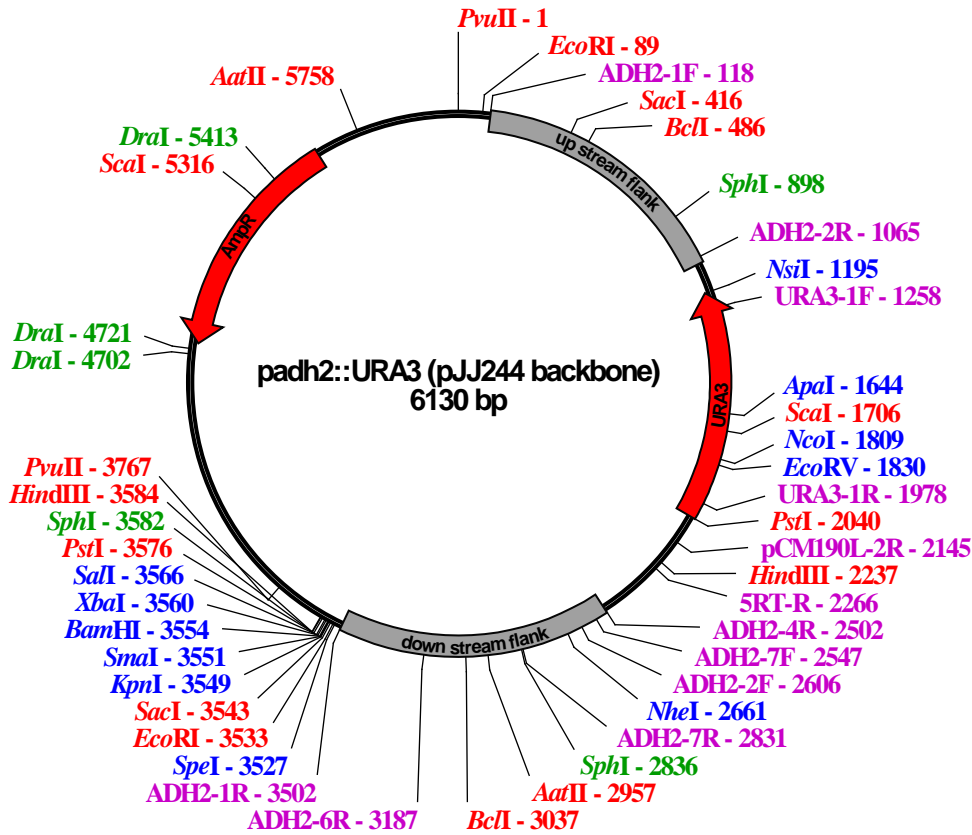


Figure Y: *padh2Δ::URA3*. *ADH2* flanking regions cloned into pJJ244 containing the *URA3* marker gene (see M & M)

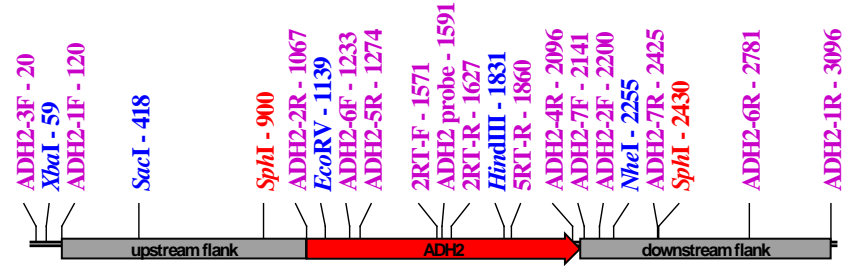


Figure Z: *ADH2* ORF and flanking regions also including 100 bp further upstream of the cloned fragment for screening

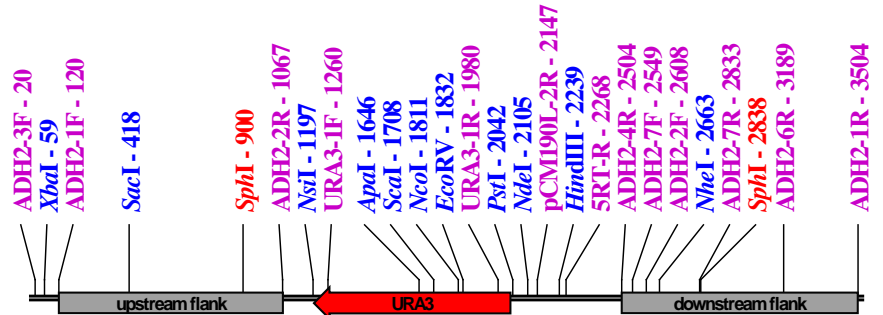


Figure AA: *URA3* and *ADH2* flanking regions also including 100 bp further upstream of the cloned fragment for screening

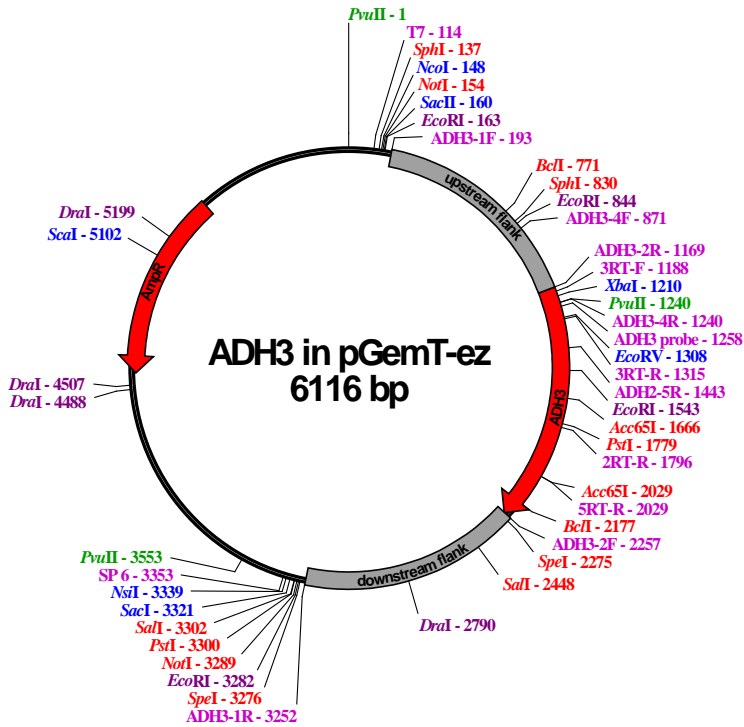


Figure AB: *pADH3*. *ADH3* ORF and 1000bp flanking regions up- and downstream cloned into pGemT-Easy

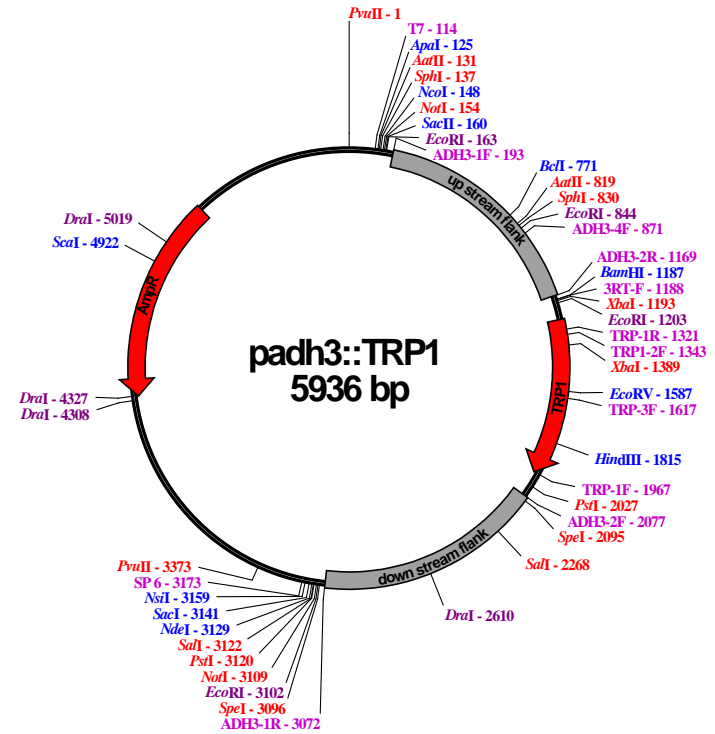


Figure AD: *padh3Δ::TRP1*. *ADH3* ORF from *pADH3* removed with PCR and replaced with the *TRP1* marker gene from pJJ248 with *BamHI* and *BgIII*

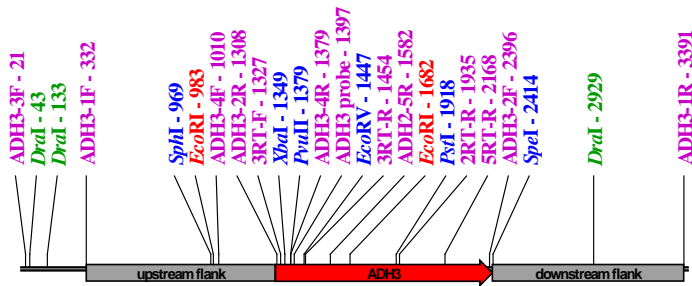


Figure AC: *ADH3* ORF and flanking regions also including 311 bp further upstream of the cloned fragment for screening

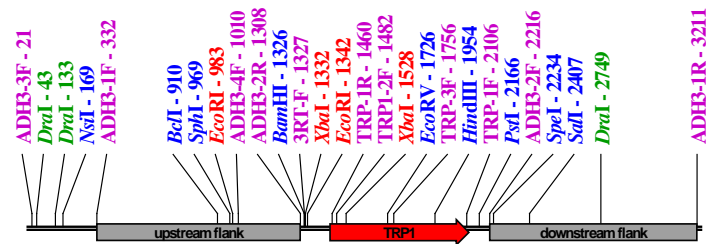


Figure AE: *TRP1* and *ADH3* flanking regions also including 311 bp further upstream of the cloned fragment for screening

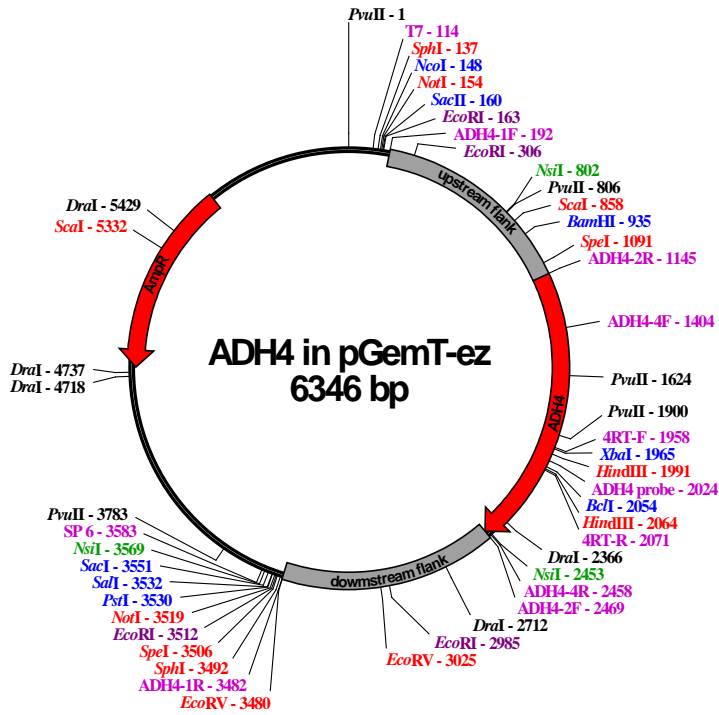


Figure AF: *pADH4*. *ADH4* ORF and 1000bp flanking regions up- and downstream cloned into pGemT-Easy

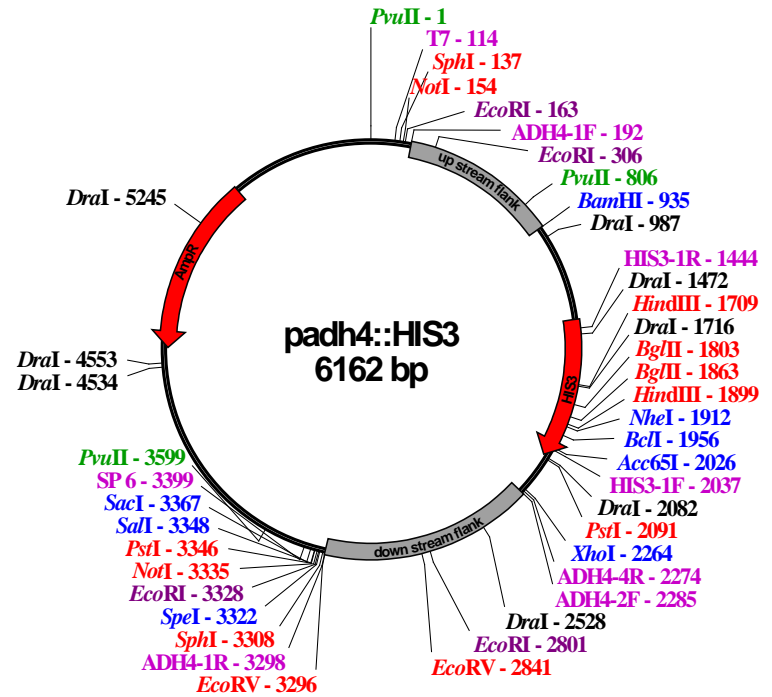


Figure AH: *padh4Δ::HIS3*. *ADH4* ORF from *pADH4* removed with PCR and replaced with the *HIS3* marker gene from pJJ217 with *BamHI* and *XhoI*

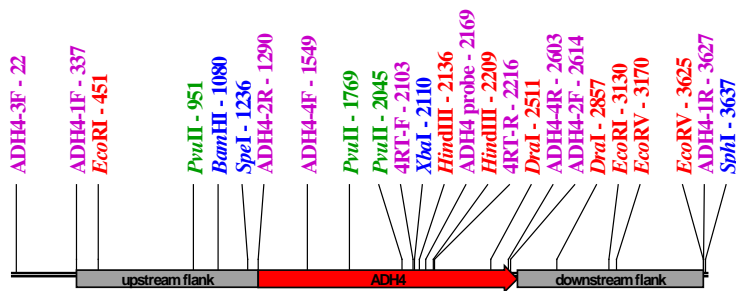


Figure AG: *ADH4* ORF and flanking regions also including 315 bp further upstream of the cloned fragment for screening

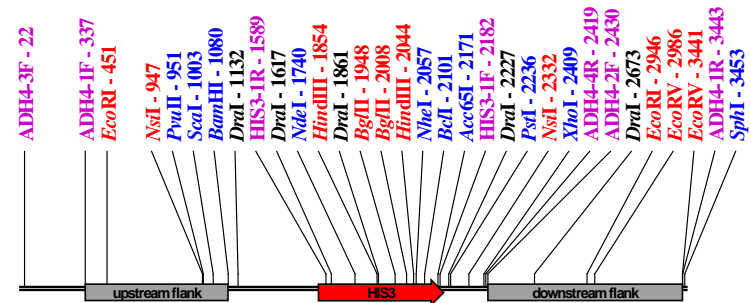


Figure AI: *HIS3* and *ADH4* flanking regions also including 315 bp further upstream of the cloned fragment for screening

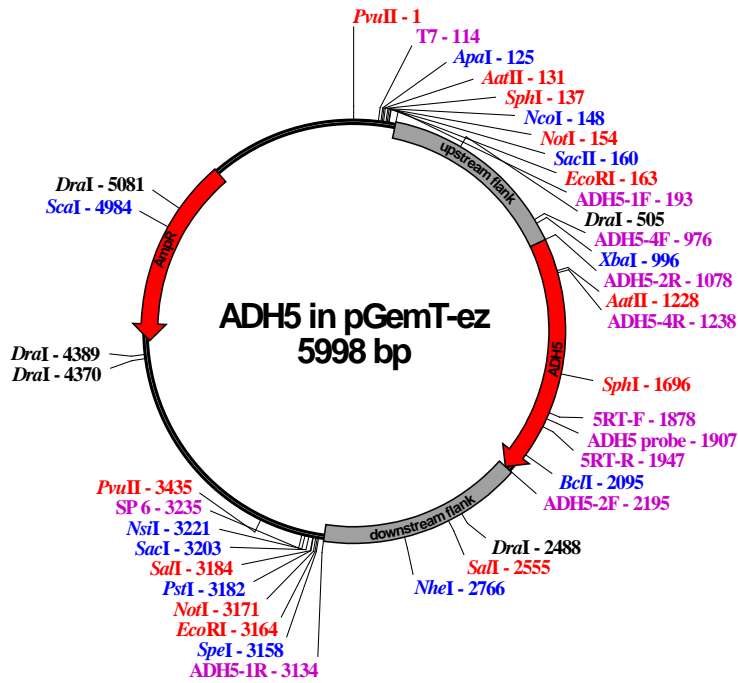


Figure AJ: pADH5. ADH5 ORF and 1000bp flanking regions up- and downstream cloned into pGemT-Easy

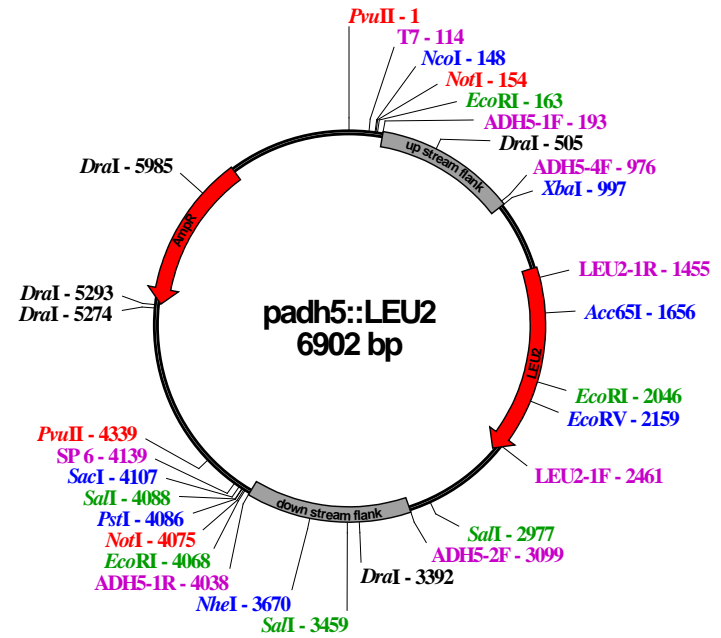


Figure AL: padh5Δ::LEU2. ADH5 ORF from pADH5 removed with XbaI and BclI and replaced with the LEU2 marker gene from pJJ252

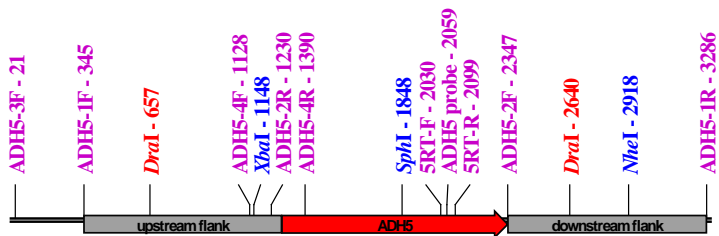


Figure AK: ADH5 ORF and flanking regions also including 324 bp further upstream of the cloned fragment for screening

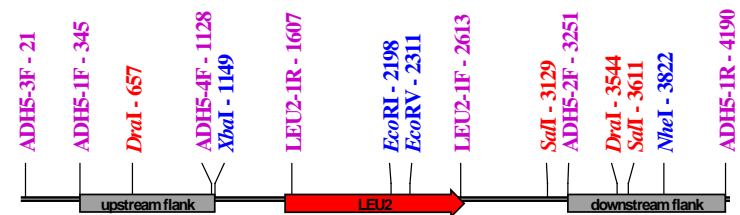


Figure AM: LEU2 and ADH5 flanking regions also including 324 bp further upstream of the cloned fragment for screening

Appendix F. PCR component concentrations and reaction conditions

Expand Long Template reaction components (Roche Applied Science)

118 ng W303-1A(a) genomic DNA or 50 ng plasmid DNA
 1X Buffer System 1 (20 mM Tris-HCl, pH 7.5, 100 mM KCl, 1mM DTT, 0.1 mM EDTA, 17.5 mM MgCl₂)
 350 μM of each dNTP
 100 nM of each primer
 2.6 units Taq polymerase

High Fidelity Taq polymerase reaction components (Roche Applied Science)

50 ng plasmid DNA or 118 ng W303-1A(a) genomic DNA
 1X Reaction Buffer (100 mM Tris-HCl, 15 mM MgCl₂, 500 mM KCl, pH 8.3)
 200 μM of dATP, dGTP, dTTP each
 6000 Ci mmol⁻¹ dCTP
 200 nM of each primer
 2 units High Fidelity Taq polymerase

Taq DNA polymerase reaction components (New England Biolabs)

1 μl of extracted yeast DNA (Appendix K) or 50 ng of plasmid DNA
 1X Reaction Buffer (20 mM Tris-HCl, 10 mM KCl, 10 mM (NH₄)₂SO₄, 2 mM MgSO₄, 0.1% Triton X-100, pH 8.8)
 200 μM of each dNTP
 200 nM of each primer
 1 unit of Taq polymerase

Programme 1: Expand Long template reaction conditions

1X	<u>94°C for 2 min</u> 94°C for 30 s
10X	X°C for 30 s <u>68°C for 3 min</u> 94°C for 30 s
20X	X°C for 30 s <u>68°C for 3 min</u> + 20 s each cycle
1X	68°C for 4 min

Programme 2: Amplification of Northern Blot probes

1X	<u>94°C for 2 min</u> 94°C for 30 s
10X	50°C for 30 s <u>72°C for 1.5 min</u> 94°C for 30 s
20X	48°C for 30 s <u>72°C for 1.5 min</u>
1X	72°C for 4 min

Programme 3: Screening with standard PCR

1X	<u>94°C for 2 min</u>
	94°C for 30 s
25-30X	X°C for 30 s
	<u>72°C for 2 min</u>
1X	72°C for 4 min

Programme 4: Screening with touchdown PCR

1X	<u>94°C for 2 min</u>
	94°C for 30 s
10X	55°C for 30 s
	<u>72°C for 2 min</u>
	94°C for 30 s
10X	50°C for 30 s
	<u>72°C for 2 min</u>
	94°C for 30 s
30X	47°C for 30 s
	<u>72°C for 2 min</u>
1X	72°C for 5 min

Programme 5: Amplification of Real-time PCR standards

1X	<u>94°C for 1 min</u>
	94°C for 30 s
10X	50°C for 30 s
	<u>72°C for 2 min</u>
	94°C for 30 s
30X	48°C for 30 s
	<u>72°C for 2 min</u>
1X	72°C for 4 min

Appendix G. Restriction enzyme digestions

Fermentas restriction enzymes were supplied by Inqaba, JHB, SA.

1. Each reaction was performed in a total volume of 10 µl.
2. A 10 fold concentrated stock solution of buffer for each enzyme was used as described by the manufacturer.
3. 0.2 units of enzyme were added to each reaction (unless otherwise specified by manufacturer).

Appendix H. Ligation reactions

1. 1 unit of T4 DNA ligase (Fermentas) and a 1 fold working concentration of ligation buffer (400 mM Tris-HCl, 100 mM MgCl₂, 100 mM DTT, 5 mM ATP pH 7.8) were added to a final reaction volume of 10 µl.
2. Template was added in 3:1 ratio fragment of interest: plasmid
3. The ligation mixture was incubated at 4°C for 12 h before transformation to *E. coli*.

Appendix I. Transformation of Rubidium chloride competent *E. coli*

1. Add 1-10 μl of plasmid to 80 μl competent cells and place on ice for 10 min.
2. Heat shock at 42°C for 45 s and place on ice for 2 min.
3. Add 800 μl LB medium and incubate at 37°C for 45 min on a shaker.
4. Centrifuge at 3 000 rpm for 2 min, remove supernatant and resuspend in 200 μl LB medium.
5. Resuspend and plate out on LB plates containing ampicillin (60 $\mu\text{g ml}^{-1}$), IPTG (9.6 $\mu\text{g ml}^{-1}$) and X-gal (40 $\mu\text{g ml}^{-1}$).

Reference: (Sambrook & Russel, 2001)

Appendix J. Transformation of yeast cells

1. Grow the culture 5 ml YPD medium for 16 h at 30°C with shaking.
2. Boil salmon sperm DNA for 10 min and place on ice for 10 min.
3. Centrifuge 800 μl of the cell culture at 13 000 rpm for 4 s.
4. Remove supernatant by aspiration and vortex slightly to loosen the pellet.
5. Add 25 μl Salmon sperm DNA (0.2 mg ml^{-1}) and 50 ng-1 μg DNA of interest.
6. Mix gently and add 100 μl pre-heated (42°C) one step buffer [0.2 M lithium acetate, 40% PEG, 0.1 M Dithiothreitol (DTT)].
7. Resuspend gently and incubate at 42°C for exactly 30 min.
8. Centrifuge at 3 000 rpm for 2 min.
9. Remove the supernatant with a pipette; resuspend the pellet gently in 250 μl YPD media and plate out on selective media.

Reference: (Chen *et al.*, 1992)

Appendix K. DNA extraction methods

Bacterial plasmid DNA extraction using alkaline lysis

1. Grow *E. coli* in 5 ml LB medium containing 60 μg ampicillin for 12 h at 37°C.
2. Centrifuge 1.5 ml of the 5 ml culture at 12 000 rpm for 5 s.
3. Resuspend the pellet in 100 μl GTE (50 mM glucose, 25 mM Tris-HCl pH 8, 10 mM EDTA).
4. Add 200 μl NaOH/SDS (0.2 mM NaOH, 1% SDS), mix by inverting 3-5 times and incubate at 25°C for 3 min.
5. Add 150 μl 5 M Potassium acetate, mix by inverting 4-6 times and place on ice for 2 min.
6. Centrifuge at 12 000 rpm for 6 min at 4°C.
7. Transfer the supernatant into a new tube and precipitate the DNA with the same volume isopropanol at 25°C for 10 min.
8. Centrifuge at 12 000 rpm for 10 min at 4°C.
9. Wash the pellet with 250 μl ice cold 70% EtOH and allow to dry.
10. Resuspend the pellet in 50 μl TE-buffer (10mM Tris-HCl, 1mM EDTA pH 8) with RNase (50 $\mu\text{g ml}^{-1}$).
11. Incubate at 37°C for 30 min
12. Store at -20°C

Reference: (Becker *et al.*, 1990)

Yeast genomic DNA extraction

1. Grow yeast strain on a YPD plates for 24 – 48 h. Place a loop full of cells in a 2 ml eppendorf tube containing 500 μ l YPD medium, vortex and centrifuge at 13 000 rpm for 5 s. Sufficient DNA can also be extracted from 2 ml of a 5 ml overnight culture.
2. Remove the supernatant and add 500 μ l lysis buffer (0.1 M Tris-HCl pH 8, 50 mM EDTA, 1% SDS) and 200 μ l ml glass beads (425-600 μ m in diameter).
3. Vortex for 2 min, add 275 μ l 7 M ammonium acetate and incubate at 65°C for 5 min.
4. Chill on ice for 5 min, add 500 μ l chloroform and mix gently by inversion.
5. Centrifuge at 11 000 rpm for 2 min at 25°C.
6. Transfer the supernatant to a new tube and add the same volume isopropanol.
7. Allow precipitation for 5 min at 25°C and centrifuge at 11 000 rpm for 2 min at 4°C.
8. Wash once with 300 μ l ice cold 70% ethanol.
9. Centrifuge at 11 000 rpm for 2 min at 4°C, remove supernatant and allow the pellet to dry.
10. Resuspend in the pellet in 50 μ l TE buffer (10 mM Tris-HCl, 1 mM EDTA, pH 8) with RNase (50 μ g ml⁻¹) and incubate at 37°C for 30 min.
11. Store at 4°C

Reference: (Labuschagne & Albertyn, 2007)

Appendix L. Construction of deletion mutants with micromanipulation.

Mating and sporulation

1. Streak the two haploid yeast strains on a YPD plate approximately 5 mm from each other and incubate at 30°C for 16 h.
2. Mix the two cultures with an inoculation needle and allow growth for at least 24 h at 30°C to ensure sufficient diploid formation (monitor the crossing process under the microscope at appropriate time intervals by checking for Schmoo structures).
3. Spread some of the culture on a potassium acetate agar plate and incubate at 25°C for at least 3 days. Monitor asci formation microscopically at appropriate time intervals.
4. When sufficient asci are visible (ca, 50%) dissection can commence.

Dissection

1. Pipette 50 μ l Zymolyase (5 mg ml⁻¹ 1 M Sorbitol) (USBiological, Swampscott, Massachusetts) in a sterile eppendorf tube and incubate at 25°C for 5 min.
2. Place a visible amount of culture from the potassium acetate agar plate aseptically into the Zymolyase (US Biological) using an inoculation loop and gently swirl the cells off.
3. Incubate at 25°C for exactly 3 min and 20 s.
4. Add 500 μ l 1 M Sorbitol very carefully to prevent rupturing of the asci.
5. Flame an inoculation loop and allow it to cool, insert vertically into the eppendorf tube down to the bottom of the tube. Remove the loop and spread the asci in a ca. 2 cm vertical line on a YPD plate (The line should be ca. 1.5 cm from the right side of the petri dish, this allows for 10 asci to be dissected 5 mm from each other).
6. Allow the liquid to dry and start the dissection; dissect only ten asci on each plate to limit contamination.
7. Allow germination at 30°C until the single spores are visible (\approx 3 days).

Replica plate screening

1. When the spores are about the size of a pin head, transferred them in an organised pattern to two fresh YPD plates.
2. Incubate one plate overnight (template for replica plating) and allow the other to grow for ca. 48 hours or until sufficient growth is visible (master).
3. Replica plate the spores onto the appropriate selective media.
4. Incubate the replica plates at 30°C for 48 hours or until growth is visible.

Reference: (Sherman & Hicks, 1991)

Appendix M. RNA isolation from *S. cerevisiae*

1. This method works effectively for samples taken from both bioreactor batch cultivations and chemostat pulse experiments. Pipette 10 ml of the culture in a test tube and centrifuge at 2000 g for 10 min at 4°C. Remove the supernatant, seal the tube and store at -80°C.
2. Add 600 µl PCI [phenol saturated solution pH 4.5: chloroform: isoamyl alcohol (25:24:1)], 200 µl glass beads (425-600 µm in diameter, washed), 500 µl extraction buffer (1 mM EDTA, 100 mM LiCl, 100 mM Tris, 10 mM Sodium acetate, pH 7.5) and 50 µl 10% SDS to frozen samples and allow thawing on ice.
3. Vortex vigorously three times for 30 s intervals, keep on ice in between.
4. Transfer the solution (without the glass beads) to a 2 ml eppendorf tube.
5. Centrifuge for 15 min at 13 000 rpm at 4°C.
6. Three phases are visible. Transfer the upper phase to a new 2 ml eppendorf tube and add 500 µl chloroform.
7. Mix and centrifuge at 12 000 rpm for 6 min at 4°C.
8. Repeat the chloroform wash step until no white inter phase is visible (usually twice).
9. Transfer the supernatant to a 1.5 ml eppendorf tube, add 1/20 volume 40% potassium acetate and fill the rest of the eppendorf tube with cold 100% ethanol.
10. Resuspend by inverting and allow precipitation at -80°C for 30 min (mix at 10 min intervals to prevent freezing).
11. Centrifuge at 10 500 rpm for 10 min at 4°C.
12. Remove the supernatant, wash the pellet with 300 µl cold 70% ethanol and allow the pellet to air dry.
13. Add 50 µl 0.1% DEPC treated water and place at 4°C over night to dissolve.
14. Store at -80°C.

Reference: (Kohrer & Domdey, 1991)

Appendix N. Northern Blotting

Electrophoresis with formaldehyde

1. Prepare a 1% agarose gel (50 ml) in NBC buffer (50 mM boric acid, 1 mM sodium citrate, 5 mM NaOH, pH 7.5)
2. Place the gel in a 65°C water bath for 15 min.
3. Add 25 µl DEPC and incubate at 65°C for 10 min, mix carefully at appropriate intervals.
4. Add 1.25 ml formaldehyde, mix, pour immediately and leave for 45 min to solidify.
5. Pre-run the gel at 80–100 V for 10 min.
6. Mix 2 µl ten fold concentrated NBC buffer (0.5 M boric acid, 0.01 M sodium citrate, 0.05 M NaOH, pH 7.5), 3 µl formaldehyde, 10 µl formamide, 2 µl loading buffer (0.25% bromophenol blue, 40% sucrose) and 1 µl ethidium bromide (1 mg ml⁻¹).
7. Add 5 µl of a 2 µg µl⁻¹ stock of RNA, mix and incubate at 65°C for 5 min.
8. Load the samples (23 µl per well) and run the gel at 80 V until the blue bands are well clear of the wells. Increase the voltage to 120 V and allow separation for at least 7 cm to facilitate ample separation of the 18s and 16s rRNA.
9. After electrophoreses photograph the gel, but keep UV exposure to an absolute minimum.

Capillary transfer to nylon membranes

1. Stack ≈ 15 paper towels and four 3 mm Chr Whatman filter papers soaked in 10X SSC (1.5 M NaCl, 0.15 M sodium citrate) in the plastic reservoir.
2. Cut the wells from the agarose gel and place it face down on the filters.
3. Cover the sides up to the gel with Glad Wrap to prevent transfer of liquid to bypass the gel.
4. Soak a HybondTM N⁺ nylon membrane (Amersham) in two fold concentrated SSC (0.3 M NaCl, 0.03 M sodium citrate) and place it on the agarose gel.
5. Cover with three soaked and three dry Whatman filter papers, stack a number of paper towels on top and keep in place with a weight.
6. Generously fill the reservoir with ten fold concentrated SSC and allow transfer for at least 10 h.
7. Remove the membrane and crosslink with UV emission in the BioRad Gene linkerTM.
8. Confirm the transfer under UV light, mark the position of the 18s and 16s rRNA with pencil and label the membrane with incisions for identification.
9. Bake at 80°C for 1 h and store between Whatman filter papers.

Hybridisation with radio active probes

1. Pre-hybridise the membrane in hybridisation solution (0.25 M Na₂HPO₄, 7% SDS, pH 7.0) for at least 1 h at 65°C in the Techne Hybridiser HB-1 roller.
2. Denature the labelled probe (labelled as described in Chapter 4) by boiling for 10 min, followed by cooling on ice/NaCl for at least 2 min.
3. Remove the liquid from the pre-hybridisation step and add 5 ml fresh hybridisation solution. Add 1 ml of the same solution to the eppendorf tube containing the probe, mix carefully and add to the roller.
4. Mix and allow hybridisation at 65°C for at least 16 h.
5. Wash twice in 100 ml Wash buffer 1 (two fold concentrated SSC, 0.1% X SDS) at 25°C for 15 min.
6. Wash twice in 500 ml pre-heated Wash buffer 2 (0.1X SSC, 0.1% SDS) at 65°C for 10 min.
7. Pour off the buffer and seal the membrane in glad rap, avoiding bubbles and folds.
8. Expose the membrane to x-ray film at -80°C for at least 24 h.
9. After exposure, remove the x-ray film and allow thawing for a few seconds.
10. Develop the x-ray film and mark with indentations similar to that of the membrane.

Appendix O. Real-time PCR

DNase I treatment

1. Total RNA concentrations were determined with the NanoDrop
2. Dilutions of ca. 200 ng μl^{-1} were prepared in DEPC treated water
3. Treat 4 μl of the RNA dilution with 2 μl of DNaseI (2U) in a 10 μl reaction containing 1 μl reaction buffer (200 mM Tris-HCl, 20 mM MgCl_2 , pH 8.3)
4. Mix carefully and spin down briefly (DNase is subject to mechanical damage)
5. Incubate at 37°C for 2 h.
6. Add 1 μl Stop solution (50 mM EDTA), mix and incubate at 70°C for 10 min
7. Cool on ice for 2 min
8. Add 29 μl DEPC treated water to obtain a final RNA concentration of ca. 20 ng μl^{-1}
9. Use 2 μl as template for real-time PCR (ca. 4 ng μl^{-1} as suggested by SensiMix One-Step Kit manufacturer) store the rest at -20°C.

Component concentrations in each reaction

3.5 mM of MgCl_2
 400 nM of primer ACT-fw
 600 nM of primer ACT-as
 200 nM of primers 1RT-F, 2RT-F, 3RT-F, 4RT-F, 5RT-F
 300 nM of primers 1RT-R, 2RT-R, 3RT-R, 4RT-R, 5RT-R
 200 nM of probes ACT, ADH5
 100 nM of probes ADH1, ADH2, ADH3, ADH4
 10U RNase inhibitor
 1X SensiMix solution (SensiMix One Step kit supplied by Quantace, London, UK)

Reaction conditions

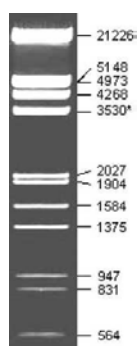
Runs were performed on the RotorGene 3000 in 10 μl vials (Corbett research, Sydney, Australia)

Hold	49°C for 40 min	
Hold	95°C for 10 min	
<u>40 cycles</u>	95°C for 15 s	Acquisition on both FAM and JOE channels
	X°C for 45 s	

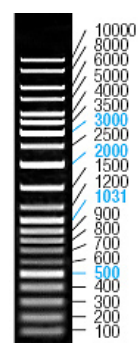
The annealing temperatures (X°C) were 59°C for the ADH1, ADH2 and ADH4 probes and 60°C for the ADH5 probe.

Appendix P: Marker DNA

Band lengths are given in base pairs (bp)



λ III
EcoRI/HindIII digested marker DNA



O'GeneRuler marker DNA

Literature cited

- Becker, J. M., G. A. Caldwell, and E. A. Zachgo.** 1990. Biotechnology, a laboratory course. Becker, J. M., Caldwell, G. A., and Zachgo, E. A. *Academic Press.* pp.
- Cakar, Z. P., U. Sauer, and J. E. Bailey.** 1999. Metabolic engineering of yeast: the perils of auxotrophic hosts. *Biotechnol. Lett.* **21**: 611-616.
- Chen, D. C., B. C. Yang, and T. T. Kuo.** 1992. One-step transformation of yeast in stationary phase. *Curr. Genet.* **21**: 83-84.
- du Preez, J. C., J. E. Mare, J. Albertyn, and S. G. Kilian.** 2001. Transcriptional repression of *ADH2*-regulated β -xylanase production by ethanol in recombinant strains of *Saccharomyces cerevisiae*. *FEMS Yeast Res.* **1**: 233-240.
- du Preez, J. C. and J. P. van der Walt.** 1983. Fermentation of D-xylose to ethanol by a strain of *Candida shehatae*. *Biotechnol. Lett.* **5**: 357-362.
- Flikweert, M. T., L. Van der Zanden, W. M. T. M. Janssen, H. Y. Steensma, J. P. van Dijken, and J. T. Pronk.** 1996. Pyruvate decarboxylase: An indispensable enzyme for growth of *Saccharomyces cerevisiae* on glucose. *Yeast* **12**: 247-257.
- Kohrer, K. and H. Domdey.** 1991. Preparation of high molecular weight RNA. *Methods Enzymol.* **194**: 398-405.
- Labuschagne, M. and J. Albertyn.** 2007. Cloning of an epoxide hydrolase-encoding gene from *Rhodotorula mucilaginosa* and functional expression in *Yarrowia lipolytica*. *Yeast* **24**: 69-78.
- Pronk, J. T.** 2002. Auxotrophic yeast strains in fundamental and applied research. *Appl. Environ. Microbiol.* **68**: 2095-2100.
- Sambrook, J. and D. W. Russel.** 2001. Molecular cloning: A laboratory manual. *Cold Spring Harbour.*
- Schulze, U., M. E. Larsen, and J. Villadsen.** 1995. Determination of intracellular trehalose and glycogen in *Saccharomyces cerevisiae*. *Anal. Biochem.* **228**: 143-149.
- Sherman, F. and J. Hicks.** 1991. Micromanipulation and dissection of asci. *Methods Enzymol.* **194**: 21-37.
- Verduyn, C., E. Postma, W. A. Scheffers, and J. P. van Dijken.** 1990. Physiology of *Saccharomyces cerevisiae* in anaerobic glucose-limited chemostat cultures. *J. Gen. Microbiol.* **136**: 395-403.